Sensing and non-destructive testing applications of terahertz spectroscopy and imaging systems: State-of-the-art and state-of-the-practice

Walter Nsengiyumva, Shuncong Zhong*, Longhui Zheng, Wei Liang, Bing Wang, Yi Huang, Xuefeng Chen, and Yaochun Shen

***Abstract*— Terahertz (THz) technology has firmly established itself as an effective sensing and nondestructive testing technique for the detection of substances and physico-chemical evaluation of materials and structural systems since its first emergence almost three decades ago. To date, both the effectiveness and accuracy of this technology have been extensively demonstrated in a myriad of applications across the spectrum of research and development all the way to process analytical technology, quality control, nondestructive testing, and structural health monitoring. These applications are generally enabled by the production and availability of advanced, versatile, robust, highly accurate, and industrially rugged THz spectroscopy and imaging systems, the unique properties of THz waves compared with other electromagnetic waves, as well as the advancements in electronics, photonics, and THz metamaterial systems development. This article presents a comprehensive state-of-the-art and state-of-the-practice review of sensing and nondestructive testing applications of THz technology and analyzes the role of THz metamaterials in enhancing the resolution and sensitivity of THz systems. The study also provides a general overview of the fundamentals of THz spectroscopy and imaging systems and discusses the suitability of THz sensing and nondestructive testing in a variety of real-world application scenarios (*e.g.* composites' defect detection and evaluation, paints and coatings thickness measurement and characterization, biomolecule detection, *etc*.). Aspects such as the noise caused by the presence of barriers, challenges with experimental implementations and operability of THz systems, long times required to acquire THz images, as well as limited customizability and portability of currently available THz systems are also discussed.**

***Index Terms*— Terahertz spectroscopy and imaging (THz-SI), Terahertz nondestructive testing (THz-NDT), Composite materials, Thermal barrier coatings (TBCs), THz metamaterial sensing, Terahertz sensing.**

I. INTRODUCTION

A. Motivation and background

In the electromagnetic spectrum, the terahertz (THz) frequency region refers to a narrow band between the microwaves (μ-Waves) and infrared (IR) regions. The radiation in this region of the electromagnetic spectrum is often referred to as THz radiation or THz waves. THz waves possess unique characteristics that make them attractive for spectroscopy and imaging applications. For example, many optically opaque materials are more transparent at THz frequencies suggesting that they can be used to reveal concealed objects through imaging, and the fact that THz wavelengths are much smaller than their μ-Waves counterparts enables THz imaging systems to resolve higher-resolution images compared to μ-Wave imaging systems [1], [2]. Also, the interaction between these waves and the matter in chemical, physical, and biological systems exhibits a wealth of fascinating and highly complex properties that are often used to evaluate and characterize the aforementioned systems [3], [4]. In particular, many molecules have unique spectral signatures at THz frequencies and this is one of the reasons why THz spectroscopy is considered an effective tool for many chemical identification and material characterization applications [5]–

This work was supported in part by the National Natural Science Foundation of China (No. 52275096, 52005108), Start-up Funding from Fuzhou University (XRC-23003), Natural Science Foundation of Fujian Province (No. 2020J05084), STS Project of Fujian-CAS (No. 2021T3026), Fuzhou-Xiamen-Quanzhou National Independent Innovation Demonstration Zone High-end Equipment Vibration and Noise Detection and Fault Diagnosis Collaborative Innovation Platform Project (No. 2022-P-022), and Fujian Provincial Major Research Project (No. 2022HZ024005). The technical staff and aegis of the International Joint Laboratory of Precision Instruments and Intelligent Measurement & Control at Fuzhou University are also acknowledged.

(Corresponding author: Shuncong Zhong).

Walter Nsengiyumva, Shuncong Zhong, Wei Liang, Bing Wang, and Yi Huang are with the Fujian Provincial Key Laboratory of Terahertz Functional Devices and Intelligent Sensing, School of Mechanical Engineering and Automation, Fuzhou University, Fuzhou, 350108, P. R. China and with the Institute of Precision Instrument and Intelligent Measurement & Control, Fuzhou University, Fuzhou 350108, P. R. China. (e-mail: nsewalt@outlook.com; sczhong@fzu.edu.cn; b.wang@fzu.edu.cn; YiHuang@fzu.edu.cn; liangwei@fzu.edu.cn).

Longhui Zheng is with CAS Key Laboratory of Design and Assembly of Functional Nanostructures, Fujian Key Laboratory of Nanomaterials, Fujian Institute of Research on the Structure of Matter, Chinese Academy of Sciences, Fuzhou, 350002, P. R. China. (e-mail: lhzheng@fjirsm.ac.cn).

Xuefeng Chen is with School of Mechanical Engineering, Xi'an Jiaotong University, Xi'an 710049, P. R. China. (e-mail: chenxf@xjtu.edu.cn).

Yaochun Shen is with the Department of Electrical Engineering and Electronics, University of Liverpool, Brownlow Hill, Liverpool L69 3GJ, United Kingdom. (e-mail: ycshen@liverpool.ac.uk).

Color versions of one or more of the figures in this article are available online at http://ieeexplore.ieee.org.

[8]. To put this into perspective, THz waves possess photon energies in the millielectronvolt (meV) range (*i.e*., usually from 1-100 meV), which enables their strong interactions with systems having their lifetime and energy transition characteristics in the picosecond and meV ranges, respectively [9], [10]. Examples of systems featuring the aforementioned lifetime and energy transition characteristics include but are not limited to free charge plasmas, excitons, transient molecular dipoles, weakly bonded molecular crystals, molecular relaxation dynamics in aqueous solutions, hydrated biological matter, *etc*. [3]. This means that by using adequate devices to detect the photon energies released following the interaction between THz waves and the target materials or chemical substances one can easily acquire specific spectroscopic and/or imaging information that could help to identify and evaluate their different features, hence the capabilities of THz systems to perform the sensing and nondestructive testing (NDT) tasks. Although the ability to perform the spectroscopy analysis of materials and structures in the far infrared has been studied since this type of analysis became technically feasible for such applications with the development and implementation of the first Fourier Transform Infrared (FTIR) spectroscopic system in the 1950s [11], [12], the development of related THz spectroscopic systems has been delayed for many years even though THz frequencies are close to the far infrared frequencies in the electromagnetic spectrum [13], [14]. Even though many technical limitations could justify the extension of the aforementioned delay, the latter has been largely attributed to the lack or inefficiency of contemporary THz emission devices and detection sensors.

In the late 1980s, significant advances in electronics and photonics have seen the development of femtosecond laser modules which enabled the generation and detection of high-power THz waves. The development of the femtosecond laser module is considered by many as the beginning of spectroscopy in the THz frequency range [3]. This method was first described by Exter *et al*. in the late 1980s and heavily relied on the optical excitation of photoconductive dipole antennas (PCA) to operate [5]. After this initial study, subsequent improvements in THz spectroscopy followed and were largely facilitated by the more general development of optoelectronics and low-scale semiconductor technologies [3], [14]. To date, THz technology has already been adopted by its earlier users and is now on the verge of its desirable plateau of productivity or simply at its technological readiness or availability levels with completely new functionalities and applications in many different fields ranging from medical diagnostics and security applications to industrial control of the processes [14], [15]. Although the principles behind THz spectroscopy are heavily related to the methods developed for μ-Wave technology and FTIR spectroscopy, they all operate in different frequency regions suggesting that the information obtained from their interactions with the target materials/structures are also different. Although the information detailing the difference between these types of radiation has been extensively documented in the literature, some aspects related to the distinct features of THz radiation are worth mentioning. In terms of their electromagnetic frequency ranges, for example, the THz region belongs to a range of loosely defined frequencies ranging from 100 GHz to 10 THz, which correspond to their range of wavelengths spanning from 3 mm to 30 μm [3]. In most cases, however, this frequency band cannot be used entirely by common THz instruments, as they only cover the frequency range between 0.1-4 THz.

Apart from the development and implementation of femtosecond laser systems, the popularity gained by THz technology and the expansion of its industrial applications in recent years were also promoted by several key properties of THz waves *vis-à-vis* the different physico-chemical substances and material systems. Typically, THz waves possess photon energy levels similar to the excitation energy levels required for different rotational and vibrational transitions of molecules in many kinds of materials and physico-chemical substances at different frequencies in the THz band. This means that some information such as low-energy molecular and intramolecular vibrational characteristics is contained in their THz spectroscopic signals, and this makes THz technology a powerful sensing and nondestructive testing (NDT) tool for the evaluation of materials as well as the detection of biological and physico-chemical substances, respectively. Compared to γ-rays and X-rays, THz waves feature low photon energy levels (*e.g*. estimated to 4 meV at 1 THz) and, therefore, form a non-ionizing type of electromagnetic radiation. Indeed, this property makes THz waves safe for use in the inspection and evaluation of biological tissues as well as the detection and analysis of any other biological samples that may be susceptible to ionization or high-energy beam damage [16]. Also, THz waves are coherent (*i.e*., meaning that they are generated by coherent laser pulses based on dipole oscillations or nonlinear optical effects driven by coherent currents), suggesting that they can be used to measure the amplitude and phase information of the electric field coherently [9], [17]. This is particularly important because not only does coherent detection achieve higher sensitivity than direct detection in THz systems, but this type of detection scheme can also achieve an increased spectral efficiency because it uses the phase, amplitude, and polarization of an optical carrier to carry information. Compared with μ-Waves and mm-Waves, THz waves possess shorter wavelengths, suggesting that THz systems can undoubtedly achieve higher penetration capability and spatial resolution than their μ-Waves and mm-Waves-based counterparts [18]. Additionally, THz pulses have good temporal resolution with their pulse width being in the picosecond to the sub-picosecond ranges [19], [20], which confers the THz systems the capability to detect and analyze transient changes taking place in electrons, atoms, molecules, and other ultra-fast processes.

Consistent with the aforementioned, THz waves have good penetration capabilities to common dielectric materials (*e.g*. inorganic materials such as glass and ceramics, rigid fibrous reinforced composites, polymers, vulcanized adhesives, elastomers and rubber-like materials, plastic films, textile fiber, resins, varnishes and silicones, *etc*.) due to their limited electromagnetic absorption levels at THz frequencies, and this gives THz technology the ability to detect dangerous goods when covered by these types of materials [9], determine the aging degree of common electrical insulators [21], *etc*. Although THz waves are heavily absorbed by most polar molecules or substances such as alcohols, water, moisture, ammonia (NH_3), *etc*. [22], the analysis of the absorption spectroscopy of THz waves passing through some samples can

also be used to reveal the quantity of these polar molecules in their midst [23], [24]. Also, the relatively low scattering losses occurring in pharmaceutical tablets due to the long wavelength of THz radiation compared to typical sizes of internal tablets/capsules common particles make THz spectroscopy and imaging (THz-SI) an extremely effective and versatile analytical tool for the analysis and evaluation of pharmaceutical capsules and tablets (*e.g*. analysis of the solid-state and amorphous formulations of pharmaceutical drug products, evaluation of small organic molecular crystals and their corresponding solid-state modifications, *etc*.) [25], [26]. All these properties combined with the aforementioned advances in the development of high-performance photonic and electronic devices have enabled the deployment of highly efficient THz-SI for several industrial applications including homeland security, aerospace, polymer science, polymer testing, evaluation of paints and coatings, characterization of wood and paper materials, evaluation of electronics and semiconductors, detection of petrochemicals, gas sensing, agricultural and food products, *etc*. [4], [14], [15], [27]. This is in contrast to what was the main sentiment among researchers in industry and academia about a decade ago when most researchers and experts could not name even a single "*killer application*" of THz sensing.

To date, THz technology has evolved into an effective sensing/NDT tool and the expansion of its applications stands at the center of current interests in the NDT community. In fact, some state-of-the-art applications that were not feasible decades ago are now being successfully implemented [28]–[30], and it appears that the commonly repeated mantra "*THz moves out of the lab*" may finally be coming true [15], [29]. Nevertheless, the number of publications in peer-reviewed journals, academic monographs, conference proceedings, book chapters, industry snippets, patent applications, *etc*. on THz sensing and NDT applications as well as THz systems development is scattered and it is becoming increasingly difficult to process it in a single reading. Also, the current expansion of deceptive and exploitative business models of countless predatory journals makes it more difficult for starters to know the publications that provide an accurate description of the facts. Therefore, having a review article that serves as a quick reference for researchers, engineers, and policymakers would help to improve their research efficiency by providing them with the most up-to-date state-of-the-art and state-of-the-practice governing the applications of THz technology in industries and research settings. Although there are currently some topical review articles on the applications of THz technology [4], [9], [25], these studies generally focus on laboratory-based testing and the detection of specific classes of materials, structures, and substances leaving the industrial applications with real-time impact on the development of THz sensing and NDT devices largely untouched. Therefore, the present study bridges these gaps and provides the readers with contemporary information on both the laboratory and industrial applications of THz technology, and outlines some of the most innovative practices involving the development, and improvement of THz technology.

B. Literature review

Industries generally need accurate and efficient NDT tools for the detection, analysis, and testing of materials, substances, and structural systems [17], [25], and this is particularly critical for products or systems that require regular testing and monitoring to guarantee their quality, material composition, properties and/or structural integrity at different stages of their lifecycles [16], [31]. Although these types of evaluation and sensing can be performed using offline testing/monitoring systems, some applications may still require the use of in-line testing/monitoring systems to allow continuous or batch processing, save resources and improve the testing/monitoring efficiency. The former can be achieved using both contact and non-contact testing/monitoring techniques, while the latter can only be achieved by using noncontact testing/monitoring techniques. Additionally, modern products such as aircraft components, pharmaceutical tablets, wind turbine blades, integrated circuits, *etc*. must comply with their application requirements as stipulated by relevant government or private agencies consistent with contemporary technological advancements [16], [25], [32]. These updates may require the use of new and advanced material systems such as composites, carbon nanotubes (CNTs), ceramics, graphene, *etc*., which also require the use of upgraded or new NDT techniques for their inspection and quality control. As a new and highly effective NDT technique, THz technology can easily detect and evaluate important structural features such as the thickness, weight, surface roughness, damage, density distribution, quality of the interfaces in multilayered structures, chemical composition, *etc*. of the target structures [4], [13], [14], [25]. Apart from the evaluation of structural features of materials and structures, THz technology can also be applied to determine numerous types of material properties including complex conductivity, dielectric properties, permittivity, refractive index, absorption coefficient, *etc*. Also, the fact that THz technology uses THz waves which combine several other characteristics such as high resolution, biosafety, the capability of evaluating the molecular vibrational characteristics, high penetration into dielectric materials, as well as the flexibility of measurement set-up, *etc*. is another added advantage [17], [33].

Taking advantage of all these properties offered by THz waves, THz technology has recently become a valuable sensing and testing technique in materials sciences, chemistry, engineering, medicine, *etc*. [15]. The technique is constantly being used to study the vibrational spectroscopy of liquids such as moisture or water molecules, different types of alcohols (*e.g*. propanol, methanol, ethanol, *etc*.), and low-frequency dielectric relaxation processes [21], [34], [35]. THz technology is also used to detect numerous types of chemical substances such as amino acids, and peptides in biomedical applications [36], [37], concealed liquid drugs, and explosives in safety and security-related applications [38], *etc*. To date, researchers are also working to optimize THz systems for the detection of bombs and other types of dangerous weaponry and initial results have produced encouraging results [39], [40]. In the field of materials science, in particular, THz-NDT is an ideal testing method to measure the density of mobile charge carriers and the electromagnetic shielding capabilities of electrically conductive and semi-conductive materials based on their

capability to reflect and absorb THz radiation [41], [42]. The recent advances in the design and implementation of new material systems have also attracted considerable attention among chemical engineers and material scientists seeking to use this technology to study the homogeneity and uniformity of emerging two-dimensional (2D) materials including bismuth selenide (Bi_2Se_3) [43], Molybdenum disulfide (MoS_2) [44], graphene, CNTs, metal carbide, and nitrides or carbonitrides (MXene) [45], [46], *etc*. Interests in using THz-NDT as a quality control technique in the pharmaceutical industry to monitor the forming and drying processes of coatings on pharmaceutical tablets and capsules, as well as measure the final thickness of the aforementioned coatings and protective layers at reduced costs and process times have also been reported [47], [48]. In the biomedical community, the use of THz technology as the diagnostic tool for certain diseases such as cancer and diabetes has also been growing in recent years [49]. In biological science, researchers are increasingly focusing on the detection of several types of microorganisms and toxins including yeast, bacteria, fungi, aflatoxins, and viruses using THz-metamaterials [50], [51].

Although THz technology is an effective sensing and NDT tool for numerous industrial and scientific applications, THz waves have longer wavelengths (*i.e*., on the order of 300 μm) than X-rays and γ-rays suggesting that THz systems can barely detect small samples or be used to perform an analysis of trace amounts of samples due to their limited resolution and/or sensitivity to these types of samples [9]. To improve their resolution and sensitivity features, researchers have developed several types of THz sub-wavelength structures commonly referred to as THz metamaterials [30]. These structures are generally fabricated by using common lithographic techniques and are primarily used to enhance the interaction between THz waves and the target samples for accurate parameter measurements and enable the evaluation of extremely small samples or the detection of substances in trace concentrations [50], [52], [53]. Advancements in the design and implementation of efficient THz metamaterial systems have also given rise to the corresponding development of high-performance THz systems' components such as filters, lenses, beam steerers, perfect absorbers, *etc*. [30], [54]. Apart from the improvement in the sensing and NDT capabilities of THz systems, researchers have also worked to diversify the configurations and measurement principles of THz systems to accommodate new applications/materials in a myriad of directions [14], [55]. As such, there are currently many published studies on THz sensing and NDT applications, and all these studies use a wide variety of THz system configurations that cannot be reviewed in a single paper. To this end, the present study only focuses on general considerations and provides illustrations and explanations pertaining to the operation of THz-SI by outlining the process through which the time-domain measurements provide the images and spectral information describing or providing the features of the structure under test. The study also illustrates the method for extracting certain structural properties and characteristics of the samples from the measured THz signals and potential pitfalls when acquiring THz time-domain spectra.

THz spectroscopy technologies are divided into three main classes namely THz frequency-domain spectroscopy (THz-FDS) and THz time-domain spectroscopy (THz-TDS) [3], [9], [14], [56], whereby the most commonly used THz systems belong to the THz-TDS class and their imaging variations. To date, numerous papers have been published describing the use of THz-SI systems and analyzing their various characteristics and operation features [3], [57], [58]. To utilize the data measured by THz-TDS systems, for example, it is necessary to understand certain performance aspects of THz-TDS systems and perform a correct interpretation of the results [15]. In their operation, THz-TDS systems use pulsed THz waves generated by exciting semiconductor heterostructures using ultrashort laser pulses [36]. The generated THz pulses will interact with the samples and the measured time-domain signals represent the temporal variation of the intensity of the spectral pulse and/or the transient electric field of THz waves. These time-domain signals can then be transformed into their frequency-domain counterparts (*i.e*., the spectral data) by applying the Fourier transformation. In most cases, THz transmission loss in the sample is visualized as the difference between the reference and sample spectra. The transformed signals or frequency-domain signals are used to calculate different types of information including the phase and amplitude, which are subsequently used to determine the sample's optical and electrical properties such as the conductivity, absorption coefficient, complex refractive index, complex conductivity, dielectric constant, *etc*. [3], [21]. The THz optical parameters of the sample are calculated from the spectral data of the reference and sample being measured [59]–[61]. For example, the sample's refractive index is obtained from the phase data, while its absorption coefficient is derived from the amplitude data but takes into consideration the previously calculated refractive index [15]. In fact, either the time domain or frequency domain can be used to analyze data measured by the THz-TDS systems for sensing and NDT applications depending on the sample's characteristics and/or features of interest.

THz-TDS operates in a signal-probe configuration and uses short pulses (*i.e*., the THz pulse length is ≈1 ps and the probe pulse length is <0.1 ps). As a result, there are no standing waves formed in the system itself or the sample being measured which further simplifies the data analysis process. Also, the THz-TDS system provides users with unambiguous measurements of the electromagnetic field amplitude and phase because it uses short pulses and coherent detection. In fact, this is also considered one of the main advantages of the THz-TDS measurements because the measured electromagnetic field amplitude and phase directly yield transmission loss and phase delay, which are subsequently used to derive the absorption coefficient and refractive index of the material measured. Although THz-TDS applications require a reference measurement in most cases (*i.e*., a dataset recorded without any sample in place or with reference material), these systems do not require repeated calibration as one measurement suffices for a specific system configuration. The nominal operational bandwidth of a typical THz-TDS system is generally between 0.1-4 THz, this bandwidth may be reduced by transmission losses (*i.e*., following a well-formulated dependence). The typical frequency resolution of most commercially available THz-TDS

is usually about 5 GHz, but better resolutions up to 1 GHz are also achievable.

THz-FDS systems are also closely related to THz-TDS systems in terms of their physical processes, technological solutions, and measurement techniques [21,22,23]. THz-FDS systems use two continuous-wave THz lasers with offset wavelengths, and dedicated semiconductor-based antennas, commonly referred to as "*photomixers*", to convert the beat signal into monochromatic THz waves. Varying the wavelength offset between the two lasers tunes the THz frequency, hence, the denomination "*frequency-tunable THz emitters or detectors*". Unlike THz-TDS systems, THz-FDS systems operate with continuous THz waves, with high temporal coherence that gives rise to standing waves that must be accounted for in measurements. Interestingly, THz-FDS systems also use coherent detection, which means that their measurements also yield information related to both THz field amplitude and phase. The typical operating range of THz-FDS systems is generally between 0.05-3 THz [24]. The main advantages of THz-FDS are a very high-frequency resolution (<5 MHz), the possibility of measuring at a user-selected, fixed frequency (or frequency range), and comparatively low system costs compared with THz-TDS systems. The general principle of operation of THz-FDS systems is similar to that of THz-TDS systems. That is, a reference signal is recorded, followed by a measurement of the sample. The phase-sensitive (coherent) detection scheme gives rise to phase "fringes" whereby the detected signal (*i.e*., the photocurrent measured in the receiver photomixer) oscillates between negative and positive values as the THz frequency is scanned. This effect is similar to scanning an interference pattern in frequency [26] and must not be confused with standing waves that arise due to multiple reflections of the beam. In general, the frequency step size in THz-FDS measurements is as small as 1 MHz which provides THz-FDS systems with high-resolution spectral measurements.

In the first post-processing step, the envelope spectrum of the phase fringes is computed to detect and identify the different features of the measured samples. The most straightforward approach is a simple identification of the phase maxima and minima [26]; however, this method fails if the linewidth of the spectral feature is narrower than the fringe period. Phase and amplitude information for each frequency step is either obtained with phase modulation techniques or by applying a Hilbert transform to the raw THz data [62]. The envelope spectrum of the sample is divided by that of the reference measurement. The square of the resulting ratio produces the transmission spectrum, where the ratio is squared because "*transmission*" refers to the intensity, whereas the envelope spectra are proportional to the electric field of the THz wave. In some studies, for example, the silicon sphere resonator with a whispering-gallery-mode resonance that has a *Q*-factor of 15,000 and a full-width half maximum (FWHM) linewidth of 42 MHz, whereby the line shape is resolved with a THz-FDS system. Indeed, this type of narrow resonance would not be detectable with a THz-TDS system, and this justifies the higher performance of THz-FDS systems over THz-TDS systems. Similar to the optical measurements in the visible and NIR, it is possible to perform THz measurements by using any suitable combination of THz sources and detectors [57], [63]–[65]. However, the challenge still lies in the inherent low-intensity levels of THz sources and the low sensitivity of most THz detectors [14]. Interestingly, advanced THz emitters and detectors operating in the lower section of the THz frequency range (*i.e*., between 0.1-1 THz) are currently being developed [15], and numerous high-performance devices such as multipixel detector arrays and video-rate THz camera systems are now being deployed for real-time industrial sensing and NDT applications.

Although THz-SI systems are highly effective sensing and NDT tools, their accuracy levels can be easily comprised because of the attenuation of the THz signals along their propagation paths and the strong dispersion of THz waves inside the specimens under test [66], [67]. As such, THz-SI systems generally require the use of adequate signal-processing methods to extract useful features that may be submerged into complex THz signals [66]. These include but are not limited to traditional signal-processing methods such as wavelet transform, short-time Fourier transform, Hilbert-Yellow transform, and sparse representation, *etc*. [67]–[69], and advanced signal-processing methods such as traditional machine learning and deep learning algorithms [70]–[74]. Although traditional signal-processing methods enhance the accuracy of THz sensing and NDT results, these methods generally rely on manually designed extractors and the professional knowledge of the users, which could potentially jeopardize feature detection and/or extraction under complex THz sensing and NDT scenarios. Also, traditional THz signal processing methods generally fail to balance their efficiency and accuracy of the measurements particularly when processing large amounts of datasets [66], [73]. To meet the constantly increasing need for constantly evolving need for automatic feature detection, evaluation, and classification in industrial inspection settings, the use of machine learning algorithms (*e.g*. support vector machines, decision tree, logistic regression, *k*-nearest neighbor, gaussian naive Bayes, *etc*. has been widely explored in recent years to enhance the sensing and NDT capabilities of THz-SI systems and achieve autonomous processing of large amounts of THz datasets [70], [75]–[78]. Although many of these signal processing methods can significantly improve the accuracy of THz measurements, the ability of traditional machine learning algorithms to provide accurate evaluation results is highly dependent on the types of selected data features when processing raw THz datasets [66]. As special and important types of machine learning algorithms, deep learning algorithms adopt data-driven approaches for feature extraction and retain deep and specific features from chaos samples [79]. As a result, these types of algorithms can effectively overcome most of the limitations of traditional machine learning algorithms, and provide users with powerful feature extraction capabilities. Also, deep learning algorithms possess significantly high resistance to signal interferences coming from complex backgrounds and are therefore capable of providing accurate test results even from noisy signals [80], [81]. To date, numerous researchers have extensively conducted research on the use of current state-of-the-art deep learning algorithms to enhance the accuracy of THz sensing and NDT results and promote autonomous feature detection and/or extraction and accurate results have been reported in the literature [72], [80]–[82]. In fact, most THz signal processing

methods using deep learning algorithms have been recently reviewed in Refs. [73], [76] and interested readers are directed to these specific studies for more information.

C. Content and contribution of the study

The majority of the studies presented in the literature indicate that THz-SI is an effective and highly accurate sensing and NDT technique for the detection of molecules and substances as well as the physico-chemical analysis and characterization of materials and structural systems. A glance into the bibliography or the present study indicates that there are currently many industrial THz systems are currently being developed worldwide, and several field trials of high-performance THz sensors and systems are proceeding apace. The literature reveals that the great majority of the proposed THz sensing and NDT applications mainly focus on the use of THz-SI systems for the detection of substances and the physico-chemical evaluation of material and structural systems where aspects such as feature characterization, thickness evaluation, defects, and damage detection and characterization, biomolecules detection, *etc*. are mainly considered. To provide readers with an updated status quo of research sensing and NDT applications, this paper presents an updated review of the current state-of-the-art and state-of-the-practice pertinent to the sensing and NDT applications of THz-SI systems. To facilitate the understanding, the study first revisits the fundamental physics relating to THz-SI, discusses the issues with the experimental implementations, and outlines the need for signal processing techniques. The study also summarizes the suitability of THz-SI technology in different sensing and NDT applications, and various challenges in real-world THz sensing scenarios where a particular interest is directed toward the effects of spectral noise arising from the presence of barriers that obstruct the measurements or absorb THz waves, long times required for image acquisition that may alter the composition and/or integrity of the samples (*i.e*., especially bio-medical samples), limited portability of the current THz-SI systems, limited customizability of the current THz-SI systems, *etc*. Finally, the study analyzes the role of THz metamaterial systems in enhancing the resolution and sensitivity of THz systems, and their applications in the sensing of biomedical, agricultural, thin films, and food samples are discussed. To cover all the aforementioned aspects, this study is divided into 5 different sections. Section 1 presents the introduction of the study outlining the information such as the motivation and background, as well as the content and contribution of the study. Section 2 presents a brief description of the THz-SI system and an introduction to THz metamaterials. Section 3 presents a broader review of the application of THz-SI in the NDT of materials and structural systems focusing on some specific areas of application such as the evaluation of composite materials, characterization of thermal barrier coatings, oil and gas sensing, artwork identification and conservation, safety inspection, *etc*. Section 4 discusses the application of metamaterials in THz spectroscopic systems for the detection and recognition of materials, structural systems, and substances. Section 5 concludes the study.

II. TERAHERTZ SPECTROSCOPY SYSTEMS AND THEIR OPERATION

As indicated earlier, the development of femtosecond laser systems in the late 1980s has enabled the development of high-performance THz spectroscopic systems [3], [9]. To date, THz spectroscopic systems have been revolutionized and they are currently being commercialized as fully-functional NDT systems for the evaluation and characterization of the physico-chemical properties of materials, and structures, as well as the sensing and recognition of substances [21], [83], [84]. Additionally, the recent development and implementation of THz metamaterial systems have also enabled the enhancement of measurable THz signals by increasing the sensitivity, selectivity, and resolution of THz systems to the extent that they are now used in many areas of fundamental science and real-world applications. In this section of the paper, the operation and detailed functions of the different components of the THz-SI systems are explained and the role of the THz metamaterials is discussed.

A. Characteristics of THz waves

The THz region of the electromagnetic spectrum is situated between the μ-Waves and IR of the electromagnetic spectrum with frequencies ranging from 100 GHz to 10 THz or the wavelengths between 3 mm to 30 μm as illustrated in Fig. 1. With the development of the THz technology in the late 1980s, this region has been constantly referred to as the "THz Gap" due to the lack of effective THz wave generators and detectors working in the THz frequency range (*i.e*., the limited density and performance of THz product and devices such as the lack of powerful THz sources and sensitive THz detectors, *etc*.). As the technology continues to evolve, this proverbial gap is constantly being reduced thanks to the rapid development of more efficient THz sources, THz detectors, and various other types of THz devices and components capable of operating at ambient temperatures and/or open-air [14], [55]. To this end, several studies outlining the use and improvement of THz technology have been extensively studied and THz technology has now become a thriving interdisciplinary field of research and development at the frontiers of science and engineering. Additionally, THz waves possess some unique properties such as biosafety, good penetration, spectral fingerprint, *etc*. that make them very exceptionally attractive for testing, sensing, and recognition of materials, structures, and chemical substances [9]. Unlike X-rays, γ-rays, or μ-waves, THz waves are also nonionizing and are, therefore, safe for even some sensitive biological molecules (*e.g*. ribonucleic acid, deoxyribonucleic acid, *etc*.) during low photon energy wave-material interactions [30], [85], [86], and these properties are indeed crucial for biosensing applications.

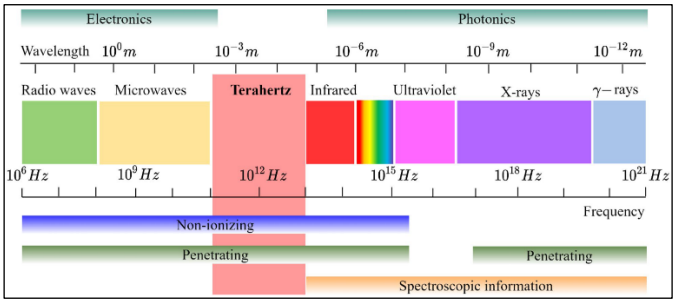

Fig. 1. Location of the THz frequency band in the electromagnetic spectrum (*i.e*., a narrow band between the microwaves and infrared regions) [13].

THz waves are also sensitive to transient rotational and vibrational modes or states of many molecules which cannot generally be detected by most of the conventional mid- and near-infrared spectroscopic systems [30]. They can also penetrate relatively thick nonconducting or dielectric matter in physico-chemical and biological systems to provide relevant sensing and NDT information [14]. Interestingly, THz spectroscopic systems using coherent detection methods are capable of measuring the transient electric field and not just its intensity, meaning that the samples' optical properties such as the absorption coefficient, transmission coefficient, refractive index, *etc*. can easily be calculated from the amplitude and phase measurements without using the Kramers-Kronig analysis or other complex/empirical models [25]. Although THz waves possess several properties that make the THz-SI systems attractive sensing and NDT tools, challenges such as weak responses of THz waves to natural materials, low spatial resolution caused by the diffraction limit, as well as the costs of THz devices still limit their adoption for common inspection and sensing applications [16]. To this end, some of the most promising solutions to achieve accurate and highly reliable THz sensing and NDT include but are not limited to the use of THz metamaterial systems, as well as the use of high-performance THz wave generators and detectors.

B. Generation and detection of THz waves

In general, THz spectroscopic systems use two different types of THz sources *viz*. continuous-wave (CW) and pulsed THz radiation. The efficient generation and detection of THz waves are key prerequisites for achieving high-performance THz spectroscopic systems. In most commercial THz spectroscopic systems, both CW and pulsed THz radiation are emitted and detected using optoelectronic systems (*e.g*. optical rectification devices) [87], [88], and electronic-based systems (*e.g*. PCA) [8]. In fact, PCA-based systems are considered the most predominant types of THz detectors and emitters for both CW and pulsed THz operations, owing to the extremely wide bandwidth available in their semiconductor electrodes at optical frequencies [1], [8], [17], [89]–[91]. The structure of a typical PCA features a metallic antenna operating at THz frequencies and a photo-absorbing semiconductor substrate (*e.g.* low temperature-grown gallium arsenide - LT-GaAs) on which a metal antenna is mounted (Fig. 2). To generate THz radiation pulses (*i.e*., pulsed THz waves), the region between the antenna arms is illuminated with a femtosecond optical pulse as illustrated in Fig. 2(a). Then an external direct current (DC) bias voltage is applied between the terminal of the aforementioned metal antenna electrodes to drift the photogenerated carriers in the active region of the PCA system and induce an ultrafast photocurrent (*i.e*., a narrow time-domain pulse having a full width at half maximum in the sub-picosecond range and corresponding to a broad THz frequency range with multiple frequency components) which drives the THz antenna into operation to generate pulsed THz waves. To detect these pulsed THz waves, femtosecond pulses are used to pump the active region of the PCA system to create photocarriers. Instead of applying an external bias field, the incident THz field induces an electric field $\vec{E}_{\mathrm{THz}}$ in the active region between the antenna arms of the PCA system. This field drifts the carriers to the antenna electrodes, and a photocurrent with a magnitude proportional to the strength of the incident THz field is induced as illustrated in Fig. 2(b) [17]. To generate or detect CW THz radiation, a dual-frequency optical beam with a THz frequency difference is heterodyned and used to pump the active region of the PCA rather than a femtosecond optical pulse (Figs. 2(c-d)) [1]. Using this configuration, frequency-tunable THz emitters or detectors are realized by changing the frequency difference of the dual-frequency optical beam [92]. In most cases, PCA systems used for cwTHz operation are usually referred to as photomixers because the generation and detection of the cwTHz waves are performed *via* the photomixing process [92], [93].

This article has been accepted for publication in IEEE Transactions on Instrumentation and Measurement. This is the author's version which has not been fully edited and content may change prior to final publication. Citation information: DOI 10.1109/TIM.2023.3318676

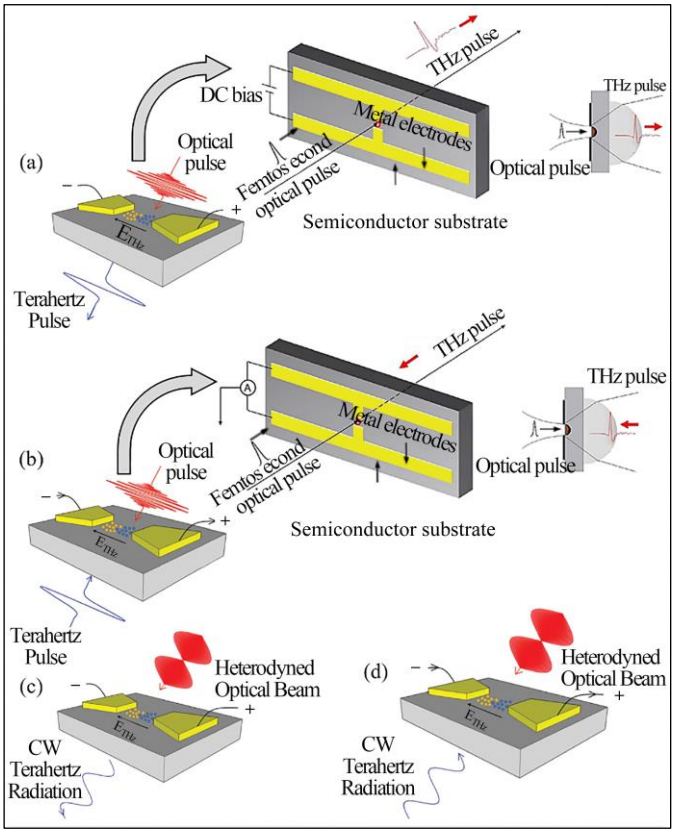

Fig. 2. The operation principle of typical THz PCA emitters and detectors: (a) configuration of the PCA used for the generation of pulsed THz radiation, (b) schematic diagram of the PCA used for the detection of pulsed THz waves, (c) schematic diagram of a PCA for the generation of CW THz radiation, and d) schematic diagram of a PCA for the detection of CW THz radiation [1], [17].

To achieve high quantum efficiency operation of PCA emitters and detectors, higher percentages of photogenerated carriers must reach the antenna's contact electrodes. However, photogenerated carriers do not travel long distances, and only carriers generated within a few hundred nanometers from the antenna's contact electrodes can adequately contribute to the ultrafast operation of the PCA system at THz frequencies [1]. As such, it is generally difficult to maintain the ultrafast operation of PCAs with a high quantum efficiency, and the tradeoff between these two factors will ultimately limit the THz emitters' radiated power and the THz detectors' sensitivity and/or responsivity levels. Recently, numerous researchers have devoted their efforts trying to improve the performance of these devices by leveraging current state-of-the-art technological advancements, of which nanotechnology and additive manufacturing seem to be the most important technologies leading the charge [1], [94], [95]. Typically, several types of nanostructure-enhanced THz PCA emitters and detectors such as plasmonic light concentrators, plasmonic contact electrodes, optical nanoantenna arrays, optical nanocavities, *etc*. have been experimentally proved to significantly improve the performance of THz PCA emitters and detectors [1], [96], [97]. Fig. 3 presents some of the aforementioned nanostructure-enhanced THz PCA emitters and detectors.

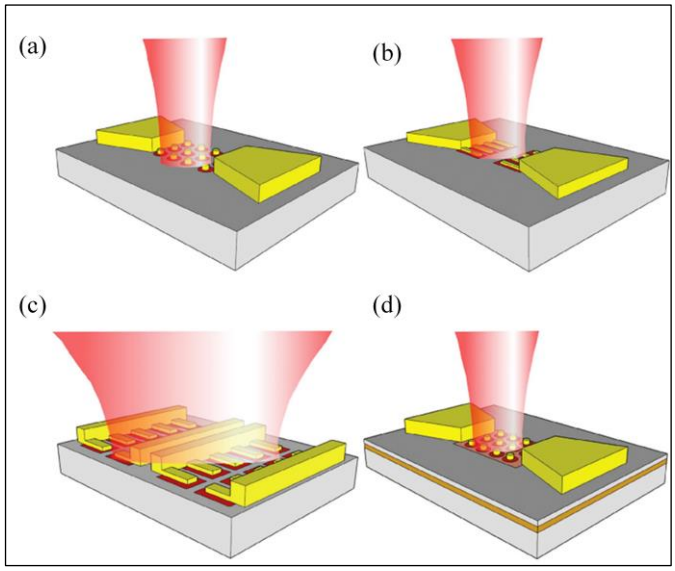

Fig. 3. Typical PCA systems based on (a) plasmonic light concentrators fabricated in the photoconductive active region to enhance the optical pump intensity, (b) plasmonic contact electrodes connected to the THz antenna to enhance the optical pump photon intensity close to the antenna, (c) nanoantenna arrays to enhance the optical field around the THz radiating elements, and (d) plasmonic nanocavity formed by a set of plasmonic nanostructures and an optical reflector to confine the optical pump photons in the active region [1].

As indicated earlier, the use of optoelectronic systems such as optical rectification devices, ultrafast spintronics, and PIN diode junctions is also a common procedure used by researchers and engineers to generate and detect THz waves. In the case of the optical rectification method, for example, a static electric field is induced while an optical field interacts with a nonlinear crystal to generate THz waves [98]. The detection of the electric field of the THz waves is performed through the electro-optical sampling method which relates to the use of the Pockels effect (*i.e*., an inverse process of the optical rectification method) where the magnitude of the THz electric field is evaluated by measuring changes in the polarization levels of the probe beam) [25], [99]. Also, ultrafast spintronics and PIN diode junctions are other options currently being explored for high-performance THz emitters and detectors [8], [100], [101]. Although these structures are also capable of providing ultrafast carrier dynamics in THz photoconductors and photomixers, they generally rely on the use of short-carrier-lifetime semiconductors [100], [102] whose manufacturing process requires the use of rare elements and non-standard processes with limited accessibility and implementation platforms [8]. To address these challenges, researchers are currently developing alternative techniques for realizing THz photoconductors and photomixers that do not rely on defect-introduced short-carrier-lifetime semiconductors, by using low-dimensional materials such as graphene, black phosphorus, *etc*. [103]–[109]. The materials are generally scalable and their continued development will undoubtedly lead to many breakthroughs

which could easily expand the availability, applications, and scalability of THz-SI systems.

In summary, both the generation and detection of THz radiation are generally performed using PCA systems for both CW and pulsed THz wave operations. These devices are generally fabricated using semiconductor materials such as LT-GaAs, which are generally difficult to manufacture and require specialized manufacturing facilities. Interestingly, recent advances in nanotechnology and additive manufacturing have recently fueled the development of high-performance PCA systems that are cost-effective and highly scalable. The key idea of these novel material development and manufacturing technologies is to take advantage of various nanostructure systems to improve the optical absorption levels of the THz waves in the active region of the PCA system and reduce the photocarrier transport path length to the THz antenna's electrodes to minimize the inherent tradeoff between ultrafast operation and high quantum efficiency [1]. The potential use of 2D nanomaterials such as graphene, black phosphorus, *etc*. is also another area being explored by researchers and engineers to manufacture high-performance PCA systems. These materials present unique electrical and optical properties not offered by many bulk semiconductor substrates (*e.g*., versatile fabrication process compatibility, broadband optical response, high charge carrier mobility, *etc.*), making them highly attractive for the fabrication of numerous optoelectronic devices operating in different electromagnetic frequency bands ranging from ultraviolet (UV) to THz [110]–[113]. The use of these advanced nanomaterials as the active region of PCA systems was successfully explored for the generation and detection of THz waves and encouraging results were reported [114]–[116]. In fact, the combination of these novel material developments and advanced manufacturing technologies would generate even better PCA systems. For example, experts believe that the use of PCA systems combining nanoplasmonic structures and optical nanocavities with 2D nanomaterials would further enhance the radiated power levels and detection sensitivities of PCA at THz frequencies. Unlike conventional semiconductors-based PCA systems, the realization of nanostructures-enhanced PCA systems usually involves several layers of challenges including but not limited to lower throughput, lower yield, and more expensive fabrication processes, *etc*. Typically, most nanostructures or cavity systems used to improve the performance of these novel PCA devices have their sizes in tens to hundreds of nanometer ranges, which are much smaller than the resolution of conventional photolithography techniques (*i.e.*, the manipulation of light to etch the desired features onto a surface). Interestingly, the use of higher-resolution nanofabrication techniques such as electron beam lithography, immersion UV lithography, nanoimprinting, soft lithography, extreme UV lithography, *etc.* can help address these challenges [117]–[119]. To this end, it is believed that the significant performance enhancement offered by various structures such as nanoantennas, nanomaterials, plasmonic nanostructures, and optical nanocavities combined with advanced nanomanufacturing techniques will pave the way for the next generation of low-cost, high-performance THz PCA emitters, and detectors with various unique spectroscopy and imaging applications.

C. Principle of operation of THz time-domain spectroscopy

As indicated earlier, the majority of THz sensing and NDT applications are performed using THz-TDS systems which may be configured differently to accommodate their application requirements [58]. Interestingly, all THz-TDS systems comprise the same main modular components *viz*. a femtosecond laser module, a THz emitter, a delay line between the pump and probe beams, as well as a time-gated THz detector and they operate based on the same principle [13], [21], [98]. Although THz measurements can be performed in transmission, reflection, or ATR modes, the literature suggests that most commercially available THz-TDS systems generally use the transmission and/or reflection modes as illustrated in Fig. 4(a) and Fig. 4(b), respectively [13], [120]. In these two geometries, the general principle of operation of THz-TDS systems is such that after the splitting of the femtosecond laser pulse into the probe and pump beams by a dedicated beam splitter, the pump beam excites the charge carriers in the PCA emitter to generate the THz radiation. The latter is then collected and guided by a set of off-axis parabolic mirrors/reflectors into the PCA detector, while the probe beam is directed toward the THz detector through the delay line. This component introduces a time delay Δt between the probe beam and pump beam, which is locked in time to the femtosecond laser pulse generating it by down-conversion [98]. The life of the probe beam pulses is generally much shorter (*i.e*., usually between 5 and 100 fs) than the THz transient. In this context, a variable time delay allows a smooth tracing of the electric field of the THz pulse, while equally sampling the electric field vector, and averaging within each optical gate pulse.

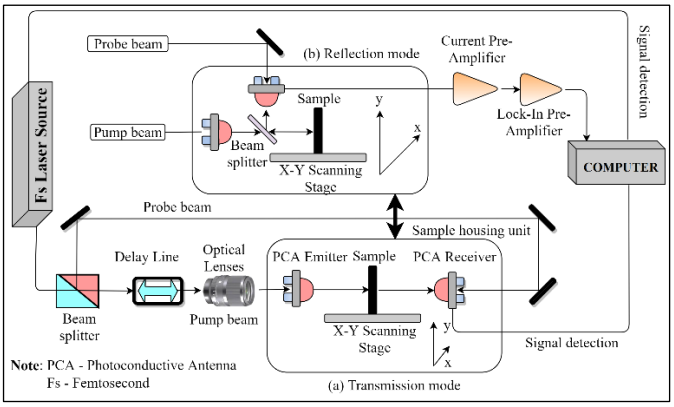

Fig. 4. The schematic diagram of the THz-SI system configured in (a) transmission, and (b) reflection geometries.

In general, two different techniques are used to implement the requisite variable time delay between the pump and probe beams of the THz-TDS system *viz*. the mechanical stages [121], [122], and optoelectronic techniques [123], [124]. The mechanical delay is the most widely used approach because it is generally cheap and simple to design as it only uses a set of mirrors/reflectors mounted on its mechanical translation stage as illustrated in Fig. 4 [13], [21]. These mirrors should have little dispersion and high broadband reflectivity levels to preserve the integrity/quality of the femtosecond laser pulse. In this way, the delay line can be adjusted by increasing or reducing the path length of the pump beam *vis-à-vis* the path

length of the probe beam to alter the phase between these two beams, and subsequently the sampling rate of the THz electric field. The magnitude of this THz electric field is usually between 10-100 V/cm and possesses an approximate time duration of a few picoseconds depending on the speed of the system's time-gated detection mechanism [90], [98]. Although mechanical time delay systems provide THz-TDS systems with excellent reproducibility, low jitter, and low noise levels, the type of time delay introduction mechanism also presents several disadvantages such as slow measurement speed, *etc*. In this context, the use of fast and highly sensitive detection methods of the THz electric field is generally required to achieve greater temporal resolution levels. However, achieving greater temporal resolution levels using direct electrical circuits and detectors is generally difficult because these types of systems usually have larger rise and fall times, and the current state-of-the-art systems can only achieve their best rise and fall times in picosecond or nanosecond time scales. As such, it is generally recommended to use optoelectronic delay methods which require two lasers with synchronized, yet slightly offset pulse repetition rates to generate and detect the time-dependent THz electric field to achieve a temporal resolution in the sub-picosecond range. Although the THz-TDS systems benefit from extremely fast data acquisition, this type of design also reduces their signal-to-noise ratio (SNR) because of shorter time intervals per data point (i.e., the SNR decreases with faster acquisition rates) and adequate singnal processing may always be required to obtain accurate results.

Consistent with the aforementioned, the measurement of the THz signals is referred to as the short read-out pulse process, and based on the description provided in the above paragraphs, this process consists of sampling an unknown electric field of the THz pulse with an intensity profile of a known femtosecond laser pulse. To extract useful information from the measured signals, the aforementioned short read-out pulse is convolved with the longer THz pulse. That is, THz detectors only measure the electric field THz pulse rather than its intensity, and the instantaneous THz signal $S(t_i)$ is obtained only when the optical read-out pulse arrives at the detector simultaneously with the THz pulse.

$$S(t_i) \propto I_{\text{Opt}}(t) E_{\text{THz}}(t_i) \quad \forall i = 1, 2, 3... \quad (1)$$

where $I_{\text{Opt}}(t_i)$ and $E_{\text{THz}}(t_i)$ denote the instantaneous values of the intensity profile of the laser pulse and the electrical field of the THz pulse at the time $t = t_i$, respectively. Although the signal $S(t_i)$ should be detected with a time resolution in the subpicosecond range, most of the currently existing THz detectors can hardly reach this resolution level, hence the convolution of the two pulses is measured instead. Also, since the optical pulse is significantly shorter than the THz pulse itself, it can be approximated to a delta function following the demonstrations presented in the following expressions.

$$S(t_i) \propto I_{\text{Opt}}(t) \circledast E_{\text{THz}}(t_i) \quad (2)$$

$$S(t_i) \propto I_{\text{Opt}}(t) \circledast E_{\text{THz}}(t_i) \approx \delta(t) \circledast E_{\text{THz}}(t_i) = E_{\text{THz}}(t_i) \quad (3)$$

The electric field of the THz pulse is measured as a function of time because the optical pulse is significantly shorter than the THz pulse and the detector is only sensitive when both pulses arrive simultaneously. Also, the fact that the THz detector is sensitive to the sign of the electrical field of the THz radiation allows the THz spectroscopic system to measure the generalized time-dependent amplitude of the THz signal $E(t)$ as opposed to other spectroscopic techniques such as the FTIR that measures the generalized intensity of the electromagnetic signal $E^2(t)$, and therefore, unable to capture the phase information. To obtain a proper measurement, precise micro-positioning of the sample is achieved using a computer-controlled positioning stage also known as the X-Y scanning stage. To minimize/eliminate the influence of moisture or water molecules in the air, the THz beam path is generally enclosed in a box filled with dry air, liquid N_2, or vacuumed using higher-level engineering designs [21], [58]. To obtain the spectral information of the THz pulse, the measured transient THz electric field is Fourier transformed as follows:

$$E(t) \xrightarrow{FT} E(\omega) = \frac{1}{\sqrt{2\pi}} \int_{-\infty}^{\infty} E(t) e^{j\omega t} dt, \ \forall \begin{cases} E(t) \in \mathbb{R} \\ E(\omega) \in \mathbb{C} \end{cases} \quad (4)$$

It follows that:

$$E(\omega) = A(\omega) e^{j\varphi(\omega)} \quad (5)$$

where $E(t)$ and $E(\omega)$ denote the time- and frequency-domain THz signals, respectively, while $A(\omega)$ and $\varphi(\omega)$ denote the amplitude and phase of the frequency-domain THz signal. The sign in the exponential function and the normalization factor $\left(1/\sqrt{2\pi}\right)$ are defined differently in different fields, algorithms, and applications/studies, so users should always ensure the above expression is used appropriately to guarantee accurate results. Also, the discrete Fourier transform (DFT) or fast Fourier transform (FFT) is used for discretized experimental data. Unlike the FTIR, THz spectroscopy uses a coherent detection scheme that eliminates environmental factors such as thermal background and incoherent signals which yields a much higher SNR. Also, the fact that only the THz electric field is measured directly rather than the intensity of the THz signal means that the data for both the phase and amplitude is measured directly as opposed to other techniques such as broadband infrared, visible spectroscopy, and single wavelength CW THz measurements. As such, the determination of the material's complex refractive index $n(\omega)$ does not require the use of Kramers-Kronig analysis [58], [125]. Additional parameters such as the material's dielectric constant and absorption coefficient are also derived directly from the amplitude of the measured THz signal by considering the refractive index.

In summary, the wide variety of applications of THz-TDS systems has resulted in quite a number of different configurations. However, all THz-TDS systems operate based on the same principle and feature the same main components albeit additional computational steps may be involved to accommodate the application requirements [58]. Their principle of operation relates to the use of single-cycle THz pulses with a complete source spectrum (broadband spectroscopic systems in nature), and the measured THz data (THz electric field) are acquired in the time domain, hence, the denomination time-domain spectroscopic systems. The spectral information (*i.e*., namely the amplitude and phase information at every frequency

in the usable bandwidth) is derived by applying the FFT to the measured time-domain data, and this information is used to evaluate properties such as the complex refractive index, conductivity, dielectric constant, *etc*. of the device under test critical for its structural characterization and/or evaluation. The system's time-domain sampling resolution can be significantly enhanced to reach the femtosecond range by adjusting the relative distance traveled by the two ultrafast laser pulses coming from the probe and pump beams.

D. Principle of operation of THz frequency-domain spectroscopy

Unlike THz-TDS systems which use pulsed THz waves generated by femtosecond laser systems, THz-FDS systems typically use a pair of cwTHz lasers with a THz frequency difference to generate and detect cwTHz waves through the photo-mixing process, which is frequency-tunable in the band of interest. Fig. 5 illustrates the general setup and principle of operation of common optoelectronic THz-FDS systems. In terms of their performance, THz-FDS systems can provide high-frequency resolution determined by the linewidth and stability of the cwTHz lasers [126]–[132], which is very hard to achieve in THz-TDS systems due to limitations in laser repetition rate and/or range of optical delay line [56]. Additionally, THz-FDS systems are compact and cost-effective because they do not require the use of expensive femtosecond laser modules used in THz-TDS systems. In fact, many THz-FDS systems operate in regular telecommunication wavelength ranges (≈1550 nm), which enables the design of systems with smaller footprints and more reliable operations at room temperature than those of regular THz-TDS systems [126]–[130]. Nevertheless, the source spectrum of a cwTHz system is relatively narrow, and only limited information can be obtained from THz-FDS systems [14]. In most cases, for example, only the intensity information of the THz signal is recorded from the THz-FDS systems' measurements [133], while THz-TDS can provide both the intensity and phase information due to their broadband emission capabilities of up to several THz.

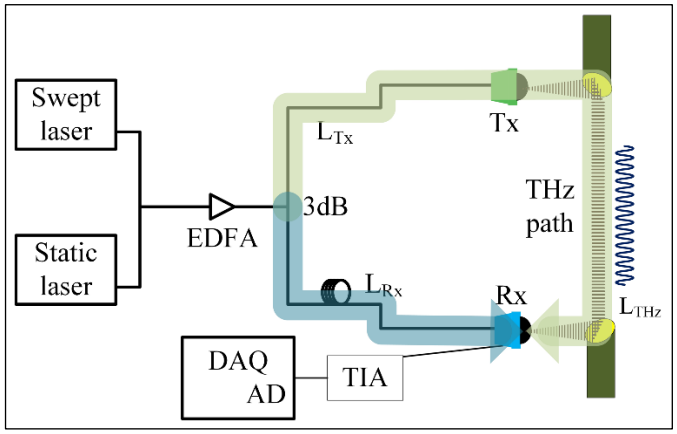

Fig. 5. Typical configuration of a common optoelectronic THz-FDS system. The system features a fixed-frequency (*i.e*., static cw-laser) and a swept laser (*i.e*., swept cw-laser), an erbium-doped fiber amplifier (EDFA), a PIN-photodiode emitter (T_x), and a photoconductive receiver (R_x) as well as a data acquisition unit (DAQ). The T_x and R_x paths are indicated with yellow- and green-shaded arrows, respectively. The different path lengths L_{Tx} and L_{Rx} indicate the path lengths relevant for the total delay time that arises from the path length asymmetry in the T_x and Rx arm of the THz-FDS system and they are a prerequisite for the operation of the THz-FDS system [134], [135].

The generation and detection of cwTHz for THz-FDS use several types of devices such as quantum cascade lasers, free-electron lasers, and short-carrier-lifetime PCAs [14], with the latter being the most commonly used type of cwTHz emitters and detectors for THz-FDS systems [126]–[132], [134]. Although short-carrier-lifetime PCAs provide THz-FDS systems with sub-picosecond photoconductive responses which enable their efficient operation at THz frequencies, their photoconductive gain, carrier mobility, and thermal conductivity levels easily degrade over time, and this greatly affects the overall performance of the host THz-FDS systems. Also, the fabrication of short-carrier-lifetime photoconductors usually requires the use of non-standard semiconductor growth processes and/or doping elements that are often difficult to access in many semiconductor manufacturing facilities [56]. Interestingly, some of these challenges can be addressed by using structures such as plasmonic and nanocavities PCAs to reduce their response times of CW THz PCA emitters and detectors even in the absence of short-carrier-lifetime photoconductors components [8], [96], [97], [110], [136]–[139]. In plasmonic PCAs, for example, the presence of plasmonic nanostructures significantly enhances the optical intensity close to the metal/semiconductor interfaces upon optical excitation [1], [137], [140]–[145], and by tight confining the optical pump photons near the plasmonic antenna, the transport path distance of most photogenerated carriers is substantially reduced, thereby enabling efficient operation of THz-FDS systems at THz frequencies. The detailed numerical electromagnetic analysis and fabrication process of the plasmonic PCA in Refs. [56], [138], and additional information on the operation and requirements of different CW THz PCA components is provided in Refs. [134], [135]. Interested readers

are directed to these specific studies for more information on these devices and operation requirements.

In summary, PCAs are considered the most common means of cwTHz generation and detection in THz-FDS systems. Although THz-FDS systems provide several advantages over THz-TDS systems, the source spectrum of common cwTHz emitters is relatively narrow and only limited information can be obtained from THz-FDS measurements [133]. Additionally, the fact that CW THz PCA systems are generally supported by relatively thick substrates with high relative permittivities usually reduces their effective radiated power levels because of the Fabry-Perot effect and unnecessary excitation of substrate surface waves [146]. To increase the effective radiated power of CW THz PCA systems and enhance the performance of THz-FDS systems, several methods such as the enhancement of the induced photocurrent inside the photoconductive semiconductor, improvement of the radiation characteristics of the antenna structure, provision of a stronger optical pump concentration, reduction of the plasmonic loss, use of a smaller barrier height for photocarriers at the metal/semiconductor interface, *etc*. are generally considered [146], [147]. Additionally, the integration of plasmonic nanostructures and gratings into the excitation gap of CW THz PCAs significantly increases their laser absorption capabilities and the resultant photocarrier generation levels which increase the THz photocurrent levels in the active area of CW THz PCAs thereby enabling ultrafast operation of the THz-FDS systems [148]–[150]. Also, the use of nanostructured electrodes in tip-to-tip or interdigitated configuration is proved to be an effective method of enhancing the electric field strength in the active area of CW THz PCAs, which equally increases the THz photocurrent levels in the active area of CW THz PCAs, and improves the performance of the host THz-FDS systems [151], [152]. Apart from improving the photocurrent generation capabilities of CW THz PCAs, the enhancement of their radiator element has also been the focus of several studies in recent years [153]–[159]. However, both the thermal damage threshold of the photoconductor and the space-charge screening effect generally limit the emitted power of CW THz PCAs below the optical pump power or the DC bias voltage [160], [161]. To overcome this limitation and achieve higher THz power, some studies suggested the use of CW THz PCA arrays instead of a single CW THz PCA system with a fixed optical pump power [162], [163]. The combination of high-mobility intrinsic photoconductors and largely reduced photocarrier transit times is also another possible solution currently being explored for the efficient operation of THz-FDS systems without relying on short-carrier-lifetime photoconductors.

D. Terahertz image acquisition process

In general, THz evaluation of materials and structures is not consistently achievable if the target samples do not exhibit any apparent features such as absorption, attenuation, or scattering peaks in the measured THz signals. Interestingly, the capability of THz systems to generate useful images and spectral information by exploiting other unique features of THz waves such as the rotational and vibrational transitions of molecules enables alternative material characterization possibilities using THz technology. To achieve that, the low power or electromagnetic energy interactions between THz waves and the matter is used to obtain the material's spectral information, which is then used to reconstruct the image establishing the structural composition of the sample [14], [15]. The process of obtaining this image is such that the THz waves pass through a sample placed at the focal plane, gets raster scanned through a set of motorize axis, or gets scanned in angular mode with a scanning mirror, and the system produces a high-contrast image that enables THz users to distinguish between the different features and/or composition of the sample (*i.e*., by analyzing the low-scattering regions of THz waves in the image).

As the diameter of the focused THz beam usually varies in size depending on the wavelength of the THz radiation in the bandwidth being used, a specific set of scanning intervals (*i.e*., usually expressed either in radians or mm and remains fixed during the entire experiment) will produce an image using on the over-sampling or under-sampling methodology depending on whether lower frequency components or higher frequency components are considered. And while the spectral interpretation of the image obtained using either one of these two methodologies remains relatively unaffected, THz users should consider this aspect when extracting features from the images. Also, there are currently several types of THz imaging methodologies to obtain THz images but most of them are based on the measurement of the amplitude, phase, or a combination of the two. All these methods provide different types of information about the composition and/or structural features of the target samples and THz users should select the best methods for their applications based on the type of information they are seeking. For example, the amplitude-based imaging method relates to the measurement of the THz signal's magnitude using numerical FFT over a particular frequency band to obtain the peak signal of the THz waveform at each pixel. The reconstruction of the THz image is performed by using the measured THz signal at each position pixel by pixel. The quality of the reconstructed image is improved by processing or denoising the measured THz signals one at a time and reconstructing the image from the processed or denoised THz signals. Image processing algorithms are generally based on the Fourier deconvolution algorithm particularly when wanting to extract the phase and amplitude information from the measured THz signals, but may also involve other image processing algorithms such as probabilistic pulse extraction, sparsity-based reflectometric methods, synthetic aperture imaging, compressive imaging, hybrid Fourier image reconstruction methods, *etc*. depending on the application requirements, accuracy levels, and type of the THz images to be processed. Individual THz signals at the different pixels also hold a wealth of information that can be extracted separately using the system's integrated digital signal processors to obtain the characteristics or features of the measured sample at each pixel.

E. Terahertz metamaterial sensing

A metamaterial is a type of artificially constructed electromagnetic material that can provide certain properties such as negative refractive index, super transparency, super absorption, negative permeability, *etc*., and structures such as cloaks, superlens, *etc*. that are not easily achievable in real-life

materials [30]. The concept of metamaterials started in 1968 when Veselago used the Maxwell equations for the theoretical prediction of the negative permittivity and permeability of materials [164]. In this study, the authors demonstrated that the materials' effective permittivity and permeability can be artificially regulated or tailored by designing artificial structures that are not naturally available. These findings were later reiterated by Pendry *et al*. [165] who further derived the mathematical expressions for both the negative permeability and effective permittivity thereby laying the theoretical foundation for research on metamaterials. To date, substantial progress has been made in the development of high-performance THz metamaterial systems and substrates, which provided scientists and engineers with new approaches for studying the functional, structural, and sensing characteristics of THz metamaterial devices as well as their correlations with the performance of THz sensors. In this context, numerous studies have demonstrated the relationship between dielectric properties and the structural design of certain metamaterial systems including left-handed materials [166], ground-plane cloaks [167], photonic crystals [168], and super magnetic materials [169], as illustrated in Fig. 6. The extraordinary properties of THz metamaterial systems have allowed the THz metamaterial sensing technology to go above and beyond the physical properties of naturally available materials with significantly high spatial confinement, and have even broken the diffraction limit of THz waves. In this context, the use of THz metamaterial devices decreases the requirement for sample preparation [170] and increases the sensitivity and selectivity of traditional THz-SI systems [171]. Also, the remarkable characteristics of THz metamaterial systems in regulating parameters such as the amplitude, phase, magnitude of the polarization impedance, *etc*. [30] have made the THz metamaterial sensing technology particularly attractive for the detection and evaluation of thin films and biomolecules.

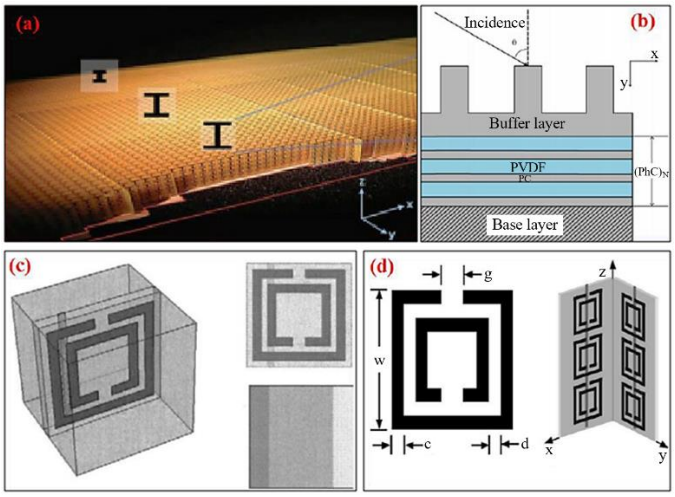

Fig. 6. Typical THz metamaterials structures: (a) a ground-plane cloak [167], (b) photonic crystals [168], (c) a split-ring resonator (SRR) [169], and (d) a left-handed metamaterial [172], [173]. There are certainly many other types of structures used for the design of THz metamaterial systems, some of which may be independent variations of these, hybrid, or completely different structures.

Although the design of ideal THz metamaterial devices requires a proper selection of functional materials to achieve a wide range of functionality or applications, a proper understanding of the underlying principles of the THz metamaterial mechanisms involved is also important especially when seeking to enhance the overall performance of the THz metamaterial devices [30]. Its operation is such that when the target sample is placed on the surface of the metamaterial system or sensor, its resonance frequency will change when certain parameters such as the concentration, permittivity, or thickness of the sample change [174], [175]. That is, the sensitivity of a THz metamaterial system can be significantly improved by simply improving the electromagnetic resonance between the THz sensing device and the target sample itself. And depending on the application, low- and high-frequency resonance may be considered. The magnitude of the low-frequency resonance of the metamaterial system is produced by the coupling between both the inductance L and capacitance C of the metamaterial as expressed in (6) [176], [177], while the high-frequency resonance denotes the plasmon resonance whose frequency is evaluated using the expression in (7) [171], [178].

$$\omega_0 \propto \frac{1}{2\pi\sqrt{LC}} = \frac{1}{2\pi\sqrt{L\left[\varepsilon_0 \int_0^{\upsilon} \varepsilon(\upsilon) E(\upsilon) d\upsilon\right]}} \tag{6}$$

$$\omega_d \propto \frac{1}{2d\sqrt{\varepsilon_{eff}}} \tag{7}$$

where d denotes the equivalent length or geometric configuration of the unit cell of the metamaterial structure, ε_0 the permittivity of vacuum, υ the space variable, and $\varepsilon(\upsilon)$ the permittivity of the material used for the design of the metamaterial structures. Additional parameters include the electric field $E(\upsilon)$ and the effective dielectric constant ε_{eff} of the environmental medium where the test is conducted. It can be seen that the magnitude of the aforementioned resonance frequency is mainly determined by two most important factors *viz*. the effective permittivity ε_{eff} of the testing or surrounding environment and the geometric parameters of the unit cell of the metamaterial system [30]. The value of the effective permittivity ε_{eff} of the testing or surrounding environment is obtained by using the following expression:

$$\varepsilon_{eff} = \varepsilon_{sub} + \lambda\varepsilon_{air} + (1-\lambda)\varepsilon_a \tag{8}$$

where the parameters ε_{sub} , ε_a , and ε_{air} denote the permittivities of the substrate, the analyte, and the air, respectively, while the parameter λ denotes the air volume ratio of the surrounding medium. In case both the metamaterial system and the material composition of the target substance change, the effective dielectric constant, and related resonance frequency will also change. In this context, it can be inferred that both the material composition of the metamaterial system and its structural topology determine the magnitude of the resonant frequency ω_0 of the corresponding metamaterial

device, and these factors should, therefore, be considered carefully to achieve the desired performance.

Apart from using the inductance-capacitance (LC) resonances of THz metamaterial systems, the plasmon resonance modes are also other parameters considered when exploiting the use of metamaterial devices in THz sensing and they include toroidal-dipolar and Fano resonances [179], [180]. To reduce the metal losses observed in plasmonic metamaterial systems with toroidal-dipolar resonance effect and obtain good performance metrics such as high-quality factor, it is generally beneficial to use high-refractive-index dielectric metamaterial such as $LiTaO_3$ micro-tubes [179]. On the other hand, the Fano resonance mode which was first observed in asymmetric split ring arrays widely exists in nearly all metamaterial systems and both the theoretical and experimental studies concurred that the associated resonance effect can be achieved by destructive interference steming from different excitation modes of the metamaterial systems [181]. Interestingly, the literature indicates that the characteristics of all the aforementioned types of resonances (*viz*. the L-C, Fano, and toroidal dipolar resonances) are closely related to the metamaterial structure, and this probably explains why the bigger part of previous research on THz metamaterial sensing has largely focused on the performance optimization of the metamaterial devices by designing high-performance metamaterial structures such those illustrated in Fig. 6 [182], [183]. In addition to structure optimization, resonators made from different metamaterial systems also exhibit different resonance characteristics [184]. Also, their resonance frequency is highly affected by the effective dielectric constant of the surrounding medium as highlighted in (6) and (7). To this end, the target substance, the measuring environment, and the metamaterial composition must be carefully controlled to ensure optimal sensing capabilities of the THz metamaterial device.

To evaluate the performance of THz metamaterial devices, several performance metrics which include the figure of merit (*FOM*), quality factor (*Q*), and sensitivity (*S*) of the THz metamaterial devices are generally used. The mathematical expression of the sensitivity ($S=\Delta\omega/\Delta n$) reflects the ratio between the change in the resonance frequency ($\Delta\omega$) and the refractive index (Δn) of the target substance. This mathematical expression suggests that the unit of the sensitivity *S* is THz/RIU where RIU denotes the refractive index unit. Similarly, the quality factor *Q* is also another performance measure for THz metamaterial devices. This parameter reflects the resonance characteristics of the THz metamaterial device and describes the the sharpness of resonance peak. Its mathematical expression ($Q=\omega$/FWHM) denotes the ratio between the center frequency of the resonance window and the full width at the FWHM frequency. This expression for the quality factor *Q* suggests that a combination of higher sensitivity and smaller FWHM will lead to a better sensing performance of the THz metamaterial device [171]. Although the expression for the quality factor *Q* suggests that this parameter is determined for a single frequency, it is important to indicate that THz metamaterial devices usually do operate in a single waveband, but rather in different wavebands. To obtain the full performance characteristics of THz metamaterial devices in different wavebands, the value of the figure of merit ($FOM=S\times Q$) is generally used as their performance indicator because it simultaneously characterizes their sensitivity and resolution levels.

In more general applications, there is a direct relationship between the sensitivity of the metamaterial device and the different physical characteristics of the target sample such as the thickness, concentration, and refractive index as well as the type of metamaterial system used to fabricate the sensor, the configuration of the different unit cells of the metamaterial system, *etc*. [30]. To indicate the performance of the current state-of-the-art THz metamaterial systems, **Table I** summarizes the detection sensitivities of the different THz metamaterial systems that have been achieved to this date and their corresponding configurations in Fig. 7. To put this into perspective, Zhong *et al*. [185] used a metasurface-enhanced THz-ART sensor (Fig. 7(a)) to detect the concentrations of sucrose in aqueous solutions from 0.03125 mol/L to 1 mol/L. Their results indicate that they manage to achieve a sensitivity level of about 0.03125 mol/L on their metasurface-enhanced THz-ATR sensor, which is 4 times higher than that of conventional THz-ATR sensors. Apart from obtaining accurate detection results, the above authors also posited that their metasurface-enhanced ATR sensor presented greater advantages in detecting analytes and measuring their concentrations in aqueous solution than metamaterial sensors featuring SRR structures or conventional THz-ATR systems. In another study [186], Yan *et al*. demonstrated the feasibility of an ultrasensitive tunable THz sensor presented in Fig. 7(b) and achieved a frequency sensitivity of about 4.2 THz/RIU with a figure of merit of about 12.5. Additional studies [168], [187], [188] have also proposed the use of thickness sensitivity and wavelength-shift sensitivity to achieve THz metamaterial systems with higher performances, and some of the most important designs are presented in Figs. 5(c-e).

TABLE I: Typical indices and detection sensitivity obtained for different device configurations of THz metamaterial systems.

No	THz metamaterials	Operating frequency	System's detection sensitivity	The figure of merit (RIU^{-1})	Refs.
1	Au	1.7 THz	0.47 THz/RIU	49	[185]
2	Graphene	2.3 THz	12.66 μm/RIU	12.66	[186]
3	InSB	0.43 THz	146600 nm/RIU	Not given	[187]
4	Au+Graphene	0.95 THz	0.2 ng/L	Not given	[188]

Note: The acronym RIU stands for "*refractive index unit*".

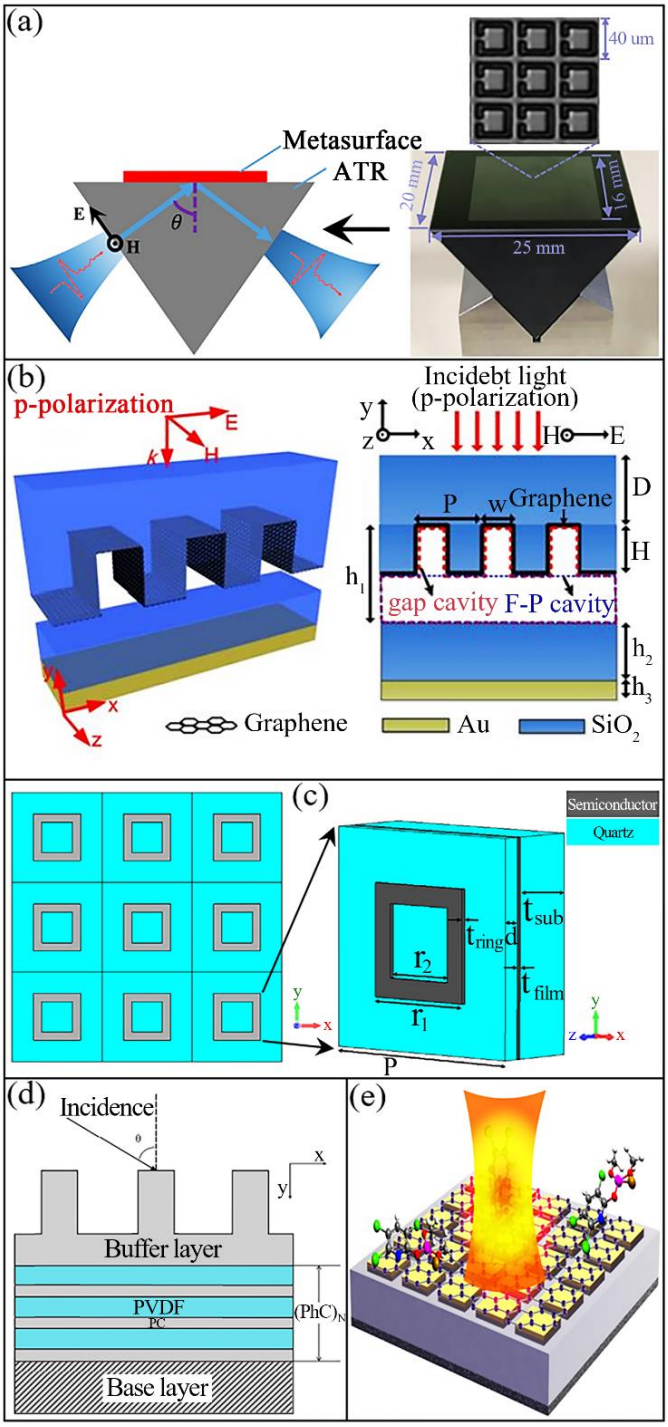

Fig. 7. Typical examples of THz metamaterial sensing device configurations with different indices: (a) the conceptual view (left) and geometrical view (right) of complementary split rings with ATR features [185], (b) the side and front views of a single layer graphene-based gratings integrated with a Fabry Perot cavity [186], (c) three-dimensional structure of a square-shaped perfect absorber [187], (d) a dielectric multilayer featuring nine alternating polyvinylidene fluoride (PVDF) and polycarbonates (PC) dielectric layers with thicknesses equal to 5 μm and 7 μm, respectively [168], and (e) a monolayer graphene-coated metamaterial system [188].

To this end, there are currently several types of metamaterial systems used for different applications, and they all operate differently. In fact, these systems can be grouped into different categories based on their operation mechanisms including metasurfaces, metallic mesh devices, metamaterial absorbers, graphene metamaterials, all-dielectric metamaterials, *etc*. with the first 3 being the most commonly used types of sensors in the THz frequency range [30], [54]. **Table II** provides a comparison between the performance characteristics of the current state-of-the-art THz metamaterials and other metamaterial sensors.

TABLE II: The performance comparison between the characteristics of the current state-of-the-art metamaterial sensors.

No	Methods	Sensitivity	Other advantages	Limitations
1	Fluorescent	Relatively high	Easy operation and rapid detection	Photobleaching
2	Calorimetric	Relatively low	Simple preparation and rapid detection	Interference from sample compositions
3	Surface plasmon resonance (SPR)	Relatively high	Label-free, and real-time detection capabilities	High cost of the instrument
4	THz metamaterials	Relatively high	Fruitful structure design and rapid detection	Complex fabrication process

III. APPLICATIONS OF TERAHERTZ SPECTROSCOPY AND IMAGING SYSTEMS

As indicated earlier, the THz-SI system enables measurements of both the phase and amplitude of THz pulses reflected from or transmitted through different types of samples. The changes in the phase and amplitude of the measured THz electric field are related to the changes in the absorption coefficient and subsequently the complex refractive index and dielectric constant of the target samples and are important for their spectroscopic and imaging characterization [17]. Recently, advanced material identification algorithms based on machine and deep learning algorithms as well as statistical pattern recognition principles have been introduced into THz applications to enable automatic samples detection and characterization and improve substance detection capabilities [189], [190]. Although the current majority of the THz spectroscopic measurements for the analysis and characterization of biological, physical, and chemical materials and/or substances have been primarily performed in single-point measurements or some cases in 2D images, developments in the three-dimensional (3D) reconstruction of the THz signals are also being implemented and 3D spectroscopic analysis is currently feasible [191]. To date, THz sensing appears to be reaching the threshold of the desirable plateau of productivity at the technology readiness or availability levels with many applications being developed, worldwide industrial installations of THz systems constantly expanding, and many field trials of THz sensors being conducted [15]. This section presents a comprehensive review of the state-of-the-art and state-of-the-practice review of the most conspicuous and

potentially promising applications of THz technology such as the NDT of composite materials, thermal barrier coatings, and the sensing of substances in biomedical and agriculture engineering settings.

A. Evaluation of polymers and polymer composites

In general, both polymers and polymer-based materials are known to be transparent or semi-transparent to THz waves, suggesting that they can easily be inspected by the THz-SI systems. The use of THz-SI for the evaluation and/or characterization of polymers and polymer-based materials is especially relevant for the determination of their macroscopic and morphological properties and the evaluation of their structural integrity [192]–[196]. Apart from simple inspection routines, polymers, and polymer-based composites are among the most important materials for the implementation of THz technology, the design of THz optical devices, as well as the fabrication of THz emitters and detectors [197], [198]. Although there are currently several types of polymers and polymer-based composites, the present section only covers pure nonconductive polymers and polymer foams, as well as polymer-based composites, and adhesives.

A. 1. Polymer materials and polymer components

The statistics indicate that one of the most important applications of THz-SI is in the field of NDT of polymers and polymer-based products, where nondestructive tests are conducted to produce high-quality polymer products and reduce material wastage during the manufacturing process [13]. The NDT of polymers and polymer-based products also help minimize their catastrophic failures during their in-service life [16], [32], [199]. This is particularly important because these types of materials have become a crucial part of our everyday lives, and the fact that they are generally nonconductive and transparent to THz waves makes them great candidates for THz-SI inspection and/or analysis [200]. In fact, recent studies [9], [16] argued that the advantages offered by the THz technology in applications such as inline inspection of plastic extrusion processes could make THz technology replace some of the most established NDT techniques for polymers and polymer-based components. Also, THz waves are considered biologically safe, suggesting that users could save costs entailed in devising and implementing extensive radiation protection processes, hiring safety officers and buying expensive personnel protective equipment (PPEs), and regular compliance documentation and/or inspection routines required for other NDT techniques such as X-ray, and neutron scanners [16]. In addition to being completely nondestructive, THz systems do not require any point of contact or contact medium with the sample systems [13], [16]. Also, THz waves can penetrate polymers, while IR waves are scattered, and ultrasonic waves are strongly damped. Compared to µ-Waves, THz waves provide greater spatial resolution and both the µm-thin polymer coatings and sub-millimeter-sized flaws can be easily and accurately detected/evaluated by THz systems.

To demonstrate the suitability of the THz-SI systems for the NDT of polymers and polymer-based components, the authors in Ref. [121] used the THz system to analyze the internal structures of a polyamide-based step wedge sample with two internal air pockets of approximately 5 mm and 10 mm in size (*i.e.*, the internal air pockets were invisible to the naked eye externally). Fig. 8 presents the THz image of the aforementioned polyamide-based step wedge with 3 distinctive regions of different thicknesses. The specimen was raster-scanned to evaluate its structural features over the area of 40 mm × 100 mm using a commercial THz-SI system. The thicknesses of the individual sections on the image of the specimen were 1 mm, 2 mm, and 4 mm (from left to right). The red and blue colors denote the regions of the specimen corresponding to the high and low transmission, respectively, which also correspond to the thinnest and thickest regions of the step wedge specimen. The authors posited that the air bubbles appear in "blue spots" because THz waves are acutely scattered at the interfaces between the air and polyamide, which significantly reduces their transmission capabilities.

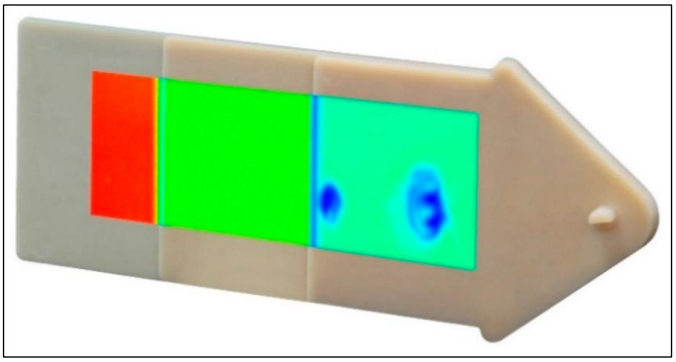

Fig. 8. A polyamide-based step wedge where the air pockets are visualized using the THz-SI system [121].

Apart from defects and damage detection and characterization, THz-SI systems can also reveal the deformations caused by thermal aging or mechanical stress in polymers and polymer-based components. These types of evaluations are generally conducted by observing changes in the static and dynamic properties of polymeric samples and correlating these changes to their thermal aging or mechanical stress levels [201]. For example, the thermal aging process of polymers and polymer-based materials can be evaluated by monitoring changes in the dielectric properties of the target samples using the THz spectroscopic systems [21], while their crystallization levels can be monitored by examining the glass transition temperatures (T_g, α and T_g, β) using temperature-variable THz spectroscopic systems [202]. Additional dynamic behaviors of polymer materials such as their polymerization [203], intermolecular vibrational modes [204], curing process [195], *etc*. can also be monitored using THz spectroscopic systems.

In summary, the application of THz-SI for the NDT of polymer materials has had a lot of success in recent years, thanks to the high optical penetration capabilities of THz waves. Although there are currently many established and cost-effective NDT techniques for polymer and polymer-based materials (*e.g*. ultrasonic sensors, X-ray scanners, and µ-wave transceivers, *etc*.), THz spectroscopic systems have now reached satisfactory levels of cost-effectiveness, modular size, performance, industrial ruggedness/robustness, measurement

speeds, and feature discrimination quality of most of the aforementioned gold standard NDT techniques for the evaluation and characterization of polymer materials [205], [206] and their applications are now expanding into the characterization of their structural abnormalities such as defects, damage and/or material degradation as well as the evaluation of their properties such as crystallization, isomerization, polymerization, intermolecular vibrational modes, and curing process among others.

A. 2. Polymer-based composite materials

In general, plastic components are not always made of pure polymers but of a blend of polymers or reinforced composite materials. In this context, the physico-mechanical characteristics of polymer materials are adapted to meet specific application requirements by incorporating reinforcements, additives, or filler materials during the compounding process to confer them with specific properties relevant to their design functions. These include, for example, dyeing with colorants, reinforcing with carbon and glass fibers or other filler materials, filling with chalk, *etc*. As such, it is important for the plastics industry to always examine certain parameters such as the additive content levels [207], homogeneity, adequate distribution or degree of dispersion of fillers [208], moisture content levels [209], the orientation of fiber in the polymeric matrix [210], the presence of internal fillers or particles [211], molecular chains composition [212], *etc*. In addition, several properties of composite materials such as their electromagnetic interference shielding and conductivity [213], [214], complex refractive index and absorption coefficient [215], dielectric properties [21], [84], *etc*. at THz frequency range can also be determined.

Taking advantage of the concept of permittivity difference, the content of carbon-based reinforcements has been extensively measured in different rubber compounds and composite materials using the THz spectroscopic systems [216], [217]. In 2013, Fischer *et al*. [215] investigated the morphology and material characteristics of wood-plastic composites using THz-SI and demonstrated moisture-contrast imaging. Figs. 9(a-b) presents both the photograph of a wood-plastic composite with a 0.6 volume percent of wood fibers and the corresponding THz image obtained by using the THz-TDS in transmission mode, which had been immersed in water for four days. To compromise between the strong THz absorption levels observed at higher frequencies and poor spatial resolution levels observed at lower frequencies, the THz image presented in Fig. 9(b) was obtained using a frequency between 0.4 and 0.5 THz. The presence of water clusters is revealed by the presence of areas of reduced THz transmission in the THz image due to the strong absorption of THz waves by the water molecules. Also, taking advantage of the fact that commonly used polymer additives (*i.e*., these are chemicals added to the base polymers during the manufacturing process of polymeric components to enhance their processability, extend their life span during their in-service stages, and/or achieve the desired chemical or physical properties of the final products, *etc*.) exhibit significantly higher dielectric permittivities than the polymer materials themselves, Wietzke *et al*. [207] used a fiber-coupled THz system to measure a variety of different additive-polymer combinations a process that is commonly referred to as the polymeric compounding process in the polymer industry. The extracted refractive indices provided reliable in-line information regarding the concentration of additives and other material combination used during the polymeric compounding processes (Fig. 9(c)), suggesting that THz-NDT could be an effective tool for quality control in polymeric compounding processes. As part of their conclusions, the above authors indicated that standard polymers are generally transparent at lower THz frequencies, but their THz properties are distinctively affected by the types of additives and their respective concentrations when processed into compounds.

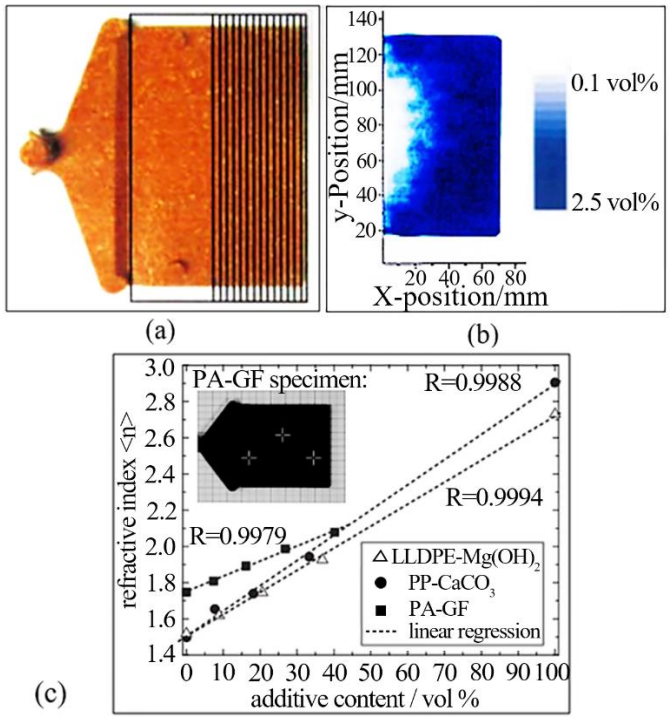

Fig. 9. (a) The photograph and (b) THz transmission image of a wood/polymer composite specimen after immersion into water for 4 days. The THz system was configured in transmission mode and the spatial distribution of the water clusters in the sample was easily detected and visualized in the THz transmission image due to significantly higher absorption levels of the water molecules compared to those of the polymeric matrix [215]. (c) The results of the refractive indices for different standard polymers (*i.e*., averaged in a dependable frequency range) with different additives (*viz*. calcium carbonate, glass-fiber, and magnesium hydroxide) at different volumetric contents. The obtained regression lines and their correlation coefficients *R* suggests there is a linear dependency of the refractive index on the additive contents/concentrations [207].

In fiber-reinforced composite materials, for example, the manufacturing defects such as the reduction in fiber content, erroneous orientation, resin shrinkage, fiber waviness, ply buckling, *etc*. significantly affect the mechanical performance of the resulting components. Given that fiber exhibits significantly higher dielectric and optical properties than the

polymeric matrix, these properties can be measured to determine the fiber concentration and orientation in fiber-reinforced composites. In [212], the authors demonstrated that the refractive index can be used to characterize the fiber content in simple GFRP composite plates, while the dielectric and optical properties to determine the ply stacking sequence of the angled GFRP composites in [192]. Earlier studies [210], [218] also showed that THz systems provide accurate information about the fiber orientation and subsequent preferential fraction patterns in GFRP composite material based on their THz birefringent properties. In addition to the aforementioned properties, the monitoring of parameters such as the degree of conversion is also crucial because it allows manufacturers to control the properties of the final product and helps them to avoid using unnecessarily extended curing cycle times during the composite manufacturing process. Additionally, the characterization of the degree of conversion of GFRP composite materials during the curing process has also been monitored using the THz spectroscopic system and demonstrated that its optical properties varied with the changes in the degree of conversion [219]. To this end, a dedicated THz system can be used for in-line monitoring of the curing process of GFRP composites [220], owing to the adequate sensitivity of THz waves to different material phase changes (*e.g.* oil composition, density changes, ply sequences, orientation, *etc*.).

In addition to the aforementioned, several studies have been conducted aiming to detect and characterize the damage and defects-related features including delamination, cracks, voids, burns, *etc*. in composite materials. For example, the lower THz absorption of air and the penetration capabilities of THz waves in composite materials make the THz spectroscopic system a suitable NDT tool for the detection of voids located at the surface and/or inner regions of polymer-based composite materials. To this end, Lu *et al*. [70] established a novel strategy to detect porosity levels in GFRP composites by analyzing the interaction mechanisms between THz waves and porous GFRP composites (*i.e*., with the porosity levels ranging from 0.29% to 4.01% and with the pore sizes estimated to 20-600 μm). They used the transmission and absorption spectra of GFRP plates and established a porosity prediction model featuring the combination of the supervised learning approach of the support vector regression and the ensemble methods and they were able to predict the porosity levels in a series of GFRP composite specimens with a coefficient of determination $R^2 = 0.976$ and a root mean square error or $RMSE = 0.174\%$. The results indicate that the combination of THz spectroscopy with algorithms such as the support vector regressor (SVR) provides a robust and accurate method for porosity analysis in GFRP composites. In an earlier study [221], Stoik *et al*. demonstrated the capabilities of the THz-SI system to detect, visualize and evaluate deeply-buried circular voids of 3 mm diameter, and other types of in-service damage such as delamination, mechanical damage, and heat damage in aircraft composite materials. Although frequency-dependent information was obtained, the above authors indicate that single-frequency amplitude or phase data proved to be enough for void detection and localization. In this study, the measurement of the electromagnetic properties of the specimens with localized heat damage did not show any noticeable change in the refractive index or absorption coefficient of the specimens with localized burn damage, but the material blistering was easily detected from the measured THz signals. Also, the depth of delamination damage was measured by evaluating the timing of the Fabry-Perot reflections occurring after the main THz pulses, while flaws such as cracks and bending stresses were visualized as distinct specimen features in the measured THz images.

Additionally, delamination damage and defects with variable sizes, shapes, and orientations have also been detected and accurately evaluated using THz-NDT in numerous studies by analyzing the transmission attenuation levels of THz waves similar to that used in the void detection setups [13], [222], or by analyzing THz signals reflected from different interfaces in the composite specimens [13], [193]. In a recent study [193], for example, the authors used the THz-SI system to visualize three delamination points with thicknesses of 96.52 μm, 109.03 μm, and 107.40 μm, respectively. Wang *et al***.** [223] used the THz-SI system to evaluate defects in polymeric composite samples and successfully determined their horizontal sizes and locations as well as their vertical depths and thicknesses in three dimensions. In a similar study [224], Wang *et al*. used the THz-SI to detect foreign objects in GFRP panels, and good results with approximately 2.26% mean measurement error were achieved, which further proved the practicality and efficacy of THz-SI in inspecting different types of polymer-based composite structures. Recently, Nsengiyumva *et al*. [13] used the THz-TDS system to detect, localize and evaluate hidden multi-delamination defects in multilayered GFRP composite samples. The measured THz signals were denoised using a de-noising algorithm based on stationary wavelet transform (SWT) and features such as the thickness and location of each delamination defect in the through-the-thickness direction were accurately calculated (Fig. 10). In an earlier study [194], the authors used this method to evaluate both intra- and inter-laminar types of damage in hybrid GFRP/CFRP composite laminates subject to low-velocity impact and successfully detected and visualized delamination damage generated by a low-velocity impact strike with corresponding thicknesses of and 150.08 μm, 139.61 μm, and 118.67 μm for 3 different points. Additional testing and analysis of polymer-based composites include the detection and analysis of burn damage and mechanical fatigue [221], water intrusion [225], impact damage [226], [227], *etc*.

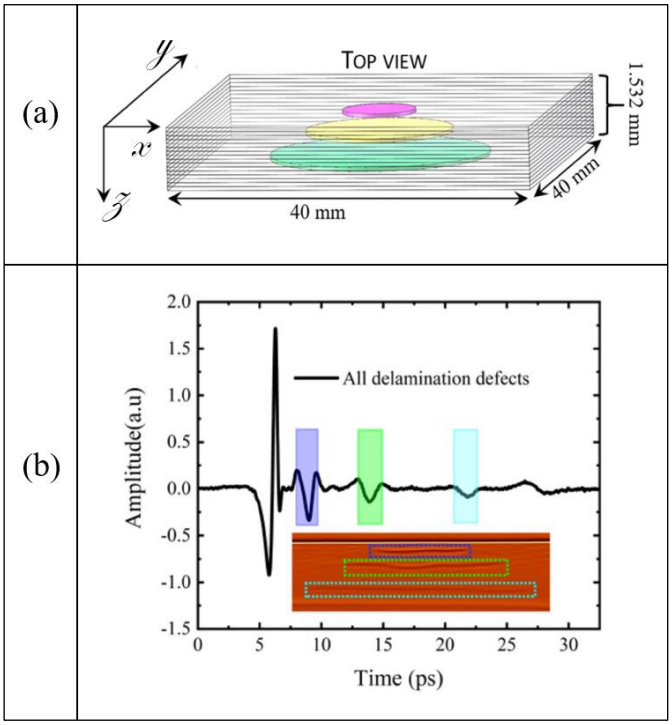

Fig. 10. (a) The schematic representation of the prepared multi-delaminated GFRP specimens, and (b) the corresponding THz time-domain signal showing all 3 levels of delamination defects. The highlighted areas in the signal indicate the peak-to-peak times at which THz waves pass through each delamination defect [13].

In summary, the above studies have proved that THz spectroscopy is a suitable technology for characterizing and analyzing both surface and underlying properties and features of nonconductive polymer-based composite materials (*e.g.* basalt, and aramid fifer-reinforced composites, *etc.*) beyond the point of proof of concept. Although the application in conductive composites such as carbon fiber-reinforced polymer-matrix (CFRP) composites is limited due to the conductivity of carbon fiber that hinders THz radiation's penetration at depth, several attempts have been made to use this technology to analyze their properties and structural integrity and some promising results have been reported although the proposed methods though still requires a lot of experiments for validation. Among these advancements include the use of polarization-resolved THz imaging which is constantly viewed as one of the most salient THz inspection methods that could help to efficiently evaluate the properties and structural integrity of CFRP composites despite their conductivity levels that quickly attenuate the in-depth propagation of THz waves [194], [227]. The use of polarization-resolved THz imaging and advanced signal processing methods can help to reveal surface and sub-surface damage as well as other finer structural features of CFRP composites by taking advantage of the sensitivity of polarized THz waves to the orientation of carbon-fiber in the composites. As such, THz spectroscopy has gradually become a popular technique for the NDT of composite materials.

A. 3. Polymer foams

In recent years, polymer foams have become one of the most important categories of polymers, albeit the growing call to limit the use of these types of materials worldwide and favor the use of eco-friendly, low-carbon emitters, and sustainable materials [228]. Polymer foams have outstanding mechanical and thermal properties at low weight and are used in industries such as aerospace, construction, automotive, and renewable energy to increase energy efficiency, maximize profits, and minimize costs. The key types of polymer foams available on the market include but are not limited to polyvinyl chloride (PVC), polyolefin, phenolic, polystyrene, melamine, and polyurethane foams [229], [230]. In the past, the techniques used to test polymer foams include but are not limited to optical or scanning electron microscopy, X-ray CT, neutron tomography, *etc*. Optical or scanning electron microscopy is used to examine the cell size distribution of the polymer foams but this approach can only examine the sample surface unless the specimen is cut into pieces to expose its internal structures [231]. Although X-ray CT [232] and neutron tomography [233] allow for 3D imaging of polymer foams, these techniques are costly and time-consuming, and their radiation is ionizing. The FTIR and Raman spectroscopic methods are the routinely used techniques for the chemical characterization and analysis of polymer foam materials [234], [235]. Also, polymer foams strongly damp ultrasound making it difficult for ultrasonic testing to reveal their inner structures and/or features. Although several techniques have been used for the testing of polymer foams, most of them are generally time-consuming, only possible offline, and partially destructive. Interestingly, polymer foams present numerous features such as very low absorption [236] and good transparency [237] to THz waves, making THz spectroscopy and imaging one of the most suitable NDT techniques for these types of materials.

THz spectroscopy and imaging systems are increasingly being used in the extrusion industry to evaluate the quality parameters and structural features of polymer foams such as the wall thickness [238], effective density, and cellular structure [239], *etc*. The cellular structure and the effective density of polymer foams can be evaluated using inline THz-NDT during the production process. It has been demonstrated that the cell size is related to both the transmission and scattering of THz waves through the foam [239], [240]. Werner *et al*. [239] demonstrated that the foam cells act as the scattering centers for THz waves, and measured their sizes by evaluating the THz loss coefficient that combines the contributions from scattering and absorption. Their study also revealed that there is a linear relationship between the material's effective THz refractive index and its bulk density, which is proportional to the thickness of the material in the THz beam path. Fig. 11(a) shows the example of the aforementioned relationship at 0.5 THz and it is observed that the refractive index increases linearly with the increasing effective density. THz imaging techniques can also be used to detect and evaluate defects and damage in polymer foams. Fig. 11(b) depicts the photograph and THz transmission image (inset) of a 100 mm × 60 mm × 20 mm specimen obtained from a PVC foam component used in rotor blade systems (*i.e*., the defects in the imaged section of the specimen are exposed as green and red dots). In another study, Abina *et*

al. [240] demonstrate that the THz-SI system has the potential to analyze the macroscopic structural features of foamed polymer materials including analysis of internal voids, inclusions, and bead distribution in a submillimetre-scale resolution range. As part of their methodology, the above authors extracted the THz spectroscopic/electromagnetic parameters of polymer foams from the measured THz data and were able to visualize the beads structures of their polymer foamed specimens by considering their structural features such as size, shape, distribution, air gaps, and interconnections. As part of their conclusions, Abina *et al*. indicated that they successfully imaged and characterized several types of defects in their foamed polymer structures including the impurities, and voids as well as the prebuilt inclusions such as thin metal wires and silica gel granules.

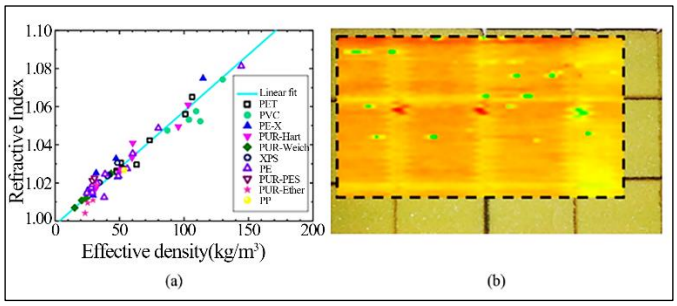

Fig. 11. Illustration of the (a) relationship between the effective density and the refractive index for various types of polymeric foams. The refractive indices reported in this graph are all calculated at 0.5 THz [208]. (b) The photograph and THz transmission image (60 mm × 100 mm) of a 20 mm-thick piece of PVC foam component as used in rotor blades of wind turbine systems [15].

In summary, the industrial use of polymer foams and their structural components is becoming gradually important due to their sustainable weight reduction and value-added properties such as their outstanding energy-absorbing capabilities that are related to the special deformation mechanisms of their cell structures (*i.e*., cell wall buckling and subsequent collapse of the cells). The testing of polymer foam materials has always been a time-consuming process, partially destructive, and only possible using *ex-situ* measurement platforms for many years. The advent of THz spectroscopic and imaging systems has changed the way NDT is administered for these types of materials, thanks to their good transparency to THz waves. Apart from the detection and analysis of the structural features of polymer foams, their decide quality parameters such as the cellular structure and the effective density can also be evaluated using THz spectroscopy and imaging systems by evaluating the transmission and scattering properties of THz waves such as their loss coefficient, absorption, and scattering levels.

A. 4. Adhesives

Adhesives or adhesive materials constitute another important category of polymers that are widely used in the construction and manufacturing industries to form adhesive joints and their NDT is still a challenge for most manufacturers of the materials and structural systems. In particular, adhesive layer connection technology is currently considered a crucial area of expertise that focuses on the optimization of the adhesive materials for uniform stress distribution, high connection efficiency, and good sealing of the host materials and structural systems as well as the development of adhesive materials with adequate lightweight and high fatigue resistance features [241]. This is particularly important because both the structural uniformity and thickness distribution of the adhesive layer are important structural features that determine the strength of the bondage/interlocking between the components. As such, these two features should be adequately examined not only to guarantee their design quality and functions but also to save the adhesive and reduce its possible contamination of the host structure [242]. To this end, one of the most critical steps in the evaluation of the glue/adhesive layer uniformity involves the determination of its exact thickness across its entire surface, and the THz-TDS appears to be one of the most promising NDT methods for the thickness evaluation and structural analysis of the adhesive layers in nonconductive materials and structural systems [195], [243]–[245]. It is also considered an alternative NDT method that could alleviate some of the most daunting limitations of conventional NDT methods such as limited inspection capabilities, time-consuming, costly, *etc*. as detailed in Ref. [240].

THz spectroscopic systems have been proven capable of accurately measuring the thicknesses of adhesive joints and evaluating their thickness distributions between polymeric components and structures [246]. As is the case with other polymeric materials, the monitoring of moisture content [245] and the curing behavior of adhesive materials can also be performed using THz-SI systems [195], [243]. In the case of a 2-component adhesive system, for example, the polymerization process starts when the two base monomers (*viz*. the hardener and the binder) are mixed, while the same process is initiated by the absorption of electromagnetic waves of appropriate wavelengths in a light-curing glue/adhesive system. Fig. 12 (a) depicts variations of pulsed THz waves transmitted through both a UV light-curing system (green) and a 2-component adhesive system (blue) during their curing process [15]. In this experiment, the Schottky diode is used to measure the intensity of pulsed THz waves [247], and the observed drops in the intensity of the transmission signals for both materials after 2 and 4 minutes mark the beginning of their polymerization reactions/processes. These reactions are exothermic for both samples, meaning that the adhesive starts by heating up, softening, and absorbing THz waves sharply. The curing process starts after the polymerization and it is marked by a significant increase in the adhesive's refractive index and a sharp decrease in the adhesive's absorption of THz waves. The essence of these variational trends relates to the fact that the increase in the adhesive system's refractive index is directly proportional to the increase in the concentration of the base polymers and their optical density, while the decrease in their absorption coefficient is explained by the decrease in the concentration of the base monomers in the adhesive system which have absorption than their polymeric forms [195]. Recently, Xing *et al*. [244] tested the polymethacrylimide (PMI) foam with an adhesive debonding structure using the THz-TDS system configured in reflection mode. The results indicate that the detection, clear identification, and quantification of the degree of adhesive debonding from about

0.1 mm to 3 mm are readily achieved with THz-NDT (Figs. 12(b-d)). In addition to the degree of adhesive debonding, the authors also managed to identify a 0.0665 mm thick paper inclusion that was used to simulate the delamination defect in the sample by both the time and frequency domain imaging.

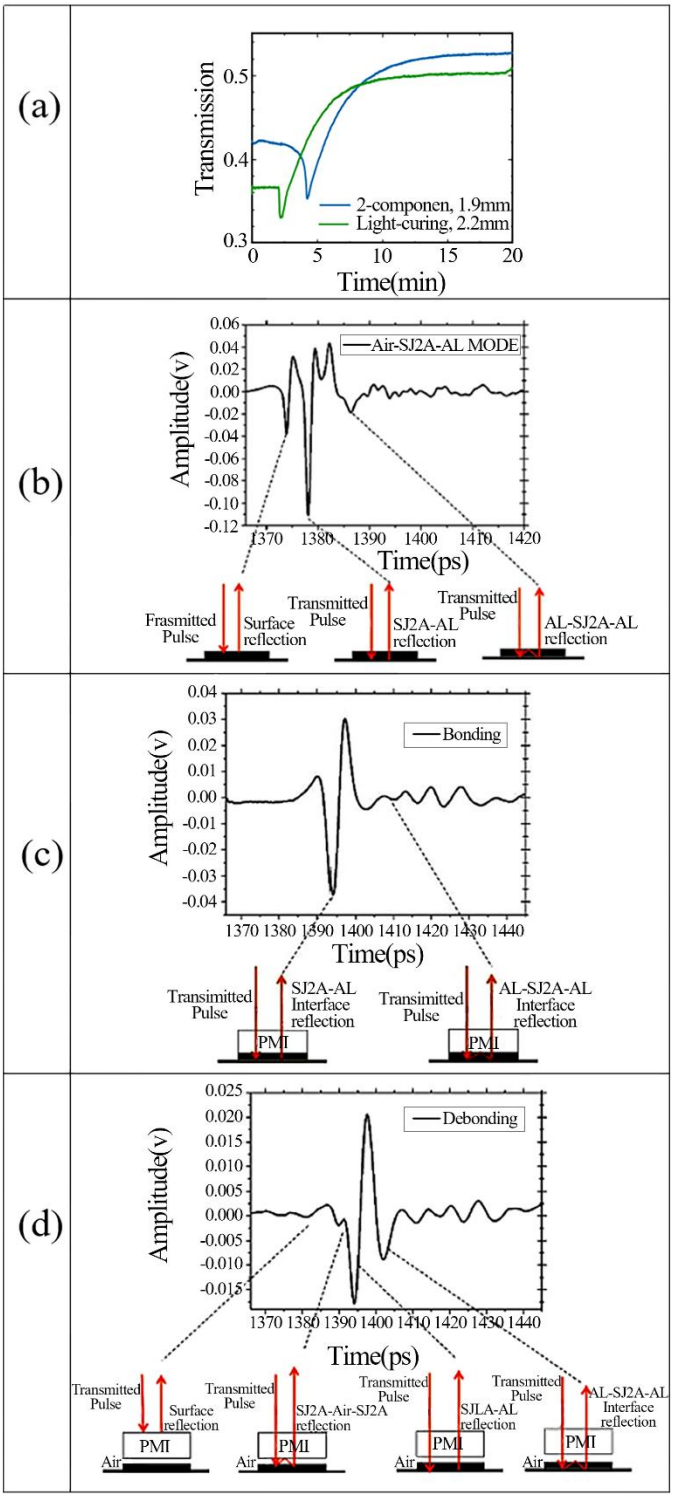

Fig. 12. Presentation of the (a) THz transmission signal obtained by measuring THz waves passing through a pure UV light-curing adhesive system and a 2-component adhesive system during their curing processes [15], (b) THz TOF signal reflected from a perfectly bonded thick nonporous honeycomb structure adhesive composed of a modified epoxy resin and its curing agent (SJ-2A) on an aluminum (Al) plate, (c) THz TOF signal reflected from a perfectly bonded polymethacrylimide bonding with the SJ-2A on an Al plate, and (d) THz TOF signal reflected from adhesive debonding damage [244]. The adhesive bonding damage exhibits multiple internal reflections of THz waves at the different interfaces which are translated into the presence of multiple peaks in the measured THz TOF signals.

In summary, THz technology has demonstrably proven to be an effective NDT technique for the detection and analysis of features in adhesive materials and it is currently considered an alternative to traditional NDT techniques for thickness measurement and quality evaluation of the adhesive layers and joints. However, special care should be taken when measuring the thicknesses of thin layers because the echo signal may partially or completely overlap due to the thin thickness of the sample, or the THz signal may be scattered and attenuated when penetrating thick adhesive layers or substrates, making the SNR of the echo signal decrease and these challenges significantly affect the accuracy and precision of the adhesive layer thickness measurement or estimation and its distribution within the entire adhesive joint [248]. To date, most of the optoelectrical properties of commonly used adhesive material systems (*e.g*. complex dielectric properties, complex refractive index, complex conductivity, *etc*.) have been evaluated in the THz frequency band [245]. This is particularly important because many of the structural features and characteristics of adhesive materials such as their thermal and fatigue aging, manufacturing defects, in-service flaws, *etc*. can be accurately detected and evaluated using the same property measurement principles, which makes THz-SI systems effective NDT tools for adhesive materials, as well as their structural joints, and systems.

B. Evaluation of paint and coatings

The evaluation of paints and coatings using THz-SI relates to the evaluation of thermal barrier coatings (TBCs), car paints, and marine coatings forming the high-tech protective surfaces in aircraft, automotive, or marine structures. Coatings are not only to protect the surfaces of the aforementioned structures operating in harsh environments such as excessive heat, frost, water, sand, stone chips, *etc*. but also to make them look visually attractive [14]. To guarantee the functional design and maintain the lifecycle of aircraft, automotive, and marine structures, the thickness and the structural integrity of their protective coatings must be adequately evaluated [15]. However, the complexity of the currently available coatings is constantly pushing the established NDT technologies to their limits, while some of them even fail to provide the measurements altogether. To this end, the magnetic gauges or eddy-current measurements fail to provide measurements when used to evaluate non-metallic substrates such as polymer, ceramic, and paints. Until recently, only destructive methods were considered the most effective techniques to evaluate protective coatings and paints of the aforementioned substrates, but their quality, debonding, and thickness can now be evaluated using the THz-SI systems [244], [249], and the

present section reviews the most important studies on this subject.

B. 1. Evaluation of thermal barrier coatings

The TBC is a type of protective layer applied onto the surface of metal substrates to provide them with high-temperature resistance capabilities [14], [250]. A TBC system consists of a ceramic topcoat and metallic bondcoat of about 200-600 μm and 100 μm thick, respectively but when the temperature of the TBC system exceeds 700 °C a thin thermally grown oxide layer (TGO) starts to grow between the topcoat and the metallic bondcoat of the system [251]. Although a relatively thin TGO can protect the alloy substrate and extend its lifecycle by reducing the oxidation rate, excessive growth of thin TGO will result in the development of thicker TGO which induces a phenomenon called topcoat thinning. The latter inflicts unbearable thermal oxidation stress on the TBC system and degrades its thermal performance. In severe cases where the thickness of TGO extends 10 μm, several types of damage such as delamination, cracks, spalling, *etc.* will start developing and propagate into the structures of the TBC system and the latter will eventually fail by peeling off from its substrate [252], [253]. Indeed, each of the aforementioned types of damage can be examined by using suitable NDT techniques and evaluating the different features of the THC system [254], and the topcoat thinning is one of the types of damage that can be detected and accurately evaluated by measuring the thickness of the topcoat layer using THz-SI systems [251], [254], [255]. In an actual evaluation of TBC systems using THz-SI, however, the research indicates that the roughness of the topcoat surface often affects the accuracy of features such as the refractive index, and thickness of the different layers, particularly because these types of measurements are conducted with the THz system configured in the reflection geometry [254]. To this end, a suitable surface roughness correction factor should be used taking into consideration the frequency characteristics of the THz-SI system to ensure accurate refractive index and thickness measurements.

THz spectroscopy has been extensively used to measure the thicknesses of topcoat and TGO layers of TBC systems and the obtained results always agreed strongly with those measured using microscope systems [255], [256]. As early as 2010, Chen *et al*. [257] conducted one of the pioneering works to measure the thickness of the TGO layer in a TBC system, where the authors used the THz-NDT to monitor the formation and growth process of the TGO. The sample was placed in a furnace and heated to 1100°C for 1350 hours to emulate the typical operational service temperature and time of the TBC system for commercial aircraft systems. The results revealed both the formation and progressive expansion of the TGO thickness from 0 to 5 mm and to 9 mm for 348 h and 1300 h thermal exposure times, respectively. In another study, Unnikrishnakurup *et al*. [258] evaluated the degradation levels of an atmospheric plasma-sprayed ceramic TBC system. In this application, the authors managed to accurately monitor the changes in the original thickness of the aforementioned TBC system by using both IRT-NDT and THz-NDT systems, and their results indicate that their THz-NDT system outperformed their IRT system further highlighting the higher efficacy of the THz-NDT as compared with other NDT systems. Recently, Waddie *et al*. [259] used a normal incidence THz reflectivity method to determine the birefringence properties and optical thickness of a ceramic TBC system and reported accurate results. Similarly, Ye *et al*. [260] explored the feasibility of THz-NDT for porosity evaluation in TBC samples and reported that porosity levels ranging from 9.09% to 21.68% were accurately measured in their TBC samples.

In summary, the application of THz-SI systems for the evaluation of ceramic TBC systems has been extensively demonstrated and numerous examples of the efficacy of these systems to effectively evaluate these structures have been presented in the literature. For example, all the demonstrations indicate that the results of the TGO or topcoat thickness measured by THz-TDS systems are always consistent with the results measured by well-established systems such as microscope systems [42,43]. Although the THz-SI system is capable of accurately measuring the thickness of TGO layers in TBC systems, the average thickness of these layers is generally a few micrometers thick (*e.g*. generally less than 10 mm during its initial formation stages), which is smaller than the pulse width of THz waves. Under these circumstances, the thickness of the TGO layers cannot be adequately resolved by THz waves and additional measures are required to achieve accurate results. To solve this problem, the development of high-resolution THz systems and the use of advanced signal processing methods should be envisioned to guarantee accurate thickness measurement. In fact, the efficacy of such developments has already been demonstrated in our previous studies where highly accurate results have been reported by leveraging the use of advanced signal processing methods with the THz systems in reflection mode [251], [261]. In addition to thickness measurements of the TGO layers, THz-SI systems are also capable of evaluating other defectious features of TBC systems such as porosity, delamination, cracks, and different types of microstructure properties, *etc*., which are all necessary to guarantee their structural design during the manufacturing process and structural integrity during their in-service stage.

B. 2. Evaluation of car paints and coatings

As indicated earlier, one of the most prominent industrial usages of THz-TDS systems is the measurement of individual layer thicknesses of multilayered structures such as coatings/paints of the car bodies or chassis. Car paints are extremely important not only because they provide the car with a beautiful and elegant look with distinct colors, but also because they provide adequate protection to the car chassis from UV radiation damage, corrosion damage, scratches, *etc*. Therefore, the car painting process is considered an important step of the entire automotive manufacturing process. In general, the thickness of paint films is one of the most critical and limiting quality parameters in the painting process for automotive or aeronautics. This is particularly because the thickness of individual paint layers is a critical factor in determining their capacity to appropriately satisfy their design requirements such as film functioning, appearance, cost, natural effect, *etc*. Each paint layer is deposited with the expectation that when film organization is finished at the end of the process, each painted layer will present a thickness inside the

predetermined target limits as defined by the designers. As such, safe testing of the dry film thickness is performed to guarantee the individual layers have the right optical and geometrical properties. Although there are currently many NDT techniques used to evaluate the thicknesses of car paints and coatings including but not limited to ultrasonic testing (UT), X-ray micro-computed tomography (X-μCT), and eddy current testing (ECT), *etc*. but many of these techniques generally do not meet the industrial standards for real-time quality control requirements and are, therefore, unsuited for deployment in industrial environments. Typically, both the sensors or measurement probes used by both UT-NDT and ECT-NDT systems require a point of contact with the target area of the painted car surface), while the safety of operating X-ray sources in industrial X-μCT systems should be carefully considered especially when using it for tests in real engineering applications.

Recently, several researchers have reported heartening results pertaining to the use of THz-SI systems for the evaluation of car paints and coatings [47], [262], [263] which prompted even further developments relating to the measurement and characterization of optically thin car paint layers using THz-SI systems. For example, the study conducted by Yasui *et al*. [264] presented a novel THz paint meter to monitor the thickness growth and drying process of thin film paint for paint films' quality control in car body painting processes. Their device used the TOF measurement of the echo signal of a THz pulse to effectively perform a 2D mapping of the thickness distribution in single- or multilayer paint films and collect adequate parameters such as monitoring the transformation of the paint layers from their wet to dry states during the drying process. In another study [265], Yasuda *et al*. presented a numerical parameter fitting algorithm similar to a multiple-regression analysis-based method to improve the sensitivity of their THz system and decrease the size of the minimum detectable thickness. Using this algorithm, the above authors managed to accurately evaluate the time delay between two temporally overlapped echo pulses in their THz thickness measurement data. In 2014, Su *et al*. [47] demonstrated the excellent performance of the THz pulsed imaging system in evaluating the thickness and structural quality of car paint films up to four layers deposited on both metallic and non-metallic substrates. The authors combined their numerical fitting algorithm with a highly accurate single-dimensional electromagnetic model simulating the propagation of THz waves in a multi-layered medium to obtain the parameters such as the extinction coefficient, and the refractive index of multilayered car paint film structures, as well as the thickness of their base paint layers as thin as 18 μm each. Fig. 13 presents the B-scan map and TOF signal of a single pixel as obtained from their thickness measurement results. It is observed that the reflection peaks stemming from the different interfaces between the individual thin film paint layers can be effectively identified using the THz-SI system. The accuracy of the thickness measured by using the THz pulsed imaging system for the aforementioned multilayered car paint specimen was also verified by other traditional methods commonly used to measure the thicknesses of car paints and coatings (*viz*. UT, ECT, and X-μCT), and the thickness measurement results obtained from these methods strongly agree with those obtained using the THz-SI system. These results indicate that THz pulsed imaging systems are ideal NDT tools for the evaluation of thickness values and structural characteristics of multilayered car paint and coating structures and the fact that the measured THz signals can effectively reveal the inner structures of the multilayered paint films similar to UT systems is another added advantage. However, it appears the THz-SI technique is more advantageous when compared with traditional NDT techniques such as UT, X-μCT, and ECT because of its noncontact nature and its capabilities of spatially obtaining the information related to the size of the thickness and its uniformity distribution from 2D THz images.

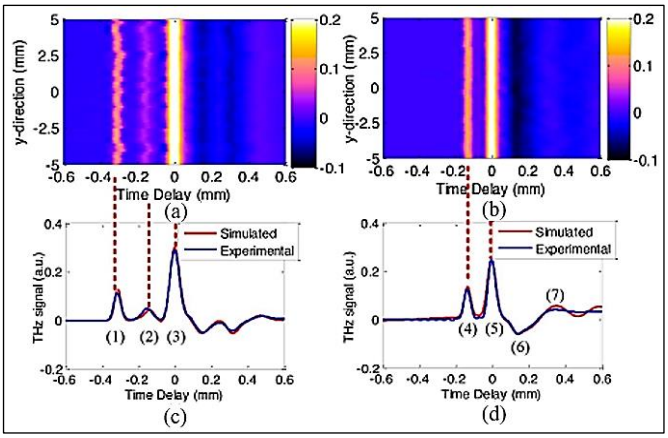

Fig. 13. THz imaging data obtained from a four-layer paint film deposited on a metal substrate as imaged by the THz-SI system configured in reflection mode: (a-b) the B-scan map of the four-layer paint film measured along the Y-direction. (c-d) the THz TOF signal of single points in the scanned area of the four-layer paint film. The labeled reflection peaks of the THz signal correspond to the following interfaces: The reflections (1), (4) denote the air-clearcoat interface, (2) the basecoat (solid black)-primer1 interface, (3), (7) the electro-coat-metal substrate interface, (5) the clearcoat-basecoat interface, and (6) the basecoat (metallic silver)-primer1 interface [47].

Considering all the aforementioned applications, it is clear that THz-SI systems are highly capable NDT tools for car paint thickness measurements and characterization but the method requires a high SNR and a large THz bandwidth to be able to resolve thin layers of car paints and coatings with thicknesses ranging from a few nanometers to a few micrometers at a relatively high speed [266]. In addition, THz-SI systems should be rendered robust, fast, portable, and cost-effective. Also, these systems should feature advanced and smart algorithms to accurately calculate the thickness of the individual layers in car paint films in real-time and be able to handle common industrial measurement conditions where factors such as excessive vibrations, electrical noise sources, high temperatures, *etc*. often influence the accuracy of the measurements. To put this into perspective, factors such as the vibration of the target automotive parts can significantly interfere with the THz signal and impede or obstruct the provision of accurate thickness measurement capabilities of the THz system. As a result, such vibrations should be measured separately using some of the current state-of-the-art optical NDT systems, and the THz pulse

traces can be adjusted or corrected in the THz data analysis software to increase the ruggedness and robustness of THz-SI systems and be able to reveal all the important features of the measured paint films. In addition to the aforementioned sources of environmental noise, it is also important to indicate that polar particles such as water molecules, moisture, or vapor in the air may jeopardize the accuracy of the measurements [5]. These substances often present multiple absorption lines in the THz frequency range which can eventually mask relevant thickness information of the target paint films leading to errors and confusion in the interpretation of the measured THz signals, thereby jeopardizing the accuracy of the measurements. Interestingly, the effect of these noise sources introducing undesired features into the measured signals can be effectively minimized numerically either by devising robust signal processing algorithms to remove them from the measured signals [267], [268], or by purging or expurgating the path of the THz pulse with dry air or other inert gases such as liquid N_2, or ideally by vacuuming the path of the THz pulse to ensure there is no contamination by polar molecules [5]. In most practices involving car paint thickness measurements, the THz reflection head is generally aligned to the car body with the help of a robot arm, and the optical sensors are used to measure the relevant distance and orientation of the robot arm to provide closed-loop positioning of the THz head relative to the car body and correct the vibration-related interferences that could potentially jeopardize the accuracy of the measurements.

In summary, THz-TDS systems offer unique advantages as the capability of measuring nondestructively and contactless as compared with the already-established NDT techniques. In addition to the TOF signals, the cross-section method is generally used as a "*golden standard*" method for thickness measurement practices even though this method also features lots of uncertainties because both the location of the measured cross-section area and the location of the microscopic investigation device significantly affect the representativeness of the measured results (*i.e*., these two parameters should always be taken into consideration). Also, for applications involving the measurements of relatively thick car paint films and coatings, the thickness of individual layers in the paints can be accurately evaluated by using the simple TOF approach and estimating their thicknesses by evaluating the position of consecutive reflections at their front and back interfaces as illustrated in Fig. 13. This generally applies to thick paint layers where the reflections from the different interfaces are distinctively separated in time such as marine paint systems. However, modern automotive and aircraft paint and coating systems can involve the application of thin paint and coating layers due to the continued desire to make lightweight and therefore fuel-saving structures, making it difficult to accurately identify the individual interface reflections associated with the individual layer thicknesses. To date, not all car body parts are manufactured using metal or alloys, but also plastics and composites, especially crash-relevant structures of the cars, which are expected to return to their original design/shape after minor car crashes. Plastic and composite structures also provide modern cars with increased noise and vibration absorption capabilities, as well as adequate intercompartmental insulation levels to absorb the kinetic energy of shocks in the case of head-on collisions or other types of road accidents. As these structures must ideally be indistinguishable from the rest of the car body for design and aesthetic purposes, they are coated with multilayer paint and coating structures to provide this function. Indeed, both the thickness and structural configuration of these paint and coating structures can also be evaluated by the THz-SI system as long as the refractive index contrast between these coatings and the substrate or the individual layers is sufficient, particularly because the performance of THz-SI does not entirely depend on the nature and composition of the metallic substrate. Several examples of such an application have been thoroughly demonstrated in the literature, particularly in the case of coating and paint evaluation on fiber-reinforced polymer-matrix composite materials such as GFRP or CFRP [269], [270], and this is of growing interest, especially because many types of structures in modern vehicles often contain these types of materials.

B. 3. Evaluation of marine coatings

In the marine industry, protective coatings play a key role in the protection of marine and/or offshore structures such as ship panels, bottoms, *etc*. Although the gradual wear and tear of these structures are almost inevitable in the long term, the deterioration, aging, or failure of their protective coatings may exacerbate their aging processes by paving the way to more serious damage (*e.g*. bubbling, rust, cracking, shedding, *etc*.). Importantly, these types of damage occur at a different pace depending on the chemical/material composition and physical characteristics (*e.g*. thickness, number of layers, *etc*.) of the coatings. As such, the chemical or material composition of the coatings should be optimized to guarantee their functional design [271]. Additionally, their thickness, which is considered the most important physical parameter of the coating's quality control and quality evaluation in the coating process by many standards, should be adequately controlled to optimize the structural performance and the life of the protective coatings altogether [249]. As such, quality control and evaluation of the thickness of the protective coatings in marine and offshore structures have always been one of the most important parameters carefully monitored during the coating process [272], and several techniques have been devised for this purpose in recent years [249], [272]. The use of THz waves for the evaluation of the thickness of marine coating has also attracted significant attention in recent years, thanks to the capabilities of THz waves to penetrate most of the materials used for protective paints and coatings on the surfaces of offshore or marine structures.

In general, THz pulse-echo reflection techniques are combined with adequate peak-finding methods to analyze the measured when measuring the thicknesses of the different types of marine coatings [251]. In the THz-TDS configured in reflection geometry, the THz echo pulses reflected from the specimen are routinely analyzed using the Fourier deconvolution algorithm to obtain the impulse response function [261], and the thickness of the marine coating can easily be evaluated from the THz TOF signals considering the reflections from the surface of the paint layer and the coating interface [261], [273]. The thickness of the marine coatings is also evaluated similarly to the evaluation of the car paint

thickness illustrated in Fig. 13. Although this method is generally effective in measuring the thickness of the coating layers using the THz-TDS systems [274], [275], the achievable depth resolution (*i.e*., the minimum detectable thickness) is generally constrained to half the coherent length of the THz pulse in the sample [265]. Typically, a bandwidth of approximately 1 THz presents a corresponding coherence length in free space of about 100 μm [276], suggesting that it is generally not possible to distinguish the reflections from any spaced interfaces (consecutive or otherwise) if the separation between them is considerably smaller than the coherence wavelength of the electromagnetic wave (*i.e*., Rayleigh criterion) [277]. To put this into perspective, the successive THz echo pulses reflected from the outmost surfaces and inner interfaces of optically thin paint layers or paint layers at their earliest painting stages cannot be utterly distinguished by the THz-SI system because of the apparent overlap between the individual reflections coming from the different surfaces and interfaces. In fact, even using the "peak-finding" would not necessarily work in this case because the method is generally used for discrete and precise thickness quantification of the different layers. In addition, the deconvolution process using traditional band-pass filters (*e.g*. Gaussian or double Gaussian filters, *etc.*) often results in unfavorable over-smoothing of the measured THz signals. As such, the loss of useful information from the measured THz signals and the subsequent inability of the THz technology to quantify thinner coating may be almost inevitable [278].

To overcome the aforementioned challenges, researchers proposed several other signal processing methods to extract the thickness and structural information from THz raw signals without using the deconvolution process [279]. These signal processing methods include the already mentioned parametric fitting method by Yasui *et al*. [264] which was used to construct the theoretical THz echo signals instead of using the numerical Fourier deconvolution method. Iwata *et al*. [280] also proposed a modified version of the partial-least-squares-1 algorithm and used it to process the THz data and were able to accurately predict the thickness of a single-layered paint film while Chady *et al*. [281] adopted the harmonic analysis method to process THz signals to accurately detect and evaluate different types of damage and defects in GFRP composite laminates which could also be used for the evaluation and characterization of marine coatings. In another study [279], Roth *et al*. extracted the power spectral density of the THz signal to evaluate the structural features of typical foams used for shuttle external tank thermal protection systems. It is important to indicate that while all these methods provide good results, their utilization should be evaluated on a case-by-case basis or improved to guarantee accurate THz-NDT results of the marine coatings. Typically, the methods proposed by Chady *et al*. [281] and Roth *et al*. [279] principally processed the measured THz time-domain signals using DFT which only represents the average spectral power distribution of the THz signal but fails to provide its time-frequency characteristics while the latter could provide relevant information for the detection and characterization of more localized features in the THz signal.

In addition to the thickness measurement, defects detection, localization, evaluation, and classification in marine coatings have also been at the top of the list of priorities. Tu *et al*. [271] used the THz-SI to evaluate the marine coatings by combining the finite-difference time-domain and stationary wavelet transform (SWT) algorithms to denoise the measured THz data. As part of their conclusion, Tu *et al*. were able to detect and evaluate the defects underneath marine protective coatings which further demonstrates the capabilities of the THz-SI for health monitoring of the marine protective coatings. Choi *et al*. [282] proposed a realistically employable method to analyze a series of THz data obtained from angled THz reflection measurements in an ambient atmosphere. Their methodology consisted of successive decomposition of the measured THz signals to identify the individual layers constituent of the marine coating specimens. Although their experimental system was largely designed to perform qualitative monitoring and evaluation of multilayered marine paint films, Choi *et al*. indicated that they managed to extract the spectrum of each paint layer that presented sufficient information for effective monitoring and evaluation of different types of features in the multilayered structures for real-world applications. Tu *et al*. [283] investigated various multilayer organic coating systems using the THz-TDS and explored the inspection capabilities of THz-NDT for marine coatings. They measured several types of defective coating samples and compared the signals measured from the pristine and damaged regions of the sample to explain the changes observed in the THz signals at the different levels of the sample. Also, the samples' structural analysis was conducted and three types of defects *viz*. paint bulge defects, corrosion defects, and paint detachment defects were clearly distinguished and quantitatively evaluated. In another study, In an earlier study [249], Tu *et al*. used the SWT combined with the neural network to enhance the THz-TDS system's capabilities of resolving thinner coating layers. Their method took advantage of the time-frequency localization characteristics of wavelet analysis and the prediction accuracy of the neural network-based algorithm to obtain a good approximation of the organic coating's thickness.

In summary, several traditional methods such as electrochemical-based techniques and some commercially available thickness measurement systems (*e.g*. eddy-current testing, ultrasonic testing, infrared thermography, *etc*.) are used to measure and evaluate the thickness and quality of protective paint coatings. However, each of the methods has its testing bottleneck, some of which lead to limitations in applications pertinent to the measurement and quality evaluation of protective coatings in marine and offshore structures. The TD-THz technology provides users with the capability to perform a noncontact inspection of organic coatings and holds greater NDT potentials not only for thickness measurement but also for the detection, localization, evaluation, and classification of the different types of damage and defects that may compromise the coatings' design performance and/or limit its life cycle. In recent years, several methods have been devised to improve the capabilities of the THz-TDS systems in these types of measurements, and THz-TDS systems can now resolve thin layers of coatings up to a few tens of micrometers.

C. Evaluation of pharmaceutical tablets and capsules

The pharmaceutical industry is a particularly favorable target area for THz-NDT applications, particularly in the R&D and NDT of pharmaceutical tablets and coatings during the manufacturing and quality control processes. This is generally because pharmaceutical tablet and capsule materials are either transparent or partially transparent to THz waves and often present specific THz spectral signatures that make their evaluation by common THz-SI systems easy, accurate, fast, and cost-effective. Also, high-precision quality monitoring of pharmaceutical tablets and their coatings is highly important because of their efficacy and safety requirements (*i.e*., accurate chemical composition, adequate microstructure, mechanical properties, *etc*.). In addition, pharmaceutical tablets are high-value products, suggesting that achieving reduced product wastage and increased product consistency brings significant cost benefits to the pharmaceutical industry [15]. Since its first emergence as an analytical method a little over 20 years ago, THz technology has been proven capable of revealing variations in molecular configurations (*e.g*. chirality, polymorphs, crystalline or amorphous states, cocrystals, *etc*.) [25], monitoring their porous microstructures [284], coatings thickness measurements [285], *etc*. Although the feasibility of the approach for all the aforementioned applications has been extensively demonstrated, our literature survey revealed that the application of THz sensing and NDT in the pharmaceutical industry has focused on two main areas *viz*. the monitoring of the porosity and pore size in pharmaceutical tablets as well as the inspection of coatings on the capsules and pharmaceutical tablets.

C. 1. Inspection of tablet and capsule coatings

As part of their structure, pharmaceutical tablets and capsules generally consist of an external soluble casing/shell containing a loose powder or fine particle blend that combines different active pharmaceutical ingredients (API) substances and excipients, while pharmaceutical tablets are made of compressed powder blends to which a coating is applied for protection and preservation purposes. To this end, the most important functions of capsule and tablet coatings are twofold *viz*. to preserve the tablet's functionality while in the storage facilities (*e.g*. mask their odor or protect them from disintegration) and to facilitate its timely dissolution (*e.g*. release control of the API in time and location of the gastrointestinal tract) when in contact with physiological fluids or water in the body [14], [26]. In most cases, the performance of pharmaceutical coatings is affected not only by their chemical composition but also by their physical characteristics including their structural uniformity, thickness, number of layers, structural composition, porous microstructure, defects, *etc*. Although the evaluation of such coatings is very challenging (especially when optically thin coatings are involved), the THz-SI systems have demonstrably proven capable of measuring the thickness of thin pharmaceutical coatings on film-coated tablets, soft gelatin capsules, controlled-release tablets, *etc*. [286], determining/predicting the dissolution profile in drug tablets [287], [288], evaluating the coating features of push-pull osmotic systems [289], *etc*. In all these testing and characterization processes, THz-SI systems do not require any sample preparation and the fact that they are capable of evaluating most of the solid pharmaceutical dosage forms with common/regular shapes and surfaces is another added advantage.

In general, the thickness of the coating on a pharmaceutical tablet is determined directly by evaluating the difference between the arrival times of THz pulses reflected from the outmost surface and inner structures of the target sample (Fig. 14(a)) [27]. In this context, the coating thicknesses can be mapped out by calculating the thickness from the time delay at each point on the outmost coating layer and other adjacent/sub-surface layers within the tablets. In 2011, May *et al*. [290] developed a highly accurate *in-situ* measurement method to determine the tablets' coating thicknesses during the film-coating process. The results of these real-time THz measurements indicated that THz-NDT is capable of providing a direct methodology to evaluate the thicknesses of pharmaceutical tablet coatings without using any chemometric calibration models (Fig. 14(d)). THz-NDT is also capable of detecting and characterizing tablets and capsules' features such as the coating defects alongside their site, depth, and size (Figs. 14(b-c)) [14], [27]. The success of THz-NDT in the evaluation of tablet and capsule coatings has been translated into the promotion of more studies that are constantly focusing on some specific industry-relevant aspects and/or features of THz technology including the development of fully automated commercial THz systems such as the use of a THz-based robotic arm to handle the tablets and position them at the THz focus with their surfaces perpendicular to the THz probe during the measurement [287], [291], [292], as well as the development of advanced signal processing algorithms to resolve thin tablet coating layers up to a few tens of micrometers [290], [293]. Although the aforementioned developments still require significant improvements for real-time industrial implementation, they are nonetheless considered the first steps toward moving the THz systems from laboratory developments to the manufacturing industry for applications such as process control, process analysis, and quality control by designing and implementing adequate film coating processes in the pharmaceutical industry.

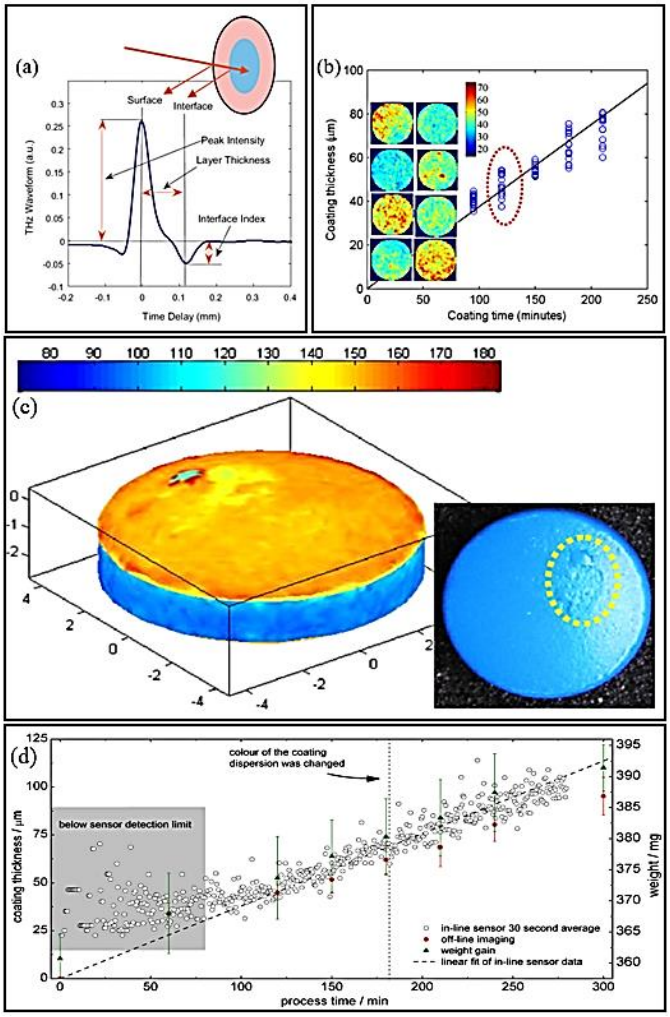

Fig. 14. (a) Typical THz waveform measured from a single-layer coated pharmaceutical tablet (this example illustrates the coating layer thickness evaluation methods based on the time delay between the reflections from the outmost surface and inner interface separating the tablet from its coating). (b) The average thickness of the coating layer on each tablet with respect to the coating time. The inset presents the coating thickness map measured from 8 different tablets in mm by using the same coating time of about 120 min and large coating thickness variations are observed [27]. (c) A 3D THz false-color image illustrating the distribution of the coating thickness on the surface and central band areas of the tablet [294]. (d) The coating thicknesses of the tablets measured using an in-line THz sensor at different time intervals of the coating process times (open circles) [290].

The possibility of evaluating the dissolution profile of the pharmaceutical tablets using THz-SI systems has also been demonstrated and accurate results have been reported. For example, Spencer *et al*. [287] confirmed that the tablet's mean dissolution time, which is the standard reference technique used to evaluate the dissolution performance of solid-dosage medicines in the pharmaceutical industry, can accurately be correlated with the average thickness of the coating on the pharmaceutical tablets. In another study [295], the authors also used THz signals to examine the possibility of estimating the dissolution performance of sustained-release tablets from the lab- and pilot-scale batches. Their results revealed that both the thickness of the coating and variations in its density distribution levels are good dissolution performance indicators for coated pharmaceutical tablets. A few years later, Malaterre *et al*. [289] used the THz time-domain signals to evaluate the coating features of push-pull osmotic systems and managed to identify some of the most important internal physical characteristics of common dosage forms affecting their drug release kinetics. Instead of using the coating's thickness and density variation data to predict the tablet's dissolution performance as previously indicated in Refs. [287], [289], [295], Ho *et al*. [288] developed another methodology that used the data obtained directly from the measured THz waveforms to accurately predict the tablets' dissolution performance and determine their *in-vitro* mean dissolution time. In another study, Ho *et al*. [296] examined the coatings conformity in a batch of round-biconvex tablets using the THz-SI system and found that the thickness of the coating of the tablets was significantly smaller around their central band domain. The measured data revealed that the central band domain of their biconvex tablet samples presented lower film coating density and higher surface roughness than their bottom and top domains. Interestingly, results from conventional dissolution performance tests concurred that the drug release process from the central band was quicker than that from the bottom and top surfaces, which further confirmed the accuracy of the feature distribution measured by the THz-SI system. In a similar study [297], Ho *et al*. also used the THz-SI system to examine the effects of features such as drug layer uniformity, the thickness of film coating, and the curing process on the *in-vitro* drug release of sustained-release coated pellets. The above authors used eight batches of pellets to conduct the study and their results indicate that drug release usually tends to slow down with the increasing thickness levels and curing time of the coatings on the tablets. The above authors also used the THz-SI system to examine the structural integrity of the coating on the aforementioned pellets and recorded significant differences in surface roughness, film coating thickness, and drug layer uniformity in all eight batches of pellets examined. Their THz-SI results were also corroborated by those measured by the SEM system.

Additionally, accurate identification and monitoring of weak spots/areas in the film coatings on pharmaceutical tablets are considered the two major pressing issues in the pharmaceutical industry, because they are vital to the success of product and process developments [15], [296]. Accurate mapping of these weak spots on pharmaceutical tablets provides scientists with useful information describing the subsequent dissolution performance. In fact, both the feasibility and utility of the approach have been extensively demonstrated in recent studies, and successful industrial applications have been presented and in some cases, THz-SI systems outperformed conventional NDT systems [293], [297]–[299]. Typical examples of such applications include the use of THz-SI as a PAT tool to evaluate numerous tablets features such as the thickness and structural integrity of the coatings applied to pharmaceutical tablets under different manufacturing conditions [298], [299], to observe the effect processing conditions of the tablets on their intra- and inter-coating thickness and porous microstructure variations [293], *etc*. The speedy and easy usage of THz-SI systems to

map up different features in the tablets' coatings may also be an attractive replacement for wet dissolution tests used to evaluate dissolution performance during the product development and process analysis stages of the tablets' manufacturing process. Although the use of THz-SI systems may be a plausible solution that could help scholars and scientists in the pharmaceutical industry to accurately evaluate the dissolution performance of common dosage forms, THz-SI tests may not always provide accurate results especially when delayed drug-release processes are involved. This is particularly because many scholars and scientists have acknowledged on numerous occasions that the delayed drug-release process or the dissolution performance of pharmaceutical tablets and capsules is rather a very complex process and depends on many other factors in addition to the coating thickness and density distribution. To this end, several studies [27], [300] have been conducted to determine the ability to control the dissolution process during the tablet scale-up process, predict the dissolution profile through tablet imaging, control process transfer of a multi-layer tablet, examine the effects of film coating process on structural integrity and performance of a finished drug product, define the compression process window, investigate failure in an enteric coated product, as well as to determine the moisture uptake and gel formation in modified release tablets, *etc*.

In summary, THz-SI has been proven to be an effective NDT tool for pharmaceutical tablet and capsule coatings evaluation. This system is capable of providing useful NDT information related to the tablets' transformation dynamics, identification, and quantification of polymorphs/hydrates in pharmaceutical tablets, off-line and online quantitative characterization of tablets and capsules' functional coatings, evaluation of the tablets' coating and dissolution profile, performing the spectroscopic imaging and chemical mapping of the pharmaceutical tablets, *etc*. In particular, factors such as the capability of using in-line THz sensors for real-time measurement of the tablets' coating thicknesses during the manufacturing/coating process combined with the many highly advantageous properties of THz waves (*e.g*. non-destructive, non-ionizing, and ability to image and probe at depth, *etc*.), make us foresee that THz-SI has the potential to become an industrial NDT measurement standard for pharmaceutical tablets evaluation practices. To live up to the enormous inherent potential of THz-SI systems, these systems have to be made fast, rugged, and affordable, which requires the development of new measurement approaches, the use of advanced signal processing algorithms, and the implementation of new system architectures that minimize the effect of environmental noise of the accuracy of the NDT measurements. In addition, it would be gratifying and extremely beneficial if the operational spectral range of the currently available THz devices could be extended from roughly 100 cm^{-1} to about 300 cm^{-1}. Extending the current range to the aforementioned range will undoubtedly allow the THz spectrum to cover both the intra- and inter-molecular vibration modes of pharmaceutical tablets in the upper THz frequency range, thereby providing the THz system with better spectral specificity and selectivity that could allow THz systems' users to achieve accurate discrimination and mapping of the physico-chemical properties of solid dosage forms. In fact, this broader spectral coverage would also allow THz users to be able to accurately evaluate and characterize optically thin tablet coating layers with higher spatial resolution. In addition to the aforementioned applications, quantum chemical modeling is also another area of interest that could provide drug manufacturers with additional knowledge on the vibration modes of pharmaceutical solids. However, the use of quantum chemical modeling processes to explore the chemical behavior of molecules and substances via quantum mechanics generally depends upon the development of adequate quantum chemistry theories and related computer algorithms, which requires the use of high-performance computational platforms to obtain accurate results. As such, the development of the aforementioned high-performance computational simulation platforms to simulate THz spectra would help scientists to fully understand and accurately interpret the vibration modes of pharmaceutical solids, which would ultimately improve our understanding of their performance, formulations, and operation processes.

C. 2. Evaluation of porosity and porous microstructures

In general, pharmaceutical tablets are manufactured by the uniaxial compaction of a mixture of granules or powders of drugs with excipients. The manufacturing process is such that the aforementioned mixture is compressed radially in a rigid die and undergoes several modification processes such as particle fracture, particle rearrangement, particle deformation, *etc*. before forming the tablet in a form of an agglomeration of inter-particulate bonds and pores. In this context, this unidirectional compaction of the API and excipients in rigid die results in the formation of tablets with anisotropic mechanical properties and the microstructure with their elongated pores being predominantly aligned in the plane of the tablet due to the nature and orientation of the compaction forces [284]. In most cases, however, factors such as the morphology, structure, and distribution of these pores in tablets greatly affect a range of their mechanical stability including their mechanical hardness, friability, tensile strength, *etc*. as well as their biopharmaceutical properties such as solubility, dissolution rate, bioavailability, *etc*. [301]. For example, the tablet's timely dissolution is considered an extremely important parameter in the drug delivery process because the kinetics of drug release must match a proper dosage form. Interestingly, this process is controlled by the liquid penetration rate into the pore networks as well as the chemical and mechanical properties of the tablet [27]. That means that certain pore properties such as their density, size, orientation, and connectivity in the tablet determine the rate at which water or physiological fluids enter the tablet to initiate the swelling of the excipient particles and break the bonds between particles. The tablet starts to disintegrate and deliver the excipients into the body when sufficient inter-particulate bonds are broken and the tablet has achieved its design disintegration threshold [284]. Therefore, accurate control and measurement of the porosity levels of pharmaceutical tablets could help scientists and drug manufacturers to understand the detailed liquid penetration kinetics into pharmaceutical tablets and the API delivery processes thereof. This information would indeed help in the design and manufacturing of high-performance tablets and pave the way toward achieving the long-coveted quality of the tablets with adequate biopharmaceutical properties.

The evaluation of porosity levels in pharmaceutical tablets is generally carried out using traditional methods such as mercury porosimetry, helium pycnometer, X-ray microcomputed tomography (X-μCT), *etc*. [25], [284]. However, most of these methods are partially destructive, harmful, and time-consuming, and cannot achieve real-time measurement of pores in pharmaceutical tablets. The pursuit of continuous and speedy NDT methods for this type of evaluation has recently ushered in the use of THz technology due to its ability to directly measure the porosity and porous microstructure of pharmaceutical tablets. This type of measurement is performed by measuring the effective refractive index of a flat-faced or biconvex tablet using the transmission geometry of the THz spectroscopic system (Fig. 15**)**. The refractive index denotes the measure propagation speed of electromagnetic radiation in the tablet with respect to the *in-vaccuo* speed of light and is termed "*effective*" because several components such as air, excipients, and API, *etc*. are mixed to form an effective medium with bulk properties that are governed by effective medium models [284]. The effective refractive index decreases almost linearly with the decreasing porosity levels because the effective interaction distance between THz waves and porous samples shortens (*i.e*., there is less substance in the path of the THz beam). Apart from the refractive index, the transmission loss can also be used to determine the porosity levels but its accuracy is always disputed because it is highly dependent on factors such as material absorption, pore geometry, pore distribution, *etc*., and combines the contributions from the absorption and scattering of the sample's materials that are difficult to evaluate.

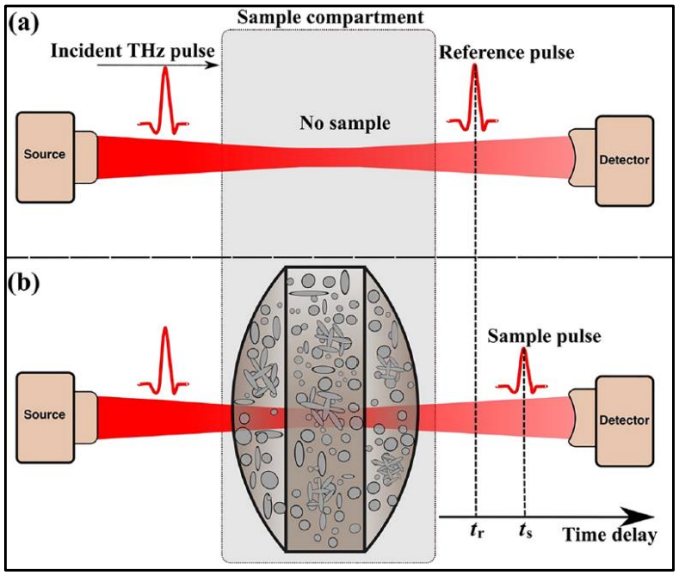

Fig. 15. Illustration of the measurement of the (a) reference and (b) sample transmission signals of pharmaceutical biconvex tablets. The time delays t_r and t_s denote the peak times of the THz pulse for the reference and sample measurements, respectively, and the difference between these two peak times denotes the TOF between these two signals [302].

The literature indicates that three approaches *viz*. traditional and anisotropic Bruggeman effective-medium approximation, as well as zero porosity approximation approaches, are generally used to detect the porosity levels in pharmaceutical tablets using THz data [284], [302]. The mathematical expressions used by these methods indicate that they are mainly based on exploiting the relationship between the porosity levels and the refractive index of the tablets in the THz frequency range, suggesting that these two parameters must be known *a priori* for these methods to be used [302]. It is important to indicate that the accurate prediction of the refractive index may be limited particularly for tablets containing a high concentration of API or composed of highly porous excipients such as functionalized calcium carbonate, and care must be taken when deciding the best prediction methods to use for such an application [302], [303]. In addition to these effective medium models, studies have also used other optical parameters in the time and frequency domains including the time delay, the effective absorption coefficient, the loss coefficient difference before and after soaking the tablet, the effective permittivity, *etc*. [301], [302], [304], [305]. The use of these parameters to predict the porosity levels of pharmaceutical tablets is particularly advantageous because they help THz users to overcome some of the limitations and difficulties associated with the aforementioned effective refractive index-based methods [284]. Apart from porosity measurement, the tablets' porous microstructure can be measured using the Wiener and Hashin-Shtrikman bounds [284], [302] which exploit the relationship between the tablet's porous microstructure and the effective dielectric constant.

In summary, THz technology has great development and application prospects for pores and porous microstructure evaluation in pharmaceutical tablets. The use of THz-SI systems for these types of applications mainly involves the quantitative analysis of the porosity levels of the tablets and the qualitative analysis of their porous microstructure. The former relates to the determination of the volume percent of the individual components in the tablets and the tablet's optical parameters such as the absorption coefficient, complex refractive index, complex permittivity, *etc*. using adequate effective medium theory models, while the latter analyzes the tablet's porous microstructure using the Hashin-Shtrikman or Wiener bounds which do not provide the specific value of the porosity levels but rather their bound limits. Although THz-SI systems have had some impressive success in the evaluation of porosity levels and porous microstructure properties of pharmaceutical tablets [284], [302], the proposed methods only use single-parameter models (*e.g*. effective refractive index, effective absorption coefficient, effective permittivity, *etc*.), meaning that the information provided by each of these models cannot be obtained simultaneously by using single-parameter models [306], [307]. To ensure accurate porosity measurement results, the development of robust porosity detection models based on multi-parameter fusion should be considered. Also, with researchers being unable to handle the strong absorption levels of THz waves by the API substances and excipients in pharmaceutical tablets [308], [309], current porosity measurement methods largely ignore the presence of these ingredients which might be affecting the accuracy of the reported results. To this end, reflection THz measurements should be considered not only to limit the effect of the strong absorption of the pharmaceutical substances, excipients, and thickness of the tablets but also because it is more practical and expedient to determine pore characteristics by reflection

measurements in industrial settings [80]. Also, reflection THz measurements are more amenable and easier to integrate into pharmaceutical processes than their transmission counterparts.

D. Analysis and characterization of electronic components

In the early days of their development, THz technologies were primarily developed to be used for the inspection of electronic devices in the electronics industry because certain electrical properties such as carrier mobility and concentration of semiconductor materials determine the magnitude of their dielectric properties in the THz frequency range [310]. THz technology is particularly effective in the spectroscopic analysis and imaging of electronic devices and circuits because of the opacity of these substrates and/or their packaging materials. To date, THz technologies are primarily used for the inspection of electronic circuits such as integrated circuits (ICs), printed circuit boards, transistor/gate scales [311], the inspection of solar cell materials such as Silicon wafers, perovskite materials [312], as well as the measurement and/or mapping of the conductivity of graphene-based thin films [313], *etc*. This section of the paper presents the main applications of THz sensing pertinent to the evaluation and/or characterization of electronic devices such as ICs, solar cell materials, and graphene.

D. 1. Inspection and characterization of integrated circuits

As opposed to X-rays or γ-rays, THz waves present long wavelengths, and the spatial resolution of most commercially available THz-SI systems is generally limited to about 1 mm, which is not sufficient for a detailed inspection of electronic circuits [15], [310]. To improve this spatial resolution and increase the details of detectable features, researchers and engineers are constantly working to develop state-of-the-art THz-SI systems capable of delivering up to the sub-wavelength resolution. These include the recent development and progressive refinement of the Laser Terahertz Emission Microscope (LTEM) and its hardware system capable of achieving a spatial resolution of a few μm when imaging photoconductive structures such as Auston-type switches, Schottky contacts, p/n junctions, *etc*. [314]–[318]. After the first demonstration of the LTEM imaging system in 2003 by Kiwa *et al*. with a spatial resolution exceeding that of the laser beam diameter of about 20 μm [319], its resolution was later enhanced to less than 3 μm in 2005 by Yamashita *et al.* [314]. In 2010, additional groundbreaking developments were also presented which primarily focused on the imaging of the transistors' p-n junctions using the LTEM devices, whereby defective transistor circuits were accurately differentiated from correctly functioning ones [316], [317]. These developments further enabled the imaging from the rear side of the transistor circuits, hence, the non-contact inspection of transistor circuits where interconnected structures prevented optical access from the front side was accurately performed [318]. To facilitate the characterization process of semiconductor devices, laser-activated THz waveforms produced from the p-n junctions in the LTEM configuration were also analyzed in detail where open defects in the multi-layered interconnections of large-scale ICs systems were accurately identified [315]. As the research continued, improvements were also being made and further developments were being achieved. It is in this spirit that Kim *et al*. [311] demonstrate the combination of a hemispherical solid immersion lens (SIL) and an LTEM with a transmission-type detection mode for the imaging of an IC device with a spatial resolution of 1.5 μm. Murakami *et al*. [320] demonstrated the capabilities of the LTEM systems were further extended and its spatial resolution was increased to 0.6 μm by incorporating near-field techniques, while a similar approach was applied to time-resolved transmission imaging [321], thereby effectively demonstrating the capabilities of the THz systems to measure the carrier mobilities and lifetimes with a spatial resolution of up to 60 μm.

In general, a spatial resolution of more than 100 nm is necessary to be able to efficiently image individual microelectronic components, and the use of the scattering near-field optical microscopy (SNOM) may be one of the solutions as it helps to achieve a resolution up to 40 nm [322]. In addition, the THz-SNOM imaging system can also be used to reveal individual transistors, identify the materials in a device, measure the carrier concentrations, *etc*. THz time-domain reflectometry (THz-TDR) is also a widely used NDT technique for detecting discontinuities and faults in electronic circuits and devices, a task that was traditionally reserved for some specific instruments such as the pulse generator or the oscilloscope [323]. Recently, Ahi *et al*. [324] developed a comprehensive set of techniques for authentication and quality control of packaged IC using the THz-SI system. Their tests revealed several features in the IC materials including the existence of features such as blacktopping layers, irregular thickness distributions in the hidden layers, unexpected materials in counterfeit components, contaminated and sanded components, as well as the dissimilarities between the morphologies of the inner structures of the counterfeit and authentic components of the ICs (Fig. 16). A simple approach of testing μ-wave monolithic and very large-scale ICs based on the electrical response generated at the circuit pins illuminated by THz waves was also reported in Ref. [325].

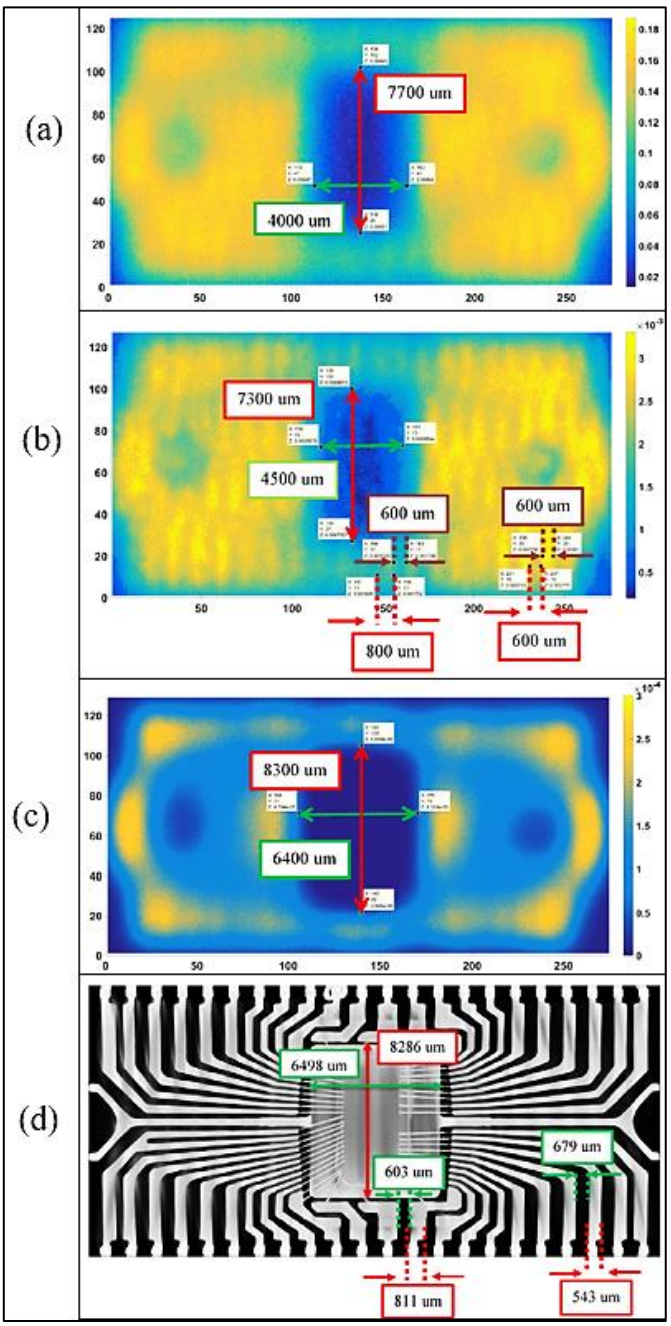

Fig. 16. (a) THz image of the authentic Intel flash-memory chip before improving the system's resolution, (b) the same THz image after improving the system's resolution in the z-plane of the die-frame, (c) the same THz image after improving the system's resolution on the z-plane of the lead-frame, and (d) the X-ray image obtained to confirm the THz imaging results. [1 pixel = 100 μm] [324].

In summary, many THz-NDT methods have been successfully devised to test and evaluate the structural integrity of ICs systems and other semiconductor devices in laboratory conditions but users still struggle with their limited cost-effectiveness for commercial applications or sometimes fail to achieve NDT results similar to those obtained by well-established NDT techniques during real-world testing in dynamic and harsh environments housing the current state-of-the-art IC manufacturing facilities. As such, THz-NDT is poised to be initially adopted by companies with significantly higher budgets and used in highly controlled or clean environments sheltering the current state-of-the-art semiconductor fabrication facilities where hostile environmental factors such as humidity, temperature, and dust, among other THz measurement-limiting factors, can be appropriately controlled and monitored. Considering their measurement capabilities, THz waves provide extreme flexibility in terms of polarizations and spectral precision across many frequencies which is highly beneficial for the implementation of highly accurate and automated product classification devices. Also, the femtosecond data collection speed and wide bandwidth of the commonly available THz systems create vast amounts of data to sort out, process, and classify, and this amount of data is expected to increase with the constant development of big data and cloud computing-related technologies. To keep up with the constantly growing cloud computing and big data-related technologies and enable real-time inspection of seemingly uncharacteristic IC features by the human operator, several technologies and algorithms are constantly being developed. Typically, artificial intelligence systems based on deep learning algorithms are being developed and combined with THz-NDT systems to enable high-quality data collection and advanced data analysis and classification capabilities with unparalleled performances. As the complexity of ICs systems and semiconductor devices continues to expand with infinitesimally smaller and high-performance features, advanced NDT methods will be needed across all scales to keep up with the demand for quality assurance and verification requirements of these systems and devices. Interestingly, preliminary investigations indicate that THz waves can allow for high-throughput passive monitoring of sensitive semiconductor devices and ICs systems during fabrication that might be damaged by induced electric currents if other NDT techniques were to be used, suggesting that THz-NDT would be the best technique to perform common NDT measurements in the semiconductor industry. Also, considering the unique and characteristic signature properties of different types of material systems in the THz frequency range, the evaluation of fingerprint characteristics of most ICs and semiconductor devices can be accurately achieved using THz spectroscopic systems. This type of information would also be used by scientists to identify materials that would uniquely enable the development of adequate THz-NDT methods to detect anomalous or counterfeit IC devices. Interestingly, the use of hybridized or data fusion-based methods featuring information from multiple NDT systems is a regime where THz-SI data can be combined with existing NDT methods to offer support to the increasingly complex failure analysis and verification requirements of ICs systems and semiconductors devices in the semiconductor industry from the nano- to macro-scale features and components. For THz-NDT systems to become self-reliant semiconductor production monitoring systems in laboratory or industrial settings, it will require a confident level of statistical process control for THz signal generation, detection, and/or processing. Taken together, all these developments and obstacles indicate that the implementation of applied and highly accurate industrial THz systems for the inspection of ICs and semiconductor devices will likely come from the combination

of research into cutting-edge THz hardware systems and the development of high-performance signal processing or signal reconstruction algorithms, as well as the widespread usage of the machine and deep learning algorithms (*i.e*., the introduction of artificial intelligence algorithms into the NDT of ICs).

D. 2. Inspection and characterization of solar cells

Application of THz-NDT for the inspection and evaluation of solar cells generally serves two separate purposes *viz*. the evaluation of solar cells' performance characteristics and the evaluation of their structural integrity. The determination of solar cells' performance characteristics involves the determination of their electrical properties to predict their performance and efficiency and the parameters measured for this purpose are typically the charge carrier density, complex conductivity, carrier mobility, as well as charge transportation and/or recombination dynamics and their dependence on solar-type illumination levels to ensure efficient interfacial transfer of photogenerated holes and electrons, *etc*. [20], [326]. These measurements are particularly important because they allow solar cell manufacturers to estimate the diffusion levels of holes and electrons, which directly affects their performances, and can all be measured by THz spectroscopic systems. Taking the carrier mobility and lifetime features as an example, the determination of these two parameters is particularly important because they are generally considered the ideal metrics for quality evaluation in semiconductor materials and provide critical guidelines for the development of more efficient semiconductor devices. In particular, adequate levels of charge carrier mobilities are generally desirable for the semiconductor materials used in photovoltaic solar cells (*i.e*., to enable efficient charge injection and extraction), and microelectronic systems (*i.e*., to increase the achievable data processing speed) [326]. In addition, the investigation into the THz field transmission through photoexcited thin films and the subsequent comparison of the different conductivity models such as the Drude conductivity, plasmon models, hopping transport, *etc*. against the THz transmission data, the type of photoconductivity of the solar cell can be easily established [41]. Indeed, this type of analysis is particularly important because it provides valuable information relevant to the determination of charge transport properties in novel semiconductor materials, which is particularly crucial for the enhancement of their optoelectronic properties during the optimization process. Apart from using simple THz spectroscopic systems, additional performance properties of solar cells such as the semiconductor's transient photoconductivity can be evaluated by combining both the photo-excitation process with the optical pump-THz-probe technique [327]. Information related to the transient photoconductivity is particularly important because it reveals other features describing the dynamics, resistivity, and mobility of photo-excited charge carriers of the solar cells directly without the need for metal contacts. The obtained information of the resistivity of the solar cell can also be used to estimate the density of the background dopant when paired with charge-carrier mobility measurements, thereby providing a complete characterization of the target solar cell structures.

In addition to the characterization of the performance properties of solar cell materials, THz technology is also used for the inspection and structural evaluation of solar cell materials and devices, which involves the detection of a variety of flaws, defects, and irregularities in solar cell structures that occurred during the manufacturing process [312]. In most practices, however, the spatial resolution of the THz system has always been reported to be a limiting factor, particularly when used for the inspection of solar cell materials. However, the introduction of the LTEM technique was welcomed by the NDT community as a significant development toward the implementation of adequate THz systems to image and analyze solar cell devices and materials. In fact, some researchers even went further and provided a detailed performance comparison of the LTEM technique with some conventional solar cell testing techniques such as electroluminescence (EL), photoluminescence (PL), and laser beam-induced current (LBIC) based methods, and similar results were recorded in the literature [328]. As part of their conclusions, the authors in [328] also pointed out that the LTEM technique is an exceptionally useful NDT technique that could be complementary to well-established NDT techniques owing to its numerous advantages such as higher spatial resolution, and its capability to accurately map out the distribution of some important solar cells' features such as electric fields, grain boundaries, surface defects, *etc*. The LTEM technique can also observe the dynamic movements of photoexcited carriers in the purlieu of the depletion layer adjacent to the surface of the solar cells, which influences a number of their properties such as their fill factor (FF) and the open-circuit voltage (V_{oc}). Interesting development surrounding the use of THz-SI systems for the evaluation of solar cells also include the use of the THz spectroscopic system in reflection mode to evaluate the structural integrity of commercial solar cells, where several types of manufacturing flaws such as defects in the soldering and tab wires, doping variations, cracks, irregular thickness distribution, *etc*. were successfully detected and evaluated [328], [329]. Additional applications featuring tip-based near-field transmission measurements were also used to map out the carrier mobility and chemical doping levels of solar cell devices were reported where significant improvement of the THz system's spatial resolution up to 10 μm in the measured images [330]. In addition to providing maps of the carrier mobility and density as well as the chemical doping levels of solar cells, THz-SI systems can also produce maps of sheet resistances capable of revealing different types of flaws in individual devices constituents of the solar cell systems, which further highlights the invaluable capabilities of THz-NDT systems for the analysis and evaluations of solar cells.

D. 3. Graphene

The history of graphene material (a type of honeycomb carbon crystal made of a one-atom-thick planar sheet) synthesis using the chemical vapor deposition method with a metallic catalyst can be traced back to the late 1960s [331]. Several years later, the first successful synthesis of monolayer graphene using mechanical exfoliation from bulk graphite was also reported in Ref. [332]. The synthesis of monolayer graphene opened up new opportunities and lead to the experimental verification of

the unique quantum electromagnetic properties in the early 2000s [333], [334]. To date, several other methods have been devised for graphene manufacturing, and the most representative methods include liquid-phase exfoliation, mechanical exfoliation, redox reaction, chemical vapor deposition, *etc*. [335]. The aforementioned advanced manufacturing achievements enabled the development of large-area graphene films and promoted the initiation of advanced research that helped to identify useful graphene properties (*i.e*., some exceptional electronic, optical, and mechanical properties) [336]. To date, the aforementioned advances have enabled the development of some state-of-the-art graphene-based electronic and/or optical devices used in a wide range of applications including but not limited to the development of THz photonic devices, optoelectronic devices, electrodes for electrochemical energy storage systems, flexible sensors, protective coating layers, advanced composite materials, biomedical devices, *etc*. [337]. In the electronic industry, for example, large-area graphene sheets are used to manufacture high-frequency THz electronic devices as well as the development of highly flexible, transparent, and durable electrodes for touch screens, monitors or displays, and solar cell devices [330]. Apart from the aforementioned devices, graphene is also used for the manufacturing of transistors and photodetector devices. In the particular case of graphene-channel transistors, for example, recent reports indicate that the use of graphene to manufacture these types of transistors has significantly increased their cutoff frequencies and the latter are now approaching the THz frequency range. Additionally, graphene-based photodetectors have also demonstrated spectacular high-speed operation capabilities in the mid-infrared frequency range and experts believe that this level of high-speed operation will soon reach the THz frequency range [337], [338]. Recently, several types of graphene-based THz devices such as plasmonic THz oscillators, graphene THz lasers, as well as graphene THz modulators (owing to the graphene's plasmon resonances with large oscillator strengths and prominent optical absorption peaks at room temperature) have all been developed.

Although graphene has had tremendous success since it was first synthesized in the 1960s, most of the aforementioned applications require the utilization of large-area high-quality graphene sheets. However, the development of large-area high-quality graphene for large-scale applications requires graphene manufacturers and users to rapidly and accurately assess its electrical properties and evaluate structural integrity for quality assurance, conformity, and validation purposes. To this end, properties such as graphene conductivity and carrier mobility must be accurately controlled and minimized, especially for applications where the spatial variability of these properties might jeopardize the smooth operation of the host systems [339]. In addition to the conductivity and carrier mobility, the quality of graphene also depends on its structural integrity and uniformity of graphene sheets. Indeed. all these quality attributes are essential for the commercialization of graphene products and require large-scale noncontact and rapid inspection techniques to ensure they remain in acceptable ranges that meet the application requirements of the final products [15], [339]. In most cases, the evaluation and characterization of the main electrical properties of graphene films generally involve the use of Raman spectroscopy combined with field-effect or Hall bar devices, though these techniques are generally complex and time-consuming, especially when used to evaluate large graphene film samples. However, graphene films usually have to be moved away from their growth substrate which may be extremely complicated if their electrical properties and/or structural integrity attributes are not properly evaluated [340]. To this end, not only is the use of highly accurate NDT systems to measure and map out the key electrical properties and structural integrity attributes of graphene films beneficial for the optimization of the graphene manufacturing process, but also for the optimization of the transfer, and structural evaluation processes. Interestingly, both THz transmission and reflection measurements allow users to perform direct and accurate mapping of graphene conductivity and carrier mobility over large areas and produce highly accurate graphene intra-band transition data similar to the Drude model analysis [313], [330]. In the THz transmission measurements, for example, the complex conductivity of graphene is evaluated using data from THz pulses transmitted through a thin graphene film layer deposited on the support. The measured THz data is then analyzed using Fresnel coefficients to determine the complex conductivity where the aforementioned graphene layer is modeled as an extremely thin conducting film. In doing so, both the drift and field-effect mobilities of the graphene film can be easily extracted by fitting the conductivity spectra to the Drude model [313] and measuring its conductivity changes as a function of the applied back-gate voltages on gate-stack support [330]. To evaluate the conductivity or carrier mobility map and obtain an adequate characterization of the electrical properties of the target graphene film, the aforementioned measurement, and analysis are repeated across the entire graphene area [330], [336]. As indicated earlier, the evaluation of structural integrity is also paramount to the quality assurance of graphene films in addition to conductivity/carrier mobility measurements, and THz systems have been equally proven capable of detecting defects in graphene on polyethylene terephthalate (PET) not visible to the naked eye nor with optical microscopy [340].

Although THz systems can provide accurate large-area spatial maps of common electrical properties as the key performance indicators for graphene films relevant to graphene production in batch production and roll-to-roll manufacturing processes, multiple legitimate hurdles still need to be addressed to achieve effective integration of THz systems into graphene manufacturing pilot plants or production lines. For example, this type of integration generally requires the establishment of well-controlled laboratory environments where factors such as measurement variabilities, instrument downtime, and artifacts can be timely and effectively dealt with for the production of high-quality graphene films. However, most commercial THz-SI devices cannot easily be implemented in graphene production facilities because of the difficulty of controlling the aforementioned factors, and the speed at which the THz measurements are performed. In addition to the aforementioned obstacles, THz systems require to be installed in electrically insulated shelters to limit the effect of environmental noise on their measurements and guarantee accurate test results. Also, establishing the long-term stability of operational THz-SI systems will guarantee the reproducibility of their

measurements and help users to eliminate false-negative and false-positive results. However, achieving adequate long-term stability of THz metrological systems in graphene manufacturing plants is not an easy task to perform and this limits the use of these systems as standard testing equipment to provide reliable performance characteristics of graphene films in large-scale graphene production settings. To this end, Whelan *et al*. [341] recently indicated that an overall good reproducibility of THz measurements is only possible when THz systems are utilized to measure graphene samples continuously over a short time scale (*i.e*., usually within a few days time-span). The same study also revealed that the electrical properties measured from the same graphene films over longer time scales often change (*i.e*., measurement variability) due to the effects of the environmental conditions in graphene pilot or production lines. In real-time production lines, mechanical disturbances such as vibration noise and mechanical drift often lead to phase errors and jeopardize the accuracy of the measurements. The vibration noise signals generally originate from other processes in the production line, the manufacturing environment, or systems in the vicinity such as the mechanical rollers in a roll-to-roll production system where the THz system is installed. In most cases, however, these types of noises cannot easily be eliminated through mechanical insulation alone, so care must be taken when selecting the place to install the THz systems [336]. Although the THz signals obtained in reflection and transmission modes can be used to evaluate the electromagnetic properties and structural integrity of graphene films, reflected THz signals are more desirable than transmitted signals because they are cost-effective, and easy to reconstruct particularly when seeking to generate property maps or NDT images. Reflected THz signals also provide higher accuracy than transmitted signals when performed on opaque or THz-absorbing materials and substrates. In terms of robustness, reflected THz signals are also far more sensitive to variations in probe-sample distance than their transmitted counterparts which generally provide inaccurate results when used to determine the carrier density and/or carrier mobility of graphene films.

In summary, THz inspection of graphene films is a highly advantageous NDT technique, but more work still needs to be done to ensure the transmission measurements can achieve the performance level of the reflection measurements. This development is generally expected to meet serious resistance from the conductivity of graphene films which already limits significant depth penetration of THz waves to probe the inner surfaces with only superficial features and/or extremely thin layers of graphene currently being measured. Interestingly, significant advances have been implemented and solutions are constantly being presented to deal with some of the aforementioned shortcomings related to THz transmission measurements. As an example, studies indicate that variations in the probe-sample distance are more critical, especially when moving from far-field to near-field transmission measurements. Indeed, the results indicate that a proper adjustment of this distance can improve the system's spatial resolution from hundreds of μm down to a few μm [338]. To date, commercial near-field THz systems that can reach 10-50 μm resolution on continuous graphene film samples are available on the market and the development of scattering-type scanning near-field microscopy operating in the THz frequency band such as that recently developed by Neaspec GmbH is expected to bring the spatial resolution down tens of nm [341]. Although these systems are primarily research tools due to their greater complexity and low measurement speed, this development has contributed to the overall understanding of non-Drude THz spectral features and the connection between these features and the physical appearances of graphene samples such as the presence of defects, grain boundaries, local contaminants, *etc*. [342]–[344], which highlights their importance on the overall research and development efforts as well as the structural feature diagnosis of graphene films. In addition to the aforementioned developments, the use of Monte Carlo simulations is also considered another possible route that could help THz users in their efforts to reconcile the measured features with the analytical understanding of graphene films. However, this method still evolving and requires additional research to adapt to the analysis of graphene films using THz systems. Therefore, the integration of the THz systems into the graphene manufacturing industry requires users to address all the aforementioned obstacles for THz systems to perform accurate contactless measurements of the key electrical properties that would in the optimization of the growth, transfer, and post-transfer processes of graphene films.

E. Gas sensing with THz systems

Gas sensing involves the detection of toxic, harmful, and natural gas leaks in areas such as coal mines, environmental monitoring, petroleum, breath analysis, chemical plants, transportation, medical diagnostics, *etc*. Interestingly, THz spectroscopy has proven to be one of the most effective gas detection systems and presents numerous advantages such as high selectivity, fast measurements, high sensitivity, reagent-free, continuous monitoring of multiple gaseous components, faster online data processing, *etc*. that makes it an attractive gas sensing tool. Its principle of operation relates to the irradiation of confined gaseous compounds by THz waves at a fixed pressure and the acquisition of their spectral information as illustrated in Fig. 17 [82], [345]. Specifically, THz waves excite the molecular bonds in the target gas and initiate the molecular roto-vibrational movements, which cause changes in the dipole moments of the affected molecules and result in the emission of specific absorption lines or bands in the THz region [346]. This is particularly interesting because most gases have relatively few absorption lines in the THz frequency range as compared to the infrared region, which facilitates their detectability by common THz spectroscopic systems. In this section of the paper, the use of THz systems in three key areas *viz*. environmental monitoring (*i.e*., particularly the pollutant monitoring and Earth observation practices), quality monitoring of natural gas in the production and supply chain as well as human breath analysis are analyzed to exemplify the effectiveness of THz systems and present the main achievements in THz gas sensing applications. Also, special features that enable THz users to achieve accurate qualitative identification and quantitative evaluation of gaseous components are presented.

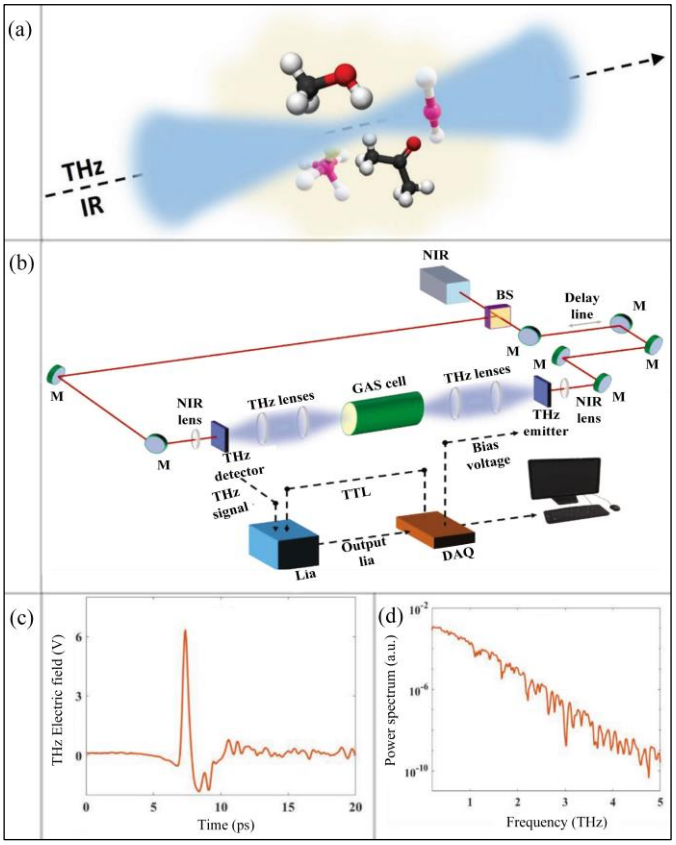

Fig. 17. Illustration of the (a) interaction mechanism between THz waves and single/multi-component gas mixtures in the THz vibrational spectroscopy, (b) schematic layout of a typical THz spectroscopic system configured in transmission mode using switched PCA in gas sensing application, (c) typical temporal profile of the THz electric field which is also referred to as the THz time-domain signal), and (d) typical THz power spectral signal which is also referred to as the THz frequency-domain signal [82].

E. 1. Environmental monitoring using THz systems

In environmental monitoring, THz technology offers effective alternative experimental systems for gas sensing and recognition for subsequent remediation of contaminants. Although gas sensing devices operating in the IR region of the electromagnetic are more advanced with so many options available on the market, THz waves offer numerous advantages such as the presence of specific and unique roto-vibrational transitions of molecules, nonflammability of common gases observed in environmental monitoring applications in the THz frequency range, as well as their resistance to aerosol scattering effects. Indeed, these features combined enable the successful usage of THz technology in various environmental monitoring applications. Nevertheless, it is important to indicate that THz waves strongly interact with or are rather absorbed by polar molecules such as alcohol, water, moisture, and NH_3, and this limits the ability of THz systems to provide accurate gas-sensing results in an open atmosphere [16], [347]. To overcome this challenge and utilize the THz systems efficiently, two different approaches have been proposed in the literature, *viz*. the use of an isolation chamber or gas cell to separate the target gas sample from the outside environment (Fig. 17) [348], [349], and the use of a strong electric field, usually the atmospheric plasma-based THz waves generation method, *etc*., to produce high-power THz waves [350], [351]. In the presence of a mixture of gases, in particular, partial overlapping of the absorption lines of the different gases in the mixture exhibits complex absorption spectra and this makes the recognition or identification of the individual gas components in the mixture difficult to achieve. This challenge is generally solved by using classic signal processing and post-processing methods based on time, frequency, and time-frequency signal processing methods, or even advanced signal processing methods featuring state-of-the-art machine learning or deep learning algorithms are often recommended [73], [82]. In addition to the use of these classic and advanced signal-processing methods, the use of gas or THz wave concentrators has also been proposed as an effective method for accurate detection, identification, and analysis of ultra-small concentrations or trace amount of different types of gas samples. For example, applications involving the detection and analysis of trace amounts of gases generally require the use of supplementary devices based on plasmonic, metamaterials, and resonant systems to extend the natural dielectric response of the target gas samples in the long-wavelength regime and overcome the THz system's optical resolution limits [175], [352]. Also, microporous structures may be used for the adsorption of the target analyte/gas samples. In this case, accurate detection and quantification of the different target gases can easily be achieved by analyzing the attenuation levels of THz waves and the variation of the overall refractive index of the sample system.

As indicated earlier, gas sensing in environmental monitoring applications relates to the detection and measurements of contaminants and pollutants in the air to meet the health, municipal/legislative, and safety regulations requirements. These types of monitoring also involve the detection and measurements of atmospheric gaseous components for climate and weather observation purposes. In all these applications, monitoring atmospheric gas composition often has less stringent requirements, while the detection and measurement of pollutants mandate highly accurate results, and the use of highly sensitive instruments with an exceptional level of selectivity and specificity is highly warranted. Interestingly, THz spectroscopic systems have proven to have all these characteristics and are therefore reliable tools for gas sensing in environmental monitoring settings. Although the use of THz systems for gas sensing applications is relatively a new technology, commercial THz spectrometers with tunable diode lasers and photomixers for trace gas sensing have already been developed almost a decade ago [346]. In a recent study, Yang *et al*. [353] presented an exhaustive list of toxic chemical compounds detectable by THz spectroscopy and pointed out the most effective THz frequency range that should be targeted by THz users to achieve accurate gas detection results. In a similar study, Smith and Arnaldo [354] examined eight different types of gases *viz*. acetaldehyde, methanol, acetonitrile, water, NH_3, propionaldehyde, ethanol, and propionitrile and demonstrated the selectivity of chemical compounds by THz spectroscopic systems. In another study [355], the authors sought to improve the sensitivity of a THz spectroscopic system and reported accurate detection of methanol, acetonitrile, carbon monoxide, and water at significantly low concentrations (*i.e*., all the

samples were detected with concentrations less than 10 ppm). To date, researchers are working to develop customized electronic systems for gas sensing applications including THz sources and detectors as well as gas cells for collecting and concentrating gas samples, *etc*.

Consistent with the aforementioned, researchers have recently proposed typical all-electronic THz systems with special types of gas cell systems to collect and concentrate gas samples to boost their detection capabilities [356], [357]. Among their many advantages, these systems are especially compact, robust, and consume extremely low power and the fact that they operate at a narrow frequency range is another added advantage. One of their main characteristics is that these systems present a narrow frequency range that can be effectively tailored to provide specific gas-sensing targets in the ppt range [358], [359], and easily meet the Clean Air Act requirements [360]. Another positive achievement relates to the development of a custom-built food spoilage monitoring system [361]. The system was designed to detect the amount of hydrogen sulfide (H_2S) at around 611.4 GHz with a sensitivity of up to 0.5 ppm. In addition to toxic gases, both the detection and recognition of particulates in the atmosphere are also vital tasks to ensure adequate air quality in pollution monitoring applications. To this end, Refs. [362], [363] published updated research on the utilization of THz systems to detect and measure the concentration levels of different types of chemical and biological particles such as pesticides, aromatic hydrocarbons, heavy metals, phenol, polychlorinated biphenyls, and dioxins, *etc*., and indicated that the mean size of particles detected in the atmosphere is generally about 2.5 μm, while the concentrations ranging from 0.001 ng/mL to 20 pg/mL can also be detected depending on the analyte. Additional developments have also initiated explorations of using compact THz systems with high-resolution and high-sensitivity features as remote toxic gas sensors at disaster sites [15], [364] as well as astronomical and atmospheric observations [365], and trials are currently underway.

In summary, THz spectroscopy presents promising opportunities for the implementation of highly accurate qualitative and quantitative gas-sensing platforms in environmental monitoring applications. These applications are largely feasible because of the capability of THz waves to provide molecular fingerprints or roto-vibrational transitions specific to different types of gases as well as the strong resistance of THz waves to particle scattering during the measurements. In addition to their molecular fingerprints characteristics, THz systems can also be used to map up the absorption and dispersion spectra for different gases which can be analyzed to obtain qualitative and quantitative information for the characterization of individual components in a mixture of different types of gases. Although THz spectroscopic are highly effective gas sensing systems, both the procurement of accurate spectroscopic parameters and the quantitative reduction of the broadband data remain challenging issues that require immediate attention. Also, gases with polar molecules have a relatively unique set of absorption lines in the THz spectral range compared to the infrared region, which facilitates their selective recognition of gaseous samples. To date, various optical configuration schemes of highly sensitive THz spectroscopic systems have been proposed with many of them currently being cost-effective, and portable systems and with low absorption losses. In particular, THz sensors can easily detect different types of gases at ambient atmospheric conditions, owing to the resistance of THz waves to environmental factors such as the aerosol scattering resistance, and the nonflammability of THz waves. However, it is important to indicate that THz waves are strongly absorbed by humidity or moisture in the air, and this limits the performance of THz spectroscopic systems in the open air. Interestingly, these limitations can be minimized by using gas cells to isolate the target gas from the outside environment, leveraging advanced signal processing techniques to discern fine sensing details specific to different gases, as well as the use of strong THz electric fields to generate THz waves. Although the latter is more effective due to the strong THz response provided by the target gas sample when irradiated by a high THz power source, the technology is in its infancy and requires further studies for validation.

E. 2. Breath analysis using the THz systems

In general, many types of gases are found in exhaled human breath (*e.g*. ethanol, methanol, acetone, *etc*.) some of which may be in larger quantities than others depending on the health conditions, diets, and environmental exposures of the person [366]. In some cases, medical doctors are required to perform an in-depth analysis of gases found in the exhaled human breath to perform early detection of certain types of disease biomarkers [367], [368]. Taking ethanol (C_2H_5OH), methanol (CH_3OH), and acetone as examples, these chemicals/gases are considered to be some of the known biomarkers for several types of diseases and metabolic disorders in humans [15]. For example, the normal level of acetone concentrations in human breath ranges from 177 ppb to 3490 ppb with an average concentration in healthy individuals of about 544-628 ppb [369]. In many instances, elevated levels of acetone concentrations have been linked to lung cancer, congestive heart failure, diabetes, brain seizures, dietary fat loss, *etc*. [370]. Under normal circumstances, typical levels of CH_3OH are estimated to be around 32-1684 ppb with their average concentrations being 457-529 ppb in healthy individuals [371]. Elevated concentration levels of CH_3OH may be linked to certain nervous system disorders [370] and abnormal levels of gut flora (*i.e*., bacteria or microorganisms living inside the intestines) associated with diseases, such as renal failure and pancreatic insufficiency [371]. Under normal conditions, levels of C_2H_5OH in breath are in the range of approximately 0-1663 ppb in healthy individuals [371], and its excessive concentration levels are associated with abnormalities such as excessive production of gut bacteria [370], hepatic steatosis, alcoholism, nonalcoholic fatty liver disease, *etc*. [372]. Additional gases that are often found in exhaled human breath include but are not limited to NH_3 (*i.e*., for a urease breath test or helicobacteriosis and the carcinoma of the lung diagnostics), carbon monoxide (CO) (*i.e*., for respiratory infection, and asthma), nitric oxide (NO) (*i.e*., for asthma, lung diseases, and bronchiectasis), acetone (*i.e*., for non-insulin diabetes), *etc*. [373]. Interestingly, THz technology is highly sensitive to all these gases, and the use of this technique for such detection

provides fast, reliable, and non-invasive means for early diagnosis and state-of-health monitoring.

The use of THz spectroscopy for breath analysis applications exhibits many advantages over conventional infrared-based spectroscopic methods because the molecular structures of common particles found in exhaled breath present their strong rotational transitions in the THz frequency range at low frequencies of around 0.1-0.5 THz [82], [374]. In fact, the literature indicates that common gases found in exhaled human breath such as C_2H_5OH, CH_3OH, acetone, *etc*. exhibit more than 1,000 absorption lines within the 0.2-0.3 THz frequency range, suggesting that this frequency band is extremely important for human breath analysis with THz spectroscopic systems [82]. For example, CH_3OH exhibits strong transitions in the 0.2-0.3 THz frequency range with easily distinguishable line intensity of approximately 8.3×10^{-23} $cm^{-1}/(molecule/cm^2)$ at 10 Pa per 1 m of absorption length [125]. Interestingly, all its absorption lines are almost equally spaced at 50 GHz, and the highest absorption peak is located at about 2.038 ± 0.015 THz. The comparison between the THz spectral absorption of acetone and CH_3OH indicates that these two gases also exhibit a different trend in this frequency region. For example, acetone generally exhibits a single and broad absorption band in the 0.2-1.2 THz frequency range (centered at approximately 0.562 ± 0.015 THz) related to a complex mixture of confined molecular rotational transitions, while CH_3OH presents many constantly spaced absorption lines related to simple molecular rotational transitions [375]. Apart from acetone and methanol, all gases found in exhaled human breath present specific optical responses and/or spectral features in the THz frequency range, which makes THz spectroscopic systems highly accurate instruments for these types of analysis.

In 2013, Fosnight *et al*. [366] used the THz-TDS system to analyze an exhaled human breath and evaluate the concentration of methanol, acetone, and ethanol of a person after consuming alcohol. In addition to being a real-time-oriented application, the authors also indicated that the selection of these chemicals as their detection target allowed them to compare their results to those obtained by common commercial breath alcohol analyzer systems or breathalyzers where acetone and methanol are considered the chemicals likely to introduce false positive results. As part of their conclusions, the above authors indicate that they managed to perform an unambiguous detection in a part per trillion dilution range with an overall sample size in the femtomolar range, thereby further confirming the accuracy of THz spectroscopic systems in breath analysis applications. In a later study [376], the authors designed a special gas cell tube and used it with the THz spectroscopic system to generate the first datasets on breathomics for the ambient air and three healthy volunteers (*i.e*., one smoking and two non-smoking healthy volunteers). In their experimental design, the probe beam was set to pass through the gas cell multiple times before being sent to the detector for measurements (*i.e*., 11 times in total). The idea was to increase the interaction time between THz waves and the target gas samples in the cell tube and strengthen the measured absorption signals for easy evaluation. The measurements were conducted in the frequency range between 220-330 GHz and a total of 21 gases were detected in the exhaled breath with a clear distinction between the samples obtained from non-smokers, smokers, and ambient air. In another study [373], Vasks *et al*. successfully used a high-precision THz spectroscopic system to detect and identify various types of biomarkers including NH_3, nitric oxide, methanol, acetone, and ethanol in the exhaled breaths of conditionally healthy and patients volunteers with different kinds of cancerous and noncancerous diseases. As part of their conclusions, the above authors indicated that not only did the THz spectroscopic system help them to successfully detect and characterize the aforementioned biomarkers and associated diseases or health conditions, but they also indicated that the THz measurements would potentially provide guide medical personnel in the choice and monitoring of therapy and prediction of the disease response to specific treatments.

In summary, breath gas analysis using THz technology is potentially a promising and non-invasive tool that offers a path toward a better understanding of metabolism for medical research/studies and medical diagnosis because it is a highly selective and very sensitive technique [377]. Although the sensitivity of the best THz spectroscopic systems is still less than that of the best chromatography-mass spectrometers, THz spectroscopy presents other distinct advantages including the unique, reliable identification of gas markers, *etc*. Indeed, this is in contrast to chromatography-mass spectrometers which can only give an identification probability. In addition to the aforementioned advantages, the THz spectroscopic system is relatively cost-effective, user-friendly, and does not require any additional high-priced components and/or consumables (*i.e*., compact and affordable sensing systems) [373]. Also, THz sensors rely on high-resolution spectra of all detectable substances or species and, therefore, these sensors offer distinct advantages in specificity and selectivity of the different gaseous substances. Although THz technology presents numerous advantages in the analysis of exhaled human breaths, progress in using THz technology for the analysis of these types of breaths in laboratory settings and routine clinical practices has been utterly slow. This is particularly because THz signals are generally affected but the moisture and polar molecules/particles in the air require cumbersome signal processing methods to remove the noise. Also, both the existence of different methodologies of breath analysis and the lack of standardization of the THz systems for breath analysis make it difficult to compare and combine the measured THz data with the data obtained from other systems. To fulfill the potential of breath analysis with THz technology within clinical and pre-clinical medicine, the standardization of some approaches to breath sampling and analysis with the THz system would be highly beneficial and would increase robustness and inter-laboratory comparisons.

E. 3. Natural gas sensing with THz systems

As indicated earlier, the technical advances in THz wave generation and detection have enabled the production and the coherent detection of THz pulses in the picosecond (ps) and even sub-picosecond ranges thereby enabling the detection and analysis of natural gas components in applications related to fuel quality analysis. In general, natural gas is primarily a mixture of three different types of hydrocarbons *viz*. ethane (C_2H_6), propane (C_3H_8), and methane (CH_4). The ratio/weight

percent of each of these three hydrocarbons determines the calorific content of the natural gas and is used as the quality indicator for most fuels in general. Additionally, natural gas usually contains an admixture of several contaminants such as carbon dioxide (CO_2), nitrous oxide (N_2O), carbon monoxide (CO), sulfur dioxide (SO_2), *etc*. which reduce the burning velocity of the resulting fuel, and ultimately the engine output and/or thermal efficiency of heating systems. As such, the quality control and monitoring of natural gas products are of significance. Unlike the THz systems used for pollution detection and breath monitoring, applications involving natural gas analysis do not require the use of THz systems with high sensitivity, selectivity, and specificity features, suggesting that common THz instruments will provide acceptable results for natural gas sensing applications. To this end, several studies have been published outlining the use of THz spectroscopy in natural gas sensing. As an example, THz-TDS was recently used to determine the mixing ratios of natural gas products based on the differences in their refractive indices [378], [379]. Apart from the monitoring quality of natural gas products for any form of contamination, pipelines are considered the most economical or cost-effective method used to transport large quantities of natural gas products, and the presence of water in these types of infrastructure will undoubtedly cause significant safety and economic issues and must be accurately and continuously monitored [380]. In summary, the application of THz technology for the analysis/sensing of fuel and natural gas products quality has been viably demonstrated in the literature and results are highly encouraging. The increasing number of research and experimental investigations on the development of new strategies and state-of-the-art THz systems for the analysis/sensing of natural gas products is an encouraging step toward the development of high-performance THz detection systems for natural gas products but requires effective planning and methodology to successfully achieve the expected objectives.

F. Inspection of wood and paper-based materials and structures

As part of their main characteristics, wood and papers are natural systems to pursue application development using THz-NDT because of their key characteristics *viz*. transparency, spatial resolution, and sensitivity to gross fiber structures that allow NDT engineers and practitioners to probe their structural integrity in a useful way. THz technology is capable of providing information related to density mapping, Water content/distribution, density, defects, and knotted areas, as well as the spectral properties of wood and paper-based materials and structures [238]. Using the aforementioned key characteristics of THz waves and inspection capabilities of THz systems, one can see why there is a lot of excitement about the application of THz technology for the NDT of wood and paper products, and the present section presents a review of the state-of-the-art and state-of-the-practice relevant to the applications of THz sensing in the wood and paper industry.

F. 1. Inspection of paper and paper products

In general, paper and its products are widely used in our daily lives (*e.g*. printed books, notebooks, banknotes, *etc*.), hence, studying the properties of these types of materials is necessary and helpful because of their numerous applications. In recent years, several investigations have been conducted using THz technology to examine the structural integrity of paper and paper products. Although most paper and paper products present high THz absorption levels, thin paper sheets have proven to have moderate-to-good THz transparency making their inspection by THz technology easier [15], [381]. THz absorption level by the paper materials is directly proportional to several parameters including their thickness, material composition, moisture or water content, and texture, suggesting that these parameters can easily be evaluated using the THz-SI system configured in the transmission mode. To this end, THz-NDT offers a solution to the paper industry's pressing need for in-line monitoring of several properties of paper materials such as their moisture content levels, thicknesses, weight per area, *etc*. In fact, several studies have been published outlining the results of successful demonstrations and ongoing investigations on the feasibility of the approach both at the laboratory and industrial scales. In the latter applications, for example, Brinkmann *et al*. [382] sought to demonstrate the industrial application of THz technology for the quality control of the cardboard boxes used in the packaging of pharmaceutical products. Their experimental setup combined the use of a pulsed THz emitter with a high-bandwidth Schottky receiver and they managed to measure the THz intensity accurately with an effective time resolution of 6.4 μs. In a proof-of-concept experiment, the above authors demonstrated that THz screening could clearly reveal the presence or the absence of package inserts inside the cardboard boxes, even for samples moving at a speed of about 20 m/s.

In laboratory setups, the inspection of paper materials was extensively demonstrated for the detection of moisture contamination [383], simultaneous composition and thickness measurements [384], as well as the determination of multiple paper parameters for quality control [385], basis weight [386], sorting and characterization, *etc*. Markov *et al*. [387] used a THz fiber Bragg grating to design a more compact THz system and used it to measure the paper thickness (*i.e*., as part of paper quality control applications). In 2017, Huber *et al*. [388] reviewed the dielectric losses of paper used in high-frequency paper-based electronic devices and provided guidelines for future research focusing on the need for inspection in controlled moisture conditions. In 2015, Vassilev *et al*. [389] used a homemade sensor to measure the moisture content in thin paper layers during an offset printing process. The study was intended to demonstrate the industrial prototype that could monitor the t moisture variations in the offset print processes and results were compared with the laboratory tests and higher accuracy was recorded. Additional applications include the study by Wang *et al*. [390] in which the authors analyzed the samples from an insulation oil-paper system for power transformers using the THz-TDS system. The results indicate that the aforementioned oil-paper samples exhibited different refractive indices in the THz frequency region at various aging stages, suggesting that this system could indeed be used to evaluate the aging stages of different insulation materials, a finding that was later confirmed in Ref. [21]. A similar study by Peccianti *et al*. [391] also used the THz spectroscopic system to measure the absorption coefficients of cellulose fiber in both ancient and modern

artifacts. As part of their conclusions, Peccianti *et al*. indicated that the THz spectral behavior of cellulose fiber is mainly determined by the superposition and organizational arrangement of hydrogen-bond networks in their midsts and involves the appearance of many-peak profile of the cellulose crystalline phases. In another study, Mousavi *et al*. [384] used the THz-TDS system to measure the moisture content and thickness of paper samples. In the latter case, the precision and accuracy of their thickness measurements surpassed that of conventional caliper measurements by a factor of two, while the performance of the THz metrology system was equivalent to that of conventional moisture measurement sensors. In an earlier study [392], Abraham *et al*. used the THz-SI system to evaluate the patterns drawn on paper using different lead grades of graphite pencils and they managed to successfully separate letters with different concentrations of graphite.

Apart from the inspection of paper materials, paper product inspection is also another area that has been explored and documented in the literature. Typical examples of such an inspection have been conducted to inspect the structural integrity of paper money or banknotes (*i.e*., a special kind of paper made mainly from cotton paper) [381], [393]. Although traditional banknote inspection methods such as UV fluorescence, and X-ray fluorescence, as well as IR and magnetic-based NDT techniques, have been thoroughly successful, the recent rise of sophisticated counterfeit notes poses new challenges to banknote inspection technologies and new methods are required to ensure effective testing results. As a new type of inspection technology, THz-TDS presents greater potential in the efforts to identify banknotes and several studies have been reported in the literature [394], [395]. Nevertheless, most studies focus on using single-frequency detection methods and limit their inspection to some parts/regions of the banknote. Experts believe that this is generally not the best way to test these notes because of the level of sophistication that is currently being introduced into the manufacturing of counterfeit notes, and the current trend is now focusing on the applicability of this technique for the inspection of a wide region on the banknote and using multiple frequencies. In this context, Ren *et al*. [381] recently used two different THz-SI systems and combined them with a spectral coverage ranging from 0.5-10 THz to evaluate the optical properties of numerous types of paper and banknote samples. Their results indicate that the measured paper and banknote samples featured remarkable THz fingerprint characteristics and absorption peaks at different frequencies including 3.05, 5.13, 6.32, and 7.03 THz. As part of their conclusions, the above authors indicated that the obtained fingerprint characteristics and absorption peaks were highly correlated to the types of vibrational transition modes that are commonly observed in cellulose which is the main component of most banknotes. Apart from the scpectroscopic measurements, THz images were also collected and the capability of the THz-SI systems to detect and identify the key anti-counterfeit labels of banknotes such as watermarks, holographic stickers, optically variable inks, scratch-off secret codes, security threads, *etc*. was utterly demonstrated.

In summary, several research groups have explored the potential of THz technology for the inspection and characterization of many paper forms and products and successful examples demonstrating the feasibility of this technique in the evaluation of the structural integrity, material compositions, as well as moisture content and distribution have been presented in the literature. Also, several studies demonstrated that THz technology can accurately evaluate paper products such as banknotes to identify some key anti-counterfeit labels such as watermarks, holographic stickers, optically variable inks, scratch-off secret codes, security threads, *etc.*, thereby providing a robust method for potential applications in testing and evaluating paper and paper products in various industries.

F. 2. Inspection of wood and wood products

Advancements in the utilization of THz-SI systems for the NDT of materials and structural systems have also extended their applications to the inspection of wood and wood products. Although these types of materials and products are generally less transparent to THz waves than papers due to factors such as larger thicknesses of samples and stronger scattering/absorption levels of THz waves by their material constituents, THz-TDS systems have shown greater potential in the NDT of wood materials and wood products. For example, the anisotropic structure of wood materials consisting of aligned fibers makes wood and wood products excellent birefringent materials, hence, it is easy to detect the orientation of fiber and other materials constituent of these structures using THz waves. Among the many applications listed in the literature include the studies by Inagaki *et al*. [396], [397] who recently indicated that THz-SI systems can accurately evaluate the moisture content and density of wood and wood products, while Jackson *et al*. [398] successfully analyzed the tree-ring in wooden cultural heritage structures for cross-dating purposes. Recently, Krügener *et al*. [399] used the THz spectroscopic system to study the optical properties (both the indices of refraction and absorption coefficients) of wooden samples from different wood species at different THz frequencies and indicated that the cell structure is one of the major elements that determine the magnitude of THz properties of wood and wood products. In another study [400], the above authors also used a THz-SI system configured in reflection mode with a robotic arm to detect internal damage in wood samples caused by burrowing “typographer” beetles and reported successful NDT tests.

In summary, the capabilities of THz waves to penetrate wood and wood materials and evaluate their density, damage levels, moisture content, and fiber orientations make the THz technology a highly attractive NDT technique for wood and wood products. The strength of solid wood, and wood composite products such as the oriented strandboard, cellulosic fiberboard, particleboard, hardboard, and plywood, derive primarily from the physical configuration, orientation, and density of the fiber that composes the structure. Interestingly, THz-SI is capable of providing sub-millimeter spatial resolution and high sensitivity to fiber orientation, and it is natural to expect THz technology to continue to penetrate the wood industry by providing some of the most advanced NDT means for research and development, quality control during the design and manufacturing processes as well as the evaluation and/or characterization of wood structures during their in-

service stage. Nevertheless, the wood elementary structures are generally of the same dimension as the THz wavelengths and this leads to an acute scattering of THz waves, this makes it difficult to know if the attenuation of the observed in the THz signals is caused by the scattering or absorption of THz waves by the wood materials or by other structural features. As this cannot be easily distinguished by using simple transmission or reflection measurements, the measured parameters will be affected by uncertainties which could also complicate the experiments and jeopardize the accuracy of the results. In this case, adequate signal processing methods should be adopted to extract the maximum information from the measured THz data and guarantee accurate test results.

G. Artwork conservation and evaluation

The conservation of artwork and historical objects/artifacts is an important aspect of preserving both artistic expression and human culture for present and future generations. However, artwork usually gets aged or deteriorates over time or can even be damaged or compromised unknowingly or involuntarily through artificial processes, suggesting that art conservators should make every effort to improve the condition of safeguarding artwork through the utilization of nondestructive preservation and restoration procedures. As such, a formal diagnosis of artworks is particularly important to correlate the nature of the materials in the artifacts to the state of decay [401] and provide art conservators with the necessary information enabling them to preserve their structural integrity. In most cases, early detection of faults or damage in artworks has been proven to be an important practice to ensure their longevity as it helps conservators to establish adequate treatment methods to maintain or restore their structural integrity. Artwork conservation has been traditionally assisted by the use of various NDT techniques including speckle pattern interferometry, photography, X-μCT, *etc*. Recently, THz technology has been introduced as a newer technology for the characterization and evaluation of artworks allowing conservators to collect even more detailed information about the structural design and fabric of artwork objects [402]. As both a spectroscopic and imaging technique, THz technology has the proven merit of contributing to the field of material and structural systems characterization by providing the materials' in-depth profiles and by revealing their finer stratigraphic information. Also, this technology can evaluate the structural characteristics of different types of artwork objects and help conservators to establish the conservation conditions of these objects and is currently becoming instrumental in the understanding of the art that defines people's cultural and artistic expressions such as canvas and panel paintings, murals, *etc*. [403], [404], thanks to the capabilities of THz waves to penetrate opaque materials and reach their in-depth structural features.

In 2019, Giovannacci *et al*. [405], used the THz-SI system to examine the structural integrity of several immovable cultural heritage materials and reported encouraging results. In an earlier study, Inuzuka *et al*. [406] used the THz-SI system to investigate the condition of the plaster layer of the Takamatsuzuka mural painting of a blue dragon. The authors indicated that they managed to identify the locations where the plaster layer appears solid on the surface but in actuality may have peeled off from the underlying tuff stone from the measured 2D images. In a recent study [407], Groves *et al*. used the THz-SI system as a secondary tool to obtain and analyze distinct features within damaged wood panel paintings, and several damage-related features were highlighted individually within the painting by analyzing the amplitude of the THz pulses, and the damaged regions were correlated to the distinct features obtained in the THz images. The authors also demonstrated that the structural damage detected on the sample paintings may reflect the existence of defects in most authentic artworks. In a later study [408], Picollo *et al*. used a portable THz-SI system to acquire THz images to determine the health conditions of various internal material layers, decorative gilding, surface degradation, and material constituents of two wooden panel paintings entirely by selecting numerous sections due size of the polyptych (*i.e*., significantly larger). Jackson *et al*. [409] used the THz-SI systems to evaluate the underdrawings and paint layers embedded within the wall paintings. Their results indicate that the metallic and dielectric paint patterns, as well as the graphite drawing of the paintings, were all accurately resolved through paint and plaster overlayer analysis, and the bulk refractive indices of four common pigments were successfully calculated and used to confirm the color domains.

Additionally, the use of THz reflectometry systems to reveal the stratigraphic information and hidden features of art paintings has attracted considerable interest with users focusing on the detection of artists' signatures [410], under-drawings [411], and modifications of earlier canvas or paintings [412]. THz reflectometry may provide useful detailed information related to the structural composition and health status by analyzing the features detectable in reflected THz signals. In the painted structures, for example, the aforementioned features may include the existence of in-depth dielectric discontinuities associated with the various layers and paint systems, suggesting that the THz time-domain echoes reflected from the various interfaces in the target object will undoubtedly exhibit different features and discontinuities at different levels in depth and transverse positions in a form of time delay and amplitude variations [413]. The stratigraphic profile of paintings in the artifact can then be reconstructed by precise extraction of THz echo parameters from reflected THz signals. To date, numerous wall and panel paintings have been studied using THz reflectometry, in which some stratigraphic details of the paintings have been revealed [408]. However, one of the commonly cited lacunas in the success of THz stratigraphic evaluation of painted structures relates to the characterization of the pre-19th century easel paintings, in which the thicknesses of the paint layers are generally less than 50 μm (*i.e*., paint-layer thicknesses vary from artist to artist and the different styles even throughout this period) [414]. In the THz frequency range, this characteristic paint-layer thickness of such paintings is considered optically thin because it is much smaller than the wavelength of THz waves which corresponds to the depth resolution of a typical THz-TDS system [415]. In some cases, the detection or identification of potentially defective or damaged regions in artwork structures using a multi-sensing approach combining THz-SI and other NDT systems [407],

[409] is also considered to be valuable for the accurate testing of artworks.

Additional studies featuring the use of THz reflectometry in artwork inspection include the recent study by Skryl *et al*. [416] which used pulsed THz waves to perform a tomographic time-domain imaging of hidden defects and other structural features in the subsurface layers of wooden panel paintings. In this study, the authors measured THz time-domain signals which they used to construct the tomographic images. The measured signals were also used to determine the different types of material systems constituents of the paint structure and their corresponding thicknesses, visualize the cross-section of the painting, as well as hidden defects in the sublayers of the paintings. The above authors also used the same THz tomographic imaging system to detect and evaluate hidden flaws in a Russian wooden panel painting. Although the THz images were taken from a region of the panel with visible surface and sub-surface cracking and degradation, their THz-SI system revealed that a kind of knot was previously removed from the panel wooden substrate and filled with a new foundational layer to restore the painting's original design. In an earlier study [414], Adam *et al*. effectively demonstrated that THz waves could be used to visualize the structural composition/configuration of the underpainting structures in canvas (*i.e*., different layers and features of material from within the canvas paintings) and further added that this technique has an even higher potential to provide the stratigraphic information of these types of painting with the lowest risk of damage when is juxtaposed with the X-ray radiation.

Although THz-NDT is generally effective in revealing the stratigraphic features of samples in the artwork conservation industry [273], [402], there may be a significant amount of spectral information present at relatively short wavelengths that are obscured in raw or unprocessed THz signals, suggesting that the implementation of state-of-the-art THz systems or signal processing methods is important to ensure all the available information is extracted from the measured signals [273], [413]. In the context of THz reflectometry, for example, THz echoes from various interfaces between the layers of optically thin paint layers will partially or even totally overlap in time and cannot be distinctively differentiated unless adequate signal processing methods are used [273], [413], [417]. To obtain the detailed stratigraphy of pre-19th-century easel paintings, Dong *et al*. [413] demonstrated that sparsity-based THz reflectometry can be used to accurately extract detailed 3D mapping of the layer structures of the 17th-century easel painting, in which the structural features such as the canvas support, underpainting, varnish layers, *etc*. were quantitatively and accurately identified and evaluated. To their credit, their approach unlocked a range of imaging applications of THz reflectometry as a potential NDT technique that could provide global and detailed stratigraphic information of easel paintings by using sparse deconvolution, without which THz reflectometry in the past has only provided a meager NDT tool for the characterization and evaluation of paintings with paint layer thicknesses less than 50 μm. In another study [273], Dong *et al*. used the THz reflective imaging combined with the frequency-wavelet deconvolution to obtain the subsurface features and stratigraphic information of artwork paintings. To resolve the optically thin paint layers, they used a deconvolution algorithm combined with the stationary wavelet shrinkage and frequency-domain filtering and used it to evaluate a mid-20th century Italian oil painting on a paperboard. The results indicate that the stratigraphic information of the painting was reconstructed using the deconvolved THz data and all the subsurface features were accurately revealed, further demonstrating that THz frequency-wavelet deconvolution is also an effective tool to characterize and evaluate stratified systems involving optically thin layers.

In summary, the THz metrology system has demonstrated great potential in the NDT of the cultural-heritage community because it can provide adequate structural information and/or stratigraphic imaging pertinent to the characterization of features in areas such as clay artifacts, wooden objects, written papyrus, ancient Egyptian mummies, stone sculpture and architecture, and tree rings. The technique can also provide information relevant to the evaluation of artifacts' physical conditions to identify and evaluate flaws. In the area of art painting, THz-SI has been used to recognize hidden features and pigments under the surface of paintings and provide information about the stratigraphic structure of artistic paintings, which helps to understand the underlying painting's creation process and the message behind the different pieces of art. Although some information may not be observed when dealing with optically thin-layer paints due to overlap between the different THz echoes, advanced signal processing methods can easily help to resolve the details and separate the details of closely-spaced paint layers. The demonstrated capabilities of THz technology for stratigraphic imaging, as well as its relatively good penetration depth, and the innocuity of THz waves make us foresee that THz spectroscopy and imaging will continue to find interesting applications in the inspection and conservation of artwork objects.

H. Analysis and detection of petrochemical products

In recent years, both the quality analysis and monitoring of the petrochemical products using THz spectroscopic systems have attracted considerable attention, owing to the high transparency of these products to THz waves and the sensitivity of THz systems to variations in their dielectric properties based on their chemical composition and/or contamination levels [418]. In their chemical composition, petrochemical products consist of hydrocarbons with different chain lengths mixed with other flammable and nonflammable impurities and contaminants such as aromatics, alcohols, *etc*. [15]. They are refined from crude oils using distillation processes that separate them into different grades based on the number of carbons present in their molecular chains. These grades are generally classified as gaseous fuels (having 1-4 carbons in their molecular chains), gasoline (having 5-12 carbons in their molecular chains), jet fuel, diesel, heating oil (having 12-20 carbons in their molecular chains), lubricating oils (having 20-30 carbons in their molecular chains), fuel oil (having 30-40 carbons in their molecular chains), and petroleum jelly or paraffin wax (having 40-50 carbons in their molecular chains). Although some may argue that petrochemicals are generally low-valued products, both their condition monitoring and quality control are of utmost importance as they can help to

increase their benefits in cost savings, improve their safety levels, and reduce the wastage during the refining process. In particular, quality control of fuels helps to improve the performance of the engine and reduce the wear and tear process of the engine parts, while condition monitoring of the lubricating oils facilitates their timely replacement and ensures the smooth operation of the host rotating machinery. As such, THz sensing has been demonstrated as a viable technology for sensing and analysis of petrochemical products.

H. 1. Crude oil and composition analysis

The application of THz sensing and evaluation of substances in the petrochemical industry has been proven to be an excellent tool for identifying and evaluating the different chemical compositions of crude oils for quality control purposes, and the classification of the different additives used to improve the quality of the different crude oil grades during the refining process. Crude oils, which are unprocessed oils exploited directly from oil wells, are generally brownish-black viscous liquids, which are combustible substances composed of various hydrocarbon grades and other chemicals such as nitrogen, sulfur, oxygen, *etc*. After exploitation from the oil wells, preliminary pretreatment of the crude oil is conducted and then it is transported to refineries for further processing through pipelines. To this end, the evaluation of the crude oils in pipelines is of great importance as it helps to determine their sources, types, and properties for subsequent processing and usage. In this context, Zhan *et al*. [419] used a combination of THz spectral data and multivariate statistical methods (*viz*. cluster analysis and principal component analysis) to identify crude oils collected from different oil fields and measured their properties, and reported accurate results. Additional studies sought to determine the oil content in oil shale [420], [421], the amount of both asphaltene [422] and wax crystals [423] in crude oil in crude oils, as well as the spectral signatures of both crude oils and coal tar [424], [425], *etc*. Additionally, THz technology has also been used to measure the amount of water content in crude oils, thanks to the strong THz absorption levels of water molecules. Jin *et al*. [426] achieved high precision measurements of low water content ranging from 0.01-0.25%, while Guan *et al*. [427] developed micron-grade samplers for the THz spectroscopic system and used them to evaluate relatively high water content ranging from 1.8% to 90.6% in crude oils. In a recent broader and more detailed study on crude oil composition measurements, oil contamination by both liquid and solid particle contamination such as water and sand was investigated and accurate concentrations of both were reported [428]. In another study [429], water, gas, and oil contents and their distribution in high-water-cut crude oil were accurately evaluated using THz spectroscopic system. The authors posited that this type of evaluation is highly important to examine the quality of crude oils, particularly the crude oils extracted from watery oil fields such as swamps, lakes, and oceans. Taken together, all these studies indicate that the THz-SI is indeed a promising NDT tool for qualitative and quantitative analysis of petrochemical products, hence, an alternative approach to complement conventional NDT methods.

H. 2. Analysis of fuels and additives

In recent years, the use of THz technology for the analysis of molecular properties and qualitative/quantitative evaluation of petrochemical products has been extensively demonstrated. In particular, researchers demonstrated that the dielectric properties of petrochemical products mainly depend on the number or the arrangements of their hydrogen bonds, the relaxation process of their dipoles, as well as their inter- and intra-molecular interactions [418]. Upon applying an external electric field, the electron cloud in non-polar molecules tends to move from lower to higher electric potential sides and this movement results in the formation of induced dipoles. Additionally, non-polar molecules will also generate additional transient dipoles even without any external electric field being applied due to factors such as the collision between the molecules and their chaotic motion in the material/substance, as well as changes in the relative positions of the nuclei and electrons of their different atoms, *etc*. [418]. In general, petroleum is a very complex mixture of carbon and hydrogen atoms and its main components include alkanes, cyclones, and aromatic hydrocarbons. For example, alkanes are non-polar molecules with a generic chemical formula of $C_nH_{2n}C_2$, and hence, great candidates for THz-NDT inspection. Under ambient pressure and temperature conditions, alkanes usually have three states *viz*. solid (C_{17} and above), liquid (C_5-C_{16}), and gas (C_1-C_4), [418], and their dielectric and optical properties [430]–[432], as well as their vibrational modes at the ambient temperature [431] have all been studied in the THz frequency range. In all these studies, the common observation is that their dielectric and optical properties increase almost linearly with the increasing number of carbon atoms, while their absorption coefficients do not have any distinct relationships with the number of carbons in their molecular chains [431]. Liquid alkanes present three vibrational modes *viz*. skeleton, rocking, and torsional vibration where the skeleton vibration is considered their primary vibrational mode in the THz frequency range.

Apart from the study of alkanes, recent studies have also been focusing on the evaluation of dielectric properties of liquid petrochemicals using THz metrology systems. In Ref. [433], for example, Arik *et al.* used the THz spectroscopic system to measure the dielectric properties, indices of refraction, and absorption coefficients of gasoline and diesel in the 0.1-1.1 THz frequency region. Results indicate that these two fuel products are non-polar liquids with weak absorption coefficients (*i.e*., insufficient transient dipole moments generated by weaker molecular collisions), but gasoline has relatively higher absorption coefficients than diesel. To this end, Arik *et al*. noted that one of the most plausible explanations for this difference in absorption coefficients of gasoline and diesel is that shorter gasoline hydrocarbon chains (C_4-C_{12}) present higher collision probability than longer diesel hydrocarbon chains (C_8-C_{40}), which generates more transient dipoles, and higher concentration of the aromatic compounds at which electrons in the p-orbitals give larger contributions to the induced dipole moments compared with the ones in the d-orbitals. Also, these two fuel oils were successfully modeled using the Debye relaxation model to investigate the relaxation dynamics after interaction with the THz electric field. The results indicate that the Debye relaxation time of the molecules in diesel is much faster than that of the molecules in gasoline due to the

differences in their intermolecular forces, hence, different dispersion forces. That is, molecular reorientation is established faster in diesel (*i.e*., faster relaxation of the molecules after the application of the THz electric field) than it is in gasoline due to its stronger intermolecular forces (*i.e*., slower relaxation of the molecules after the application of the THz electric field). Another particularly important feature of the THz spectroscopic systems in fuel analysis is its capability to quantify fuel octane number [434]–[437] and distinguish the different fuel components such as the mixtures of gasoline and diesel [438], different gasoline grades [435], and diesel-engine-road-vehicle fuel, also known as white diesel, road diesel or simply derv fuel oils [436], *etc*. In particular, experiments indicate that fuels with high-octane numbers (*i.e*., fuels with shorter carbon chain lengths) present lower absorption coefficients and refractive indices and are lower than those of low-octane fuels (*i.e*., fuels with longer carbon chain lengths) [15], and this is yet another feature that could be exploited to discriminate between fuels with different octane numbers.

Additionally, THz spectroscopy can also identify and evaluate common additive substances used to enhance the quality and efficiency of liquid petrochemicals. In Ref. [437], for example, the authors used the THz metrology system to evaluate the cetane number in biodiesel-diesel blends, while several other authors managed to accurately measure the concentration of ethanol in ethanol-gasoline mixtures with an accuracy of up to 1% [439], [440]. In the latter case, in particular, it is important to indicate that the addition of ethanol to the mixture strongly increases its absorption coefficient and refractive index of the mixture compared with those of pure gasoline because ethanol is a polar liquid. Also, several types of benzene derivatives such as ethylbenzene, toluene, and xylene which commonly include a significant volume fraction of gasoline have been identified by using the THz spectroscopic system [156]. The concentrations of methyl methacrylate (*i.e*., a kind of fuel additive that is generally used to lower the freezing temperature of diesel) have been detected in diesel down to 0.2% [440]. Likewise, the contamination of fuel by sulfur products was also examined using the THz spectroscopic system, and low concentrations of sulfur in gasoline up to 0.2 ppm were detected [440], [441]. It is important to indicate that the presence of sulfur even at low concentrations increases the THz absorption levels of the target samples, similar to other types of contaminants and/or additives that are not pure hydrocarbons.

In summary, THz waves strongly interact with the intermolecular hydrogen-bond network and this confers to the THz-TDS or more generally the THz-SI the capability to evaluate several types of liquid petrochemicals properties such as their optical and dielectric properties as well as their dynamic behavior such as their molecular vibration and dipoles relation processes. These clear differences in optical and dielectric properties of different fuel grades provide THz systems users with a simple yet effective way to discriminate different types of fuel oils from one another by using THz spectroscopy without any danger of decomposition and/or combustion of the samples. This approach may also be used to determine the quality of fuel oils at different processing stages. Additionally, the strong interaction with unique characteristics between THz waves and liquid petrochemicals offers a methodology for the classification of these products inside the containers, and hence THz spectroscopy is a suitable sensing tool capable of detecting bottled liquid petrochemicals and their additives remotely. In most cases, the application of THz sensing for the evaluation and characterization of liquid petrochemicals has mainly focused on the determination of certain properties such as their dielectric constant, absorption coefficients, and refractive index, and analyzed the inter-/intra-molecular interactions, as well as the molecular/relaxation dynamics of liquid petrochemicals. In addition, both the quantitative analysis and qualitative identification of liquid petrochemicals using THz spectroscopy have been reported either in combination with chemometrics or using THz metamaterial sensing and all the studies have been successful.

H. 3. Analysis of lubricating and insulating oils

In general, lubricating and insulating oils are extracted from petroleum and they contain complex mixtures of different types of hydrocarbons. These types of oils are used to reduce wear rate and the friction intensity between movable metallic joints and their functions include but are not limited to the lubrication, cooling, antirust, cleaning, sealing, and buffering of metallic mechanical and electrical parts. Insulating and lubricating oils generally differ from fuels because their performance critically depends on their specific viscoelasticity or dielectric properties, suggesting that they are generally highly purified and their compositions are tightly specified. Additionally, insulating and lubricating oils are generally degraded or contaminated with impurities over time even in the process of normal operation, and they should be periodically monitored to ensure the timely detection of contamination or degradation and replacement for a continued smooth operation of the lubricated and/or insulated parts [442], [443]. The main performance indices of lubricating and insulating oils include but are not limited to the lubricant's viscosity level, number of saturated hydrocarbon content, and sulfur content level [418], and all these properties can be accurately measured by THz technology.

Consistent with the aforementioned, Naftaly *et al*. [444] were the first to investigate the relationships between THz absorption level, chemical composition, and optical properties of 4 different types of machine oils namely Tonna, HVI 160B, HVI 650, and Risella MH. As part of their compositions, both HVI 160B and HVI 650 are hydrocarbon oils with no additives (*i.e*., the former being a lighter oil with shorter chains, while the latter is a medium-heavy oil with much longer chains). Risella is a light and highly refined type of oil and does not have any polycyclic aromatic hydrocarbons. Tonna is a medium-heavy oil with additives. Using the THz-TDS system, Naftaly *et al*. managed to measure the absorption coefficients of the aforementioned lubricating oils and discovered that the length of hydrocarbon chains had little to no effect on the THz absorption levels. However, the above authors emphasized that both the height and profile of the absorption curves are sensitive to factors such as the degree of refinement and the types of additives used. In a later study, Tian *et al*. [443] analyzed the optical features of 6 different types of lubricating oils using a THz-TDS system in the 0.3-1.6 THz frequency range. The experimental results revealed that lubricating oils are generally

more sensitive to THz waves than near-infrared waves, and present different spectral features that can be used to easily identify them in the THz frequency range. This study also showed that the absorption coefficient of the lubricating oil increases and its refractive index decreases in the presence of gasoline, with contamination levels up to 4% easily detectable.

Engine oil is a particular kind of lubricating oil that consists of complex mixtures of hydrocarbons with a molecular weight between 250 and 1000 UMW (*i.e*., usually in the range of 250-1000 units of molecular weight). To increase its lubricating performance, variable amounts and types of additives are added to achieve different objectives such as inhibiting the oxidation or degradation of the lubricant, decreasing the fluidity point, improving the viscosity index, avoiding foaming or settling of solid particles, *etc*. In 2010, Zhu *et al*. [445] utilized the THz-TDS system to examine the optical properties of 6 different types of engine oils in the 0.6-2.5 THz frequency range. Their results indicate that both the time delay and refractive indices of the engine oils were different but increased linearly with the increasing viscosity, which indicates that engine oils can be easily identified by examining their THz spectral features. In a later study [442], the authors used the THz-TDS system to identify gasoline engine oils with three different grades and viscosity levels in the 0.5-2.0 THz frequency range. The results suggest the existence of a linear relationship between their THz refractive indices and viscosity levels, which also increased linearly with the increasing number of carbons atoms in the molecular chains of the individual grades.

Additional studies have also revealed that THz sensing is sensitive to polar oxidation products in oils (*i.e*., particularly carbonyl and hydroxyl compounds), and can therefore be used to detect these compounds at low concentrations [446]. Also, THz systems have been demonstrated capable of evaluating water contamination and subsequent degradation levels of engine oils where water is a product of fuel burning [447], [448]. All these examples suggest that THz technology can effectively be used to monitor the behavior of lubricating and insulating oils during their oxidation process. Indeed, such an application has already been tested when Nishimura *et al*. [449] used the THz system to study the molecular behavior of alkylbenzene (*i.e*., a type of insulating oil for ultra-high voltage cables) during the oxidation process. In their study, the authors evaluated the oxidation process of this insulating oil under different conditions (*i.e*., open air, under oxygen flow, under nitrogen flow). Their results indicate that there was a significant increase in the absorption coefficient of alkylbenzene degraded by heating in the open air and under the presence of oxygen in the frequency range between 6-7 THz, but did not see any significant change in the insulator's absorption coefficient when heated under the presence of nitrogen. To this end, they inferred that this increase in the absorption coefficient in the air and under the flow of oxygen was caused by the presence of hydroxyl groups from the oxidation process, and further added that the benzene ring in alkylbenzene could also have affected its absorption characteristics. They concluded that the absorption band reflects the degree of hydrogen bonding, and can be used as an efficient indicator in the sensing and/or NDT of the aging degree of the insulating oils.

I. Applications in the agriculture and food industry

Agricultural and food commodities are available in a wide range of varieties in terms of type, chemical contents, size, shape, color, *etc*. and as their market grows more demanding, agricultural and food products are subdivided into numerous categories based on their market segments. To this end, the definition and characterization of different attributes of agricultural and food products are very important not only for business flexibility but also for consumer or customer satisfaction purposes, making it compulsory for agricultural and food industries to establish the norms of standardization and classification to make commercial trading more efficient and promote higher awareness to the of consumers. This is crucial because factors such as the demand for good and better quality food and agricultural products at a lower cost and consumer awareness are all considered the most important factors toward achieving the implementation of reliable, efficient, accurate, and low-cost methods as well as effective monitoring and evaluation of safety and quality requirements in food industries [450]. To this end, researchers have demonstrated that THz imaging is capable of revealing defects in agricultural and food products and distinguishing between live and dead insects. Researchers also indicated that combining chemometric methods with the THz metrology system can easily help users not only accurately discriminate between transgenic and nontransgenic seeds, but also to detect harmful substances such as poisonous plants and pesticides [4], and up to 100% classification results for genetically and non-genetically modified crops have been achieved [4], [450]. In recent years, THz spectroscopy has also been used for the detection of buried organic objects and heavy metals in the soil, and more recently studies detailing the use of THz technology for the detection and evaluation of pesticides and other harmful compounds in crops have been published. In more innovative NDT approaches, THz technology has proven to be an accurate NDT technique for the evaluation of drought stress, quantities of water content in plant leaves, and crop yield as well as distinguishing between flowers, leaves, and fruits.

As indicated earlier, THz metrological systems have been used to evaluate the quantity of water content in plant leaves and discern the drought stress response in plants. In general, water is an essential nutrient in leaves and it is involved in most of the physiological processes taking place in the plants. To this end, monitoring the levels of water content in plant leaves has a vital role as it helps farmers to describe the growth, and productivity of crops, as well as the management of the irrigation systems and the planning thereof. The study of water content levels in plant leaves by the THz technology is enabled by the high sensitivity and absorption of THz waves by the water molecules in plant leaves as well as their penetration properties in watery plant leaves [451], [452]. Although THz technology may seem to be an effective NDT technique for the monitoring of water content levels in plant leaves, the process still presents several layers of hurdles including finding the different transmission and absorption spectra for different water content levels of plant leaves, and this makes accurate quantification of water content levels in plant leaves difficult. Experts believe this problem can be solved by combining THz technology with chemometric or advanced mathematical

modeling methods [4]. Using any of these combinations may also e difficult because the combination with chemometric methods requires an extensive investigation into different chemometric methods to determine the most efficient model for a particular leaf, while the combination with advanced mathematical modeling requires advanced mathematical and modeling knowledge. This shows the need for additional research into the prediction of water content levels in plant leaves and plant species, particularly for high-water-content crops under drought or dehydration stress in the field.

In addition to the applications involving the detection of water levels in plant leaves, THz technology is also used for the investigation of soil and soil material contents [453]. In particular, soil texture (*e.g*. particle distribution, particle size, *etc*.) generally influences the shape of the THz transmission signals due to the Mie (more dominant for small particles) and Rayleigh (less dominant for small particles) scattering effects. In a recent study [454], Lee *et al*. used the THz system at a frequency range between 0.2-2 THz to explore the effect of both the soil particle size and moisture content on the overall extinction coefficients of 3 different types of soil materials. They observed that the extinction coefficients of their soil samples varied with the porosity levels and particle sizes as well as their distribution within the soil samples. As part of their conclusions, they indicated that the Mie scattering effect was mainly responsible for this type of variation because the dimensions of the wavelengths of the THz radiation were almost similar to those of the soil particles in their samples. Lee *et al*. also indicated that the presence of higher water content levels in their soil samples significantly affected the intensity of transmittance or THz absorption levels and increased the extinction coefficients of the soil samples.

Although the THz-SI is considered a promising NDT tool for soil remote sensing applications, its detection accuracy should be improved by using more powerful THz sources and more THz sensitive detectors to counter issues related to limited soil penetration capabilities of THz waves which currently stand at 2 mm below the surface of the sand layers [4]. Also, there is still a pronounced limitation in applying THz technology for soil measurement applications because of the scattering of THz waves by the soil particles, soil ingredients as well as their inhomogeneous distribution which cause variations in the refractive index of the soil (*i.e*., low reproducibility of refractive index data) and adversely affects the quality monitoring process. It is believed that the low reproducibility of the technique can be eliminated by using the absorption spectra of diluted soil samples [455] or soil sensors with wedge sample holders that can accurately align soil samples for accurate measurements [456] but additional research is clearly needed to solve all the difficulties related to soil penetration, instrument spatial resolution limitation, as well as the influence of particle size and soil ingredients to guarantee accurate THz evaluation of some important physical soil properties such as soil texture, composition, and contamination levels, *etc*. Although pesticides, insecticides, and herbicides increase crop yield and prevent agricultural and food products from contamination, as well as damage by pests and insects, these chemicals also create adverse environmental pollution and health hazard. As such, the detection of pesticide, insecticide, and herbicide residuals is thus very important to provide safe food to consumers and several studies have used the THz technology for this type of detection and reported accurate results [457]–[459]. Additional applications include seed characterization and classification of crops [460]–[462], discrimination of the origin, types, or varieties of crops, as well as the discrimination between the genetically and non-genetically modified groups [463]–[465], identification of microbes and toxins in agricultural and food commodities [466]–[469], quality control, adulterants, and additives detection applications [470]–[472], food spoilage monitoring [361], contamination by foreign materials and defects identification [6], [473], crop yield and water content levels estimation [4], *etc*.

In summary, THz-SI systems have been proven capable of performing both qualitative and quantitative evaluations of agricultural and food products in the agriculture and food sectors, respectively. These techniques are primarily used to identify defects, monitor water levels, and soil characteristics, and detect and evaluate the quantity of pesticides and harmful chemicals present in food commodities, transgenic seeds, and poisonous plants. THz spectroscopy has also been used for soil inspection and detection of heavy metals and deeply buried objects in the soil. Also, recent technological advances have enabled the development of powerful THz sources and detectors, which subsequently enabled THz users to obtain high-resolution images through ultra-fast scanning methods. To date, researchers can differentiate between fresh and old leaves using these new THz technologies. These technologies can also help researchers to monitor the water status levels in plants, and estimate crop yields, which enable farmers to take subsequent actions such as irrigation and harvest planning and control. Although THz technology has been proven to be an effective tool that could help farmers to achieve adequate soil inspection and quality control of their agricultural products, the technique still presents several layers of limitations including a low limit of detection for pesticides, low spatial resolution, limited application to products with high moisture content levels, the limited penetration depth of THz waves, high thickness-dependency, scattering of THz waves, relatively low SNR, the effect of particle size and plant surface or fruit roughness, variations in the workable standoff distance (especially for high-water-content crops), high-cost of THz installations and very application-specific, *etc*. Interestingly, researchers around the world are currently working to overcome all these limitations and increase the technology's industrial and practical applications to ensure its economic benefits are significantly transcended into the agricultural and food sectors. Typically, new developments are now focusing on extending the applications of THz systems in the agriculture and food industry by developing more rugged, sensitive, and portable THz systems, decreasing the cost of THz technology and its enabling devices (*e.g*. THz spectrometers, detectors, and sources, *etc*), building a THz database for fast and reliable signal processing techniques (*e.g*. machine learning, deep learning, *etc*.), improve the instruments' efficiency and SNR features, and increasing the instruments' hardware and software performances. The development of new metamaterials and devices is also being constantly introduced to enhance the sensitivity of THz-SI systems for various real-time sensing and NDT applications in the agriculture and food industry.

J. Applications in the biomedical field

Applications of THz sensing in the biomedical field have been rapidly growing in recent years [9], [474], owing to the intermediate properties of THz waves between μ-Waves and IR such as the spectral fingerprints of biomolecules, biosafety, *etc*. [474]. For example, the energy of THz photons is relatively low, which makes these nonionizing and nondestructive waves great candidates for biomedical studies, medical diagnosis, and non-destructive quality control of complex biomolecules [475]. Additionally, THz waves are strongly absorbed by intermolecular bonds such as the N-H bonds present in proteins and hydrogen bonds present in water molecules and while the biomolecules have limited absorption of THz waves. This means that THz waves are very sensitive to subtle changes in biological tissues such as the increase in blood flow or water content in these tissues [474] due to factors such as the presence of disease, physiological changes, or tissue abnormalities [476]. In particular, the hydrogen-bond network in water presents several broadband relaxation modes at different frequencies in the GHz and THz bands. In the THz frequency range, in particular, these broadband relaxation modes are the root cause of high THz permittivity and THz absorption levels that makes THz waves sensitive to water molecules in watery samples and aqueous solutions [477]. This feature of THz waves combined with their penetrating capabilities and their relatively high spatial resolution (*i.e*., generally in the μm range) make THz spectroscopy a promising NDT tool in the biomedical field [478]. In the biomedical field, in particular, this technology is specifically used to detect several types of biomolecules (*e.g*. amino acid and polypeptide, deoxyribonucleic acid (DNA), *etc*.) from their THz spectral characteristics [479] or diagnose different types of diseases by visualizing the contrasts between healthy and diseased tissues (*i.e*., for both *ex-vivo* and *in-vivo* spectroscopy and imaging) [49]. In most studies focusing on the diagnosis of cancer tissues, for example, excised tissues are tested using THz-SI systems and the obtained results are compared with gold-standard histology for validation and accuracy verification. In most cases, the measured THz results strongly agree with those of the gold-standard histology, and this demonstrates the efficacy of THz-SI systems for biomedical applications.

In the early 2000s, Fischer *et al*. [480] were among the first researchers to utilize the THz spectroscopic system to record the vibrational modes of the four nucleobases, *viz*. guanine (G), cytosine (C), adenine (A), and thymine (T) and their corresponding nucleosides that constituting the building blocks of the deoxyribonucleic acid (DNA) molecules. The results indicate that the THz spectrum of each of the aforementioned molecules features a series of resonances within the 1-3.5 THz frequency range (Figs. 18(a-b)). In a later study, Zhang *et al*. [481] measured the strong THz absorption fingerprints of DNA molecules using THz photo-mixing spectrometer with a custom conical-horn coupling (Figs. 18(c-d)). In their experiments, the above authors used a linear, single-stranded (ss), 13-mer polynucleotide DNA specimen that was diluted in buffer solution to have a concentration of about 0.15 μmoL/mL. Their results indicate that a solution with ssDNA molecules cross-linked up to 0.48% exhibited the strongest THz absorption coefficient centered around 0.717 THz and with the strength, linewidth, and damping time of about 2.5×10^{16} cm^{-1}/moL, 0.048 THz, and 6.6 ps, respectively. The above authors indicated that their method was extremely sensitive and easily enabled the analysis of the trace amount of their cross-linked ssDNA samples up to 1.29×10^{-5} nmoL in a small volume of about 0.0355 μL. The signature obtained at 0.72 THz could be attributed to the random cross-linking between two ssDNA strands in the solution, the presence of local hydrogen bondings, or a single strand self-bonds by looping. Interestingly, the obtained THz signature characteristics were consistent with *prior* FTIR experimental results conducted on elastic lattice models and Na-/Li-DNA salts [482]. In another study [483], Tsurkan *et al*. used 2 different THz spectroscopic methods, *viz*. High Q cavity (H-Qc) frequency synthesizer and Backward-Wave Oscillator (BWO), to analyze the degradation levels of DNA molecules in herrings (*i.e*., silvery fish that is most abundant in coastal waters) based on their THz spectral information. Their results indicate that DNA molecules of herrings present specific absorption peaks at different lower THz frequencies including 306 GHz, 339 GHz, and 375 GHz. Apart from providing them with important guidelines for an effective and accurate structural analysis of the herrings' DNA molecules, this information also provided them with a novel and more accurate methodology to analyze the structural integrity of DNA molecules using THz spectra. Recently, Tang *et al*. [484] successfully developed a novel method that accurately performed a label-free analysis of single-base mutations in DNA molecules, while Yang *et al*. [478] highlighted successful detections of several types of biomolecules including amino acids and polypeptides, proteins, protein dynamics, as well as DNA and changes in DNA characteristics by THz-SI system. In Ref. [485], the authors indicated that molecular resonances in aqueous solutions of genomic DNA from cancer cell lines could be monitored using THz-TDS systems, and the quantification of the resonance signals could lead to accurate identification of cancer cells with some level of DNA methylation as indicated in Figs. 18(e-f). This demonstrates that DNA molecules in cancer cells also present specific THz fingerprint spectra, a feature that could be used to diagnose cancers at the molecular level [486] and/or treat cancer (*i.e*. effective demethylation of melanoma cells) using THz waves [52].

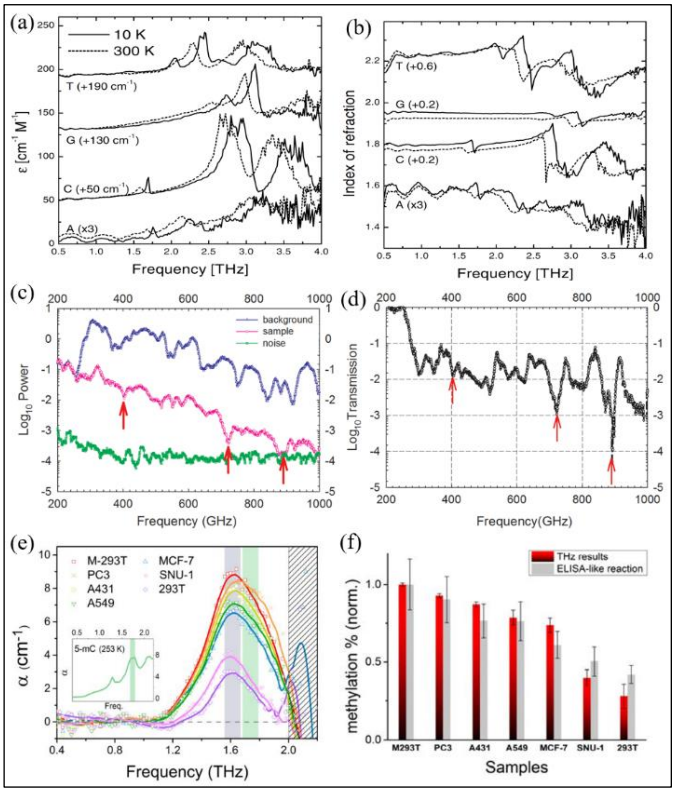

Fig. 18. (a) The absorption coefficients and (b) indices of refraction of the nucleobases A, G, C, and T recorded at temperatures equal to 10 K and 300 K, indicated by solid curves and dashed curves, respectively [480]. The THz spectra of μL of DNA solution: (c) background, sample, and noise floor, and (d) THz transmission spectrum of the sample with locally cross-linked ssDNA molecules after the removal of the background noise effects [481]. (e) THz resonance peaks for different DNA samples after the baseline correction, which indicates that the genomic DNA from different types of cancer cells (A549, MCF-7, PC3, A431, and SNU-1) presents the same resonance peak at 1.67 THz [485], and (f) the corresponding THz and ELSA-like reaction results demonstrating the degree of DNA methylation in each of the above DNA samples [485].

In addition to the detection and characterization of biomolecules, recent applications also suggest that THz-SI is potentially an effective method for cancer diagnosis. An effective liver cancer diagnosis has been reported in Ref. [487] where the authors used THz spectroscopy to examine large areas of tissue specimens using a wide range of wavelengths. The results highlighted the existence of a significant contrast of liver cancer tissue imaged by the THz transmission imaging at 3.6 THz. In a later study [488], the authors used THz pulsed imaging system to study the tissues of oral cancer at 0.2-1.2 THz. Their results indicate that not only does the THz imaging of frozen cancerous tissue offer greater sensitivity in distinguishing the cancerous areas from the surrounding areas than regular histological examination systems, but they also revealed that there is a larger THz-frequency spectral difference between the cancerous and normal samples imaged at room temperature. In another study, Rahman *et al*. [489] used THz systems with different configurations to identify features in human skin biopsy samples diagnosed for basal cell carcinoma (BCC) and compared them with healthy skin samples. The latter exhibit regular cellular pattern 3D images while the BCC skin samples do not have regular cell patterns.

In Ref. [490], the authors proposed a THz-SI-based cancer diagnosis method capable of distinguishing the vertical and horizontal transverse sections of breast cancer tissues to depths over 1 mm. THz-SI has also been used for the diagnosis of prostate, skin, gastric, colon, and liver cancers, *etc*. [49], [478]. An earlier study [491] used the THz system to identify human breast cancer tissues based on their optical properties and reported that cancerous samples presented higher absorption coefficients and refractive indices in the 0.15-2.0 THz frequency range. The continued popularity of artificial intelligence techniques such as machine learning and deep learning has also extended their applications in cancer diagnosis where they are used to examine THz data for automatic cancer cell detection. In Ref. , for example, the use of machine/deep learning algorithms for the automatic detection of breast invasive ductal carcinoma (IDC) cells from THz spectral information has been demonstrated using three different types of machine learning methods *viz*. support vector machine (SVM), k-nearest neighbor (kNN), and ensemble. The results indicate that all these algorithms scored more than 0.89% with the ensemble algorithm reaching a precision of up to 92.85%. These results are particularly interesting because the best breast IDC identification systems currently present the estimated performances in terms of specificity, sensitivity, and precision of about 96.67%, 89.66%, and 92.85%, respectively, making the the use of machine learning algorithms to analyze THz-SI data an effective biomedical NDT tool for the detection and evaluation of different breast tissues [492]. In addition to the detection of cancers, THz-SI is also an important sensing and/or NDT tool in many biomedical applications including but not limited to continuous monitoring and assessment of the severity and extent of burn injury [493], the study of the effect of hydrofluoric acid on osseous tissues [494], the study of dental caries [495], water content level in organs, and *ex-vivo* porcine corneas [496], the classification of bacterial colonies [497], and the diagnosis of diseases such as diabetes [498], [499], *etc*. Although the biomedical applications of THz technology have been extensively studied considering the examples provided in this section of the paper, studies examining the biological effects of THz radiation on living organs, biomolecules, cells, and tissues, are still warranted to provide related qualitative and quantitative information [500] before applying THz technology in clinical practices for therapeutic and diagnostic purposes.

In summary, the biomedical applications of THz technology span a wide range of scale examinations and diagnostics from molecules to cells and tissues in both *in-vivo* and *ex-vivo* applications, particularly for the qualitative and quantitative analyses of biomacromolecules, the detection, and recognition of tumor cells, biomarkers, traditional herbal medicines, as well as the monitoring and treatment of burn injuries and dental caries, *etc*. To this end, several topical review articles have been presented detailing these applications, including topical reviews on THz cancer diagnosis [500], [501], human skin analysis and characterization [502], as well as other more general reviews on biomedical applications in refs. [476], [478] and interested readers are directed to these studies for more

information. Although the applications of THz technology in the biomedical field have been thoroughly successful, there are still no technical standards governing the procurement of THz signals in the biomedical field, with great effort currently being invested into the development of high-performance THz instrumentation, the improvement of signal processing techniques, as well as the investigation into the effects of THz radiation on biological tissues, living organisms, cells, and biomolecules, *etc*. To date, the technology's key bottlenecks still appear to be the THz image acquisition speed and registration processes, whereby long measurement times often lead to a systematic shift in the measured THz data and jeopardize the accuracy and consistency of the measurements [478], [479]. In fact, researchers argue that these bottlenecks could render the discrimination between the diseased and healthy tissues challenging given the dependency of the accuracy of these types of measurements on water content levels in the specimens. Also, the slower the inspection or measurement process, the longer the target subject must remain fixed in place or standing still, in good contact with the system's measuring window, and at the same distance with respect to the positions of the THz detector and emitter. This is particularly important because any changes occurring in these parameters during the measurement will create significant knock-on effects on the quality and effectiveness of the image registration while equally exacerbating the issues of temperature and pressure whose effects have not yet been fully examined in the THz frequency band. Improvements in THz imaging speed and the continued quest for the development of near-video or photograph rates THz imaging systems could help to dispel some of these pressing issues, and several research groups worldwide are already working on the development of such systems [503]–[505]. Additionally, near-video or photograph rates THz imaging systems would also enable multidimensional imaging of transient events to reveal some of the most important ultrafast mechanisms governing some of the transient biological and/or physical processes, thereby overcoming the issues of THz image acquisition speed and registration processes for effective biomedical applications of the THz technology.

K. Applications for safety and security inspections

The use of spectroscopic systems for the detection of trace quantities of explosives and different kinds of energetic materials and substances has become a high priority in public safety, defense, and global counter-terrorism industries [506], [507]. The detection/identification of these types of substances is particularly crucial to the protection of human lives, properties, and infrastructure [508]. In many different countries around the globe, law enforcement forces are often encouraging scientists and researchers to develop effective systems to detect and identify explosives concealed in public places such as airports, railways, or bus stations. The development of analytical tools to analyze the remanence of explosive substances is also important for forensic analysis of explosions and criminal investigations after successful terrorist attacks or criminal acts. Apart from the detection and analysis of explosive materials/substances, additional applications of THz sensing in safety and security inspections also include soil pollution, water contamination, and air contamination, as well as the analysis of health problems caused by the exploded explosives. All these applications are extremely important for the safety and security of people and goods, and the development of faster, more selective, and more sensitive THz systems to detect concealed explosives and their remenances, and analyze contaminants and dangerous materials is vital to guarantee the safety of humans, animals, and objects/properties.

In 2015, Sleiman *et al*. [509] used the THz-TDS to measure the absorption spectra of different types of explosives including pentaerythritol tetranitrate also known as penthryte (PETN), hexahydro-1,3,5-trinitro-1,3,5-triazine also known as hexogen (RDX), and their mixtures and predict their relative contents in the samples. Although this analysis was challenging because significant spectral overlap prevented the identification of the spectral fingerprint of each type of explosive in the mixture, the authors managed to get rid of the overlapping of important spectral lines by using the series of partial least squares regression models and successfully predicted the concentrations of PETN in mixture samples. In a similar study, Rahman [510] used the THz-TDS system to characterize the 2,4,6-trinitrotoluene (TNT), PETN, and RDX. The samples were prepared by mixing each of these explosives with methanol to obtain solutions of 1 mg/mL. The test results indicate that both the intensity and shape of the time-domain signals for each explosive were distinctively different, and these unique characteristics enabled them to easily detect and identify the different species (*i.e.*, within each spectral signal having distinct absorption peaks that are used to identify the different species). In another study, Palk [511] used the THz spectral signals obtained from a THz system configured in transmission and reflection (*i.e*., specular and stand-off) modes to detect pure samples made of different types of explosives, *viz*. RDX, 1,3,5,7-tetranitro1,3,5,7-tetrazocine also known as octogen (HMX), PETN, their mixtures (RDX+PETN and RDX+HMX), and simulants (sugar, 4-aminobenzoic acid (PABA), and tartaric acid) in the in 0.1-3 THz frequency range. The measured peaks absorbance values of all the substances were closely related to the calculated values of their reflectance characteristics, which further confirmed the capabilities of THz-NDT to detect and identify different types of explosives.

In 2014, Choi *et al*. [512] used the THz-TDS system in reflection mode to analyze nitramine explosives (HMX and RDX) in the 0.3-3 THz frequency range. The samples were prepared using pure explosives without any additional additives or binders. The results indicate that the primary absorption peaks were found at 0.84, 1.08, 1.50, 1.92, and 2.30 THz for the RDX samples, while those for HMX samples were found at 1.75, 2.50, and 2.90 THz. Interestingly, both the RDX and HMX samples presented completely different spectra in the THz frequency range, which made it easier for the authors to distinguish them. In another study [513], the above authors also presented an additional set of experimental results where they managed to detect and identify different explosive species using the THz-TDS system. The samples were composed of a 60% RDX and 40% TNT mixture (S-A) and a 70% PETN and 30% TNT mixture (S-B). The authors collected the THz spectra for both samples and proposed a novel signal-processing method for *in-situ* detection of compound explosives using the THz-

TDS system. Their signal processing method achieved a 22.7% and 48.8% noise reduction for S-A and S-B, respectively. In addition to obtaining accurate results, the authors also pointed out the important factors to be considered when using the THz-TDS system for explosive detection, which could be used as the guideline for accurate detection and identification of explosives for safety and security-related applications. In 2015, Puc *et al*. [514] examined the effect of different background noises on the spectral features of different explosive simulants and developed a signal-processing method to enhance the detection accuracy of the THz-TDS system. They developed a new methodology to detect explosive materials by combining the organic-crystal-based THz-TDS and the spectral peak analysis method and demonstrated that hidden simulants can be quickly and accurately detected and identified using this method in the 1.5 to 4.0 THz frequency region. In an earlier study, Liu *et al*. [7] analyzed the absorption spectrum of the RDX obtained from the THz reflectance spectrum and managed to distinguish this type of explosive from other materials (*i.e*., the RDX was easily identified by using the THz diffuse reflection measurement even when the RDX sample was covered with certain optically opaque materials because of its strong absorption at 0.82 THz). In 2007, Chen *et al*. [515] used the THz-TDS system to study the absorption spectra of 17 different types of explosives in the 0.1-2.8 THz frequency range. Their results indicate that the explosives presented specific THz absorption characteristics that could be used to establish a relevant database for these types of explosives and used as a reference for future detection and identification practices. In another study [514], Puc *et al*. also considered that these types of explosives are usually concealed, and went on and studied their absorption spectra under different types of cover materials to prove that the THz system can indeed be used to accurately detect and identify hidden explosives. They used RDX and HMX samples covered by cotton, plastic, and leather and their results indicate that the THz transmission spectra of these two explosives strongly agree with those of the samples alone in the 0.1-3 THz frequency range, and further confirmed that barrier materials that are transparent to THz waves would not obstruct the detection and recognition of explosives.

In the actual security inspection, it is important to understand that samples are generally not single-component explosives but rather a mixture of explosives or illicit drugs. To this end, more robust methods should be developed to guarantee accurate inspection results, and subsequently the safety and security of people and their goods. In 2011, Chen *et al*. [516] proposed a THz spectral uncertainty analysis based on a micro-genetic algorithm to detect and identify the original pure explosives, related compounds, and concentrations in the mixture from these known spectral data of the pure explosive components (*i.e*., application of an intelligent computing method to the analysis and optimization of the THz spectral data of mixed explosives). Their results indicate that the mixture of p-toluic, o-toluic acid, and benzoic acid acids was analyzed and each of these species was detected and accurately identified. Recently, Trofimov *et al*. [517], [518] proposed several methods to accurately analyze different types of explosives using THz spectroscopy and evaluate their spectral dynamics. In Ref. [518], for example, the above authors devised an efficient THz system and used it to detect and identify different types of substances in ternary explosive mixtures with similar THz spectral properties and reported highly accurate results. In addition to the detection and identification of explosives, other applications of THz technology in safety and security inspections involve the detection of different types of contrabands such as illicit drugs [38], [519], [520], concealed dangerous objects or weaponry [521], [522], whereby the measured THz images and/or spectral signals were processed and analyzed for the rapid detection of concealed firearms and knives [520]. As the development of THz-SI systems for security screening applications continues to mature into the establishment of robust, industrially rugged, and reliable NDT tools, the state-of-the-art THz security inspection equipment is constantly emerging and put into practical applications for adequate detection and analysis of illicit drugs, concealed weapons, and explosive materials [521], [522].

In summary, the use of THz-NDT to detect and identify explosives from various sources has attracted considerable attention in recent years and researchers concur that this technique has been proven to be ideal for real-time analysis of trace amounts of explosives with high resolution, selectivity, and precision, and the fact that it does not require extraneous sample preparation routines is another added advantage [506]. Although the feasibility of the approach has thoroughly been demonstrated in safety and security inspections and accurate detection of trace amounts of explosives has been reported, additional studies are still warranted to help THz users to understand not only the effect of different barrier materials on the detection capabilities of the THz systems and also their respective properties and features that could be obtained from the measured THz spectral profiles [514]. Also, current THz spectroscopic systems allow the collection of spectral information in a narrow THz window which limits their capabilities in the detection of explosives and chemicals whose spectral information might not be distinctively extracted in this narrow window. In this range, many explosives compounds and substances may appear to be similar, hence, this frequency range is technically not sufficient to distinguish explosive materials from their matrices. As such, the use of a wider THz bandwidth is expected to identify the salient features unique to each molecule of the explosives in the acquired THz spectrum such as their roto-vibrational fingerprints/transitions [82]. Also, since the reflected THz signals of hazardous or explosive materials are generally weak and strongly depend on the quality of the surface of the host objects, THz measurements usually require a more sensitive arrangement and advanced signal processing methods to achieve reliable detection results. To avoid the problems caused by peak broadening, waveguide-based time-domain spectroscopic techniques can be employed in which crystal planes are highly oriented to incident THz waves. It is believed that the continued development of more advanced THz systems will open up newer and more precise applications, as the quest and the implementation of fast, accurate, and reliable THz detection systems continue to grow.

IV. Metamaterials-enhanced THz spectroscopy and Imaging

Although THz-SI offers great advantages in the detection and analysis of substances and structural features in different types

of specimens, this technique is also subject to some limitations. Typically, THz waves have longer wavelengths compared to γ-ray and X-rays, and this implies that their sensitivity and resolution are not high enough to facilitate the detection and evaluation of small and trace amounts of samples in THz sensing and/or NDT applications. To solve the problems related to the sensitivity and resolution of THz-SI systems, researchers have proposed the use of THz metamaterials to improve the quality of the interaction between THz waves and the target samples, and subsequently the sensitivity and resolution of the THz-SI systems [30], [523]. These are artificial media structured on a size scale smaller than the wavelength of the external stimuli (*i.e*., subwavelength unitary structures), which exhibit both the strong localization and enhancement of electromagnetic fields and provide novel tools used to significantly improve the resolution and sensitivity of THz sensors and open up a whole range of new opportunities in the THz sensing/NDT practices [9], [30], [524]. The distribution of the design parameters of THz metamaterials unitary structures normally follows an arbitrary or specific spatial arrangement to achieve the desired physical properties (*e.g*. super transparency, super absorption, negative permeability, negative permittivity, zero refraction, negative refractive index, *etc*.) that cannot or are generally difficult to obtain from natural materials and/or by using traditional technologies [9], [30]. In THz sensing and NDT applications, rationally designed metamaterial units are used to enhance and/or make the resonance signals with THz waves appear as needed, thus providing THz technology with higher sensitivity for the detection and evaluation of substances and materials.

The history of THz metamaterial systems can be traced back to the early 2000s when Yen *et al*. from the University of California in Los Angeles [169] first demonstrated this technology where they demonstrated that inherently nonmagnetic metamaterials can exhibit magnetic response at THz frequencies, thereby increasing the possible range in which magnetic and negative-index materials can be achieved by roughly two orders of magnitude. Since then, the technology has expanded rapidly and it now touches many areas from fundamental science to real-world applications. Today, metamaterial-enhanced THz spectroscopy is recognized as one of the emerging technologies, and its main applications include but are not limited to food safety analysis, detection of biomolecules in biomedicine, detection of chemical substances in environmental monitoring, material characterization, seeds, and soil characterization in the agricultural industry, safety inspection, *etc*. Fig. 19 illustrates the major applications of metamaterial-enhanced THz technology and the roadmap of some representative state-of-the-art THz metamaterial systems created in the past decade.

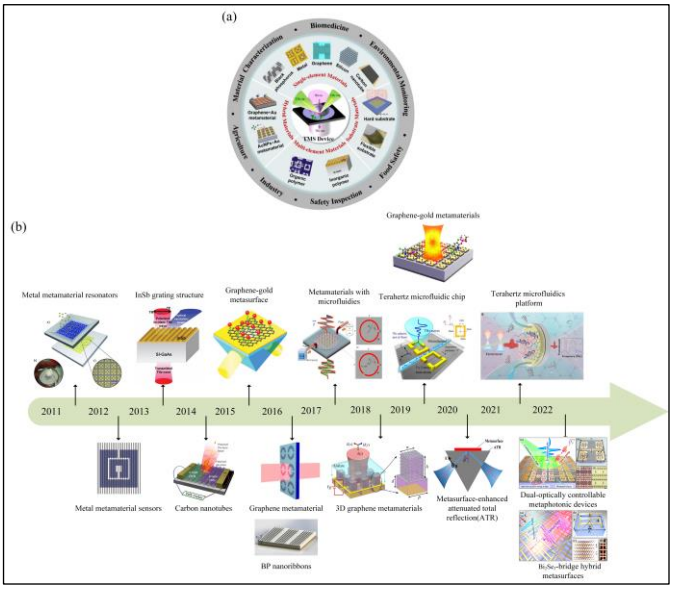

Fig. 19. Illustration of the (a) major applications of metamaterial-enhanced THz technology, and (b) the roadmap of some representative state-of-the-art THz metamaterial systems created in the past decade [30], [185], [188], [525]–[537].

A. THz metamaterial sensing and testing in biomedical science and engineering

The metamaterial-enhanced THz spectroscopy has a wide range of practical applications in biomedical sensing related to the detection of complex biomolecules such as DNA molecules, and proteins, the detection of other biological microorganisms such as viruses, and bacteria, as well as in medical diagnosis for the detection and evaluation of cancer cells, owing to its capabilities of ultra-trace amounts and collective vibration modes detection of many complex biomolecules in the THz regime. For example, Yang *et al*. [538] designed a planar array featuring highly sensitive Au-based SRRs and used it to discriminate transgenic and wild-type genome DNA molecules as illustrated in Fig. 20(a), while Park *et al*. [539] used the same type resonators to perform a highly sensitive detection of viruses as depicted in Fig. 20(b). Although THz metamaterial-based sensing provides good sensing results in biomedical applications, the main challenge in these types of applications relates to the limitation caused by the strong absorption of THz waves by polar solvents and physiological liquids, which prevents THz users from extracting accurate sensing information for solute molecules [2]. To address this challenge, researchers integrated THz metamaterial sensors with microfluidic technology, which allows a small amount of liquid to pass through and enhances the detection capabilities of the THz metamaterial sensor [2,64]. Applications involving this type of configuration were tested by Geng *et al*. [531] who proposed an Au-based THz metamaterial biosensor integrated with a microfluidic channel (*i.e*., a THz-SRR metamaterial system integrated with microfluidic technology depicted in Fig. 20(c)) to detect glutamine transferase isozyme II (GGT-II) and alpha-fetoprotein (AFP) which are the biomarkers for liver cancers/tumors. Their results indicate that they managed to accurately detect lower concentrations of the aforementioned

substances with their respective concentration estimated at 0.02524 μg/mL and 1 μg/mL, which indicates that the THz systems could be used to detect these types of tumors at their early stages. Apart from the integration of the THz metamaterial system with microfluidic technology, another well-known technique capable of overcoming or minimizing the absorption of THz waves by polar solvents is the use of the THz time-domain ATR (THz-TD-ATR) technique as first presented by Hirori *et al*. in 2004 [540]. In this design, a dove prism is inserted into the THz beam (Fig. 20(f)), which generates traveling evanescent waves on the surface of the designed dove prism [541]. The change in the reflection and phase due to the interaction between THz waves and the target sample placed near the prism are evaluated by comparing the TDS signals measured with and without target samples in place. In this context, it is easy to study the dynamics of the solute molecules as a function of characteristics such as their hydration levels [542]. As opposed to several picoseconds in bulk water, the hydrating water molecules are generally bound to the surface of the biomolecules with a relaxation time of up to 10^{-7} s which is long enough to enable THz users to evaluate the dielectric constant and subsequently the hydration number of the target biomolecules at THz frequencies. The feasibility of the THz-TD-ATR technique in biomedical applications has been extensively demonstrated in the literature [543]–[546] and the accuracy of the reported results indicates that THz-TD-ATR is undoubtedly an important sensing/NDT technique for biomedical applications.

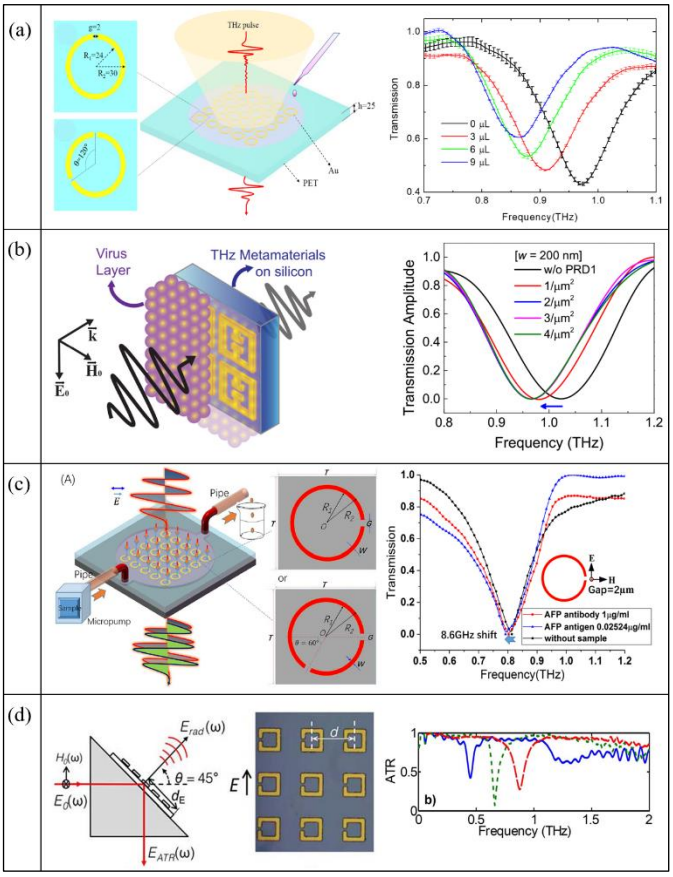

Fig. 20. Examples of ordinary and noble metal-based THz metamaterials used for the detection of complex biomolecules in biomedical science: (a) a planar array of Au-based SRRs [538], (b) THz-SRRs with nanogap widths [539], (c) an Au-based biosensor chip integrated with a series of microfluidic channels and examples of THz spectral signals of liver cancer antibody AFP (1 μg/mL) and liver cancer serum antigen (0.02524 μg/mL) detected using SRR structures with 2 μm gaps. The THz transmission spectra shifted by 8.6 GHz before and after the injection of the AFP antibody and the serum antigen [531]. (d) Illustration of SRR structures featuring an ATR platform [541].

Recently, Wang *et al*. [547] fabricated a THz metamaterial system with polarization-insensitive features and used it for the detection of bovine serum albumin (BSA) water solutions with different concentrations. The detection setup and the microscopic image of the fabricated polarization-insensitive metamaterial (PMI) biosensor are presented in Fig. 21(a), and the measured data in Figs. 19(b-c). In Fig. 21(b), the pink, blue, and red curves denote the responses from the biosensor with 3 mmoL/L, 1.5 mmoL/L, and 0.75 mmoL/L of the BSA aqueous solutions, respectively, while the black curve indicates the response from the biosensor without any BSA molecules (0 mmoL/L). The corresponding resonant frequencies for all these 4 solutions are found to be f_1=1.188 THz, f_2=1.3 THz, f_3=1.413 THz, and f_4=1.463 THz, respectively for the 3 mmol/L, 1.5 mmol/L, 0.75 mmol/L, and 0 mmol/L BSA solutions. These results indicate that the resonant frequency is red-shifted when the content in the BSA molecules increases in the target aqueous solution, suggesting that higher concentrations of the

biological analyte (*i.e*., which is the BSA molecules in this case) led to a corresponding increase in the effective dielectric constant of the target BSA solutions. Interestingly, it was observed that changes in resonant frequency followed an approximately linear pattern following the changes in the concentrations of the BSA aqueous solutions. To this end, the displacement of the resonance can be considered a linear function of changes in the concentration levels of the BSA molecules in these solutions. Additionally, the above authors also investigated the influence of the rotation of the metamaterial biosensor on the resonant frequency. They found that their biosensor was polarization insensitive, and obtained the highest resonant frequency difference equal to 1.68 GHz with the highest resolution equal to 17.7 μmoL/L under the rotations of the full angular range.

Similar to other applications, the strong absorption of THz waves by polar solvents such as water, ethanol, isopropyl alcohol, glycerin, and propylene glycol still pauses a major challenge for the effective use of THz spectroscopy in biomedicine. Nevertheless, interesting developments have already been implemented to overcome this challenge using THz metamaterial systems some of which are worth mentioning. In 2018, for example, Tang *et al*. [548] managed to overcome the difficulty of THz absorption by polar solvents by combining the microfluidic chip with THz metamaterial systems to detect DNA oligonucleotides with base mutations. In a later study, Yan *et al*. [170] proposed a THz metamaterial biosensor based on Fano resonance to detect and analyze cancer cells and achieved a theoretical sensitivity of about 455.7 GHz/RIU. In another study, Karmakar *et al*. [549] proposed a stacked metasurface system for the detection of different types of samples including thin layers, different types of chemicals, and unknown analytes. To detect the unknown analytes, for example, the target samples were placed between the metasurfaces that formed the Fano cavity to achieve substantial energy confinement inside the dielectric spacer between the two resonators due to broadside coupling of the unit cell resonators and strong light-matter interaction features. These features enabled the attainment of ultra-sensitive sensing, hence, the unknown analytes were easily detected. As part of their conclusions, the above authors indicated that the use of broadside coupling of the unit cell resonators helped them to achieve much stronger near-field and large-area interactions between THz waves and the target substances leading to ultrasensitive sensing, capable of achieving >1 THz/RIU (=1.76 $\times 10^5$ nm/RIU) and a figure of merit of about 14.05 in the THz frequency range. In 2021, Ahmadivand *et al*. [550] used the THz metamaterial system to detect SARS-CoV-2 stinger proteins at femtomolar concentrations and reported fast and accurate detection results. This application provided a rapid and convenient method that could be used to detect COVID-19. In their recent studies, Cui *et al*. [177], [551] devised different types of highly sensitive THz metamaterial biosensors to detect early cancer biomarkers carcinoembryonic antigen (CEA) with concentrations ranging from 0 to 500 ng/mL as depicted in Figs. 21(d-f) [177], and breast cancer marker carbohydrate antigen 125 with the concentration ranging from 0 to 20 μg/mL as depicted in Figs. 21(g-k) [551] and reported accurate results (Figs. 21(e-f) and Figs. 21(h-k), respectively). In the first study, their biosensor was fabricated based on the classic double SRR structure as depicted in Fig. 21(d) [177], while their second sensor was fabricated based on a bowtie triangle ring (BTR) as depicted in Fig. 21(g) [551]. As part of their conclusions, the above authors pointed out that their design and detection methods could provide a potential route for the early warning stages of cancer [177] and/or detection of proteins and small molecules [551]. The above authors indicated that the sensitivities of these two sensors were significantly improved and reached the maximum values of about 387 GHz/RIU and 498 GHz/RIU, respectively.

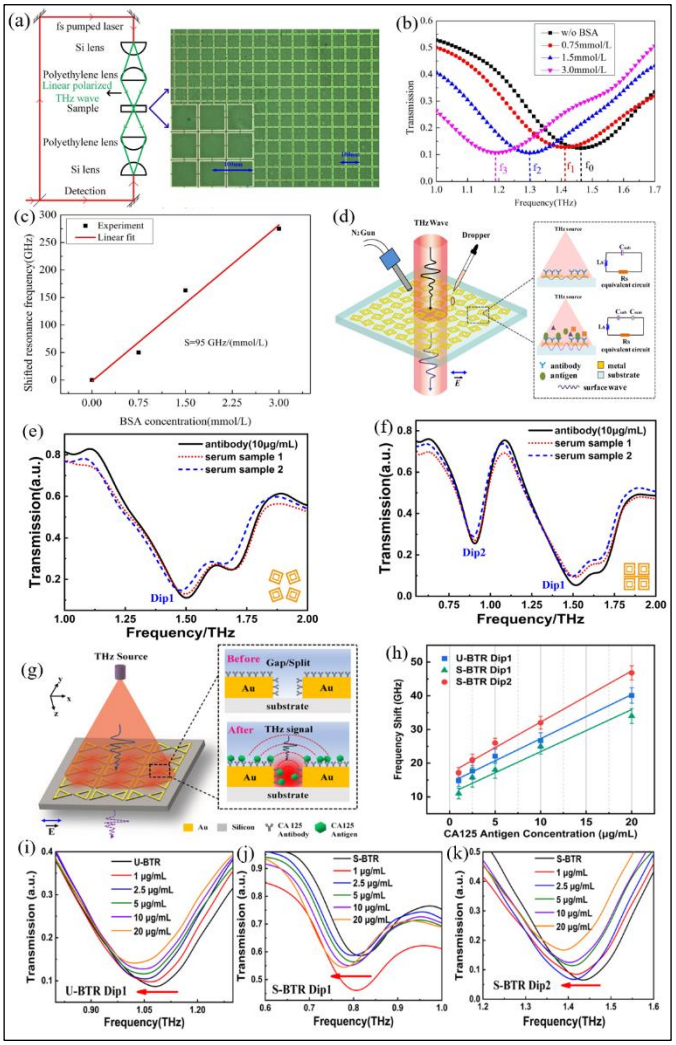

Fig. 21. (a) Experimental setup for THz spectroscopy combined with the metamaterial system and the microscopic image of the resulting PIM biosensor, (b) THz transmission spectra of the BSA aqueous solutions as measured by the PIM biosensor, (c) least squares fitting of experimental data of the resonant frequencies for the different BSA aqueous solutions [547], (d) schematic diagram of THz metamaterial biosensor chip (*i.e*., the inset represents the measurement principle and the equivalent circuit for classic double SRRs and both Csub and Csam denote the capacitances of the substrates and sample, respectively, while Ls denotes the inductance of the classic double SRRs). The measured THz results for different CEA protein concentrations: (e) The results of serum detected using rotating double SRRs, (f) the results of serum measured using grating double SRRs [177]. (g) The schematic diagram of the BTR metamaterial biosensor chip where the insert indicates the reaction mechanism of the electromagnetic field and the target analytes, (h) the frequency shift observed by measuring different concentrations of the CA125 protein and fixed concentrations of its antibody. The transmission spectra of the (i) U-BTR Dip1, (j) split BTR Dip1, and (k) split BTR Dip2 under different concentrations of the CA125 protein [551].

As early as 2007, Yoshida *et al*. [552] proposed a label-free biological sensor made of thin metallic mesh and used it with the THz spectroscopic system to detect small amounts of protein horseradish peroxidase in aqueous solutions (0 pg/mm^2, 300 pg/mm^2, 500 pg/mm^2, 1100 pg/mm^2, and 2100 pg/mm^2). The authors used a commercially available printer to spread small amounts of the aforementioned samples on the sensor's surface to form the sample systems, which were then measured using THz spectroscopic system in transmission mode. Their results indicate a clear frequency shift of the transmission dip for the samples with the concentrations of the horseradish peroxidase between 500-2100 pg/mm^2 compared to bare metallic mesh (0 pg/mm^2). As part of their conclusions, the above authors indicated that the THz sensing with thin metallic meshes was extremely sensitive as it enabled the detection of small amounts of biomolecules with a sensitivity equal to that of conventional methods using antibody-labeled horseradish peroxidase. In another study [553], Bui *et al*. used a micron-scale thin-slab metamaterial system to enhance the absorption signal of the THz vibration of ultrathin-adsorbed layers made of large and small organic molecules. Samples with large biomolecules were obtained from BSA solutions, while the samples for small biomolecules were obtained from the solutions of 3,3'-diethylthiatricarbocyanine iodide (DTTCI) and Rhodamine 6G (Rh6G). The results indicate that their metamaterial system significantly amplified the signal strength of solutions with bulky BSA which displayed a vibration signal at 4.8 THz, while those with DTTCI and Rh6G remained inactive due to the lack of low-frequency vibrational modes in the frequency region of interest. As part of their conclusions, the above authors indicated that the use of THz metamaterial sensing could improve the sensitivity and selectivity of THz systems, which could be used to detect and/or monitor other large biomolecules such as proteins or pathogenic enzymes.

In addition to the detection of biomolecules using THz metamaterial systems, the use of this technology to detect microorganisms has been frequently researched partly because of the comparable sizes of most of the microorganisms and the atoms of THz metamaterial systems. In 2014, for example, Park *et al*. [554] proposed a set of THz sensing systems each featuring several slot antenna arrays fabricated on different substrates and used them to detect yeast cells. In their results, Park *et al*. observed that the addiction of yeast cells to the slot area of the antenna arrays caused a noticeable shift in the resonant frequency of the metamaterial systems though the sensitivity was different for sensors fabricated on quartz and silicon substrates. Using the substrate's permittivity as the classification indicator for these sensor systems, Park *et al*. indicate that sensors fabricated on low permittivity substrates such as quartz demonstrated higher sensitivity and vertical range of the effective sensing volume than those fabricated on high permittivity substrates such as silicon. Park *et al*. also observed that the frequency shift decreased with the increasing width of the slot antenna for a fixed coverage of yeast films, which highlights the field enhancement effect of their THz metamaterial system. To analyze the vertical range of the effective sensing volume and the field enhancement effect, the above authors used their design to detect yeast films deposited on the THz metamaterial systems with different thicknesses and slot widths sizes and found that their sensitivity was higher for smaller slot width metamaterial systems than bigger slot width metamaterial systems. To put this into perspective, the

metamaterial system with a 2 μm slot width caused approximately 13 GHz in resonant frequency shift when covered with a 4 μm yeast film and saturated at 3.5 μm for the same slot width.

In many instances, researchers also argued that the sensitivity levels of THz metamaterial systems used to detect microorganisms in biomedical samples very much depend on the shape and size of the individual microorganisms in the samples suggesting that these two factors should always be taken into consideration to devise an effective sensing protocol and achieve accurate sensing results thereof. In fact, this was recently verified by Park *et al*. [555] who used an electrical SRR-based sensor with the THz system to detect and evaluate star-shaped, ovular, spherical, and lens-shaped polystyrene microbead samples. The results indicated that the star-shaped microbeads presented the best sensitivity in the low-density regime which was approximately three times that of the spherical-shaped microbeads. They also found that the frequency shift of their metamaterial system saturated at 60-80 GHz when all the gap areas were fully covered by the microbead samples. In 2016, Zhang *et al*. [556] constructed a flexible THz metamaterial system featuring a planar array of five concentric subwavelength gold ring resonators on a 10-μm-thick polyimide substrate. The resulting flexible THz metamaterial system was sensitive to small external changes in dielectric environments and was then used to monitor the health status of oral cancer cells with and without sanative drugs. Their results revealed the existence of a linear relationship between the relative change of resonant frequencies of their metamaterial sensor and the cell's apoptosis measured by flow cytometric technique. Although Zhang *et al*. did not provide quatitative information outlining the number of cured and uncured cancer cells in their samples, they nonetheless indicated that the frequency shift of the metamaterial's resonant peak with cured cancer cell samples was much smaller than that of control samples with uncured cancer cells. They concluded that this was because and concluded that this was due to the fact that number of cured oral cancer cells was smaller than the number of uncured cells in the control samples, and further added that their study was of general importance for the effective development of label-free, cost-effective, and *in-situ* detection tools.

The implementation of label-free THz biosensing platforms was also demonstrated in several studies with interesting results. For example, Hasebe *et al*. [557] used thin metallic mesh devices featuring a PVDF membrane to show that both the transmittance attenuation of THz waves and the shift of the dip frequency of the metamaterial system very much depended on the bonding levels of the target samples. The metallic mesh devices were designed to have sharp dip features in the transmitted THz spectra and exhibit anomalous transmission phenomena when subjected to resonant excitations of the surface waves. Their results indicate that their metallic mesh devices were extremely sensitive to changes in the refractive index of the samples attached to the metallic mesh, and managed to detect the lectin-sugar interactions using this method. Additional analysis of these types of interactions also revealed that parameters such as the phase peak shift of the derivative spectra, as well as the transmittance attenuation and dip shift of the resonant frequency of the metamaterial system very much depended on the bonding levels between lectin-sugar interactions. Using this method to determine the avidin-biotin interactions, the above authors managed to detect small amounts of biotin ups to 0.17 pg/mm^2, which further highlighted the extreme sensitivity of their design. In a similar study [558], the above authors reported a label-free analysis of single- and double-stranded DNA samples using surface waves in the THz frequency region. They posited that the free-space THz measurements could not measure the optical properties of a small number of DNA molecules because of their low absorption coefficients, but emphasized that the use of metallic mesh provided their THz system with enhanced sensitivity levels to detect small changes in the optical properties (*i.e*., refractive indices) of their DNA samples at the concentration levels of 2 μg/mm^2 as estimated from a dip frequency shift of the metallic mesh device.

In addition to the aforementioned, several researchers also used THz metamaterial systems featuring SRR structures to detect self-assembled and functionalized alkanethiol molecules. In [559], for example, Wu *et al*. demonstrated that surface-enhanced electromagnetic response in the resonant regions of the SSR structures offers an extremely sensitive device for the evaluation of surface dipoles formed by alkanethiol molecules with THz waves through the use of the differential transmission (DT) spectroscopic method. In their configuration, the THz-DT signals mainly came from the interaction between metamaterials and alkanethiols by electron transfer and/or variations in the dielectric constant and cooperatively captured variations in the frequency shift and the damping constant of the resonance of the metamaterial system. This method was then used to demonstrate the sensing feasibility for the chain length dependence of the alkanethiol molecules and the obtained results revealed that the improved THz response near resonant regions of the metamaterial system enabled users to read out the number of carbon atoms in self-assembled alkanethiol molecular monolayers. Interestingly, Wu *et al*. believed that their results could be extended to other wavelength regions of the electromagnetic spectrum as well as other shapes of metamaterial system analysis. In another study [560], Wu *et al*. used a highly sensitive and label-free biosensor based on the THz metamaterial system and functionalized by octadecan thiols and biotins. The sensor was then used to detect streptavidin-agarose (SA). Their results indicate that both low and high-frequency resonance modes of their metamaterial system were useful for the detection of SA, and the high-frequency mode exhibited a frequency shift as high as 6.76 GHz for undiluted commercial SA solutions. The high-frequency mode originated from the plasmonic dipole oscillator, while the low-frequency mode was attributed to LC oscillation and both of which were highly sensitive to micro-environmental changes. They also observed that the adsorption of the SA solutions with different concentrations caused different frequency shifts, and the replacement of high refractive-index substrates with low refractive-index substrates increased the overall sensitivity of their experimental system. They indicated that their experimental results well agreed with the numerical simulation results, and further added that the sensitivity of their design to certain types of biomolecules could still be improved by further optimizing the design of their metamaterial systems.

Park *et al*. [50] demonstrated that the SRR-patterned THz metamaterials provide extremely selective and sensitive microbial sensors capable of performing high-speed *in-situ* identification of microorganisms under both aqueous and ambient environmental conditions. Using these sensors, the above authors managed to detect extremely small amounts of microorganism samples with sizes equal to the micro-gaps of SRR metamaterial structure as depicted in Fig. 22(a). They also investigated the resonant frequency shift of their THz metamaterial systems based on the dielectric constants and the number density of the microorganisms, which they successfully interpreted by changing the effective dielectric constant of the gap area size (*i.e*., gap sizes of 2-3 μm) and structure (*i.e*., using either single or double SRRs). Their results indicate that not only did the resonant frequency shift increase linearly with the increasing number of fungi in the gap areas, but this resonant frequency shift was also higher for the higher dielectric constants. Fig. 22(b) presented the results of the visible transmittance spectra of the quartz substrate coated by Escherichia coli (*E. coli*) with a density of 0.078 mm^2 in aqueous (red line) and ambient air (black line) conditions, and Figs. 22(c-d) presents the results of *E. coli* metamaterial sensing in an aqueous environment. In this study, a blue shift of the resonant peak was observed by adding 0.019 μm^{-2} of *E. coli* because the refractive index of *E. coli* cells was lower than that of water. As the exciting electric field was at several tens of micrometer levels, the absorption of water was not strong and this made it easier to use the THz metamaterial sensor for liquid sensing. Although their study was successful and accurate results were obtained during their measurements, the above authors noted that free space THz sensing was not easy to perform because the most sensitive area of their metamaterial sensor was located at the gap of the SRR structure.

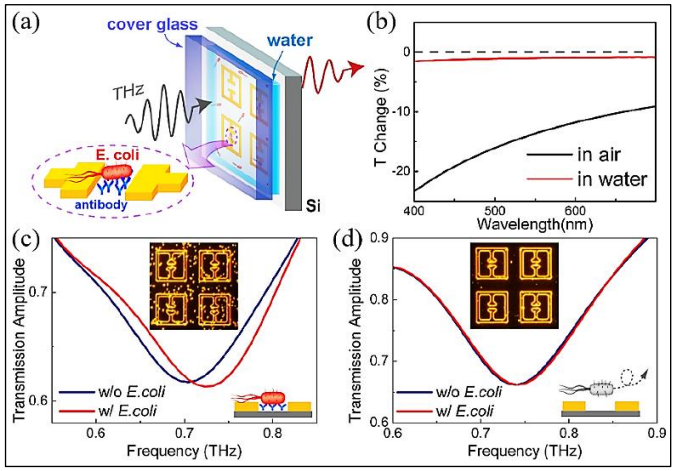

Fig. 22. Results of THz metamaterial sensing of *E. coli* in an aqueous solution with the structure of the THz metamaterial system used in the study: (a) the schematic representation of selective bacteria (*E. coli*) detection in an aqueous solution (the Si substrate is coated with antibodies specific to *E. coli*), (b) the visible transmittance spectra of the quartz substrate coated by *E. coli* (with the density of 0.078 mm^2) under the ambient (black line) and aqueous (red line) environmental conditions, (c) the THz transmission spectra obtained before (blue line) and after (red line) depositing *E. coli* bacteria on the functionalized THz metamaterial systems in aqueous environments (the inset depicts a typical corresponding dark-field microscopic image obtained after depositing *E. coli* bacteria on the metamaterial systems), and (d) the THz transmission spectra of THz waves measured before (blue line) and after (red line) depositing *E. coli* bacteria on the microbial sensors without surface functionalization (the inset depicts the corresponding dark-field microscopic image after depositing *E. coli* bacteria on the metamaterial systems) [50].

In summary, THz metamaterial-based sensing has found an increasing number of applications in biomedical science and engineering in recent years. In addition to its capabilities of enhancing features such as the selectivity, sensitivity, and accuracy of common THz-SI systems, its broader applicability in this area was also encouraged by the possibility of using these systems to accurately predict collective vibration modes of many types of proteins and DNA molecules in the THz frequency range [552]. For example, the absorption coefficients and refractive indices of single and double-stranded DNA molecules are different from one another in the THz frequency range, and these distinguishable features can be used to accurately distinguish between these two types of molecules. Apart from the study and evaluation of DNA molecules, credible reports have also been published on the use of THz metamaterial systems for the detection and evaluation of complex biomolecules and their interactions such as avidin-biotin and lectin-sugar complex as well as the spectroscopy and imaging of artificial or synthetic RNA molecules [561], [562]. Additional advancements have also revealed potential applications of label-free sensing systems for many types of biomolecules by using THz waves. To date, most label substrates, which might involve a radioisotope, an enzyme reaction, or a fluorescence are used for protein detection, which

are generally complex and time-consuming. The use of label-free detection methods with THz metamaterial systems is considered to be one the most convenient techniques that could be used to detect and evaluate these types of molecules faster and easier than the aforementioned methods.

B. THz metamaterial sensing and testing in the agriculture and food industry

The addition of chemicals such as pesticides and antibiotics to agricultural products and food exhibits fingerprint spectra in the THz frequency region and these features could be used to detect these substances similar to other chemical substances as indicated in the previous sections. To demonstrate the feasibility of such an application agriculture and food industry, Qin *et al*. [563] used THz spectroscopy to detect the carbendazim solutions in different concentrations and used the THz metamaterial system to improve the THz system sensitivity and alleviate the burden of complicated data processing. The obtained results indicate that the designed metamaterial system could detect carbendazim solutions in different concentrations down to 5 mg/L. In another study, Qin *et al*. [564] also designed a THz metamaterial system and used it for the detection of tetracycline hydrochloride (*i.e*., an antibiotic residue that is widely used in animals that can cause human health issues once in excessive quantity in food) as depicted in Figs. 23(a-b). The THz transmission spectra obtained from the tetracycline hydrochloride solutions deposited on the THz metamaterial system with concentrations varying from 0.01-10000 mg/L are presented in Fig. 23(c). Although samples with tetracycline hydrochloride concentrations lower than 0.1 mg/L generally do not show any significant difference in the amplitudes of their transmission spectra, this study demonstrated that the addition of metamaterials greatly improved the sensitivity as compared to the direct use of the THz system and enabled the successful detection of tetracycline hydrochloride as low as 0.01 mg/L. In a similar study [565], Xu *et al*. used the THz metamaterial system to detect chlorpyrifos-methyl solutions with concentrations between 0.2-1.0 mg/L. In their experiments, the authors configured their metamaterial system to operate in reflection mode (Fig. 23(d)) and used it to detect 10 µL of chlorpyrifos-methyl solutions of different concentrations. Experiments were repeated 3 times, and reflection spectra measured from the different chlorpyrifos-methyl solutions as well as their frequency shifts are presented in Figs. 23(e-f). The results of the normalized reflection indicate that the indicate that the resonant peaks regularly shifted to lower frequencies (Fig. 23(e)), and the value of the frequency shift increased with the increasing concentration of chlorpyrifos-methyl in the measured solution. Xu *et al*. effectively demonstrated that the frequency shift value could be estimated as a function of chlorpyrifos-methyl concentration and their verification results were subsequently presented in Fig. 23(f). In fact, one can easily notice that there there is a strong linear relationship between the concentration of the chlorpyrifos-methyl samples and the resulting frequency shifts of the reflected spectra which further verifies the accuracy of their results. This study was particularly interesting because the obtained results highlighted a significant improvement in the THz system enabled by the use of metamaterials, and a limit of detection for the aforementioned substance reaching 0.204 mg/L, lower than that recommended by the World Health Organization's provisional guideline limit for chlorpyrifos-methyl in vegetables (1 mg/L). In a similar study, Nie *et al*. [566] designed an all-dielectric broadband THz metamaterial absorber to detect chlorpyrifos with an increased detection limit of up to 0.1 mg/L. The results indicate that their design has an interaction efficiency of over 99% at 1.33 THz, with the bandwidth featuring a center frequency of approximately 600 GHz. Interestingly, both the system's stability and sensitivity were effectively maintained under different temperature levels, time scales, and humidity conditions.

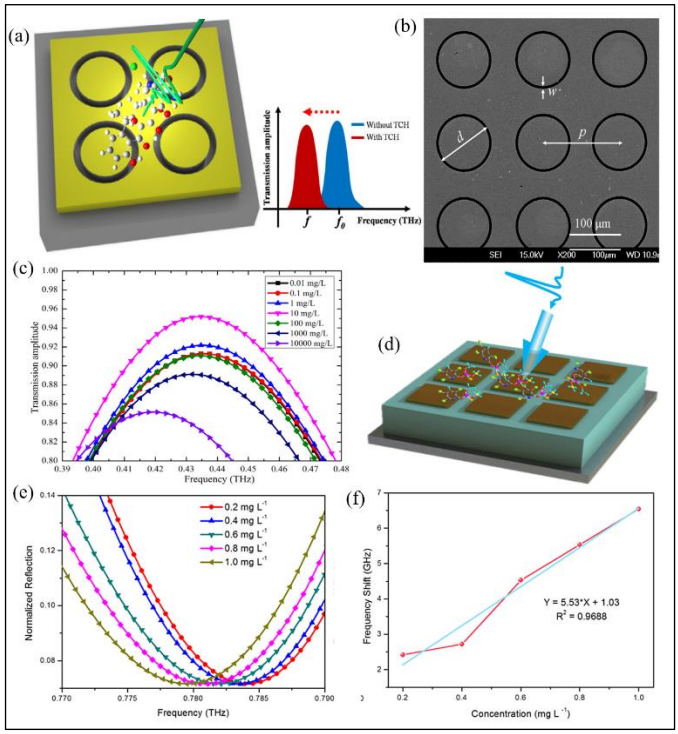

Fig. 23. Presentation of the (a) THz metamaterial system used for the detection of tetracycline hydrochloride and (b) resulting scanning electron microscope images, (c) the THz transmission spectra of tetracycline hydrochloride deposited on the metamaterial system (these transmission spectra are obtained from samples with different concentrations of tetracycline hydrochloride) [564], (d) the THz metamaterial system used for the detection of chlorpyrifos-methyl, (e) the THz reflectance spectra of chlorpyrifos-methyl at different concentrations (ranging from 0.2 mg/L to 1.0 mg/L), and (f) the frequency shift results of chlorpyrifos-methyl at different concentrations (ranging from 0.2 mg/L to 1.0 mg/L) (the blue curve depicts a linear fit to the THz data measured from the chlorpyrifos-methyl) [565].

Recently, a metasurface system made of square-shaped slits on a high-resistance silicon substrate with extraordinary optical transmission resonance at approximately 0.3 THz was used for kanamycin sulfate detection in Ref. [567], and an extraordinary sensitivity was reached with the minimum detectable concentration reaching down to 100 pg/L which is approximately 10^{10} times enhancement compared to its lowest

detectable concentration on bare silicon estimated to approximately 1 g/L. In ref. [565], the authors used a THz metamaterial absorber to detect a kind of pesticide named chlorpyrifos-methyl and assessed the sensitivity improvement by comparing the sensing performances of the Teflon plates and the developed THz metamaterial absorbers. The detection limit was found to be 0.204 mg/L which was lower than the provisional guideline set by the World Health Organization establishing the allowable concentration limit of chlorpyrifos-methyl in vegetables (1 mg/L). Liu *et al*. [568] used a THz metamaterial system with SRR structures and successfully calculated tiny refractive index differences between non-transgenic and transgenic products based on clearly distinguished SRR response peaks. Recent studies have also demonstrated that the THz wave could be guided onto the surface of the metamaterial systems by using the scattering edge coupling technique [569], [570]. The results indicate that broadband spectral signals could be experimentally obtained from corrugated metallic surfaces made of linear arrays of subwavelength grooves [570]. As part of their conclusion, the above authors also noted that the improved interactions between the light-matter that occurred in the vicinity of the spoof plasmon surface which enabled a more efficient use of the limited power of current THz sources and the subsequent detection lactose at 300 ng/mm^2. In ref. [571], You *et al*. designed a THz plasmonic sensor featuring a hybrid planar waveguide with a diffraction metal grating and a subwavelength plastic ribbon waveguide. To demonstrate the robustness detection capabilities of their conceptual design, they used it to detect Bi_2CuISe_3 in different concentration levels. The results indicate that the minimum detectable amount of their target analyte (Bi_2CuISe_3) in powder form reached 17.3 nmol/mm^2. This level of accuracy means that this sensor could accurately detect particles in general-purpose pollution or chemical reaction monitoring applications. Recently, Liu [572] used high-sensitivity THz metamaterial systems to evaluate the organochlorine pesticide residues based on a loop-shaped absorber that had a strong interaction with the THz wave. Their results indicate that the frequency of their loop-shaped absorber resonance peak was red-shifted when the dielectric environment indicated by the absorber changed. Also, the interaction between the THz electric field generated by the aforementioned loop-shaped absorber and the target samples was considerably improved by the use of metamaterial systems compared to the direct detection of these pesticide residues using conventional THz spectroscopic systems. The sample signal could also be amplified. They concluded that the use of the loop-shaped absorber can improve the interaction between THz waves and the target samples, and further added that the frequency shift signal of the resonance peak of the metamaterial absorber can be used to enhance the sensitivity of the sample detection, and enable the detection and analysis of trace amounts of samples. In another study, Li *et al*. [573] successfully combined THz spectroscopy with metamaterial systems to detect quinolone antibacterial drug (noroxin) in low concentrations. Interestingly, the noroxin detection limit for their method was determined to be 0.01 μg/mL, and this study proved that THz metamaterial sensing could indeed be highly effective method for the rapid detection of quinolone antibiotic residues in food matrices.

In summary, the constantly growing demand for food quality, food safety, higher production, lower food wastage, time-saving processing mechanisms, lower workforce requirements, and unwavering food security in the agricultural and food industries have stimulated great interest in the use of THz metamaterial systems for the identifications of defects in food and agricultural products, monitor water level, examine the soil characteristics for crop growth and maintain food safety and quality during the production process. THz metamaterial systems provide regular THz systems with faster, more accurate, reliable, non-invasive, cost-effective, and simpler features for safety monitoring and quality evaluation for crops and food commodities greatly contributing to their continued expansion into the NDT of food and agricultural products [4], [450]. THz metamaterial systems also offer users the capability to classify between pristine and defective food and agricultural products, owing to their unique properties such as transmission capacity, spectral fingerprint, unique water absorption property, and little scatter effect, as well as the great potential of extracting useful spectral features from the samples amplitude and phase information. Although THz metamaterial systems are still not adopted as a standard NDT technique in agricultural and food industries, the aforementioned properties continue to encourage the extensive applications of these devices and many researchers and engineers in agricultural and food industries now consider THz metamaterial systems as an effective, non-invasive, highly accurate, and cost-effective NDT technique.

C. THz metamaterials for thin-film sensing and testing

In sensing applications, the detection of subwavelength sample thicknesses imposes great difficulties on conventional THz spectroscopic systems. However, sensing and measuring these types of samples is essential for a large number of applications in biological, chemical, physical, and medical sciences. The desire to obtain accurate sensing information in these applications encouraged the continued quests for the development of high-performance sensing modalities with improved sensitivity, selectivity, and specificity for biological, physical, and chemical thin-film samples [574]. To date, experts believe that THz thin-film sensing is one of the most promising applications of THz metamaterial sensors, thanks to the specific interactions between THz waves and analytes in biological and physico-chemical thin-film samples. These applications are generally enabled by the fact that thin film samples are flat, easy to measure, and possess specific optical properties that can easily be evaluated using THz metamaterial systems [575], [576]. Although many types of metamaterial structures such as ground-plane cloaks, photonic crystals, SRR, left-handed metamaterials, *etc*. [30], the literature indicates that the majority of metamaterial systems capitalize on improving and modifying the structure of SRRs, which seems to be the most commonly used type of metamaterial structure for thin film sensing applications [172]. In most cases, modifications of the SRR structure are generally performed to achieve adequate natural oscillation frequencies, which generally depend on parameters such as the dielectric constant of the substrate, the size of the width or diameter of the rings, gaps or cuts of the rings, separation distance between consecutive rings, as well as the depth of the rings in the SRR structures. In biological and

chemical sciences, for example, the use of SRR-based sensors is considered a viable candidate for the detection and evaluation of highly sensitive biological and chemical thin film samples because these resonators are extremely small and exhibit tunable resonant frequency responses [577]. This is the case for pathogen detection, where the target pathogens, such as bacteria, are captured on the surface of the biosensor by specific antibodies to form a monolayer of bacteria with a thickness in the μm range detectable by THz metamaterial sensors [578]. A combination of these properties and the uniqueness of THz wave characteristics have recently fueled significant interests in THz metamaterial sensing where the detection of several types of biological and physico-chemical substances/analytes in the form of thin film samples have been the point of focus [480], [515], and this makes THz metamaterial systems more acquiescent to thin film sensing applications.

Consistent with the aforementioned, the detection of trace quantities of substances in the form of thin films using THz metamaterial systems is now one of the most important research directions in the THz sensing industry, and numerous studies have been published on this topic thanks to the increased knowledge of key optical and dielectric properties of countless biological and chemical substances in the THz regime. In Ref. [579], for example, Zhang *et al*. used a waveguide THz spectroscopic system with adequate sensitivity to characterize layers of water in the nanometer range. In their experiments, Zhang *et al*. deposited a 20 nm layer of water on the surface of a parallel-plate metal waveguide and managed to measure the absorption coefficient and refractive index and found that they were in good agreement with those of bulk water samples due to the increased effective interaction time between water molecules and THz waves. In another study, Driscoll *et al*. [176] demonstrated that THz spectroscopic system can accurately detect small quantities of a silicon-nanospheres-ethanol solution (30 μL) containing less than 1 ng of silicon deposited as an overlayer or thin film on a planar THz metamaterial. In their study, Driscoll *et al*. demonstrated the possibility of performing a fine-tuning of the magnetic resonance frequency of a fixed SRR array by adding inclusion materials near the split-ring elements. Also, by applying drops of their silicon-nanospheres-ethanol sample to the surface of their samples, they observed a noticeable decrease in the magnetic resonance frequency of their split-ring array sensors. This property provided these sensors with high sensitivity to subwavelength volumes and opened up new possibilities for using these types of sensor devices for real-time THz thin film sensing applications. In a similar study, O'Hara *et al*. [580] sought to investigate the obstacles and limitations of using THz metamaterial systems as sensing devices and used the THz-TDS system to measure the dielectric properties of several types of dielectric overlayers deposited on planar metamaterial systems. O'Hara *et al*. deposited uniform dielectric overlayers with varying thicknesses from 100 nm to 16 μm onto fixed SRR arrays to shift the resonance frequency of the electric response. Their results indicate that the overlayer of 100 nm quickly approached the limit of detectability in their metamaterial design. Although their results largely agreed with previous findings in [176], [581], they emphasized that the measured results were not always consistent with simulations, particularly those involving very thin films with thicknesses less than 200 nm, and concluded that experimental verification is always necessary when using SRR-based sensors to ensure adequate simulation structures and reveal the practical difficulties of analyte deposition on the metamaterial sensors. Interestingly, this study also pointed out some of the important factors involved in sensing optimization (*e.g*., the limitations of the THz measurement system, resonance effects, ring geometry, analyte composition and deposition, substrate composition, *etc*.), which could be utilized in the design and implementation of high-performance SRR and/or frequency selective surface-based sensors.

Apart from the detection and analysis of thin-film analytes, metal hole arrays (MHA) were also used to study the effects of dielectric films on the overall performance of THz thin-film sensing applications. In Ref. [582], for example, the authors studied the effect of attaching dielectric films on the surface of MHAs on their THz reflection spectra. The results indicate that the frequencies of the reflection dips, attributed to the excitation of surface waves in the vicinity of the MHA surface, shifted from higher to lower frequencies with the increasing thickness of the dielectric film (≥50 μm). Additionally, their results also indicate that thinner MHAs provided better sensitivity than their thicker counterparts, and are there suitable for applications involving highly sensitive THz detections. In a similar study, Tanaka *et al*. [583] investigated the effect of depositing thin dielectric layers on the transmission characteristics of MHA devices in the THz frequency range. As part of the experiments, Tanaka *et al*. deposited a 50 μm dielectric layer on the surface of an MHA device and recorded a significant decrease in parameters such as the THz transmission peaks and SNR of the device due to the mismatch between the resonance frequencies of its two sides and the cutoff effect of its metal holes, making the measurement of its resonant peak utterly difficult.

THz metamaterial systems with good sensitivity were also used for thin-film thickness measurements. Yoshida *et al*. [584] used the THz system featuring a metallic mesh device to measure the thickness of 3 μm, 4 μm, and 5 μm thick poly(ethylene terephthalate) thin-film samples, whereby a 1 μm difference in thickness could be easily detected. Also, the authors recorded several 2D images of metallic mesh devices with thin film samples attached to their surfaces where the differences between the thicknesses of these thin film samples were easily distinguished by analyzing features in their 2D images. In a similar study, Suzuki *et al*. [585] used the THz system with a metallic mesh sensor to measure the thickness of a sub-mm-thick SiO_2 thin film, while Reinhard *et al*. [586] easily achieved a minimum thickness resolution of about 12.5 nm in Si thin films which was approximately 16000 times smaller than the wavelength of the incident THz waves. In another study [587], a near-field THz spectroscopic system was built to reduce the spot size of the THz beam in a THz metamaterial sensing setup. The proposed design significantly reduced the number of resonators and the minimum sensing area of the thin film by placing the metasurface sensing platform close to the sub-diffraction THz source (*i.e*., with the distances set to 25 μm and 50 μm). An additional advantage of this design is that the aforementioned reduction in the number of exciting resonators also decreased the inter-cell coupling strength, which subsequently increased the resonance Q-factor

of the metamaterial system. Recently, Park *et al*. [588] demonstrated the feasibility of one of the most highly sensitive metamaterial systems for THz thin film sensing applications where a 1 nm thick thin film was detected (*i.e*., this thickness was estimated to be almost 10^6 times smaller than the wavelengths of the incident THz waves). Their metamaterial system used nanogaps (≤10 nm gaps) to confine THz waves and improve the sensitivity of their sensor device. In another study, You *et al*. [589] used the THz plasmonic waveguide for nanofilm sensing applications. They demonstrated that a high-aspect-ratio metallic rod array can easily produce and propagate THz surface plasmonic waves capable of detecting 300 nm-thick ZnO and SiO_2 nanofilms coated on 100 μm-thick polypropylene films.

In summary, THz thin-film sensing is one of the rapidly expanding branches of THz science and it increasingly appears to be amenable to numerous practical applications in biological, chemical, physical, and medical sciences. THz thin-film sensing has great scientific significance because it represents a special configuration in which trace amounts of many biological and physico-chemical substances are ideally analyzed to reveal some of their THz properties and features such as the magnitude/variability of their refractive indices, thickness, and volume, spacers of metamaterial absorbers, metamaterial resonance types, thicknesses of metasurface substrates, *etc*. Although thin-film samples are generally difficult to evaluate using conventional THz spectroscopic systems, THz thin-film sensing based on metamaterial systems is considered one of the most promising THz sensing applications, thanks to its capabilities to provide accurate, precise, stable, and reliable measurements of thin film samples in the THz sub-wavelength range. In recent years, interesting developments have been achieved including the recent development of a high-performance THz chemical microscope [590], [591], and THz metamaterial structures (*e.g*., resonant structures, guided waves, noise cancellation, *etc*.) for improved sensitivity of THz spectroscopic systems [574]. Although it would be optimal to compare the performance of all these configurations using a single quantitative sensitivity parameter, this is generally not possible because the boundary between thick and thin samples is usually difficult to establish for some researchers as it only depends on the limitation of their experimental THz-TDS under normal operating conditions (*i.e*., samples are considered thin or thin-films when conventional THz–TDS can no longer distinguish them from the reference materials). To avoid reporting conflicting performance parameters, this section only presents the reviewed results based on the measured and/or anticipated characteristic performance as well as the general guidelines on features such as their complexity, utility, advantages, and disadvantages. Taken together, the literature revealed that THz thin-film sensing is still in its infancy, partly because numerous demonstrations have been singular events introducing the concept but rarely pursued to achieve real-time implementation while others were only marginally implemented. Interestingly, the success of these advancements is considerably impressive, and if these advancements provide tangible hints on future opportunities for THz thin-film sensing, then the general outlook for this technology is highly promising. However, it appears much remains to be discovered in basic metamaterials and THz science, and more so in practical THz technology development to accommodate even more sophisticated thin-film sensing applications.

D. Other THz metamaterials-based sensing and testing applications

Although THz waves present smaller wavelengths compared to their μ-waves counterparts, their wavelengths are still larger than those of X-rays or γ-rays which severely limited their interactions with nano-sized samples (*e.g*. nanoparticles, nanorods, and large biological molecules). Interestingly, researchers have recently demonstrated that by fabricating THz metamaterials with a nanometer-sized gap, their electric field could be significantly improved and this could help overcome the aforementioned challenges and expand the application scopes of THz-SI systems [592]. As an example, the above authors indicated that the use of THz dipole nanoantennas spaced by 20 nm nanogaps allowed for the extraction of the spectroscopic signature of a monolayer of cadmium selenide quantum dots (CdSe-QDs) at 5.65 THz, thereby generating a Fano-like interference between the phonon resonance of the quantum dots and the fundamental antenna mode with an absorption improvement factor (η_{TOT}) up to or greater than 10^6 times in the center of the nanogaps [592]. In a similar study [593], Ji *et al*. developed virus-sized gold nanogaps with a gap width of 20 nm using the atomic layer lithography and devised an ultra-sensitive virus THz detection platform working. Their results indicate that the large-area nanogap-loop array achieved up to 580 times in field enhancement, thereby enabling the accomplishment of extreme light-matter interactions near the gap. Using these two studies as an example, it is evident that the capabilities of trapping THz waves into nano-sized volumes might enable scientists and engineers to develop highly sensitive as well as selective THz sensors.

Additionally, the capability of THz waves to transmit through an array of nanogaps with variable structural sizes, arrangements, and periodicities has enabled the use of thin film single-walled CNTs in THz sensing applications [594]. Also, oil does not exhibit noticeable absorption of THz waves compared with polar liquids such as ethanol and water, thereby enabling easy oil detection even in free space THz sensing setups. A recent study used an SRR patterned THz metamaterial system for oil sensing application and the authors managed to identify specific parameters for gasoline 93# and 97#, further highlighting the capabilities of THz-SI to identify the different types of gasoline derivatives [595]. Recently, Yi *et al.* [175] developed an ultra-precision direct phase readout THz sensing device by combining both the ATR and steerable plasmonic resonance of THz waves. These authors revealed that the often neglected information related to THz phase jumps in SPR-based sensing applications could actually provide THz users with relevant information that could help them to develop more effective and reliable THz plasmonic sensing devices for polar liquids and/or aqueous solutions. In particular, their detailed analysis indicated that the reflected THz phase exhibits two different jump responses in the coupling gap. The Q-factor of phase spectra for optimal coupling gaps was found to be within the range of 9.7 to 43.4 corresponding to approximately 4 to 26

times higher than that of its counterpart in amplitude measurements in liquids sensing and higher than that of fixed coupling gaps. The accuracy of their sensing device was also verified using several types of liquid samples including gasoline, alcohol, liquid paraffin, glycerin, and water, and accurate results were reported. As part of their conclusion, they indicated that their sensing device performed better free from the interference of the fixed gap, and can be used for higher resolution in the spectral characterization of biological and/or physiological samples due to the ultrahigh Q-factor of the phase spectra. Also, small changes in the reflective index of the target samples were easily detected by measuring changes in phase jumps of their sensing device with ultrahigh sensitivity of about 0.370 THz/RIU, and this level of sensitivity could be exploited to establish real-time monitoring of very small changes in the target samples associated with certain activities such as biological and chemical reactions.

E. Challenges and prospects of THz metamaterials sensing and testing

The use of THz metamaterial systems in THz sensing and NDT applications has provided novel opportunities for developing new-generation THz sensing and NDT devices in recent years. For example, THz metamaterials have enabled the development of THz sensors with improved mechanical, optical, and electromagnetic properties, which subsequently promoted the development of cutting-edge sensor systems such as single molecular biosensors and high throughput sensor arrays. Although THz metamaterial systems present numerous advantages and potentially several industrial applications, they also face many challenges like other emerging technologies. Typically, the accuracy of THz metamaterial-based sensors is generally limited by fluctuations in the measured signals caused by various internal and/or external noise sources. External noise sources include quantum noise (also referred to as shot noise), signal processing circuit noise, as well as photodetector noise, while internal noise mainly originates from the desorption/removal and adsorption/adhesion of the sample particles into the metamaterial system or from the metamaterial system to the sample [524], [596]. In fact, the literature indicates that both the adsorption and desorption noises remain the main limiting factors of the ultimate performance of THz metamaterial devices. This is particularly because many of these devices consist of metal-dielectric structures (*e.g*. conventional SPR sensors, nanoplasmonic structures, *etc*.) which are often exposed to measuring environments that generally influence the effect of adsorption and desorption noises and subsequently affect the overall performance of these devices during their operation.

To guarantee the design performance of the THz metamaterial devices and minimize the influence of the noise on the sensors' readout, the aforementioned types of noise sources and measurement interferences should be limited/controlled. To this end, several solutions have been proposed in the literature including but not limited to the optimization of the THz sensing systems, selection of adequate the metamaterial system for the intended application, design of adequate sensing environments, isolation of the measurement systems from the external noise sources, *etc*. [596]. Specific types of noises such as the noise bandwidth can also be eliminated by implementing state-of-the-art noise-insensitive designs such as the use of an auxiliary reference channel close to the sensor, the use of low thermo-optic dielectric materials as the resonance material, the use of sensors working in an aqueous environment, as well as the use of an increased number of averaging scans to eliminate false negative and/or false positive results [171]. There are certainly other solutions and design considerations that can be implemented to achieve the best performance of the metamaterial systems many of which can perform better in specific applications than others, and their implantation should be carefully considered based on the applications and the parameters surrounding the measurements such as the chemical properties of the target sample, required sensing levels/accuracy, specificity or selectivity of the sensor, surface functional requirements, *etc*. To illustrate the importance of sensors and material selections for specific applications, a few examples are worth mentioning consistent with the aforementioned noise sources. In Ref. [597], for example, Djurić *et al*. sought to decrease the influence of adsorption and desorption noise and achieve the best possible performance of metamaterial-based sensors and analyzed the effect of adsorption and desorption noise on the performance and efficacy of microelectromechanical systems (MEMS). Their results indicate that the aforementioned noise was mostly generated by the instantaneous variations in the adsorption and desorption rates of the analyte particles which caused a molecular contamination at the surface of the resonator and limited its sensing capabilities. In this particular instance, the above authors specifically highlighted that the analyte particles were continuously adsorbed onto or absorbed by the MEMS resonator surface, which increased the mass of the resonator and caused continuous fluctuations in its resonant frequency. A later study by Jakšić *et al*. [598] also analyzed the operation and accuracy of metamaterial-based sensors and found that their sensing performance was largely limited by fluctuations in their refractive index caused by the above-mentioned adsorption and desorption noise sources. To minimize this type of noise, one of the possible solutions is to minimize losses and scaling issues by using purely dielectric metamaterial systems instead of metal-structured metamaterial systems which exhibit higher losses and scaling issues [599].

In the design of THz metamaterial systems for spectral modulation applications, for example, several factors such as the system's efficiency, system configuration, bandwidth, and the incident angle of the THz beam should be carefully controlled to achieve accurate sensing and testing results consistent with the application requirements. It is important to indicate that not only should a good THz absorber have a wide bandwidth and high absorptivity, but its structural properties and characteristics should also remain stable over a wide incident angle to accommodate slight variations in the incident angle of the THz beam. Additionally, a high Q-value should be equally envisioned to improve the sensor's detection sensitivity, while the provision of wide operating bandwidth and insensitivity to small variations in the incident angles of the THz beam should be prioritized to achieve high-performance polarization-modulated metamaterial systems. The literature indicates that most of the currently available THz metamaterial devices suffer from issues such as the possession of a single

modulation function (*i.e*., only a few multi-functional THz metamaterial devices are available), complicated processing, and fixed shape. To achieve a highly integrated THz system, the development of advanced THz metamaterial systems/devices featuring two or more modulation functions should be considered. Also, although THz metamaterial-based sensors have been extensively demonstrated, these types of sensors may not provide accurate results in applications such as biomedical engineering where highly accurate measurement results are often required. As such, it is estimated that THz metamaterial-based biosensors still require additional accuracy and sensitivity improvements, mainly because it is difficult to achieve high-resolution, or any other micro- or nano-scale features on the sensor's substrates where conventional photo-lithographic techniques are difficult to use (*i.e*., impossible to use microfabrication techniques with chemical solutions in conventional photo-lithographic techniques).

It appears that the use of advanced, versatile, and fast fabrication techniques should be considered when manufacturing THz metamaterial-based biosensors to guarantee accurate and reliable detection and testing capabilities of the resulting sensors (particularly for biomedical science and/or biomedical engineering applications). To date, it has been reported that state-of-the-art THz metamaterial systems are currently fabricated using lithography technology, but this processing technology is generally complicated, costly, and relatively time-consuming despite its well-recognized high-precision features. To this end, additional fabrication processes should be explored to provide designers with additional tools to achieve high-performance THz metamaterial systems at a cheap price and in a relatively short time. As a fast-developing and cheap material processing technology, additive manufacturing technology is currently being explored for the fabrication of THz metamaterial systems, and its unique advantages of fabricating multilayered structures are expected to bring additional features into the THz metamaterial community for novel sensing and testing applications. For example, the use of miniaturized wearable devices is currently developing toward its implementation, and not only will it be difficult to integrate the existing metamaterial devices with hard substrates into curved surface systems, but it will also be somewhat impossible to achieve conformal surfaces to accommodate these systems. To this end, it is necessary to further investigate flexible metamaterial devices that could be used for these types of applications.

In addition to the aforementioned, accurate detection of the electromagnetic responses by THz metamaterial systems in the THz frequency range can begin a new era of THz photonics-related applications in the implementation of safety and security imaging systems, remote sensing devices, *etc*. Apart from the aforementioned additive manufacturing and photolithographic techniques, the advent of micro- and nano-fabrication methods is also going to inspire new sensing and testing possibilities as they will enable practical implementations of different THz metamaterial systems and this field is already attracting a considerable number of researchers worldwide [600], [601]. Also, active THz metamaterial devices present a wide range of application prospects, particularly in all-optical controlled devices owing to their advantages of performing flexible functions while equally being highly reusable. However, factors such as inexact projection, and low modulation efficiency still hinder the development of efficient all-optical controlled metamaterial systems. As a result, it is important to devise strategies and methods to improve the projection accuracy of optical antennas and the modulation efficiency of all-optical controlled metasurfaces. Also, the modulation rate of active metamaterial systems should be optimized further to guarantee the adequate performance of the host THz systems.

F. Summary of metamaterials-enhanced THz spectroscopy

In summary, significant progress has been made in THz-metamaterial sensing and NDT applications and new approaches have been developed to improve the THz spectroscopic systems' sensing and detection capabilities for biological and physico-chemical substances. The literature survey indicates that there is continuous progress in the design and manufacturing of THz metamaterial systems up to the submicron and nanometer scales, and both new and enhanced properties of THz metamaterial systems are constantly being created while others are being uncovered. To this end, it appears the interdisciplinary boundary between THz metamaterial science and other sub-branches of THz technology, has recently become an overwhelmingly fertile ground for novel scientific discoveries and technological expansions and this justifies the abundance and constantly growing number of publications in peer-reviewed journals, academic monographs, conference proceedings, book chapters, industry snippets, and patents on THz metamaterial systems and related applications. In this context, substantial developments in THz metamaterial sensors have been made in recent years, which led to corresponding developments in the manufacturing of THz metamaterial-based components capable of detecting and evaluating structural information of numerous types of biological and physico-chemical substances in regular and trace concentrations. Although information regarding the sensing mechanisms and indices of THz metamaterial systems would be valuable to understand the synergistic utilization of these types of devices in THz sensing and NDT applications, this information is outside the prevue of the present article and is not discussed herein. Instead, interested readers are advised to read Refs. [30], [89] for information on these particular topics.

V. Sensing and NDT Applications successes of THz-SI Systems, related challenges, and possible solutions

A. Key sensing and NDT application successes of THz-SI

The literature survey revealed that THz technology has experienced tremendous interest since its first emergence almost 30 years ago. The success of THz-SI as a useful NDT tool has been promoted by several factors including the prevalent geopolitical, ecological, and financial situations of different countries and research institutions around the world, advancements in photonics, electronics, and laser technology, as well as the advantageous properties of THz waves (*e.g*. biosafety, spectral fingerprints of different materials and substances, good penetration of non-conducting matters, high resolution, *etc*.) [14], [55]. Advances in all these fronts continuously intensified since the beginning of the 21st century

and this prompted a significant increase in THz sensing and NDT applications, particularly in the fields of medical diagnostics, chemical substance detection, and biological features detection followed by the physico-chemical evaluation of materials and structural systems in the fields of material science as well as the process monitoring and product quality evaluation in the manufacturing industry [16], [25], [298], [602]. In addition to classic technological advancements, the recent introduction of THz metamaterial systems has also increased the resolution and sensitivity of the THz systems and prompted their applications for the detection and/or identification of micro or even trace amount of samples or physico-chemical substances.

Consistent with the aforementioned, the early prediction of the potential widespread usage of THz systems for the sensing and physico-chemical evaluation of materials and structural systems came true about a decade ago. In the past 5 years, in particular, state-of-the-art THz-SI systems for applications such as the evaluation and characterization of protective paints and coatings in automotive and marine industries [14], [262], [271], [283], detection of complex biomolecules in medical diagnostics [576], [603], as well as process analytical technology for quality monitoring in the pharmaceutical industry [288], [289] have all been registered with so many other systems currently being developed. The continued desire to use THz-SI systems for sensing and NDT applications complex systems and structures combined with advances in photonics, electronics, and computer technology also fuelled the development of new and efficient types of THz sources and detectors [1], [108], novel imaging methods and analyses of the measured signals [55], [66], [289], smarter THz system configurations [153], [577], *etc*. To increase the performance of the currently available THz systems for general-purpose spectroscopic and imaging applications, recent studies have been focusing on addressing aspects related to the acquisition speed of THz signals by using state-of-the-art single detectors with spatial light modulators and compressive imaging techniques or by using graphene or silicon-based technologies, which are inherently scalable and capable of promoting the development of more compact, portable and cost-effective THz-SI systems [116], [604]–[609]. In fact, the literature indicates that the fast development of graphene or silicon-based technologies has contributed to the development of contemporary THz components and devices, which subsequently contributed to the surge of applications of THz technology to new areas including biomedicine, agriculture, composite material, structural systems, liquid petrochemical, *etc*. In many cases, the constantly increasing performance of THz-SI systems and the continued discoveries of their spectroscopy and imaging capabilities in the detection and analysis of biological substances as well as the physico-chemical evaluation of materials and structural systems have attracted significant attention from users in the NDT community seeking to optimize THz-SI systems to fit their measurement requirements by improving their technological features such as speed, configuration, performance, cost, *etc*. which are extremely important for their performance and strategic applications.

In the pharmaceutical industry, for example, THz sensing is capable of revealing a wealth of information detailing the microstructure, coating thickness, and contrasts between the adjacent coating structures of pharmaceutical tablets and capsules [25], [27], [284], [285]. These applications are enabled by the capabilities of THz waves to penetrate through thick dosage form coatings and provide a full characterization without being affected by the scattering losses caused by the embedded pigments, additives, and/or air bubbles. However, it is noted that while THz sensing can resolve coatings greater than 35 μm without using complicated data processing methods, THz-SI systems cannot generally resolve tablets coatings with sharp edges or embossing nor can the devices fully image through the entire tablet volumes largely due to the types of optics used by currently available THz systems. To solve this issue and achieve large-scale usage and deployability of THz technology across the pharmaceutical industry like its competing near-infrared and Raman spectroscopic systems, this technology requires the development of faster and more reliable image acquisition systems with adequate laser operational stability, power sources, and affordability levels [55]. Additionally, the development of advanced signals processing techniques capable of overcoming the scattering losses caused by the sharp edges at depth should be considered to be able to resolve all the in-depth spectral signatures of the tablets and perform a 3D mapping of their chemical composition [294]. Also, the improvement of the currently existing waveform selection algorithms, as well as addressing the issue of data management or sampling strategies should be envisioned to harness the many advantages of THz sensing in the pharmaceutical industry [25], [302], [610].

In applications related to safety and security, the literature indicates that the initial intense thrust in these areas such as the detection of concealed explosives and weaponry from a distance was quickly diminished about a decade ago partly because of the anticipated “over-expectation” by the users of this technology [55]. This is particularly because the THz technology was relatively in its early stages of implementation with very rudimentary types of software and hardware systems for data acquisition and processing when it started [3], [14]. This was also exacerbated by the existence of the “THz Gap” and the extreme absorption of THz waves by polar molecules in the air such as moisture or humidity. As such, the likelihood of detecting certain types of concealed explosives either alone or mixed with stabilizers or accelerant agents located at a relatively long stand-off distance using diffused THz reflection (*i.e*., located at a few meters to a dozen meters away from the target [611]) was simply a stretch too far and researchers quickly lost interest in this types of application. This was particularly because of the contemporary limited power of the THz source and sensitivity of the THz detector, as well as the concealment through a combination of barriers and the length of the stand-off distance between the measuring device and the target. To this end, one of the most effective scenarios is to reduce the magnitude of the diffused reflectance of the THz spectra measured from high-energy materials and substances, given that these spectra are generally broad in frequency, weak, and tend to overlap with THz signals coming from other substances in the target samples thereby making their detectability difficult and the discrimination between the

different substances in the mixture almost impossible [612], [613]. Additionally, although THz spectroscopic information obtained using the coherent optical gating mechanism provides substantial SNR albeit using weak THz sources this configuration generally restricts the range of the distance over which accurate THz spectroscopic inspection can be achieved. Also, both the probe and the pump arms of the THz-SI system should have the same optical path lengths to ensure accurate measurements in the coherent detection scheme. However, the system implementation of this nature with large stand-off detection distances is utterly challenging mostly because it requires a precise and strict dispersion control of the ultrafast optical laser at its THz wave generation and detection terminals. As such, the detection of any highly energetic material systems (with spectral lines that can reach 2 THz or more) simply becomes impractical under the aforementioned concealment and stand-off measurement conditions [55]. Quite surprisingly though, some research groups continue with this effort to this day with unconvincing results still being reported [614], [615].

To overcome the issues related to stand-off-based THz inspections in safety and security-related applications, current research efforts are constantly being orientated toward the development of effective remote detection tools with highly maneuverable robotic systems (*i.e.*, to increase the scope of THz inspection in unsafe environments, confined spaces, or hard-to-reach areas without the need of human interventions) which is one of the technological by-products of THz sensing/NDT arising from intense developments in its industrial applications [48]. The success of such an endeavor is generally reliant on the recent development of powerful fiber-coupled PCA-based THz wave generators and detectors driven by ultrafast laser systems featuring high-performance optical sampling devices that are capable of acquiring more than 10^4 THz spectroscopic scans per second [124]. However, these types of systems also require the use of advanced signal/image analysis to accurately interpret the measured results and be able to overcome the concealment factors and counter different types of frequency-dependent measurement uncertainties introduced by numerous environmental and system operation factors during the measurements. Indeed, the most important metrics used to determine the performance of THz systems in security and safety screening applications are stand-off capability or remote maneuverability of the system as well as the flexibility of using advanced image/signal analysis and interpretation methodologies for feature extraction and recognition [81], [616]. Although the cost might not always be an issue when considering the loss of lives that might be involved if an explosive is to detonate in public spaces, both the system portability and image/signal acquisition speed are other important developments to be considered to ensure the practical feasibility of THz sensing/NDT in safety and security-related applications. To date, there are only a few imaging systems based on THz sensing/NDT for security screening applications worldwide, and numerous research groups worldwide are actively pursuing this objective to improve the sensing/NDT capabilities of THz systems in safety and security-related applications using modern THz technological advancements [81], [616]–[618].

In the biomedical field, the rapid progress in THz technology has enabled the development of portable and ergonomic THz-SI systems for diagnostic and therapeutic applications [474]–[476], [478], [479]. The extreme sensitivity of THz waves to the content and/or states of water molecules either as a free substance or bound with the body tissues provided novel opportunities for biomedical engineers and medical doctors using THz medical imaging as a diagnostic tool to apply this instrument in areas such as the examination of traumatic injuries, label-free diagnosis of benign or malignant neoplasms with different nosological classification and/or localization levels, detection of tissue viability, diagnosis of diabetes mellitus, as well as the therapy for certain inflammatory diseases and tumors/cancers [9], [479]. Also, THz waves are generally considered biologically safe and have a wide range of spectroscopic signatures for several types of biomolecules with potentially numerous biomedical application advantages. Although THz-SI systems present enormous opportunities for biomedical applications, numerous factors such as the lack of appropriate parts, the complexity of the hardware systems, costly hardware configurations, limited software integration, low power of common THz waves generators, limited sensitivity of THz detectors for biological samples, substantial water absorption levels, and low penetration depths still limit the high-performance imaging of THz-SI systems and effectively hinder the mass-market introduction of THz medical imaging. To put this into perspectives, THz medical imaging remains a novel research direction where significantly fewer data relating to the THz-wave-biological-tissue interactions have been presented, as compared to their visible and IR frequency ranges counterparts, which currently provide the most common diagnostic instruments to study and analyze the properties of biological tissues [55]. To this end, it is crucial to conduct further studies to gather enough information related to the optical properties of biological and molecules tissues in the THz frequency band and analyze the underlying physical effects of THz waves on these types of samples, which could also help researchers to identify the advantages of using THz medical imaging and spectroscopic systems over other types of medical imaging and spectroscopic systems. Although THz medical imaging and spectroscopic systems are highly accurate devices that could revolutionize the medical spectroscopy and imaging industry, the use of these instruments for medical diagnostics is still very rare, particularly because they are cumbersome, have less penetration capability of THz waves in biological samples/tissues, and are relatively expensive compared to other well-established medical imaging systems. To this end, it would be extremely beneficial to develop some cost-effective, high-performance, and portable THz-SI systems and components for biomedical applications with a special emphasis on the development of new THz materials to manufacture high-performance THz emitters and detectors as well as high-performance optical devices such as highly resistant and flexible waveguides that could be used to deliver THz waves to internal or hardly-accessible biological tissues and/or organs. In addition to the aforementioned, improving the spatial resolution of THz-SI systems beyond the diffraction limit with the performance up-to- or close-to-real-time inspection capabilities (*i.e.*, which is generally required to avoid long hour measurements that would result in the distortion of

the biological samples) is highly warranted to achieve an effective competition of THz-SI with the existing state-of-the-art medical spectroscopy and imaging modalities. Finally, the data variability observed for most of the label-free sensing methods for malignancy diagnosis is also observed in THz data obtained from the measurements of biological tissues [619]. A combination of THz-SI systems with other label-free imaging systems could be an effective method that could help THz users to obtain comprehensive diagnostic information on biological tissues as such combinations would take advantage of the diagnostic capabilities of different systems to provide accurate descriptions/characterizations of the target samples [478], [479], [620].

In the petrochemical industry, THz sensing/NDT is used to determine the complex optical and dielectric properties, analyze inter- and intramolecular interactions, investigate the molecular and relaxation dynamics, as well as the qualitative identification and quantitative analysis of petrochemical products [74], [418], [436], [437], [440], [446]. Although many of the tests and detection applications have been performed using the THz systems with regular THz emitters and detectors, the literature survey indicates recent developments have been focusing on the use of THz metamaterials sensing to obtain better sensitivity and accurate testing results [175]. To date, several research directions using THz technology to analyze the chemical compositions and contamination levels of petrochemical products are constantly being pursued in numerous laboratories and research institutions around the globe to improve the applicability and efficacy of THz-SI for the examination and detection of substances and products in the petrochemical industry [418]. These include but are not limited to the development of 2D and 3D THz imaging systems and the miniaturization of THz devices capable of distinguishing interfaces between different petroleum products in pipeline transportation systems. These developments also include the use of THz-SI systems to analyze the state and composition of refined petrochemicals, evaluate the chemical accessories and/or additive contents, inspect and characterize the different types of protective coatings for pipeline systems, *etc*.

In the artwork conservation industry, THz-NDT is used in the conservation of cultural artifacts and artwork structures at rather a phenomenal rate, thanks to the non-contact, non-destructive, and non-ionizing features of the THz-SI systems [405]. In addition to these general advantages, THz waves also offer other specific advantages such as the provision of chemical specificities or spectral fingerprints of complex molecules in different types of physico-chemical substances such as dye, ink, paints, glaze, and metal oxides found in gemstones and artifacts as well as considerable penetration capabilities for dielectric materials such as textiles, clothing, wood, marble, paper, bones, ivory, *etc*. found in artwork and cultural heritage structures [402], [410], [416]. Additionally, most THz-SI systems are surprisingly capable of performing a tomographic inspection of materials and structures used in the artwork industry, which allows users to establish accurate depth profiling of countless artifacts and cultural heritage structures in their natural states.

B. Existing challenges and possible solutions

Although both the hardware and software systems of THz-SI systems have developed rapidly since the beginning of the 21st century, many challenges still limit their widespread adoption by regular spectroscopic and imaging systems users. For example, factors such as the low signal/image acquisition speed, lack of efficient signal analysis/processing algorithms, limited miniaturization capabilities of current technologies and/or portability of THz-SI systems, limited customizability of THz-SI for specific applications, the cost of current state-of-the-art THz systems are some of the many issues that require immediate attention from researchers and engineers to achieve a realistic implementation of this technique [55]. Fig. 24 depicts the fundamental premise behind the lingering issues related to the realistic implementation of THz-SI systems and their subsequent sensing and NDT applications in real-world scenarios.

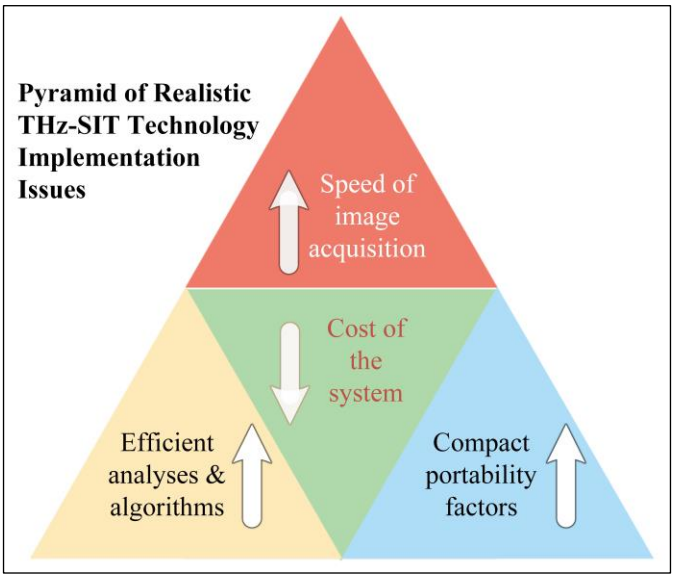

Fig. 24: Typical technical system and software limitations of current THz-SI systems. The directions of the arrows indicate the current movements of the parameters indicated in the pyramid (*e.g*. the speed of the image acquisition mechanisms is increasing, the cost of the system is reducing, *etc*.).

Although significant progress has been made in improving the operation of THz-SI systems in recent years, the pre-requisite optical delay line, the inefficiency of THz laser sources, and the use of single-pixel detectors are the major factors limiting the imaging speed of THz-SI systems [621]. In THz-TDS systems featuring an optical delay line with a linear mechanical motion, for example, the best performance period of the aforementioned optical delay is estimated to be in the millisecond range [621], [622]. Interestingly, the THz signals' collection rates can be significantly improved up to the kilohertz range by eliminating the mechanical motion of the delay line and replacing it with some state-of-the-art optical sampling methods such as asynchronous optical sampling, electronically controlled optical sampling, and laser cavity tuning [623]–[626]. To obtain better images with all useful features and at significantly high-resolution levels, advanced

THz imaging techniques *viz*. THz tomography and near-field imaging techniques have been developed [321], [322], [627]–[629]. The former is capable of performing 3D imaging of specimens while the latter can provide high-resolution images of specimens (*e.g*. generally in the nanometer range) [621]. However, THz tomography imaging is still a slow imaging method that requires the development of adequate mechanisms to achieve simultaneous parallel measurement of pixel data, achieve the third dimension or corner rotation measurements of the specimens, *etc*. to reduce the data acquisition time [621], [629] and increase the ability to capture projected images and reconstruct them at a variety of angles for accurate visualization and presentation of the 3D map of the specimen under test [621]. As such, these systems already meet the requirements of providing fast TOF signals, the capability of running at room temperature, and avoiding external interference, but the development of fast imaging components that could facilitate the promotion of further breakthroughs toward the development of real-time THz imaging systems is still lacking.

In terms of their cost, for example, the current state-of-the-art THz-SI systems are considerably expensive, owing mostly to their expensive photonic components and high-end electronic systems [15], [55]. In particular, the fabrication of PCA emitters and detectors faces unrelenting cost-effectiveness and large-scale production viability issues. Although low-temperature GaAs are the most preferred type of semiconductor material for the fabrication of PCA devices, the properties of this semiconductor material are extremely difficult to reproduce, even when grown under the same nominal conditions. Additionally, the growth of low-temperature GaAs materials requires must be performed in molecular-beam-epitaxy machines, which is an expensive method and hence not available on a larger scale [630]. As a result, the successful implementation of cost-effective compact and on-chip THz-SI systems will heavily rely on a substantial reduction of their "*ticket price*" and that of their modular components.

Although THz-SI systems are highly efficient sensing and NDT tools, useful features are often submerged into complex THz datasets thereby jeopardizing the accuracy of THz measurements. To this end, numerous traditional and machine learning-based signal processing techniques have been developed to improve the accuracy of THz measurements []. However, traditional signal processing techniques generally use manual feature extraction methods, which are generally not accurate or fast enough to provide a timely analysis of the constantly increasing amount of THz signals under complex sensing and NDT application scenarios [66]. Also, while machine learning algorithms can address some of these issues, these algorithms need good-quality datasets and require an accurate selection of features of interest [81]. However, a reliable database with full consideration of environmental factors (*e.g*. temperature and humidity, *etc*.) is generally difficult to obtain, and most specimens are relatively complex and their material/substance constituents often have unique THz spectral fingerprints in the THz frequency range. To this end, the effective integration of intelligent THz-SI systems into sensing and NDT applications will heavily rely on the quality and representativity of the THz datasets to train and test these algorithms. Finally, the feature information can be easily covered by noise particularly for signals with low SNR levels, making it difficult to extract useful features during the analysis of the results. As such, more effective algorithms should be envisioned when extracting useful features from THz signals.

In addition, the strong absorption of THz waves by polar substances or molecules in the air constitutes a clear hindrance to the widespread applications of THz sensing, and hence the use of dry air or liquid nitrogen to provide a measurement/test medium free from polar molecules is often considered. In the absence of dry air or liquid nitrogen, experiments can also be conducted under vacuum conditions to eliminate the effect of polar molecules in the sample housing unit of the THz system. Nevertheless, these types of conditions are usually not available on a large scale for practical applications, which limits the fast detection of substances and physico-chemical characterization of materials and structures. In addition, although THz waves have a relatively high penetration capability for relatively thick samples, their depth penetration is still limited, particularly when samples are concealed or overshadowed by obstacles containing polar liquids such as water or covered by conductive materials such as metals [16], [32], [55]. To this end, further improvements in the optimization of metamaterial structures, the development of newer metamaterial systems similar to microfluidic channels, as well as the development of newer and effective data processing algorithms to extract all usable information and achieve accurate detection and inspection results. Additionally, it is necessary to further reduce the cost of THz systems which are still relatively high compared to other NDT systems, increase their detection limit and imaging speed, and further improve their resolution and SNR levels through the development of new THz measuring approaches and system architectures.

In addition to the aforementioned technological challenge that challenges, the chip-scale integration of numerous THz components as well as the design of compact, rugged, efficient, room-temperature-operated, and portable THz-SI systems in tactical and/or commercial sectors are also limited and require considerable attention to enable the feasibility of field inspections/measurements in the THz frequency range [55]. Although numerous advancements in the design and manufacturing of high-performance THz optoelectronic and photonic devices in recent years, the resultant THz systems still present cumbersome modular designs. To this end, it is recommended that as new THz sensing and NDT modalities and measurement approaches continue to be developed, the design of compact, rugged, room-temperature-operated, and portable systems be considered to satisfy all levels of the THz sensing and NDT application scenarios. Also, information about their suitability and performance for different sensing and NDT applications should equally be made available to help potential users be more efficient and easily figure out the best practice possible to use them and achieve accurate sensing and testing results.

In summary, all the aforementioned developments are expected to extend the applications of THz-SI systems in real-world sensing/NDT settings and boost their acquisition by industries with limited budgets which cannot currently afford to pay even for general-purpose THz-SI systems due to their elevated prices. Additionally, the spectral range of currently

available THz-SI instruments should be extended to improve their spatial resolution and achieve effective NDT of materials and structural systems capable of detecting incipient structural damage and/or defects in thin film systems. Advanced signal and image processing methods capable of extracting and recognizing features from the measured signals with weak defect information are also required to achieve high-performing THz-SI systems. The penetration depth of THz waves should also be investigated and establish an inspection limits profile that could help users quickly decide when to use the THz-SI systems. The development of high-power THz sources, which can enable the inspection of thick materials, is highly warranted to ensure the expansion of THz-NDT in high-end engineering applications.

VI. Emerging Trends and Possible Breakthroughs

As indicated in the introduction section, the aim of this study is not merely to present the fundamental concept that was put forward by the masters of THz-SI systems and then assess its applicability and challenges related to their sensing and NDT applications, but also to extrapolate what could be its future scope of application, design, and implementation. To conceptualize the future projection of the THz technology's footprints, it is important to invoke some of the masters of this technology. In [374], for example, De Lucia examined the application prospects of the sub-mm range spectroscopy and went on and addressed the pessimism previously expressed by his peers on the fading "excitement of molecular spectroscopy". In most of the next frontiers and opportunities highlighted by the author, he rightfully indicated that spectroscopy will be a "*useful servant*" in all human scientific discoveries. The sentiment expressed by De Lucia is not only timelessly true for a discipline like molecular spectroscopy but also relevant for THz-SI technology. Indeed, the latter is an epic multidimensional spectroscopic tool with both surface and volume mapping capability using non-ionizing radiation. Its current applications are innumerable and are expected to grow even further. Perhaps, one of the easiest approaches to foretell the future of THz-SI technology would be to revisit the fundamentals of the science and the techniques behind its spectroscopy and imaging techniques as published in recent tutorials [58], [61], [302]. This could also be supplemented by some recently reported innovative concepts of THz-SI for high-end applications such as medical diagnostics, security screening, and/or material science.

Consistent with the aforementioned, the following are considered to be the most important emerging trends from the bibliography of this study. First, the fabrication of different diffractive, refractive, and reflective optics for THz imaging applications using novel technology such as 3D printing. Apart from the source and the detector, beam-steering optics form the most crucial part of an imaging arrangement for any sort of application. One of the reasons for the limited growth of THz-SIT technology in the past is the lack of customizability of such optics because of limited options of materials and easy routes of fabrication. Lately, however, this limitation has been replaced by the liberation of ideas and concepts with the help of groundbreaking technologies (*e.g*. additive manufacturing) [117]–[119]. Using these toolsets and advanced computer modeling and graphics, high-performance THz imaging components are being made, literally, out of nothing but outstanding sheer innovation [631]–[635], and these developments are expected to "*break the mold*" of future applications of THz-SI in different sensing and NDT applications with faster image acquisition, and compact, portable, and economical THz-SI system configurations. Second, the design and implementation of THz plasmonic-based chip-scale spectroscopic components are currently being explored as a potential roadmap toward the miniaturization of THz-SI systems [55], [116], [323]. Instead of using conventional operational routes (*i.e*., the use of frequency upconversion and down-conversion methods), chip-scale THz plasmonic devices use simple physics such as the use of tiny transistor gates (*e.g*. gates in plasmonic field-effect-transistors) to select the operational frequencies [55]. In plasmonic field-effect-transistors, for example, the operational frequency selection process is controlled by both the density of charge carriers (*i.e*., tunable by tailoring the conductivity levels of the layers in the base materials) and their length (*i.e*., the distance between their source and drain layers) [636]. Interestingly, most 2D plasmons generated in this manner are highly confined in a dimension scale much smaller than the diffraction limit of THz wavelengths, hence the possibility of miniaturizing on-chip sensing, frequency mixing, and modulation processes [637]. These advances are also expected to drive the implementation of THz-SI systems with an added advantage of fabrication scalability [604]–[609], and hopefully a reduced price tag for THz-SI systems [55]. Third, the fact that long-range free-space propagation has never been and never will be a strong suit in the THz frequency range, researchers are currently working to adapt the THz-SI technology in a "*very near*" range or in "*near-field*" mode where the technique implementation, required hardware, data processing mechanisms, *etc*. are different from those of the "*far-field*" mode [638]–[640]. In fact, these implementations have recently opened up a whole new world of information (*e.g*. the visualization of the interaction between THz radiation and single biological cells or atoms) which almost defies the rules of physics and optics [641]–[643]. Indeed, this "*near-field*" spectroscopy and imaging will undoubtedly have far-reaching effects on the understanding of the fundamental behavior of substances in biology, physics, and chemistry. Fourth, there is also the technology merging by bringing together multiple orthogonal spectroscopic techniques in a single detection platform. This is particularly important because the THz-SI systems also have limited spatial resolutions, suggesting that merging their measurements with those obtained from other sensing and mapping systems operating in other regions of the electromagnetic spectrum such as Raman spectroscopy, FTIR, *etc*. techniques having far greater spatial resolution and greater sensitivity to the presence of trace amounts of physico-chemical substances, would provide adequate sensing and NDT measurements in areas such as biosciences, artwork conservation, *etc*. [619], [644], [645]. It is estimated that system combination or data fusion will also lower the cost of current THz-SI systems and increase their adaptability to new application areas, while equally enabling users to obtain accurate measurements [199]. Finally, exploiting mature technology by optical conversion of THz signal is also another area taking steam in recent years.

Although it has been almost 25 years since the first sets of spectral THz images were obtained, THz-SI systems still suffer from a relatively "*low level*" of technological and engineering maturity compared to systems operating the infrared- or optical frequency ranges. To this end, researchers are currently converting THz signals into infrared or optical signals, thereby overcoming the struggle against the limitations of current THz-SI systems [646]–[649]. Evidence has shown that converted infrared or optical signals/images can easily be stored, transferred, or even transformed via several technological pathways available in those ranges. Indeed, this trend is considered the most out-of-the-box notion that could be the most effective of all the current trends in the successful implementation and applications of THz sensing and NDT devices.

Also, the fabrication of PCA emitters and detectors faces unrelenting cost-effectiveness and large-scale production viability issues particularly because the majority of these devices are fabricated using low-temperature GaAs material whose properties are extremely difficult to reproduce (*i.e*., even when grown under the same nominal conditions) and which is grown in molecular-beam-epitaxy machines (*i.e*., an expensive method and not available on a larger scale) [630]. Also, both the relatively low radiation power and detection sensitivity of common PCA devices place limitations on the SNR ratio and operation bandwidth of the host THz-SI systems. To address these technical challenges, several techniques have been devised, and the most promising ones by leveraging the advantages provided by advanced techniques such as nanotechnology for the fabrication of PCA devices with nanostructures (*e.g*. nanoantennas, nanomaterials, plasmonic nanostructures, and optical nanocavities, *etc*.) that increase the interaction of the optical pump beam with the photoconductive semiconductor [1], [650] and the use of 3D printing technology to achieve (*e.g*. electron beam lithography, immersion UV lithography, nanoimprinting, soft lithography, extreme UV lithography, *etc.*) manufacture cost-effective THz PCA devices with higher THz power throughput and yield [117]–[119]. Therefore, the significant performance enhancement offered by various types of nanostructures combined with advanced nanomanufacturing techniques will pave the way for the next generation of low-cost, high-performance PCA emitters, and detectors with numerous sensing and NDT applications.

In summary, advances in computer modeling and computer simulation technologies coupled with advances in additive manufacturing (e.g. 3D printing technology) are driving the design and manufacturing of on-demand THz optical components for high-end THz-SI systems. In particular, it is estimated that highly confined 2D plasmons below the diffraction limit of THz waves could perform on-chip THz sensing, frequency mixing, modulation, spectroscopy, THz imaging, *etc*. with ease of operation and fabrication scalability. Also, the exploitation of the near-field interaction of THz waves with the matter in chemical, physical, and biological systems opens the possibility of spectroscopic analysis and imaging of extreme material features such as the dynamic behaviors of single biological cells or atoms, which are critical for advanced studies in biological and material sciences. To increase the spatial resolution or enhance the limited sensitivity of THz-SI systems to amounts of samples, orthogonal spectral mapping technologies are currently being merged with the THz frequency range to produce comprehensive and rugged imaging platforms. Finally, the conversion of detected THz signals, either in IR or visible ranges is expected to unlock the processing and recording pathways of THz signals by relatively mature and economical spectroscopic and imaging technologies.

VII. Concluding remarks

The present paper provides an updated review of the state-of-the-art and state-of-the-practice pertinent to the utilization of THz technology for sensing and NDT applications in different types of industries and areas of research for the detection, evaluation, and recognition of substances across the spectrum of research and development all the way to process analytical technology, quality control, nondestructive testing, and structural health monitoring owing to the unique combination of characteristics, such as chemical specificity, dielectric penetrability, higher spatial resolution compared to microwaves, extremely low to no biological concerns in terms of radiation safety, *etc*. The literature survey indicates that THz-SI has experienced a considerable uptake in the fields of biochemistry, cultural heritage conservation, safety and security, medical diagnostics, biosensing, industrial process control, material characterization and evaluation, hydration analysis of biological tissues, food quality control, and agri-photonics in recent years, thanks to the developments in areas such as computer technology, optoelectronics, nanotechnology, and phononics. In fact, these developments have recently opened up a whole new world of extremely important information where the interaction between THz waves and the matter in chemical, physical, and biological systems (e.g. single biological cells, single atoms, *etc*.) can be easily visualized in ways that almost defy the rules of physics and optics.

Although THz-SI systems have experienced steep growth in their fabrication, design improvements, and various sensing and NDT applications, the literature survey also revealed that their utilization continues to suffer from low image acquisition speed, high costs for their modular components, considerable footprint/size of their imaging systems, limited spectral contrast in the through-barrier mode, low spatial resolution (usually ~ 1 μm), *etc*. Unlike other modes of commercially successful and mature spectroscopy and imaging technologies such as Fluorescence, Raman, and FTIR systems, most of the issues related to THz sensing and NDT are not dictated by common laws of optics and physics. Experts believe that this probably makes it difficult to establish clear operational principles, signal processing techniques, and measurement requirements, which subsequently affect the determination of unequivocal improvement pathways. In particular, major issues plaguing the sensing and NDT applications of THz-SI systems are, in most cases, the consequences of slow technological progress in implementation pathways and continuing concerns over the accessibility of powerful THz emitters/sources, highly sensitive THz detectors, and other passive and active THz optics. Interestingly, with the recent push towards fundamental material research, nanotechnology, and device manufacturing technology (*e.g*. 3D printing or additive manufacturing

technology), tremendous developments are continuously being registered with the rapid development of more efficient THz sources/emitters, extremely sensitive THz detectors, and various other types of high-performance THz components, which are, in most cases, driven by several radical concepts. Increasingly, techniques from both the electronic side and the photonic side of the THz frequency range are successfully being merged for the first time leading to emerging THz sensing and NDT concepts including THz topological photonics, optical conversion of THz signals, chip-scale THz hybrid architectures, *etc*. and these constitute a clear path toward successful implementation of high-end THz-SI systems, the miniaturization of THz-SI modular components and the fabrication of chip-scale and/or portable THz-SI systems.

Additionally, traditional technological strategies of frequency down-conversion from the photonics side or up-conversion from the electronics side to generate or detect THz signals are considered a thing of the past in these new developments. For example, direct digital-to-impulse architecture, excitation of surface and collective modes, and antenna-coupled heterostructures with precise nano-particle inclusions are some of the hallmark characteristics of these technological shifts. Interestingly, this type of paradigm shift in the technological growth of THz-SI is very crucial because it paves the way for the development of high-end compact, rugged, scalable, and energy-efficient components which are also reconfigurable based on the application requirements. Considering the past 5 years as a time scale measurement for these technological developments, the bibliography of this study indicates that even within this short period, THz-SI technology is already experiencing parallel growth in the THz-SI system-level implementation, and THz-SI systems' operational concepts in numerous areas of application, and this trend is expected to continue for years to come. To this end, it is perhaps not too unrealistic to foresee that THz-SI would certainly overcome some of the aforementioned key challenges given the current sensing and NDT application successes, and current trends in the development of high-end THz-SI systems.

References

[1] N. T. Yardimci and M. Jarrahi, "Nanostructure-Enhanced Photoconductive Terahertz Emission and Detection," *Small*, vol. 14, no. 44, p. 1802437, 2018, doi: 10.1002/smll.201802437.

[2] M. Tonouchi, "Cutting-edge terahertz technology," *Nature Photon*, vol. 1, no. 2, pp. 97–105, Feb. 2007, doi: 10.1038/nphoton.2007.3.

[3] P. U. Jepsen, D. G. Cooke, and M. Koch, "Terahertz spectroscopy and imaging - Modern techniques and applications," *Laser & Photon. Rev.*, vol. 5, no. 1, pp. 124–166, Jan. 2011, doi: 10.1002/lpor.201000011.

[4] L. Afsah-Hejri, E. Akbari, A. Toudeshki, T. Homayouni, A. Alizadeh, and R. Ehsani, "Terahertz spectroscopy and imaging: A review on agricultural applications," *Computers and Electronics in Agriculture*, vol. 177, p. 105628, Oct. 2020, doi: 10.1016/j.compag.2020.105628.

[5] M. van Exter, Ch. Fattinger, and D. Grischkowsky, "Terahertz time-domain spectroscopy of water vapor," *Opt. Lett.*, vol. 14, no. 20, p. 1128, Oct. 1989, doi: 10.1364/OL.14.001128.

[6] H. J. Shin, S.-W. Choi, and G. Ok, "Qualitative identification of food materials by complex refractive index mapping in the terahertz range," *Food Chemistry*, vol. 245, pp. 282–288, Apr. 2018, doi: 10.1016/j.foodchem.2017.10.056.

[7] H.-B. Liu, Y. Chen, G. J. Bastiaans, and X.-C. Zhang, "Detection and identification of explosive RDX by THz diffuse reflection spectroscopy," *Opt. Express, OE*, vol. 14, no. 1, pp. 415–423, Jan. 2006, doi: 10.1364/OPEX.14.000415.

[8] P.-K. Lu *et al.*, "Ultrafast carrier dynamics in terahertz photoconductors and photomixers: beyond short-carrier-lifetime semiconductors," *Nanophotonics*, vol. 11, no. 11, pp. 2661–2691, Jun. 2022, doi: 10.1515/nanoph-2021-0785.

[9] X. Fu, Y. Liu, Q. Chen, Y. Fu, and T. J. Cui, "Applications of Terahertz Spectroscopy in the Detection and Recognition of Substances," *Front. Phys.*, vol. 10, p. 869537, May 2022, doi: 10.3389/fphy.2022.869537.

[10] K. S. Kumar, G. L. Prajapati, R. Dagar, M. Vagadia, D. S. Rana, and M. Tonouchi, "Terahertz Electrodynamics in Transition Metal Oxides," *Adv. Optical Mater.*, vol. 8, no. 3, p. 1900958, Feb. 2020, doi: 10.1002/adom.201900958.

[11] E. V. Loewenstein, "The History and Current Status of Fourier Transform Spectroscopy," *Appl. Opt.*, vol. 5, no. 5, p. 845, May 1966, doi: 10.1364/AO.5.000845.

[12] K. D. Möller and W. G. Rothschild, "Far-infrared spectroscopy," *New York: Wiley*, 1971.

[13] W. Nsengiyumva, S. Zhong, M. Luo, and B. Wang, "Terahertz Spectroscopic Characterization and Thickness Evaluation of Internal Delamination Defects in GFRP Composites," *Chinese Journal of Mechanical Engineering*, vol. 36, no. 1, p. 6, Jan. 2023, doi: 10.1186/s10033-022-00829-7.

[14] S. Zhong, "Progress in terahertz nondestructive testing: A review," *Front. Mech. Eng.*, vol. 14, no. 3, pp. 273–281, Sep. 2019, doi: 10.1007/s11465-018-0495-9.

[15] M. Naftaly, N. Vieweg, and A. Deninger, "Industrial Applications of Terahertz Sensing: State of Play," *Sensors*, vol. 19, no. 19, Art. no. 19, Jan. 2019, doi: 10.3390/s19194203.

[16] W. Nsengiyumva, S. Zhong, J. Lin, Q. Zhang, J. Zhong, and Y. Huang, "Advances, limitations and prospects of nondestructive testing and evaluation of thick composites and sandwich structures: A state-of-the-art review," *Composite Structures*, vol. 256, pp. 112951–113002, Jan. 2021, doi: 10.1016/j.compstruct.2020.112951.

[17] D.-H. Han and L.-H. Kang, "Nondestructive evaluation of GFRP composite including multi-delamination using THz spectroscopy and imaging," *Composite Structures*, vol. 185, pp. 161–175, Feb. 2018, doi: 10.1016/j.compstruct.2017.11.012.

[18] H.-W. Hübers, R. Eichholz, S. G. Pavlov, and H. Richter, "High Resolution Terahertz Spectroscopy with Quantum Cascade Lasers," *J Infrared Milli Terahz Waves*, vol. 34, no. 5, pp. 325–341, Jun. 2013, doi: 10.1007/s10762-013-9973-7.

[19] P. Han, X. Wang, and Y. Zhang, "Time-Resolved Terahertz Spectroscopy Studies on 2D Van der Waals Materials," *Adv. Optical Mater.*, vol. 8, no. 3, p. 1900533, Feb. 2020, doi: 10.1002/adom.201900533.

[20] H. Němec, P. Kužel, and V. Sundström, "Charge transport in nanostructured materials for solar energy conversion studied by time-resolved terahertz spectroscopy," *Journal of Photochemistry and Photobiology A: Chemistry*, vol. 215, no. 2, pp. 123–139, Sep. 2010, doi: 10.1016/j.jphotochem.2010.08.006.

[21] W. Nsengiyumva *et al.*, "Terahertz spectroscopic study of optical and dielectric properties of typical electrical insulation materials," *Optical Materials*, p. 111837, Dec. 2021, doi: 10.1016/j.optmat.2021.111837.

[22] Q. Jin, Y. E, K. Williams, J. Dai, and X.-C. Zhang, "Observation of broadband terahertz wave generation from liquid water," *Appl. Phys. Lett.*, vol. 111, no. 7, p. 071103, Aug. 2017, doi: 10.1063/1.4990824.

[23] M. Borovkova, M. Khodzitsky, P. Demchenko, O. Cherkasova, A. Popov, and I. Meglinski, "Terahertz time-domain spectroscopy for non-invasive assessment of water content in biological samples," *Biomed. Opt. Express*, vol. 9, no. 5, p. 2266, May 2018, doi: 10.1364/BOE.9.002266.

[24] Z. Zang *et al.*, "Terahertz spectroscopy for quantification of free water and bound water in leaf," *Computers and Electronics in Agriculture*, vol. 191, p. 106515, Dec. 2021, doi: 10.1016/j.compag.2021.106515.

[25] P. Bawuah and J. A. Zeitler, "Advances in terahertz time-domain spectroscopy of pharmaceutical solids: A review," *TrAC Trends in Analytical Chemistry*, vol. 139, p. 116272, Jun. 2021, doi: 10.1016/j.trac.2021.116272.

[26] S. Zhong *et al.*, "Non-destructive quantification of pharmaceutical tablet coatings using terahertz pulsed imaging and optical coherence tomography," *Optics and Lasers in Engineering*, vol. 49, no. 3, pp. 361–365, Mar. 2011, doi: 10.1016/j.optlaseng.2010.11.003.

[27] Y.-C. Shen, "Terahertz pulsed spectroscopy and imaging for pharmaceutical applications: A review," *International Journal of Pharmaceutics*, vol. 417, no. 1, pp. 48–60, Sep. 2011, doi: 10.1016/j.ijpharm.2011.01.012.

[28] C. M. Armstrong, "The truth about terahertz," *IEEE Spectrum*, vol. 49, no. 9, pp. 36–41, Sep. 2012, doi: 10.1109/MSPEC.2012.6281131.

[29] T. Hochrein, "Markets, Availability, Notice, and Technical Performance of Terahertz Systems: Historic Development, Present, and Trends," *J Infrared Milli Terahz Waves*, vol. 36, no. 3, pp. 235–254, Mar. 2015, doi: 10.1007/s10762-014-0124-6.

[30] S. Shen *et al.*, "Recent Advances in the Development of Materials for Terahertz Metamaterial Sensing," *Advanced Optical Materials*, vol. 10, no. 1, p. 2101008, Jan. 2022, doi: 10.1002/adom.202101008.

[31] O. Ahmed, X. Wang, M.-V. Tran, and M.-Z. Ismadi, "Advancements in fiber-reinforced polymer composite materials damage detection methods: Towards achieving energy-efficient SHM systems," *Composites Part B: Engineering*, vol. 223, p. 109136, Oct. 2021, doi: 10.1016/j.compositesb.2021.109136.

[32] S. Zhong and W. Nsengiyumva, *Nondestructive Testing and Evaluation of Fiber-Reinforced Composite Structures*. Singapore: Springer, 2022. doi: 10.1007/978-981-19-0848-4.

[33] J. Dong, B. Kim, A. Locquet, P. McKeon, N. Declercq, and D. S. Citrin, "Nondestructive evaluation of forced delamination in glass fiber-reinforced composites by terahertz and ultrasonic waves," *Composites Part B: Engineering*, vol. 79, pp. 667–675, Sep. 2015, doi: 10.1016/j.compositesb.2015.05.028.

[34] M. C. Beard, G. M. Turner, and C. A. Schmuttenmaer, "Measuring Intramolecular Charge Transfer via Coherent Generation of THz Radiation," *J. Phys. Chem. A*, vol. 106, no. 6, pp. 878–883, Feb. 2002, doi: 10.1021/jp013603l.

[35] A. Chakraborty, T. Inagaki, M. Banno, T. Mochida, and K. Tominaga, "Low-Frequency Spectra of Metallocenium Ionic Liquids Studied by Terahertz Time-Domain Spectroscopy," *J. Phys. Chem. A*, vol. 115, no. 8, pp. 1313–1319, Mar. 2011, doi: 10.1021/jp108097q.

[36] T. Li, Q. Yu, L. Zhang, and L. Jiang, "Terahertz spectroscopy of amino acid crystals based on dispersion-correction functional theory," *Spectroscopy Letters*, vol. 53, no. 1, pp. 55–62, Jan. 2020, doi: 10.1080/00387010.2019.1690524.

[37] J. Neu and C. A. Schmuttenmaer, "Terahertz Spectroscopy and Density Functional Theory Investigation of the Dipeptide L-Carnosine," *J Infrared Milli Terahz Waves*, vol. 41, no. 11, pp. 1366–1377, Nov. 2020, doi: 10.1007/s10762-019-00636-7.

[38] A. G. Davies, A. D. Burnett, W. Fan, E. H. Linfield, and J. E. Cunningham, "Terahertz spectroscopy of explosives and drugs," *Materials Today*, vol. 11, no. 3, pp. 18–26, Mar. 2008, doi: 10.1016/S1369-7021(08)70016-6.

[39] C. Jansen, S. Wietzke, V. Astley, D. M. Mittleman, and M. Koch, "Mechanically flexible polymeric compound one-dimensional photonic crystals for terahertz frequencies," *Appl. Phys. Lett.*, vol. 96, no. 11, p. 111108, Mar. 2010, doi: 10.1063/1.3341309.

[40] G. Gallot, S. P. Jamison, R. W. McGowan, and D. Grischkowsky, "Terahertz waveguides," *J. Opt. Soc. Am. B*, vol. 17, no. 5, p. 851, May 2000, doi: 10.1364/JOSAB.17.000851.

[41] J. Lloyd-Hughes and T.-I. Jeon, "A Review of the Terahertz Conductivity of Bulk and Nano-Materials," *J Infrared Milli Terahz Waves*, vol. 33, no. 9, pp. 871–925, Sep. 2012, doi: 10.1007/s10762-012-9905-y.

[42] I. Kawayama, C. Zhang, H. Wang, and M. Tonouchi, "Study on terahertz emission and optical/terahertz pulse responses with superconductors," *Supercond. Sci. Technol.*, vol. 26, no. 9, p. 093002, Sep. 2013, doi: 10.1088/0953-2048/26/9/093002.

[43] F. Giorgianni *et al.*, "Strong nonlinear terahertz response induced by Dirac surface states in Bi2Se3 topological insulator," *Nat Commun*, vol. 7, no. 1, p. 11421, Sep. 2016, doi: 10.1038/ncomms11421.

[44] X. Wang, J. Wang, Z.-D. Hu, G. Liu, and Y. Feng, "Angle insensitive broadband terahertz wave absorption based on molybdenum disulfide metamaterials," *Superlattices and Microstructures*, vol. 135, p. 106246, Nov. 2019, doi: 10.1016/j.spmi.2019.106246.

[45] K. Hussain *et al.*, "Terahertz time-domain spectroscopy of thin and flexible CNT-modified MXene/polymer composites," *Appl. Phys. A*, vol. 127, no. 5, p. 382, May 2021, doi: 10.1007/s00339-021-04525-6.

[46] S. Li, S. Xu, K. Pan, J. Du, and J. Qiu, "Ultra-thin broadband terahertz absorption and electromagnetic shielding properties of MXene/rGO composite film," *Carbon*, vol. 194, pp. 127–139, Jul. 2022, doi: 10.1016/j.carbon.2022.03.048.

[47] K. Su, Y.-C. Shen, and J. A. Zeitler, "Terahertz Sensor for Non-Contact Thickness and Quality Measurement of Automobile Paints of Varying Complexity," *IEEE Transactions on Terahertz Science and Technology*, vol. 4, no. 4, pp. 432–439, Jul. 2014, doi: 10.1109/TTHZ.2014.2325393.

[48] F. Ellrich *et al.*, "Terahertz Quality Inspection for Automotive and Aviation Industries," *J Infrared Milli Terahz Waves*, vol. 41, no. 4, pp. 470–489, Apr. 2020, doi: 10.1007/s10762-019-00639-4.

[49] P. Zhang *et al.*, "Application of Terahertz Spectroscopy and Imaging in the Diagnosis of Prostate Cancer," *Curr. Opt. Photon.*, vol. 4, no. 1, pp. 31–43, Feb. 2020, doi: https://doi.org/10.1364/COPP.4.000031.

[50] S. J. Park *et al.*, "Detection of microorganisms using terahertz metamaterials," *Sci Rep*, vol. 4, no. 1, p. 4988, May 2015, doi: 10.1038/srep04988.

[51] S. W. Jun and Y. H. Ahn, "Terahertz thermal curve analysis for label-free identification of pathogens," *Nat Commun*, vol. 13, no. 1, p. 3470, Dec. 2022, doi: 10.1038/s41467-022-31137-2.

[52] H. Cheon, H.-J. Yang, M. Choi, and J.-H. Son, "Effective demethylation of melanoma cells using terahertz radiation," *Biomed. Opt. Express*, vol. 10, no. 10, p. 4931, Oct. 2019, doi: 10.1364/BOE.10.004931.

[53] A. Keshavarz and Z. Vafapour, "Water-Based Terahertz Metamaterial for Skin Cancer Detection Application," *IEEE Sensors J.*, vol. 19, no. 4, pp. 1519–1524, Feb. 2019, doi: 10.1109/JSEN.2018.2882363.

[54] W. Xu, L. Xie, and Y. Ying, "Mechanisms and applications of terahertz metamaterial sensing: a review," *Nanoscale*, vol. 9, no. 37, pp. 13864–13878, Sep. 2017, doi: 10.1039/C7NR03824K.

[55] A. Bandyopadhyay and A. Sengupta, "A Review of the Concept, Applications and Implementation Issues of Terahertz Spectral Imaging Technique," *IETE Technical Review*, vol. 39, no. 2, pp. 471–489, Mar. 2022, doi: 10.1080/02564602.2020.1865844.

[56] P.-K. Lu and M. Jarrahi, "Frequency-domain terahertz spectroscopy using long-carrier-lifetime photoconductive antennas," *Opt. Express*, vol. 31, no. 6, p. 9319, Mar. 2023, doi: 10.1364/OE.483746.

[57] H. Guerboukha, K. Nallappan, and M. Skorobogatiy, "Toward real-time terahertz imaging," *Adv. Opt. Photon., AOP*, vol. 10, no. 4, pp. 843–938, Dec. 2018, doi: 10.1364/AOP.10.000843.

[58] J. Neu and C. A. Schmuttenmaer, "Tutorial: An introduction to terahertz time domain spectroscopy (THz-TDS)," *Journal of Applied Physics*, vol. 124, no. 23, p. 231101, Dec. 2018, doi: 10.1063/1.5047659.

[59] L. Duvillaret, F. Garet, and J.-L. Coutaz, "A reliable method for extraction of material parameters in terahertz time-domain spectroscopy," *IEEE J. Select. Topics Quantum Electron.*, vol. 2, no. 3, pp. 739–746, Sep. 1996, doi: 10.1109/2944.571775.

[60] I. Pupeza, R. Wilk, and M. Koch, "Highly accurate optical material parameter determination with THz time-domain spectroscopy," *Opt. Express, OE*, vol. 15, no. 7, pp. 4335–4350, Apr. 2007, doi: 10.1364/OE.15.004335.

[61] P. U. Jepsen, "Phase Retrieval in Terahertz Time-Domain Measurements: a 'how to' Tutorial," *J Infrared Milli Terahz Waves*, vol. 40, no. 4, pp. 395–411, Apr. 2019, doi: 10.1007/s10762-019-00578-0.

[62] D. W. Vogt and R. Leonhardt, "High resolution terahertz spectroscopy of a whispering gallery mode bubble resonator using Hilbert analysis," *Opt. Express, OE*, vol. 25, no. 14, pp. 16860–16866, Jul. 2017, doi: 10.1364/OE.25.016860.

[63] D. M. Mittleman, "Twenty years of terahertz imaging," *Opt. Express, OE*, vol. 26, no. 8, pp. 9417–9431, Apr. 2018, doi: 10.1364/OE.26.009417.

[64] K. Sengupta, T. Nagatsuma, and D. M. Mittleman, "Terahertz integrated electronic and hybrid electronic–photonic systems," *Nat Electron*, vol. 1, no. 12, Art. no. 12, Dec. 2018, doi: 10.1038/s41928-018-0173-2.

[65] D. M. Mittleman, "Perspective: Terahertz science and technology," *Journal of Applied Physics*, vol. 122, no. 23, p. 230901, Dec. 2017, doi: 10.1063/1.5007683.

[66] X. Wang *et al.*, "DA-CNN-based similar terahertz signal identification for intelligent characterization of internal debonding defects of composites under high-resolution mode," *Composite Structures*, vol. 322, p. 117412, Oct. 2023, doi: 10.1016/j.compstruct.2023.117412.

[67] J.-Y. Zhang, J.-J. Ren, L.-J. Li, J. Gu, and D.-D. Zhang, "THz imaging technique for nondestructive analysis of debonding defects in ceramic matrix composites based on multiple echoes and feature fusion," *Opt. Express, OE*, vol. 28, no. 14, pp. 19901–19915, Jul. 2020, doi: 10.1364/OE.394177.

[68] Y. Xu, X. Wang, L. Zhang, R. Yan, and X. Chen, "Terahertz nondestructive quantitative characterization for layer thickness based on sparse representation method," *NDT & E International*, vol. 124, p. 102536, Dec. 2021, doi: 10.1016/j.ndteint.2021.102536.

[69] D. W. Vogt, M. Erkintalo, and R. Leonhardt, "Coherent Continuous Wave Terahertz Spectroscopy Using Hilbert Transform," *J Infrared Milli Terahz Waves*, vol. 40, no. 5, pp. 524–534, May 2019, doi: 10.1007/s10762-019-00583-3.

[70] X. Lu *et al.*, "Accurate detection of porosity in glass fiber reinforced polymers by terahertz spectroscopy," *Composites Part B: Engineering*, vol. 242, p. 110058, Aug. 2022, doi: 10.1016/j.compositesb.2022.110058.

[71] Y. Xu, H. Hao, D. S. Citrin, X. Wang, L. Zhang, and X. Chen, "Three-dimensional nondestructive characterization of delamination in GFRP by terahertz time-of-flight tomography with sparse Bayesian learning-based spectrum-graph integration strategy," *Composites Part B: Engineering*, vol. 225, p. 109285, Nov. 2021, doi: 10.1016/j.compositesb.2021.109285.

[72] Y. Xu *et al.*, "Real-time terahertz characterization for composite delamination using a lightweight CPU adaptive network," *Composites Part B: Engineering*, vol. 247, p. 110354, Dec. 2022, doi: 10.1016/j.compositesb.2022.110354.

[73] Y. Jiang *et al.*, "Machine Learning and Application in Terahertz Technology: A Review on Achievements and Future Challenges," *IEEE Access*, vol. 10, pp. 53761–53776, 2022, doi: 10.1109/ACCESS.2022.3174595.

[74] H. Zhu, H. Wang, J. Liu, W. Wang, R. Gao, and Y. Zhang, "Application of terahertz dielectric constant spectroscopy for discrimination of oxidized coal and unoxidized coal by machine learning algorithms," *Fuel*, vol. 293, p. 120470, Jun. 2021, doi: 10.1016/j.fuel.2021.120470.

[75] T. Chen, L. Ma, Z. Tang, and L. X. Yu, "Identification of coumarin-based food additives using terahertz spectroscopy combined with manifold learning and improved support vector machine," *Journal of Food Science*, vol. 87, no. 3, pp. 1108–1118, 2022, doi: 10.1111/1750-3841.16064.

[76] S. Helal, H. Sarieddeen, H. Dahrouj, T. Y. Al-Naffouri, and M.-S. Alouini, "Signal Processing and Machine Learning Techniques for Terahertz Sensing: An overview," *IEEE Signal Process. Mag.*, vol. 39, no. 5, pp. 42–62, Sep. 2022, doi: 10.1109/MSP.2022.3183808.

[77] Siuly, X. Yin, S. Hadjiloucas, and Y. Zhang, "Classification of THz pulse signals using two-dimensional cross-correlation feature extraction and non-linear classifiers," *Computer Methods and Programs in Biomedicine*, vol. 127, pp. 64–82, Apr. 2016, doi: 10.1016/j.cmpb.2016.01.017.

[78] H. Park and J.-H. Son, "Machine Learning Techniques for THz Imaging and Time-Domain Spectroscopy," *Sensors*, vol. 21, no. 4, Art. no. 4, Jan. 2021, doi: 10.3390/s21041186.

[79] Q. Rong, H. Wei, X. Huang, and H. Bao, "Predicting the effective thermal conductivity of composites from cross sections images using deep learning methods," *Composites Science and Technology*, vol. 184, p. 107861, Nov. 2019, doi: 10.1016/j.compscitech.2019.107861.

[80] X. Yang *et al.*, "Super-resolution reconstruction of terahertz images based on a deep-learning network with a residual channel attention mechanism," *Appl. Opt., AO*, vol. 61, no. 12, pp. 3363–3370, Apr. 2022, doi: 10.1364/AO.452511.

[81] C. Wang, F. Shi, M. Zhao, J. Ao, C. Jia, and S. Chen, "Convolutional Neural Network-Based Terahertz Spectral Classification of Liquid Contraband for Security Inspection," *IEEE Sensors Journal*, vol. 21, no. 17, pp. 18955–18963, Sep. 2021, doi: 10.1109/JSEN.2021.3086478.

[82] V. Galstyan, A. D'Arco, M. D. Fabrizio, N. Poli, S. Lupi, and E. Comini, "Detection of volatile organic compounds: From chemical gas sensors to terahertz spectroscopy," *Reviews in Analytical Chemistry*, vol. 40, no. 1, pp. 33–57, Jan. 2021, doi: 10.1515/revac-2021-0127.

[83] B. Ferguson and X.-C. Zhang, "Materials for terahertz science and technology," *Nature Mater*, vol. 1, no. 1, Art. no. 1, Sep. 2002, doi: 10.1038/nmat708.

[84] W. Nsengiyumva *et al.*, "Theoretical and experimental analysis of the dielectric properties of 3D orthogonal woven GFRP composites in the terahertz frequency range," *Optik*, vol. 260, p. 169105, Jun. 2022, doi: 10.1016/j.ijleo.2022.169105.

[85] A. Houard, Y. Liu, B. Prade, V. T. Tikhonchuk, and A. Mysyrowicz, "Strong Enhancement of Terahertz Radiation from Laser Filaments in Air by a Static Electric Field," *Phys. Rev. Lett.*, vol. 100, no. 25, p. 255006, Jun. 2008, doi: 10.1103/PhysRevLett.100.255006.

[86] H.-T. Chen, W. J. Padilla, M. J. Cich, A. K. Azad, R. D. Averitt, and A. J. Taylor, "A metamaterial solid-state terahertz phase modulator," *Nature Photon*, vol. 3, no. 3, pp. 148–151, Mar. 2009, doi: 10.1038/nphoton.2009.3.

[87] R. D. V. Ríos, S. Bikorimana, M. A. Ummy, R. Dorsinville, and S.-W. Seo, "A bow-tie photoconductive antenna using a low-temperature-grown GaAs thin-film on a silicon substrate for terahertz wave generation and detection," *J. Opt.*, vol. 17, no. 12, p. 125802, Dec. 2015, doi: 10.1088/2040-8978/17/12/125802.

[88] Y. J. Ding, "Progress in terahertz sources based on difference-frequency generation [Invited]," *J. Opt. Soc. Am. B*, vol. 31, no. 11, p. 2696, Nov. 2014, doi: 10.1364/JOSAB.31.002696.

[89] J. He, X. He, T. Dong, S. Wang, M. Fu, and Y. Zhang, "Recent progress and applications of terahertz metamaterials," *J. Phys. D: Appl. Phys.*, vol. 55, no. 12, p. 123002, Mar. 2022, doi: 10.1088/1361-6463/ac3282.

[90] P. U. Jepsen, R. H. Jacobsen, and S. R. Keiding, "Generation and detection of terahertz pulses from biased semiconductor antennas," *J. Opt. Soc. Am. B, JOSAB*, vol. 13, no. 11, pp. 2424–2436, Nov. 1996, doi: 10.1364/JOSAB.13.002424.

[91] G. Zhao, R. N. Schouten, N. Van Der Valk, W. Th. Wenckebach, and P. C. M. Planken, "Design and performance of a THz emission and detection setup based on a semi-insulating GaAs emitter," *Review of Scientific Instruments*, vol. 73, no. 4, pp. 1715–1719, Apr. 2002, doi: 10.1063/1.1459095.

[92] Y.-D. Hsieh *et al.*, "Terahertz Frequency-Domain Spectroscopy of Low-Pressure Acetonitrile Gas by a Photomixing Terahertz Synthesizer Referenced to Dual Optical Frequency Combs," *J Infrared Milli Terahz Waves*, vol. 37, no. 9, pp. 903–915, Sep. 2016, doi: 10.1007/s10762-016-0277-6.

[93] E. Ohmichi, Y. Shoji, H. Takahashi, and H. Ohta, "Frequency-domain electron spin resonance spectroscopy using continuously frequency-tunable terahertz photomixers," *Applied Physics Letters*, vol. 119, no. 16, p. 162404, Oct. 2021, doi: 10.1063/5.0065649.

[94] N. T. Yardimci, H. Lu, and M. Jarrahi, "High power telecommunication-compatible photoconductive terahertz emitters based on plasmonic nano-antenna arrays," *Applied Physics Letters*, vol. 109, no. 19, p. 191103, Nov. 2016, doi: 10.1063/1.4967440.

[95] K. Peng and M. B. Johnston, "The application of one-dimensional nanostructures in terahertz frequency devices," *Applied Physics Reviews*, vol. 8, no. 4, p. 041314, Dec. 2021, doi: 10.1063/5.0060797.

[96] N. T. Yardimci, D. Turan, S. Cakmakyapan, and M. Jarrahi, "A high-responsivity and broadband photoconductive terahertz detector based on a plasmonic nanocavity," *Applied Physics Letters*, vol. 113, no. 25, p. 251102, Dec. 2018, doi: 10.1063/1.5066243.

[97] N. T. Yardimci, D. Turan, and M. Jarrahi, "Efficient photoconductive terahertz detection through photon trapping in plasmonic nanocavities," *APL Photonics*, vol. 6, no. 8, p. 080802, Aug. 2021, doi: 10.1063/5.0055332.

[98] E. Bründermann, H.-W. Hübers, and M. F. Kimmitt, *Terahertz Techniques*, vol. 151. in Springer Series in Optical Sciences, vol. 151. Berlin, Heidelberg: Springer Berlin Heidelberg, 2012. doi: 10.1007/978-3-642-02592-1.

[99] K.-E. Peiponen, A. Zeitler, and M. Kuwata-Gonokami, *Terahertz spectroscopy and imaging*, vol. 171. Springer, 2012.

[100] A. El-Ghazaly, J. Gorchon, R. B. Wilson, A. Pattabi, and J. Bokor, "Progress towards ultrafast spintronics applications," *Journal of Magnetism and Magnetic Materials*, vol. 502, p. 166478, May 2020, doi: 10.1016/j.jmmm.2020.166478.

[101] M. B. Jungfleisch *et al.*, "Control of Terahertz Emission by Ultrafast Spin-Charge Current Conversion at Rashba Interfaces," *Phys. Rev. Lett.*, vol. 120, no. 20, p. 207207, May 2018, doi: 10.1103/PhysRevLett.120.207207.

[102] A. Comstock *et al.*, "Spintronic Terahertz Emission in Ultrawide Bandgap Semiconductor/Ferromagnet Heterostructures," *Advanced Optical Materials*, vol. 11, no. 1, p. 2201535, 2023, doi: 10.1002/adom.202201535.

[103] J. Yang, H. Qin, and K. Zhang, "Emerging terahertz photodetectors based on two-dimensional materials," *Optics Communications*, vol. 406, pp. 36–43, Jan. 2018, doi: 10.1016/j.optcom.2017.05.041.

[104] M. Mittendorff, S. Winnerl, and T. E. Murphy, "2D THz Optoelectronics," *Advanced Optical Materials*, vol. 9, no. 3, p. 2001500, 2021, doi: 10.1002/adom.202001500.

[105] Z. Shi *et al.*, "Two-dimensional materials toward Terahertz optoelectronic device applications," *Journal of Photochemistry and Photobiology C: Photochemistry Reviews*, vol. 51, p. 100473, Jun. 2022, doi: 10.1016/j.jphotochemrev.2021.100473.

[106] M. Wang and E.-H. Yang, "THz applications of 2D materials: Graphene and beyond," *Nano-Structures & Nano-Objects*, vol. 15, pp. 107–113, Jul. 2018, doi: 10.1016/j.nanoso.2017.08.011.

[107] T. Otsuji *et al.*, "Emission and Detection of Terahertz Radiation Using Two-Dimensional Electrons in III–V Semiconductors and Graphene," *IEEE Transactions on Terahertz Science and Technology*, vol. 3, no. 1, pp. 63–71, Jan. 2013, doi: 10.1109/TTHZ.2012.2235911.

[108] J. Tong, M. Muthee, S.-Y. Chen, S. K. Yngvesson, and J. Yan, "Antenna Enhanced Graphene THz Emitter and Detector," *Nano Lett.*, vol. 15, no. 8, pp. 5295–5301, Aug. 2015, doi: 10.1021/acs.nanolett.5b01635.

[109] X. Yang, A. Vorobiev, A. Generalov, M. A. Andersson, and J. Stake, "A flexible graphene terahertz detector," *Applied Physics Letters*, vol. 111, no. 2, p. 021102, Jul. 2017, doi: 10.1063/1.4993434.

[110] N. T. Yardimci, S. Cakmakyapan, S. Hemmati, and M. Jarrahi, "A High-Power Broadband Terahertz Source Enabled by Three-Dimensional Light Confinement in a Plasmonic Nanocavity," *Sci Rep*, vol. 7, no. 1, Art. no. 1, Jun. 2017, doi: 10.1038/s41598-017-04553-4.

[111] C. Neumann *et al.*, "Probing electronic lifetimes and phonon anharmonicities in high-quality chemical vapor deposited graphene by magneto-Raman spectroscopy," *Applied Physics Letters*, vol. 107, no. 23, p. 233105, Dec. 2015, doi: 10.1063/1.4936995.

[112] O. Balci, E. O. Polat, N. Kakenov, and C. Kocabas, "Graphene-enabled electrically switchable radar-absorbing surfaces," *Nat Commun*, vol. 6, no. 1, Art. no. 1, Mar. 2015, doi: 10.1038/ncomms7628.

[113] X. Chen *et al.*, "Widely tunable black phosphorus mid-infrared photodetector," *Nat Commun*, vol. 8, no. 1, Art. no. 1, Nov. 2017, doi: 10.1038/s41467-017-01978-3.

[114] L. Prechtel, L. Song, D. Schuh, P. Ajayan, W. Wegscheider, and A. W. Holleitner, "Time-resolved ultrafast photocurrents and terahertz generation in freely suspended graphene," *Nat Commun*, vol. 3, no. 1, Art. no. 1, Jan. 2012, doi: 10.1038/ncomms1656.

[115] M. Mittendorff, R. J. Suess, E. Leong, and T. E. Murphy, "Optical Gating of Black Phosphorus for Terahertz Detection," *Nano Lett.*, vol. 17, no. 9, pp. 5811–5816, Sep. 2017, doi: 10.1021/acs.nanolett.7b02931.

[116] N. Hunter *et al.*, "On-Chip Picosecond Pulse Detection and Generation Using Graphene Photoconductive Switches," *Nano Lett.*, vol. 15, no. 3, pp. 1591–1596, Mar. 2015, doi: 10.1021/nl504116w.

[117] D. P. Sanders, "Advances in Patterning Materials for 193 nm Immersion Lithography," *Chem. Rev.*, vol. 110, no. 1, pp. 321–360, Jan. 2010, doi: 10.1021/cr900244n.

[118] L. J. Guo, "Nanoimprint Lithography: Methods and Material Requirements," *Advanced Materials*, vol. 19, no. 4, pp. 495–513, 2007, doi: 10.1002/adma.200600882.

[119] H. R. Bardolaza *et al.*, "Integrated optics spiral photoconductive antennas coupled with 1D and 2D micron-size terahertz-wavelength plasmonic metal arrays," *Opt. Mater. Express, OME*, vol. 12, no. 4, pp. 1617–1626, Apr. 2022, doi: 10.1364/OME.455044.

[120] L. Yu *et al.*, "The medical application of terahertz technology in non-invasive detection of cells and tissues: opportunities and challenges," *RSC Adv.*, vol. 9, no. 17, pp. 9354–9363, 2019, doi: 10.1039/C8RA10605C.

[121] N. Vieweg *et al.*, "Terahertz-time domain spectrometer with 90 dB peak dynamic range," *J Infrared Milli Terahz Waves*, vol. 35, no. 10, pp. 823–832, Oct. 2014, doi: 10.1007/s10762-014-0085-9.

[122] D. Molter *et al.*, "High-speed terahertz time-domain spectroscopy of cyclotron resonance in pulsed magnetic field," *Opt. Express, OE*, vol. 18, no. 25, pp. 26163–26168, Dec. 2010, doi: 10.1364/OE.18.026163.

[123] Y. Kim and D.-S. Yee, "High-speed terahertz time-domain spectroscopy based on electronically controlled optical sampling," *Opt. Lett., OL*, vol. 35, no. 22, pp. 3715–3717, Nov. 2010, doi: 10.1364/OL.35.003715.

[124] M. Yahyapour *et al.*, "Fastest Thickness Measurements with a Terahertz Time-Domain System Based on Electronically Controlled Optical Sampling," *Applied Sciences*, vol. 9, no. 7, Art. no. 7, Jan. 2019, doi: 10.3390/app9071283.

[125] P. Bawuah, P. Silfsten, A. Sarkar, K. Kordas, J.-P. Mikkola, and K.-E. Peiponen, "On the complex refractive index of N-doped TiO2 nanospheres and nanowires in the terahertz spectral region," *Vibrational Spectroscopy*, vol. 68, pp. 241–245, Sep. 2013, doi: 10.1016/j.vibspec.2013.08.008.

[126] D. Stanze, A. Deninger, A. Roggenbuck, S. Schindler, M. Schlak, and B. Sartorius, "Compact cw Terahertz Spectrometer Pumped at 1.5 µm Wavelength," *J Infrared Milli Terahz Waves*, vol. 32, no. 2, pp. 225–232, Feb. 2011, doi: 10.1007/s10762-010-9751-8.

[127] L. Liebermeister, S. Nellen, R. Kohlhaas, S. Breuer, M. Schell, and B. Globisch, "Ultra-fast, High-Bandwidth Coherent cw THz Spectrometer for Non-destructive Testing," *J Infrared Milli Terahz Waves*, vol. 40, no. 3, pp. 288–296, Mar. 2019, doi: 10.1007/s10762-018-0563-6.

[128] M. Deumer *et al.*, "Continuous wave terahertz receivers with 4.5 THz bandwidth and 112 dB dynamic range," *Opt. Express, OE*, vol. 29, no. 25, pp. 41819–41826, Dec. 2021, doi: 10.1364/OE.443098.

[129] S. Hisatake, Y. Koda, R. Nakamura, N. Hamada, and T. Nagatsuma, "Terahertz balanced self-heterodyne spectrometer with SNR-limited phase-measurement sensitivity," *Opt. Express, OE*, vol. 23, no. 20, pp. 26689–26695, Oct. 2015, doi: 10.1364/OE.23.026689.

[130] T. Göbel, D. Stanze, B. Globisch, R. J. B. Dietz, H. Roehle, and M. Schell, "Telecom technology based continuous wave terahertz photomixing system with 105 decibel signal-to-noise ratio and 3.5 terahertz bandwidth," *Opt. Lett., OL*, vol. 38, no. 20, pp. 4197–4199, Oct. 2013, doi: 10.1364/OL.38.004197.

[131] C. Baker, I. S. Gregory, M. J. Evans, W. R. Tribe, E. H. Linfield, and M. Missous, "All-optoelectronic terahertz system using low-temperature-grown InGaAs photomixers," *Opt. Express, OE*, vol. 13, no. 23, pp. 9639–9644, Nov. 2005, doi: 10.1364/OPEX.13.009639.

[132] F. Hindle, A. Cuisset, R. Bocquet, and G. Mouret, "Continuous-wave terahertz by photomixing: applications to gas phase pollutant detection and quantification," *Comptes Rendus Physique*, vol. 9, no. 2, pp. 262–275, Mar. 2008, doi: 10.1016/j.crhy.2007.07.009.

[133] C. Yu, S. Fan, Y. Sun, and E. Pickwell-MacPherson, "The potential of terahertz imaging for cancer diagnosis: A review of investigations to date," *Quant Imaging Med Surg*, vol. 2, no. 1, pp. 33–45, Mar. 2012, doi: 10.3978/j.issn.2223-4292.2012.01.04.

[134] L. Liebermeister *et al.*, "Terahertz Multilayer Thickness Measurements: Comparison of Optoelectronic Time and Frequency Domain Systems," *J Infrared Milli Terahz Waves*, Dec. 2021, doi: 10.1007/s10762-021-00831-5.

[135] L. Liebermeister *et al.*, "Optoelectronic frequency-modulated continuous-wave terahertz spectroscopy with 4 THz bandwidth," *Nat Commun*, vol. 12, no. 1, Art. no. 1, Feb. 2021, doi: 10.1038/s41467-021-21260-x.

[136] P.-K. Lu, D. Turan, and M. Jarrahi, "High-power terahertz pulse generation from bias-free nanoantennas on graded composition InGaAs structures," *Opt. Express, OE*, vol. 30, no. 2, pp. 1584–1598, Jan. 2022, doi: 10.1364/OE.447733.

[137] D. Turan *et al.*, "Wavelength conversion through plasmon-coupled surface states," *Nat Commun*, vol. 12, no. 1, Art. no. 1, Jul. 2021, doi: 10.1038/s41467-021-24957-1.

[138] P.-K. Lu, D. Turan, and M. Jarrahi, "High-sensitivity telecommunication-compatible photoconductive terahertz detection through carrier transit time reduction," *Opt. Express, OE*, vol. 28, no. 18, pp. 26324–26335, Aug. 2020, doi: 10.1364/OE.400380.

[139] D. Turan, N. T. Yardimci, and M. Jarrahi, "Plasmonics-enhanced photoconductive terahertz detector pumped by Ytterbium-doped fiber laser," *Opt. Express, OE*, vol. 28, no. 3, pp. 3835–3845, Feb. 2020, doi: 10.1364/OE.386368.

[140] J. A. Schuller, E. S. Barnard, W. Cai, Y. C. Jun, J. S. White, and M. L. Brongersma, "Plasmonics for extreme light concentration and manipulation," *Nature Mater*, vol. 9, no. 3, Art. no. 3, Mar. 2010, doi: 10.1038/nmat2630.

[141] C. W. Berry, N. Wang, M. R. Hashemi, M. Unlu, and M. Jarrahi, "Significant performance enhancement in photoconductive terahertz optoelectronics by incorporating plasmonic contact electrodes," *Nat Commun*, vol. 4, no. 1, Art. no. 1, Mar. 2013, doi: 10.1038/ncomms2638.

[142] D. Turan, S. C. Corzo-Garcia, N. T. Yardimci, E. Castro-Camus, and M. Jarrahi, "Impact of the Metal Adhesion Layer on the Radiation Power of Plasmonic Photoconductive Terahertz Sources," *J Infrared Milli Terahz Waves*, vol. 38, no. 12, pp. 1448–1456, Dec. 2017, doi: 10.1007/s10762-017-0431-9.

[143] S.-H. Yang, M. R. Hashemi, C. W. Berry, and M. Jarrahi, "7.5% Optical-to-Terahertz Conversion Efficiency Offered by Photoconductive Emitters With Three-Dimensional Plasmonic Contact Electrodes," *IEEE Transactions on Terahertz Science and Technology*, vol. 4, no. 5, pp. 575–581, Sep. 2014, doi: 10.1109/TTHZ.2014.2342505.

[144] N. T. Yardimci, S.-H. Yang, C. W. Berry, and M. Jarrahi, "High-Power Terahertz Generation Using Large-Area Plasmonic Photoconductive Emitters," *IEEE Transactions on Terahertz Science and Technology*, vol. 5, no. 2, pp. 223–229, Mar. 2015, doi: 10.1109/TTHZ.2015.2395417.

[145] N. Wang, S. Cakmakyapan, Y.-J. Lin, H. Javadi, and M. Jarrahi, "Room-temperature heterodyne terahertz detection with quantum-level sensitivity," *Nat Astron*, vol. 3, no. 11, Art. no. 11, Nov. 2019, doi: 10.1038/s41550-019-0828-6.

[146] E. Rahmati and M. Ahmadi-Boroujeni, "Design of terahertz photoconductive antenna arrays based on defective photonic crystal substrates," *Optics & Laser Technology*, vol. 114, pp. 89–94, Jun. 2019, doi: 10.1016/j.optlastec.2019.01.044.

[147] N. Khiabani, Y. Huang, Y.-C. Shen, and StephenJ. Boyes, "Theoretical Modeling of a Photoconductive Antenna in a Terahertz Pulsed System," *IEEE Transactions on Antennas and Propagation*, vol. 61, no. 4, pp. 1538–1546, Apr. 2013, doi: 10.1109/TAP.2013.2239599.

[148] S. Jafarlou, M. Neshat, and S. Safavi-Naeini, "A hybrid analysis method for plasmonic enhanced terahertz photomixer sources," *Opt. Express, OE*, vol. 21, no. 9, pp. 11115–11124, May 2013, doi: 10.1364/OE.21.011115.

[149] C. W. Berry, M. R. Hashemi, S. Preu, H. Lu, A. C. Gossard, and M. Jarrahi, "Plasmonics enhanced photomixing for generating quasi-continuous-wave frequency-tunable terahertz radiation," *Opt. Lett., OL*, vol. 39, no. 15, pp. 4522–4524, Aug. 2014, doi: 10.1364/OL.39.004522.

[150] S. Ghorbani, M. Bashirpour, J. Poursafar, M. Kolahdouz, M. Neshat, and A. Valinejad, "Thin film tandem nanoplasmonic photoconductive antenna for high performance terahertz detection," *Superlattices and Microstructures*, vol. 120, pp. 598–604, Aug. 2018, doi: 10.1016/j.spmi.2018.06.029.

[151] M. Awad, M. Nagel, H. Kurz, J. Herfort, and K. Ploog, "Characterization of low temperature GaAs antenna array terahertz emitters," *Appl. Phys. Lett.*, vol. 91, no. 18, p. 181124, Oct. 2007, doi: 10.1063/1.2800885.

[152] N. Khiabani, Y. Huang, L. E. Garcia-Muñoz, Y.-C. Shen, and A. Rivera-Lavado, "A Novel Sub-THz Photomixer With Nano-Trapezoidal Electrodes," *IEEE Transactions on Terahertz Science and Technology*, vol. 4, no. 4, pp. 501–508, Jul. 2014, doi: 10.1109/TTHZ.2014.2320824.

[153] M. Tamagnone, J. S. Gómez-Díaz, J. R. Mosig, and J. Perruisseau-Carrier, "Reconfigurable terahertz plasmonic antenna concept using a graphene stack," *Applied Physics Letters*, vol. 101, no. 21, p. 214102, Nov. 2012, doi: 10.1063/1.4767338.

[154] N. Zhu and R. W. Ziolkowski, "Photoconductive THz Antenna Designs With High Radiation Efficiency, High Directivity, and High Aperture Efficiency," *IEEE Trans. THz Sci. Technol.*, vol. 3, no. 6, pp. 721–730, Nov. 2013, doi: 10.1109/TTHZ.2013.2285568.

[155] R. Emadi, H. Emadi, R. Emadi, R. Safian, and A. Z. Nezhad, "Analysis and Design of Photoconductive Antenna Using Spatially Dispersive Graphene Strips with Parallel-Plate Configuration," *IEEE J. Select. Topics Quantum Electron.*, vol. 24, no. 2, pp. 1–9, Mar. 2018, doi: 10.1109/JSTQE.2017.2693261.

[156] I. Woo, T. K. Nguyen, H. Han, H. Lim, and I. Park, "Four-leaf-clover-shaped antenna for a THz photomixer," *Opt. Express, OE*, vol. 18, no. 18, pp. 18532–18542, Aug. 2010, doi: 10.1364/OE.18.018532.

[157] S. M. Duffy, S. Verghese, A. McIntosh, A. Jackson, A. C. Gossard, and S. Matsuura, "Accurate modeling of dual dipole and slot elements used with photomixers for coherent terahertz output power," *IEEE Transactions on Microwave Theory and Techniques*, vol. 49, no. 6, pp. 1032–1038, Jun. 2001, doi: 10.1109/22.925487.

[158] M. Tamagnone, J. S. Gómez-Díaz, J. R. Mosig, and J. Perruisseau-Carrier, "Analysis and design of terahertz antennas based on plasmonic resonant graphene sheets," *Journal of Applied Physics*, vol. 112, no. 11, p. 114915, Dec. 2012, doi: 10.1063/1.4768840.

[159] K. Han, T. K. Nguyen, I. Park, and H. Han, "Terahertz Yagi-Uda Antenna for High Input Resistance," *J Infrared Milli Terahz Waves*, vol. 31, no. 4, pp. 441–454, Apr. 2010, doi: 10.1007/s10762-009-9596-1.

[160] M. Khabiri, M. Neshat, and S. Safavi-Naeini, "Hybrid Computational Simulation and Study of Continuous Wave Terahertz Photomixers," *IEEE Transactions on Terahertz Science and Technology*, vol. 2, no. 6, pp. 605–616, Nov. 2012, doi: 10.1109/TTHZ.2012.2213596.

[161] G. C. Loata, M. D. Thomson, T. Löffler, and H. G. Roskos, "Radiation field screening in photoconductive antennae studied via pulsed terahertz emission spectroscopy," *Applied Physics Letters*, vol. 91, no. 23, p. 232506, Dec. 2007, doi: 10.1063/1.2823590.

[162] A. Rivera-Lavado *et al.*, "Arrays and New Antenna Topologies for Increasing THz Power Generation Using Photomixers," *J Infrared Milli Terahz Waves*, vol. 34, no. 2, pp. 97–108, Feb. 2013, doi: 10.1007/s10762-013-9954-x.

[163] C. W. Berry, M. R. Hashemi, and M. Jarrahi, "Generation of high power pulsed terahertz radiation using a plasmonic photoconductive emitter array with logarithmic spiral antennas," *Appl. Phys. Lett.*, vol. 104, no. 8, p. 081122, Feb. 2014, doi: 10.1063/1.4866807.

[164] V. G. Veselago, "Electrodynamics of substances with simultaneously negative electrical and magnetic permeabilities," *Soviet Physics Uspekhi*, vol. 10, no. 4, pp. 504–509, 1968.

[165] J. B. Pendry, A. J. Holden, W. J. Stewart, and I. Youngs, "Extremely Low Frequency Plasmons in Metallic Mesostructures," *Phys. Rev. Lett.*, vol. 76, no. 25, pp. 4773–4776, Jun. 1996, doi: 10.1103/PhysRevLett.76.4773.

[166] R. A. Shelby, D. R. Smith, and S. Schultz, "Experimental Verification of a Negative Index of Refraction," *Science*, vol. 292, no. 5514, pp. 77–79, Apr. 2001, doi: 10.1126/science.1058847.

[167] R. Liu, C. Ji, J. J. Mock, J. Y. Chin, T. J. Cui, and D. R. Smith, "Broadband Ground-Plane Cloak," *Science*, vol. 323, no. 5912, pp. 366–369, Jan. 2009, doi: 10.1126/science.1166949.

[168] C. Zhang, S. Shen, Q. Wang, M. Lin, Z. Ouyang, and Q. Liu, "Highly Sensitive THz Gas-Sensor Based on the Guided Bloch Surface Wave Resonance in Polymeric Photonic Crystals," *Materials*, vol. 13, no. 5, p. 1217, Mar. 2020, doi: 10.3390/ma13051217.

[169] T. J. Yen *et al.*, "Terahertz Magnetic Response from Artificial Materials," *Science*, vol. 303, no. 5663, pp. 1494–1496, Mar. 2004, doi: 10.1126/science.1094025.

[170] X. Yan *et al.*, "The terahertz electromagnetically induced transparency-like metamaterials for sensitive biosensors in the detection of cancer cells," *Biosensors and Bioelectronics*, vol. 126, pp. 485–492, Feb. 2019, doi: 10.1016/j.bios.2018.11.014.

[171] R. Sun, W. Li, T. Meng, and G. Zhao, "Design and optimization of terahertz metamaterial sensor with high sensing performance," *Optics Communications*, vol. 494, p. 127051, Sep. 2021, doi: 10.1016/j.optcom.2021.127051.

[172] M. Kafesaki, T. Koschny, R. S. Penciu, T. F. Gundogdu, E. N. Economou, and C. M. Soukoulis, "Left-handed metamaterials: detailed numerical studies of the transmission properties," *J. Opt. A: Pure Appl. Opt.*, vol. 7, no. 2, p. S12, Jan. 2005, doi: 10.1088/1464-4258/7/2/002.

[173] D. R. Smith *et al.*, "Left-Handed Metamaterials," in *Photonic Crystals and Light Localization in the 21st Century*, C. M. Soukoulis, Ed., in NATO Science Series. Dordrecht: Springer Netherlands, 2001, pp. 351–371. doi: 10.1007/978-94-010-0738-2_25.

[174] S.-H. Lee, D. Lee, M. H. Choi, J.-H. Son, and M. Seo, "Highly Sensitive and Selective Detection of Steroid Hormones Using Terahertz Molecule-Specific Sensors," *Anal. Chem.*, vol. 91, no. 10, pp. 6844–6849, May 2019, doi: 10.1021/acs.analchem.9b01066.

[175] Y. Huang, S. Zhong, T. Shi, Y. Shen, and D. Cui, "Terahertz plasmonic phase-jump manipulator for liquid sensing," *Nanophotonics*, vol. 9, no. 9, pp. 3011–3021, Sep. 2020, doi: 10.1515/nanoph-2020-0247.

[176] T. Driscoll *et al.*, "Tuned permeability in terahertz split-ring resonators for devices and sensors," *Appl. Phys. Lett.*, vol. 91, no. 6, p. 062511, Aug. 2007, doi: 10.1063/1.2768300.

[177] N. Cui *et al.*, "Design and application of terahertz metamaterial sensor based on DSRRs in clinical quantitative detection of carcinoembryonic antigen," *Opt. Express, OE*, vol. 28, no. 11, pp. 16834–16844, May 2020, doi: 10.1364/OE.393397.

[178] W. J. Padilla, A. J. Taylor, C. Highstrete, M. Lee, and R. D. Averitt, "Dynamical Electric and Magnetic Metamaterial Response at Terahertz Frequencies," *Phys. Rev. Lett.*, vol. 96, no. 10, p. 107401, Mar. 2006, doi: 10.1103/PhysRevLett.96.107401.

[179] J. Li, J. Shao, Y.-H. Wang, M.-J. Zhu, J.-Q. Li, and Z.-G. Dong, "Toroidal dipolar response by a dielectric microtube metamaterial in the terahertz regime," *Opt. Express*, vol. 23, no. 22, p. 29138, Nov. 2015, doi: 10.1364/OE.23.029138.

[180] T. Kaelberer, V. A. Fedotov, N. Papasimakis, D. P. Tsai, and N. I. Zheludev, "Toroidal Dipolar Response in a Metamaterial," *Science*, vol. 330, no. 6010, pp. 1510–1512, Dec. 2010, doi: 10.1126/science.1197172.

[181] R. Singh, I. A. I. Al-Naib, M. Koch, and W. Zhang, "Sharp Fano resonances in THz metamaterials," *Opt. Express*, vol. 19, no. 7, p. 6312, Mar. 2011, doi: 10.1364/OE.19.006312.

[182] S. Wang, X. Zhao, S. Wang, Q. Li, J. Zhu, and L. Han, "The investigation of the electromagnetic coupling effect in terahertz toroidal metasurfaces and metamaterials," *Journal of Materials Research and Technology*, vol. 9, no. 3, pp. 3935–3942, May 2020, doi: 10.1016/j.jmrt.2020.02.019.

[183] Y. Qi *et al.*, "A tunable terahertz metamaterial absorber composed of elliptical ring graphene arrays with refractive index sensing application," *Results in Physics*, vol. 16, p. 103012, Mar. 2020, doi: 10.1016/j.rinp.2020.103012.

[184] L. Min and L. Huang, "Perspective on resonances of metamaterials," *Opt. Express*, vol. 23, no. 15, p. 19022, Jul. 2015, doi: 10.1364/OE.23.019022.

[185] Y. Zhong, L. Du, Q. Liu, L. Zhu, and B. Zhang, "Metasurface-enhanced ATR sensor for aqueous solution in the terahertz range," *Optics Communications*, vol. 465, p. 125508, Jun. 2020, doi: 10.1016/j.optcom.2020.125508.

[186] F. Yan *et al.*, "Ultrasensitive Tunable Terahertz Sensor With Graphene Plasmonic Grating," *J. Lightwave Technol.*, vol. 37, no. 4, pp. 1103–1112, Feb. 2019, doi: 10.1109/JLT.2018.2886412.

[187] M. Aslinezhad, "High sensitivity refractive index and temperature sensor based on semiconductor metamaterial perfect absorber in the terahertz band," *Optics Communications*, vol. 463, p. 125411, May 2020, doi: 10.1016/j.optcom.2020.125411.

[188] W. Xu *et al.*, "Terahertz biosensing with a graphene-metamaterial heterostructure platform," *Carbon*, vol. 141, pp. 247–252, Jan. 2019, doi: 10.1016/j.carbon.2018.09.050.

[189] A. C. Kak, M. Slaney, and G. Wang, "Principles of Computerized Tomographic Imaging," *Med. Phys.*, vol. 29, no. 1, pp. 107–107, Jan. 2002, doi: 10.1118/1.1455742.

[190] J. W. Handley, A. J. Fitzgerald, E. Berry, and R. D. Boyle, "Wavelet compression in medical terahertz pulsed imaging," *Phys. Med. Biol.*, vol. 47, no. 21, pp. 3885–3892, Nov. 2002, doi: 10.1088/0031-9155/47/21/328.

[191] X. Yin, B. W.-H. Ng, B. Ferguson, and D. Abbott, "Wavelet based local tomographic image using terahertz techniques," *Digital Signal Processing*, vol. 19, no. 4, pp. 750–763, Jul. 2009, doi: 10.1016/j.dsp.2008.06.009.

[192] D.-W. Park, G.-H. Oh, and H.-S. Kim, "Predicting the stacking sequence of E-glass fiber reinforced polymer (GFRP) epoxy composite using terahertz time-domain spectroscopy (THz-TDS) system," *Composites Part B: Engineering*, vol. 177, p. 107385, Nov. 2019, doi: 10.1016/j.compositesb.2019.107385.

[193] C.-H. Ryu, S.-H. Park, D.-H. Kim, K.-Y. Jhang, and H.-S. Kim, "Nondestructive evaluation of hidden multi-delamination in a glass-fiber-reinforced plastic composite using terahertz spectroscopy," *Composite Structures*, vol. 156, pp. 338–347, Nov. 2016, doi: 10.1016/j.compstruct.2015.09.055.

[194] J. Dong, A. Locquet, N. F. Declercq, and D. S. Citrin, "Polarization-resolved terahertz imaging of intra- and inter-laminar damages in hybrid fiber-reinforced composite laminate subject to low-velocity impact," *Composites Part B: Engineering*, vol. 92, pp. 167–174, May 2016, doi: 10.1016/j.compositesb.2016.02.016.

[195] S. Sommer, T. Probst, E. Kraus, B. Baudrit, G. E. Town, and M. Koch, "Cure monitoring of two-component epoxy adhesives by terahertz time-domain spectroscopy," *Polym. Sci. Ser. B*, vol. 58, no. 6, pp. 769–776, Nov. 2016, doi: 10.1134/S1560090416060154.

[196] R. Valery A., "Manifestation of the Relationship between Molecular Relaxation Processes and Vibrational Dynamics of Polymers at Terahertz Frequencies in their IR Spectra," *Journal of Macromolecular Science, Part B*, vol. 0, no. ja, pp. 1–6, Nov. 2022, doi: 10.1080/00222348.2022.2145742.

[197] S. F. Busch, E. Castro-Camus, F. Beltran-Mejia, J. C. Balzer, and M. Koch, "3D Printed Prisms with Tunable Dispersion for the THz Frequency Range," *J Infrared Milli Terahz Waves*, vol. 39, no. 6, pp. 553–560, Jun. 2018, doi: 10.1007/s10762-018-0488-0.

[198] T. Kaji, Y. Tominari, T. Yamada, S. Saito, I. Morohashi, and A. Otomo, "Terahertz-wave generation devices using electro-optic polymer slab waveguides and cyclo-olefin polymer clads," *Opt. Express, OE*, vol. 26, no. 23, pp. 30466–30475, Nov. 2018, doi: 10.1364/OE.26.030466.

[199] W. Nsengiyumva, S. Zhong, M. Luo, Q. Zhang, and J. Lin, "Critical insights into the state-of-the-art NDE data fusion techniques for the inspection of structural systems," *Struct Control Health Monit*, Sep. 2021, doi: 10.1002/stc.2857.

[200] X. Zhang, Q. Guo, T. Chang, and H.-L. Cui, "Broadband stepped-frequency modulated continuous terahertz wave tomography for non-destructive inspection of polymer materials," *Polymer Testing*, vol. 76, pp. 455–463, Jul. 2019, doi: 10.1016/j.polymertesting.2019.04.001.

[201] S. Engelbrecht, K.-H. Tybussek, J. Sampaio, J. Böhmler, B. M. Fischer, and S. Sommer, "Monitoring the Isothermal Crystallization Kinetics of PET-A Using THz-TDS," *J Infrared Milli Terahz Waves*, vol. 40, no. 3, pp. 306–313, Mar. 2019, doi: 10.1007/s10762-019-00570-8.

[202] S. Santitewagun, R. Thakkar, J. A. Zeitler, and M. Maniruzzaman, "Detecting Crystallinity Using Terahertz Spectroscopy in 3D Printed Amorphous Solid Dispersions," *Molecular Pharmaceutics*, Jun. 2022, doi: 10.1021/acs.molpharmaceut.2c00163.

[203] E. V. Yakovlev, K. I. Zaytsev, I. N. Dolganova, and S. O. Yurchenko, "Non-Destructive Evaluation of Polymer Composite Materials at the Manufacturing Stage Using Terahertz Pulsed Spectroscopy," *IEEE Trans. THz Sci. Technol.*, vol. 5, no. 5, pp. 810–816, Sep. 2015, doi: 10.1109/TTHZ.2015.2460671.

[204] H. Hoshina *et al.*, "Terahertz Spectroscopy in Polymer Research: Assignment of Intermolecular Vibrational Modes and Structural Characterization of Poly(3-Hydroxybutyrate)," *IEEE Transactions on Terahertz Science and Technology*, vol. 3, no. 3, pp. 248–258, May 2013, doi: 10.1109/TTHZ.2013.2253154.

[205] Y. H. Tao, A. J. Fitzgerald, and V. P. Wallace, "Non-Contact, Non-Destructive Testing in Various Industrial Sectors with Terahertz Technology," *Sensors*, vol. 20, no. 3, p. 712, Jan. 2020, doi: 10.3390/s20030712.

[206] E. V. Yakovlev, K. I. Zaytsev, I. N. Fokina, V. E. Karasik, and S. O. Yurchenko, "Nondestructive testing of polymer composite materials using THz radiation," *Journal of Physics: Conference Series*, vol. 486, p. 012008, Mar. 2014, doi: 10.1088/1742-6596/486/1/012008.

[207] S. Wietzke, C. Jansen, F. Rutz, D. M. Mittleman, and M. Koch, "Determination of additive content in polymeric compounds with terahertz time-domain spectroscopy," *Polymer Testing*, vol. 26, no. 5, pp. 614–618, Aug. 2007, doi: 10.1016/j.polymertesting.2007.03.002.

[208] N. Krumbholz *et al.*, "Degree of dispersion of polymeric compounds determined with terahertz time-domain spectroscopy," *Polym Eng Sci*, vol. 51, no. 1, pp. 109–116, Jan. 2011, doi: 10.1002/pen.21798.

[209] C. Jördens, S. Wietzke, M. Scheller, and M. Koch, "Investigation of the water absorption in polyamide and wood plastic composite by terahertz time-domain spectroscopy," *Polymer Testing*, vol. 29, no. 2, pp. 209–215, Apr. 2010, doi: 10.1016/j.polymertesting.2009.11.003.

[210] C. Jördens *et al.*, "Terahertz spectroscopy to study the orientation of glass fibres in reinforced plastics," *Composites Science and Technology*, vol. 70, no. 3, pp. 472–477, Mar. 2010, doi: 10.1016/j.compscitech.2009.11.022.

[211] M. Okano and S. Watanabe, "Inspection of internal filler alignment in visibly opaque carbon-black–rubber composites by terahertz polarization spectroscopy in reflection mode," *Polymer Testing*, vol. 72, pp. 196–201, Dec. 2018, doi: 10.1016/j.polymertesting.2018.10.020.

[212] F. Rutz, T. Hasek, M. Koch, H. Richter, and U. Ewert, "Terahertz birefringence of liquid crystal polymers," *Appl. Phys. Lett.*, vol. 89, no. 22, p. 221911, Nov. 2006, doi: 10.1063/1.2397564.

[213] D. Polley, A. Barman, and R. K. Mitra, "EMI shielding and conductivity of carbon nanotube-polymer composites at terahertz frequency," *Opt. Lett., OL*, vol. 39, no. 6, pp. 1541–1544, Mar. 2014, doi: 10.1364/OL.39.001541.

[214] D. Polley, A. Barman, and R. K. Mitra, "Controllable terahertz conductivity in single walled carbon nanotube/polymer composites," *Journal of Applied Physics*, vol. 117, no. 2, p. 023115, Jan. 2015, doi: 10.1063/1.4905958.

[215] B. M. Fischer *et al.*, "Investigating Material Characteristics and Morphology of Polymers Using Terahertz Technologies," *IEEE Trans. THz Sci. Technol.*, vol. 3, no. 3, pp. 259–268, May 2013, doi: 10.1109/TTHZ.2013.2255916.

[216] K. Berdel, J. G. Rivas, P. H. Bolivar, P. de Maagt, and H. Kurz, "Temperature dependence of the permittivity and loss tangent of high-permittivity materials at terahertz frequencies," *IEEE Transactions on Microwave Theory and Techniques*, vol. 53, no. 4, pp. 1266–1271, Apr. 2005, doi: 10.1109/TMTT.2005.845752.

[217] Y. Hirakawa *et al.*, "Nondestructive Evaluation of Rubber Compounds by Terahertz Time-Domain Spectroscopy," *J Infrared Milli Terahz Waves*, vol. 32, no. 12, pp. 1457–1463, Dec. 2011, doi: 10.1007/s10762-011-9832-3.

[218] F. Rutz, M. Koch, S. Khare, M. Moneke, H. Richter, and U. Ewert, "Terahertz Quality Control of Polymeric Products," *Int J Infrared Milli Waves*, vol. 27, no. 4, pp. 547–556, Jul. 2007, doi: 10.1007/s10762-006-9106-7.

[219] M. Naftaly and R. E. Miles, "Terahertz Time-Domain Spectroscopy for Material Characterization," *Proc. IEEE*, vol. 95, no. 8, pp. 1658–1665, Aug. 2007, doi: 10.1109/JPROC.2007.898835.

[220] E. Frauendorfer, A. Wolf, and W.-D. Hergeth, "Polymerization Online Monitoring," *Chem. Eng. Technol.*, vol. 33, no. 11, pp. 1767–1778, Nov. 2010, doi: 10.1002/ceat.201000265.

[221] C. D. Stoik, M. J. Bohn, and J. L. Blackshire, "Nondestructive evaluation of aircraft composites using transmissive terahertz time domain spectroscopy," *Opt. Express*, vol. 16, no. 21, p. 17039, Oct. 2008, doi: 10.1364/OE.16.017039.

[222] T. Chady and P. Lopato, "Testing of glass-fiber reinforced composite materials using terahertz technique," *JAE*, vol. 33, no. 3–4, pp. 1599–1605, Oct. 2010, doi: 10.3233/JAE-2010-1290.

[223] Q. Wang *et al.*, "Nondestructive imaging of hidden defects in aircraft sandwich composites using terahertz time-domain spectroscopy," *Infrared Physics & Technology*, vol. 97, pp. 326–340, Mar. 2019, doi: 10.1016/j.infrared.2019.01.013.

[224] J. Wang, J. Zhang, T. Chang, L. Liu, and H.-L. Cui, "Terahertz nondestructive imaging for foreign object detection in glass fibre-reinforced polymer composite panels," *Infrared Physics & Technology*, vol. 98, pp. 36–44, May 2019, doi: 10.1016/j.infrared.2019.02.003.

[225] M. Mieloszyk, K. Majewska, and W. Ostachowicz, "THz spectroscopy application for detection and localisation of water inclusion in glass composite," *Composite Structures*, vol. 192, pp. 537–544, May 2018, doi: 10.1016/j.compstruct.2018.03.040.

[226] F. Destic and C. Bouvet, "Impact damages detection on composite materials by THz imaging," *Case Studies in Nondestructive Testing and Evaluation*, vol. 6, pp. 53–62, Nov. 2016, doi: 10.1016/j.csndt.2016.09.003.

[227] J. Dong *et al.*, "Visualization of subsurface damage in woven carbon fiber-reinforced composites using polarization-sensitive terahertz imaging," *NDT & E International*, vol. 99, pp. 72–79, Oct. 2018, doi: 10.1016/j.ndteint.2018.07.001.

[228] G. Wang *et al.*, "Strong and super thermally insulating in-situ nanofibrillar PLA/PET composite foam fabricated by high-pressure microcellular injection molding," *Chemical Engineering Journal*, vol. 390, p. 124520, Jun. 2020, doi: 10.1016/j.cej.2020.124520.

[229] K. Skleničková, S. Abbrent, M. Halecký, V. Kočí, and H. Beneš, "Biodegradability and ecotoxicity of polyurethane foams: A review," *Critical Reviews in Environmental Science and Technology*, vol. 52, no. 2, pp. 157–202, Jan. 2022, doi: 10.1080/10643389.2020.1818496.

[230] M. Tomin and Á. Kmetty, "Polymer foams as advanced energy absorbing materials for sports applications-A review," *Journal of Applied Polymer Science*, vol. 139, no. 9, p. 51714, 2022, doi: 10.1002/app.51714.

[231] A. Elmoutaouakkil, G. Fuchs, P. Bergounhon, R. P res, and F. Peyrin, "Three-dimensional quantitative analysis of polymer foams from synchrotron radiation x-ray microtomography," *J. Phys. D: Appl. Phys.*, vol. 36, no. 10A, pp. A37–A43, May 2003, doi: 10.1088/0022-3727/36/10A/308.

[232] E. Solórzano *et al.*, "Comparison between neutron tomography and X-ray tomography: A study on polymer foams," *Nuclear Instruments and Methods in Physics Research Section B: Beam Interactions with Materials and Atoms*, vol. 324, pp. 29–34, Apr. 2014, doi: 10.1016/j.nimb.2013.11.023.

[233] E. Solórzano, E. Laguna-Gutierrez, S. Perez-Tamarit, A. Kaestner, and M. A. Rodriguez-Perez, "Polymer foam evolution characterized by time-resolved neutron radiography," *Colloids and Surfaces A: Physicochemical and Engineering Aspects*, vol. 473, pp. 46–54, May 2015, doi: 10.1016/j.colsurfa.2015.02.006.

[234] M. B. B. Monroe, A. D. Easley, K. Grant, G. K. Fletcher, C. Boyer, and D. J. Maitland, "Multifunctional Shape-Memory Polymer Foams with Bio-inspired Antimicrobials," *ChemPhysChem*, vol. 19, no. 16, pp. 1999–2008, 2018, doi: 10.1002/cphc.201701015.

[235] A. Wesełucha-Birczyńska *et al.*, "Application of Raman spectroscopy to study of the polymer foams modified in the volume and on the surface by carbon nanotubes," *Vibrational Spectroscopy*, vol. 72, pp. 50–56, May 2014, doi: 10.1016/j.vibspec.2014.02.009.

[236] G. Pastorelli *et al.*, "Characterisation of historic plastics using terahertz time-domain spectroscopy and pulsed imaging," *Anal Bioanal Chem*, vol. 403, no. 5, pp. 1405–1414, May 2012, doi: 10.1007/s00216-012-5931-9.

[237] Y. Oyama, L. Zhen, T. Tanabe, and M. Kagaya, "Sub-terahertz imaging of defects in building blocks," *NDT & E International*, vol. 42, no. 1, pp. 28–33, Jan. 2009, doi: 10.1016/j.ndteint.2008.08.002.

[238] A. Abina, U. Puc, A. Jeglič, and A. Zidanšek, "Applications of Terahertz Spectroscopy in the Field of Construction and Building Materials," *Applied Spectroscopy Reviews*, vol. 50, no. 4, pp. 279–303, Apr. 2015, doi: 10.1080/05704928.2014.965825.

[239] M. Werner, C. Kolb, G. Schober, and S. Kremling, "Charakterisierung Von Polymerschäumen Mittels Zeitaufgelöster Terahertz-Spektroskopie," *DGZfP-Jahrestagung: Berlin, Germany*, 2017.

[240] A. Abina, U. Puc, A. Jeglič, and A. Zidanšek, "Structural analysis of insulating polymer foams with terahertz spectroscopy and imaging," *Polymer Testing*, vol. 32, no. 4, pp. 739–747, Jun. 2013, doi: 10.1016/j.polymertesting.2013.03.004.

[241] R. Aradhana, S. Mohanty, and S. K. Nayak, "High performance epoxy nanocomposite adhesive: Effect of nanofillers on adhesive strength, curing and degradation kinetics," *International Journal of Adhesion and Adhesives*, vol. 84, pp. 238–249, Aug. 2018, doi: 10.1016/j.ijadhadh.2018.03.013.

[242] X. Yang *et al.*, "Accurate Characterization of the Adhesive Layer Thickness of Ceramic Bonding Structures Using Terahertz Time-Domain Spectroscopy," *Materials*, vol. 15, no. 19, Art. no. 19, Jan. 2022, doi: 10.3390/ma15196972.

[243] T. Probst *et al.*, "Monitoring the Polymerization of Two-Component Epoxy Adhesives Using a Terahertz Time Domain Reflection System," *J Infrared Milli Terahz Waves*, vol. 36, no. 6, pp. 569–577, Jun. 2015, doi: 10.1007/s10762-015-0155-7.

[244] L. Xing *et al.*, "Nondestructive examination of polymethacrylimide composite structures with terahertz time-domain spectroscopy," *Polymer Testing*, vol. 57, pp. 141–148, Feb. 2017, doi: 10.1016/j.polymertesting.2016.11.022.

[245] E. Stübling *et al.*, "THz Properties of Adhesives," *J Infrared Milli Terahz Waves*, vol. 39, no. 6, pp. 586–593, Jun. 2018, doi: 10.1007/s10762-018-0492-4.

[246] C. Jansen, S. Wietzke, H. Wang, M. Koch, and G. Zhao, "Terahertz spectroscopy on adhesive bonds," *Polymer Testing*, vol. 30, no. 1, pp. 150–154, Feb. 2011, doi: 10.1016/j.polymertesting.2010.11.005.

[247] F. Rettich, N. Vieweg, O. Cojocari, and A. Deninger, "Field Intensity Detection of Individual Terahertz Pulses at 80 MHz Repetition Rate," *J Infrared Milli Terahz Waves*, vol. 36, no. 7, pp. 607–612, Jul. 2015, doi: 10.1007/s10762-015-0162-8.

[248] W. Withayachumnankul and M. Naftaly, "Fundamentals of Measurement in Terahertz Time-Domain Spectroscopy," *J Infrared Milli Terahz Waves*, vol. 35, no. 8, pp. 610–637, Aug. 2014, doi: 10.1007/s10762-013-0042-z.

[249] W. Tu, S. Zhong, Y. Shen, A. Incecik, and X. Fu, "Neural network-based hybrid signal processing approach for resolving thin marine protective coating by terahertz pulsed imaging," *Ocean Engineering*, vol. 173, pp. 58–67, Feb. 2019, doi: 10.1016/j.oceaneng.2018.12.051.

[250] L. Wang, Y. Di, Y. Liu, H. Wang, H. You, and T. Liu, "Effect of TGO on the tensile failure behavior of thermal barrier coatings," *Front. Mech. Eng.*, vol. 14, no. 4, pp. 452–460, Dec. 2019, doi: 10.1007/s11465-019-0541-2.

[251] Z. Zhang *et al.*, "Time of flight improved thermally grown oxide thickness measurement with terahertz spectroscopy," *Front. Mech.*

Eng., vol. 17, no. 4, p. 49, Dec. 2022, doi: 10.1007/s11465-022-0705-3.

[252] P. Jiang, L. Yang, Y. Sun, D. Li, and TiejunWang, "Local residual stress evolution of highly irregular thermally grown oxide layer in thermal barrier coatings," *Ceramics International*, vol. 47, no. 8, pp. 10990–10995, Apr. 2021, doi: 10.1016/j.ceramint.2020.12.220.

[253] H. E. Evans, "Oxidation failure of TBC systems: An assessment of mechanisms," *Surface and Coatings Technology*, vol. 206, no. 7, pp. 1512–1521, Dec. 2011, doi: 10.1016/j.surfcoat.2011.05.053.

[254] T. Fukuchi, T. Ozeki, M. Okada, and T. Fujii, "Nondestructive inspection of thermal barrier coating of gas turbine high temperature components," *IEEJ Transactions on Electrical and Electronic Engineering*, vol. 11, no. 4, pp. 391–400, 2016, doi: 10.1002/tee.22255.

[255] T. Fukuchi *et al.*, "Topcoat Thickness Measurement of Thermal Barrier Coating of Gas Turbine Blade Using Terahertz Wave," *Electrical Engineering in Japan*, vol. 189, no. 1, pp. 1–8, 2014, doi: 10.1002/eej.22624.

[256] T. Fukuchi, N. Fuse, M. Okada, T. Fujii, M. Mizuno, and K. Fukunaga, "Measurement of Refractive Index and Thickness of Topcoat of Thermal Barrier Coating by Reflection Measurement of Terahertz Waves," *Electronics and Communications in Japan*, vol. 96, no. 12, pp. 37–45, 2013, doi: 10.1002/ecj.11551.

[257] C.-C. Chen, D.-J. Lee, T. Pollock, and J. F. Whitaker, "Pulsed-terahertz reflectometry for health monitoring of ceramic thermal barrier coatings," *Opt. Express, OE*, vol. 18, no. 4, pp. 3477–3486, Feb. 2010, doi: 10.1364/OE.18.003477.

[258] S. Unnikrishnakurup, J. Dash, S. Ray, B. Pesala, and K. Balasubramaniam, "Nondestructive evaluation of thermal barrier coating thickness degradation using pulsed IR thermography and THz-TDS measurements: A comparative study," *NDT & E International*, vol. 116, p. 102367, Dec. 2020, doi: 10.1016/j.ndteint.2020.102367.

[259] A. J. Waddie, P. J. Schemmel, C. Chalk, L. Isern, J. R. Nicholls, and A. J. Moore, "Terahertz optical thickness and birefringence measurement for thermal barrier coating defect location," *Opt. Express, OE*, vol. 28, no. 21, pp. 31535–31552, Oct. 2020, doi: 10.1364/OE.398532.

[260] D. Ye *et al.*, "In-situ evaluation of porosity in thermal barrier coatings based on the broadening of terahertz time-domain pulses: simulation and experimental investigations," *Opt. Express, OE*, vol. 27, no. 20, pp. 28150–28165, Sep. 2019, doi: 10.1364/OE.27.028150.

[261] M. Luo, S. Zhong, L. Yao, W. Tu, W. Nsengiyumva, and W. Chen, "Thin thermally grown oxide thickness detection in thermal barrier coatings based on SWT-BP neural network algorithm and terahertz technology," *Appl. Opt., AO*, vol. 59, no. 13, pp. 4097–4104, May 2020, doi: https://doi.org/10.1364/AO.392748.

[262] S. Krimi, J. Klier, J. Jonuscheit, G. von Freymann, R. Urbansky, and R. Beigang, "Highly accurate thickness measurement of multi-layered automotive paints using terahertz technology," *Appl. Phys. Lett.*, vol. 109, no. 2, p. 021105, Jul. 2016, doi: 10.1063/1.4955407.

[263] A. I. Hernandez-Serrano and E. Castro-Camus, "Determination of automobile paint thickness using non-contact THz-TDS technique," in *2015 40th International Conference on Infrared, Millimeter, and Terahertz waves (IRMMW-THz)*, Aug. 2015, pp. 1–1. doi: 10.1109/IRMMW-THz.2015.7327427.

[264] T. Yasui, T. Yasuda, K. Sawanaka, and T. Araki, "Terahertz paintmeter for noncontact monitoring of thickness and drying progress in paint film," *Appl. Opt., AO*, vol. 44, no. 32, pp. 6849–6856, Nov. 2005, doi: 10.1364/AO.44.006849.

[265] T. Yasuda, T. Iwata, T. Araki, and T. Yasui, "Improvement of minimum paint film thickness for THz paint meters by multiple-regression analysis," *Appl. Opt., AO*, vol. 46, no. 30, pp. 7518–7526, Oct. 2007, doi: 10.1364/AO.46.007518.

[266] L. Liebelt *et al.*, "Influence of bandwidth and dynamic range on thickness determination using terahertz time-domain spectroscopy," in *2019 44th International Conference on Infrared, Millimeter, and Terahertz Waves (IRMMW-THz)*, Sep. 2019, pp. 1–2. doi: 10.1109/IRMMW-THz.2019.8874124.

[267] W. Withayachumnankul, B. M. Fischer, and D. Abbott, "Numerical removal of water vapour effects from terahertz time-domain spectroscopy measurements," *Proc. R. Soc. A.*, vol. 464, no. 2097, pp. 2435–2456, Sep. 2008, doi: 10.1098/rspa.2007.0294.

[268] Y. Wang, Z. Chen, Z. Zhao, L. Zhang, K. Kang, and Y. Zhang, "Restoration of terahertz signals distorted by atmospheric water vapor absorption," *Journal of Applied Physics*, vol. 105, no. 10, p. 103105, May 2009, doi: 10.1063/1.3129308.

[269] K.-H. Im, I.-Y. Yang, S.-K. Kim, J.-A. Jung, Y.-T. Cho, and Y.-D. Woo, "Terahertz scanning techniques for paint thickness on CFRP composite solid laminates," *J Mech Sci Technol*, vol. 30, no. 10, pp. 4413–4416, Oct. 2016, doi: 10.1007/s12206-016-0903-1.

[270] K. H. Im, S. K. Kim, D. K. Hsu, and J. A. Jung, "Coating Thickness Characterization of Composite Materials Using Terahertz Waves," *MSF*, vol. 878, pp. 70–73, Nov. 2016, doi: 10.4028/www.scientific.net/MSF.878.70.

[271] W. Tu, S. Zhong, Y. Shen, and A. Incecik, "Nondestructive testing of marine protective coatings using terahertz waves with stationary wavelet transform," *Ocean Engineering*, vol. 111, pp. 582–592, Jan. 2016, doi: 10.1016/j.oceaneng.2015.11.028.

[272] W. Tu, S. Zhong, Q. Zhang, Y. Shen, and A. Incecik, "Quality evaluation of organic protective paints using terahertz pulse imaging technology based on wavelet packet energy method," *Ocean Engineering*, vol. 267, p. 113282, Jan. 2023, doi: 10.1016/j.oceaneng.2022.113282.

[273] J. Dong *et al.*, "Terahertz frequency-wavelet domain deconvolution for stratigraphic and subsurface investigation of art painting," *Opt. Express, OE*, vol. 24, no. 23, pp. 26972–26985, Nov. 2016, doi: 10.1364/OE.24.026972.

[274] D. J. Cook, S. J. Sharpe, S. Lee, and M. G. Allen, "Terahertz Time Domain Measurements of Marine Paint Thickness," in *Optical Terahertz Science and Technology (2007), paper TuB5*, Optica Publishing Group, Mar. 2007, p. TuB5. doi: 10.1364/OTST.2007.TuB5.

[275] D. J. Cook, S. Lee, S. J. Sharpe, and M. G. Allen, "Accuracy and linearity of time-domain THz paint thickness measurements," presented at the Integrated Optoelectronic Devices 2008, K. J. Linden and L. P. Sadwick, Eds., San Jose, CA, Feb. 2008, p. 68930H. doi: 10.1117/12.763900.

[276] J. L. Johnson, T. D. Dorney, and D. M. Mittleman, "Interferometric imaging with terahertz pulses," *IEEE Journal of Selected Topics in Quantum Electronics*, vol. 7, no. 4, pp. 592–599, Jul. 2001, doi: 10.1109/2944.974230.

[277] J. L. Johnson, T. D. Dorney, and D. M. Mittleman, "Enhanced depth resolution in terahertz imaging using phase-shift interferometry," *Appl. Phys. Lett.*, vol. 78, no. 6, pp. 835–837, Feb. 2001, doi: 10.1063/1.1346626.

[278] Y. Chen, Y. Sun, and E. Pickwell-Macpherson, "Improving extraction of impulse response functions using stationary wavelet shrinkage in terahertz reflection imaging," *Fluct. Noise Lett.*, vol. 09, no. 04, pp. 387–394, Dec. 2010, doi: 10.1142/S0219477510000319.

[279] D. J. Roth, J. P. Seebo, L. B. Trinh, J. L. Walker, and J. C. Aldrin, "Signal Processing Approaches for Terahertz Data Obtained from Inspection of the Shuttle External Tank Thermal Protection System Foam," *AIP Conference Proceedings*, vol. 894, no. 1, pp. 415–424, Mar. 2007, doi: 10.1063/1.2718002.

[280] T. Iwata, S. Yoshioka, S. Nakamura, Y. Mizutani, and T. Yasui, "Prediction of the Thickness of a Thin Paint Film by Applying a Modified Partial-Least-Squares-1 Method to Data Obtained in Terahertz Reflectometry," *J Infrared Milli Terahz Waves*, vol. 34, no. 10, pp. 646–659, Oct. 2013, doi: 10.1007/s10762-013-0015-2.

[281] T. Chady, P. Lopato, and B. Szymanik, "Terahertz and thermal testing of glass-fiber reinforced composites with impact damages," *Journal of Sensors*, vol. 2012, 2012.

[282] J. Choi, W. S. Kwon, K.-S. Kim, and S. Kim, "Nondestructive evaluation of multilayered paint films in ambient atmosphere using terahertz reflection spectroscopy," *NDT & E International*, vol. 80, pp. 71–76, Jun. 2016, doi: 10.1016/j.ndteint.2016.02.011.

[283] W. Tu, S. Zhong, M. Luo, and Q. Zhang, "Non-Destructive Evaluation of Hidden Defects Beneath the Multilayer Organic Protective Coatings Based on Terahertz Technology," *Front. Phys.*, vol. 9, p. 676851, Jun. 2021, doi: 10.3389/fphy.2021.676851.

[284] X. Lu, H. Sun, T. Chang, J. Zhang, and H. Cui, "Terahertz detection of porosity and porous microstructure in pharmaceutical tablets: A review," *International Journal of Pharmaceutics*, vol. 591, p. 120006, Dec. 2020, doi: 10.1016/j.ijpharm.2020.120006.

[285] D. Alves-Lima *et al.*, "Review of Terahertz Pulsed Imaging for Pharmaceutical Film Coating Analysis," *Sensors*, vol. 20, no. 5, Art. no. 5, Jan. 2020, doi: 10.3390/s20051441.

[286] A. J. Fitzgerald, B. E. Cole, and P. F. Taday, "Nondestructive Analysis of Tablet Coating Thicknesses Using Terahertz Pulsed

Imaging," *Journal of Pharmaceutical Sciences*, vol. 94, no. 1, pp. 177–183, Jan. 2005, doi: 10.1002/jps.20225.

[287] J. A. Spencer *et al.*, "Delayed release tablet dissolution related to coating thickness by terahertz pulsed image mapping," *Journal of Pharmaceutical Sciences*, vol. 97, no. 4, pp. 1543–1550, 2008, doi: 10.1002/jps.21051.

[288] L. Ho *et al.*, "Monitoring the Film Coating Unit Operation and Predicting Drug Dissolution Using Terahertz Pulsed Imaging," *Journal of Pharmaceutical Sciences*, vol. 98, no. 12, pp. 4866–4876, Dec. 2009, doi: 10.1002/jps.21766.

[289] V. Malaterre, M. Pedersen, J. Ogorka, R. Gurny, N. Loggia, and P. F. Taday, "Terahertz pulsed imaging, a novel process analytical tool to investigate the coating characteristics of push–pull osmotic systems," *European Journal of Pharmaceutics and Biopharmaceutics*, vol. 74, no. 1, pp. 21–25, Jan. 2010, doi: 10.1016/j.ejpb.2008.10.011.

[290] R. K. May *et al.*, "Terahertz In-Line Sensor for Direct Coating Thickness Measurement of Individual Tablets During Film Coating in Real-Time," *Journal of Pharmaceutical Sciences*, vol. 100, no. 4, pp. 1535–1544, Apr. 2011, doi: 10.1002/jps.22359.

[291] H. Lin, Y. Dong, Y. Shen, and J. Axel Zeitler, "Quantifying Pharmaceutical Film Coating with Optical Coherence Tomography and Terahertz Pulsed Imaging: An Evaluation," *Journal of Pharmaceutical Sciences*, vol. 104, no. 10, pp. 3377–3385, Oct. 2015, doi: 10.1002/jps.24535.

[292] R. K. May *et al.*, "Hardness and Density Distributions of Pharmaceutical Tablets Measured by Terahertz Pulsed Imaging," *Journal of Pharmaceutical Sciences*, vol. 102, no. 7, pp. 2179–2186, Jul. 2013, doi: 10.1002/jps.23560.

[293] H. Lin *et al.*, "Impact of Processing Conditions on Inter-tablet Coating Thickness Variations Measured by Terahertz In-Line Sensing," *Journal of Pharmaceutical Sciences*, vol. 104, no. 8, pp. 2513–2522, Aug. 2015, doi: 10.1002/jps.24503.

[294] L. Ho *et al.*, "Analysis of sustained-release tablet film coats using terahertz pulsed imaging," *Journal of Controlled Release*, vol. 119, no. 3, pp. 253–261, Jun. 2007, doi: 10.1016/j.jconrel.2007.03.011.

[295] L. Ho *et al.*, "Applications of terahertz pulsed imaging to sustained-release tablet film coating quality assessment and dissolution performance," *Journal of Controlled Release*, vol. 127, no. 1, pp. 79–87, Apr. 2008, doi: 10.1016/j.jconrel.2008.01.002.

[296] L. Ho *et al.*, "Investigating dissolution performance critical areas on coated tablets: A case study using terahertz pulsed imaging," *Journal of Pharmaceutical Sciences*, vol. 99, no. 1, pp. 392–402, 2010, doi: 10.1002/jps.21845.

[297] L. Ho *et al.*, "Effects of film coating thickness and drug layer uniformity on in vitro drug release from sustained-release coated pellets: A case study using terahertz pulsed imaging," *International Journal of Pharmaceutics*, vol. 382, no. 1, pp. 151–159, Dec. 2009, doi: 10.1016/j.ijpharm.2009.08.025.

[298] M. Dohi *et al.*, "Application of terahertz pulse imaging as PAT tool for non-destructive evaluation of film-coated tablets under different manufacturing conditions," *Journal of Pharmaceutical and Biomedical Analysis*, vol. 119, pp. 104–113, Feb. 2016, doi: 10.1016/j.jpba.2015.11.046.

[299] T. Chang, Q. Guo, L. Liu, and H.-L. Cui, "Nondestructive Thickness Inspection of Capsule Coating by Terahertz Time-Domain Spectroscopy," *IEEE Trans. THz Sci. Technol.*, vol. 8, no. 6, pp. 688–695, Nov. 2018, doi: 10.1109/TTHZ.2018.2867265.

[300] M. Haaser, K. C. Gordon, C. J. Strachan, and T. Rades, "Terahertz pulsed imaging as an advanced characterisation tool for film coatings—A review," *International Journal of Pharmaceutics*, vol. 457, no. 2, pp. 510–520, Dec. 2013, doi: 10.1016/j.ijpharm.2013.03.053.

[301] K.-E. Peiponen, P. Silfsten, J. Pajander, and J. Ketolainen, "Broadening of a THz pulse as a measure of the porosity of pharmaceutical tablets," *International Journal of Pharmaceutics*, vol. 447, no. 1, pp. 7–11, Apr. 2013, doi: 10.1016/j.ijpharm.2013.02.041.

[302] P. Bawuah *et al.*, "Terahertz-Based Porosity Measurement of Pharmaceutical Tablets: a Tutorial," *J Infrared Milli Terahz Waves*, vol. 41, no. 4, pp. 450–469, Apr. 2020, doi: 10.1007/s10762-019-00659-0.

[303] D. Markl *et al.*, "Characterization of the Pore Structure of Functionalized Calcium Carbonate Tablets by Terahertz Time-Domain Spectroscopy and X-Ray Computed Microtomography," *Journal of Pharmaceutical Sciences*, vol. 106, no. 6, pp. 1586–1595, Jun. 2017, doi: 10.1016/j.xphs.2017.02.028.

[304] P. Bawuah, T. Ervasti, N. Tan, J. A. Zeitler, J. Ketolainen, and K.-E. Peiponen, "Noninvasive porosity measurement of biconvex tablets using terahertz pulses," *International Journal of Pharmaceutics*, vol. 509, no. 1, pp. 439–443, Jul. 2016, doi: 10.1016/j.ijpharm.2016.06.023.

[305] M. Juuti *et al.*, "Optical and terahertz measurement techniques for flat-faced pharmaceutical tablets: a case study of gloss, surface roughness and bulk properties of starch acetate tablets," *Meas. Sci. Technol.*, vol. 20, no. 1, p. 015301, Nov. 2008, doi: 10.1088/0957-0233/20/1/015301.

[306] L. Lin, J. Chen, X. Zhang, and X. Li, "A novel 2-D random void model and its application in ultrasonically determined void content for composite materials," *NDT & E International*, vol. 44, no. 3, pp. 254–260, May 2011, doi: 10.1016/j.ndteint.2010.12.003.

[307] L. Lin, X. Zhang, J. Chen, Y. Mu, and X. Li, "A novel random void model and its application in predicting void content of composites based on ultrasonic attenuation coefficient," *Appl. Phys. A*, vol. 103, no. 4, pp. 1153–1157, Jun. 2011, doi: 10.1007/s00339-010-6061-x.

[308] K.-E. Peiponen, P. Bawuah, M. Chakraborty, M. Juuti, J. A. Zeitler, and J. Ketolainen, "Estimation of Young's modulus of pharmaceutical tablet obtained by terahertz time-delay measurement," *International Journal of Pharmaceutics*, vol. 489, no. 1, pp. 100–105, Jul. 2015, doi: 10.1016/j.ijpharm.2015.04.068.

[309] P. Bawuah, P. Silfsten, T. Ervasti, J. Ketolainen, J. A. Zeitler, and K.-E. Peiponen, "Non-contact weight measurement of flat-faced pharmaceutical tablets using terahertz transmission pulse delay measurements," *International Journal of Pharmaceutics*, vol. 476, no. 1, pp. 16–22, Dec. 2014, doi: 10.1016/j.ijpharm.2014.09.027.

[310] M. Herrmann, M. Tani, K. Sakai, and R. Fukasawa, "Terahertz imaging of silicon wafers," *Journal of Applied Physics*, vol. 91, no. 3, pp. 1247–1250, Feb. 2002, doi: 10.1063/1.1429772.

[311] S. Kim, H. Murakami, and M. Tonouchi, "Transmission-Type Laser THz Emission Microscope Using a Solid Immersion Lens," *IEEE Journal of Selected Topics in Quantum Electronics*, vol. 14, no. 2, pp. 498–504, Mar. 2008, doi: 10.1109/JSTQE.2007.913425.

[312] W. Ghann, A. Rahman, A. Rahman, and J. Uddin, "Interaction of Sensitizing Dyes with Nanostructured TiO2 Film in Dye-Sensitized Solar Cells Using Terahertz Spectroscopy," *Sci Rep*, vol. 6, no. 1, Art. no. 1, Jul. 2016, doi: 10.1038/srep30140.

[313] J. D. Buron *et al.*, "Terahertz wafer-scale mobility mapping of graphene on insulating substrates without a gate," *Opt. Express, OE*, vol. 23, no. 24, pp. 30721–30729, Nov. 2015, doi: 10.1364/OE.23.030721.

[314] M. Yamashita, K. Kawase, C. Otani, T. Kiwa, and M. Tonouchi, "Imaging of large-scale integrated circuits using laser terahertz emission microscopy," *Opt. Express, OE*, vol. 13, no. 1, pp. 115–120, Jan. 2005, doi: 10.1364/OPEX.13.000115.

[315] M. Yamashita *et al.*, "THz emission characteristics from p/n junctions with metal lines under non-bias conditions for LSI failure analysis," *Opt. Express, OE*, vol. 19, no. 11, pp. 10864–10873, May 2011, doi: 10.1364/OE.19.010864.

[316] M. Yamashita, C. Otani, K. Kawase, K. Nikawa, and M. Tonouchi, "Noncontact inspection technique for electrical failures in semiconductor devices using a laser terahertz emission microscope," *Appl. Phys. Lett.*, vol. 93, no. 4, p. 041117, Jul. 2008, doi: 10.1063/1.2965810.

[317] M. Yamashita *et al.*, "Laser THz emission microscope as a novel tool for LSI failure analysis," *Microelectronics Reliability*, vol. 49, no. 9, pp. 1116–1126, Sep. 2009, doi: 10.1016/j.microrel.2009.07.047.

[318] M. Yamashita *et al.*, "Backside observation of large-scale integrated circuits with multilayered interconnections using laser terahertz emission microscope," *Appl. Phys. Lett.*, vol. 94, no. 19, p. 191104, May 2009, doi: 10.1063/1.3133346.

[319] T. Kiwa, M. Tonouchi, M. Yamashita, and K. Kawase, "Laser terahertz-emission microscope for inspecting electrical faults in integrated circuits," *Opt. Lett., OL*, vol. 28, no. 21, pp. 2058–2060, Nov. 2003, doi: 10.1364/OL.28.002058.

[320] H. Murakami *et al.*, "Scanning laser THz imaging system," *J. Phys. D: Appl. Phys.*, vol. 47, no. 37, p. 374007, Sep. 2014, doi: 10.1088/0022-3727/47/37/374007.

[321] N. J. J. van Hoof, S. E. T. ter Huurne, J. G. Rivas, and A. Halpin, "Time-resolved terahertz time-domain near-field microscopy," *Opt. Express, OE*, vol. 26, no. 24, pp. 32118–32129, Nov. 2018, doi: 10.1364/OE.26.032118.

[322] A. J. Huber, F. Keilmann, J. Wittborn, J. Aizpurua, and R. Hillenbrand, "Terahertz Near-Field Nanoscopy of Mobile Carriers in Single Semiconductor Nanodevices," *Nano Lett.*, vol. 8, no. 11, pp. 3766–3770, Nov. 2008, doi: 10.1021/nl802086x.

[323] M. Nagel, A. Michalski, and H. Kurz, "Contact-free fault location and imaging with on-chip terahertz time-domain reflectometry," *Opt. Express, OE*, vol. 19, no. 13, pp. 12509–12514, Jun. 2011, doi: 10.1364/OE.19.012509.

[324] K. Ahi, S. Shahbazmohamadi, and N. Asadizanjani, "Quality control and authentication of packaged integrated circuits using enhanced-spatial-resolution terahertz time-domain spectroscopy and imaging," *Optics and Lasers in Engineering*, vol. 104, pp. 274–284, May 2018, doi: 10.1016/j.optlaseng.2017.07.007.

[325] M. Shur, S. Rudin, G. Rupper, M. Reed, and J. Suarez, "Sub-terahertz testing of millimeter wave Monolithic and very large scale integrated circuits," *Solid-State Electronics*, vol. 155, pp. 44–48, May 2019, doi: 10.1016/j.sse.2019.03.007.

[326] H. Hempel *et al.*, "Predicting Solar Cell Performance from Terahertz and Microwave Spectroscopy," *Advanced Energy Materials*, vol. 12, no. 13, p. 2102776, 2022, doi: 10.1002/aenm.202102776.

[327] A. M. Ulatowski, L. M. Herz, and M. B. Johnston, "Terahertz Conductivity Analysis for Highly Doped Thin-Film Semiconductors," *J Infrared Milli Terahz Waves*, vol. 41, no. 12, pp. 1431–1449, Dec. 2020, doi: 10.1007/s10762-020-00739-6.

[328] H. Nakanishi, A. Ito, K. Takayama, I. Kawayama, H. Murakami, and M. Tonouchi, "Comparison between laser terahertz emission microscope and conventional methods for analysis of polycrystalline silicon solar cell," *AIP Advances*, vol. 5, no. 11, p. 117129, Nov. 2015, doi: 10.1063/1.4935913.

[329] L. Minkevičius *et al.*, "Detection of tab wire soldering defects on silicon solar cells using terahertz time-domain spectroscopy," *Electron. Lett.*, vol. 48, no. 15, p. 932, 2012, doi: 10.1049/el.2012.1995.

[330] J. D. Buron *et al.*, "Graphene mobility mapping," *Sci Rep*, vol. 5, no. 1, Art. no. 1, Jul. 2015, doi: 10.1038/srep12305.

[331] J. W. May, "Platinum surface LEED rings," *Surface Science*, vol. 17, no. 1, pp. 267–270, Sep. 1969, doi: 10.1016/0039-6028(69)90227-1.

[332] K. S. Novoselov *et al.*, "Electric Field Effect in Atomically Thin Carbon Films," *Science*, vol. 306, no. 5696, pp. 666–669, Oct. 2004, doi: 10.1126/science.1102896.

[333] K. S. Novoselov *et al.*, "Two-dimensional gas of massless Dirac fermions in graphene," *Nature*, vol. 438, no. 7065, Art. no. 7065, Nov. 2005, doi: 10.1038/nature04233.

[334] Y. Zhang, Y.-W. Tan, H. L. Stormer, and P. Kim, "Experimental observation of the quantum Hall effect and Berry's phase in graphene," *Nature*, vol. 438, no. 7065, Art. no. 7065, Nov. 2005, doi: 10.1038/nature04235.

[335] Y. Yang *et al.*, "From Materials to Devices: Graphene toward Practical Applications," *Small Methods*, vol. 6, no. 10, p. 2200671, 2022, doi: 10.1002/smtd.202200671.

[336] H. Lin *et al.*, "Contactless graphene conductivity mapping on a wide range of substrates with terahertz time-domain reflection spectroscopy," *Sci Rep*, vol. 7, no. 1, Art. no. 1, Sep. 2017, doi: 10.1038/s41598-017-09809-7.

[337] T. Otsuji *et al.*, "Graphene-based devices in terahertz science and technology," *J. Phys. D: Appl. Phys.*, vol. 45, no. 30, p. 303001, Jul. 2012, doi: 10.1088/0022-3727/45/30/303001.

[338] H. Pandey *et al.*, "All CVD Boron Nitride Encapsulated Graphene FETs With CMOS Compatible Metal Edge Contacts," *IEEE Transactions on Electron Devices*, vol. 65, no. 10, pp. 4129–4134, Oct. 2018, doi: 10.1109/TED.2018.2865382.

[339] D. M. A. Mackenzie *et al.*, "Quality assessment of graphene: Continuity, uniformity, and accuracy of mobility measurements," *Nano Res.*, vol. 10, no. 10, pp. 3596–3605, Oct. 2017, doi: 10.1007/s12274-017-1570-y.

[340] P. R. Whelan *et al.*, "Conductivity mapping of graphene on polymeric films by terahertz time-domain spectroscopy," *Opt. Express, OE*, vol. 26, no. 14, pp. 17748–17754, Jul. 2018, doi: 10.1364/OE.26.017748.

[341] P. R. Whelan *et al.*, "Case studies of electrical characterisation of graphene by terahertz time-domain spectroscopy," *2D Mater.*, vol. 8, no. 2, p. 022003, Feb. 2021, doi: 10.1088/2053-1583/abdbcb.

[342] T. Ostatnický, V. Pushkarev, H. Němec, and P. Kužel, "Quantum theory of terahertz conductivity of semiconductor nanostructures," *Phys. Rev. B*, vol. 97, no. 8, p. 085426, Feb. 2018, doi: 10.1103/PhysRevB.97.085426.

[343] T. L. Cocker *et al.*, "Microscopic origin of the Drude-Smith model," *Phys. Rev. B*, vol. 96, no. 20, p. 205439, Nov. 2017, doi: 10.1103/PhysRevB.96.205439.

[344] P. Kužel and H. Němec, "Terahertz Spectroscopy of Nanomaterials: a Close Look at Charge-Carrier Transport," *Advanced Optical Materials*, vol. 8, no. 3, p. 1900623, 2020, doi: 10.1002/adom.201900623.

[345] D. Popa and F. Udrea, "Towards Integrated Mid-Infrared Gas Sensors," *Sensors*, vol. 19, no. 9, p. 2076, May 2019, doi: 10.3390/s19092076.

[346] M. Theuer, S. S. Harsha, D. Molter, G. Torosyan, and R. Beigang, "Terahertz Time-Domain Spectroscopy of Gases, Liquids, and Solids," *ChemPhysChem*, vol. 12, no. 15, pp. 2695–2705, Oct. 2011, doi: 10.1002/cphc.201100158.

[347] J. Dong, A. Locquet, and D. S. Citrin, "Enhanced Terahertz Imaging of Small Forced Delamination in Woven Glass Fibre-reinforced Composites with Wavelet De-noising," *J Infrared Milli Terahz Waves*, vol. 37, no. 3, pp. 289–301, Mar. 2016, doi: 10.1007/s10762-015-0226-9.

[348] D. M. Slocum, E. J. Slingerland, R. H. Giles, and T. M. Goyette, "Atmospheric absorption of terahertz radiation and water vapor continuum effects," *Journal of Quantitative Spectroscopy and Radiative Transfer*, vol. 127, pp. 49–63, Sep. 2013, doi: 10.1016/j.jqsrt.2013.04.022.

[349] W. D. Kimura, "Tunable CO2 laser system with subnanosecond-pulse-train output," *Optics & Laser Technology*, vol. 88, pp. 263–274, Feb. 2017, doi: 10.1016/j.optlastec.2016.09.022.

[350] R. K. Singh, S. Kumar, and R. P. Sharma, "Generation of electromagnetic waves in the terahertz frequency range by optical rectification of a Gaussian laser pulse in a plasma in presence of an externally applied static electric field," *Contributions to Plasma Physics*, vol. 57, no. 6–7, pp. 252–257, Jul. 2017, doi: 10.1002/ctpp.201700029.

[351] K. Liu, A. D. Koulouklidis, D. G. Papazoglou, S. Tzortzakis, and X.-C. Zhang, "Enhanced terahertz wave emission from air-plasma tailored by abruptly autofocusing laser beams," *Optica*, vol. 3, no. 6, p. 605, Jun. 2016, doi: 10.1364/OPTICA.3.000605.

[352] J. Homola, "Surface Plasmon Resonance Sensors for Detection of Chemical and Biological Species," *Chem. Rev.*, vol. 108, no. 2, pp. 462–493, Feb. 2008, doi: 10.1021/cr068107d.

[353] L. Yang, T. Guo, X. Zhang, S. Cao, and X. Ding, "Toxic chemical compound detection by terahertz spectroscopy: a review," *Reviews in Analytical Chemistry*, vol. 37, no. 3, Sep. 2018, doi: 10.1515/revac-2017-0021.

[354] R. M. Smith and M. A. Arnold, "Selectivity of Terahertz Gas-Phase Spectroscopy," *Anal. Chem.*, vol. 87, no. 21, pp. 10679–10683, Nov. 2015, doi: 10.1021/acs.analchem.5b03028.

[355] B. Graber, C. Kim, and D. H. Wu, "High SNR single measurements of trace gas phase spectra at THz frequencies," *Appl. Phys. Lett.*, vol. 111, no. 22, p. 221107, Nov. 2017, doi: 10.1063/1.4996910.

[356] A. Tekawade *et al.*, "Towards realization of quantitative atmospheric and industrial gas sensing using THz wave electronics," *Appl. Phys. B*, vol. 124, no. 6, p. 105, May 2018, doi: 10.1007/s00340-018-6974-1.

[357] K. Schmalz, N. Rothbart, M. H. Eissa, J. Borngräber, D. Kissinger, and H.-W. Hübers, "Transmitters and receivers in SiGe BiCMOS technology for sensitive gas spectroscopy at 222 - 270 GHz," *AIP Advances*, vol. 9, no. 1, p. 015213, Jan. 2019, doi: 10.1063/1.5066261.

[358] I. R. Medvedev, M. Behnke, and F. C. De Lucia, "Fast analysis of gases in the submillimeter/terahertz with 'absolute' specificity," *Appl. Phys. Lett.*, vol. 86, no. 15, p. 154105, Apr. 2005, doi: 10.1063/1.1897442.

[359] C. F. Neese, I. R. Medvedev, G. M. Plummer, A. J. Frank, C. D. Ball, and F. C. De Lucia, "Compact Submillimeter/Terahertz Gas Sensor With Efficient Gas Collection, Preconcentration, and ppt Sensitivity," *IEEE Sensors J.*, vol. 12, no. 8, pp. 2565–2574, Aug. 2012, doi: 10.1109/JSEN.2012.2195487.

[360] D. Popp, "Pollution control innovations and the Clean Air Act of 1990," *J. Pol. Anal. Manage.*, vol. 22, no. 4, pp. 641–660, 2003, doi: 10.1002/pam.10159.

[361] F. Hindle *et al.*, "Monitoring of food spoilage by high resolution THz analysis," *Analyst*, vol. 143, no. 22, pp. 5536–5544, Nov. 2018, doi: 10.1039/C8AN01180J.

[362] C. Wu, X. Miao, and K. Zhao, "Identifying PM2.5 samples collected in different environment by using terahertz time-domain

spectroscopy," *Front. Optoelectron.*, vol. 11, no. 3, pp. 256–260, Sep. 2018, doi: 10.1007/s12200-018-0805-1.

[363] H. Zhan, K. Zhao, R. Bao, and L. Xiao, "Monitoring PM2.5 in the Atmosphere by Using Terahertz Time-Domain Spectroscopy," *J Infrared Milli Terahz Waves*, vol. 37, no. 9, pp. 929–938, Sep. 2016, doi: 10.1007/s10762-016-0283-8.

[364] M. Araki, Y. Tabata, N. Shimizu, and K. Matsuyama, "Terahertz spectroscopy of CO and NO: The first step toward temperature and concentration detection for combustion gases in fire environments," *Journal of Molecular Spectroscopy*, vol. 361, pp. 34–39, Jul. 2019, doi: 10.1016/j.jms.2019.05.007.

[365] K. Kikuchi, S. Kohjiro, T. Yamada, N. Shimizu, and A. Wakatsuki, "Compact terahertz passive spectrometer with wideband superconductor-insulator-superconductor mixer," *Review of Scientific Instruments*, vol. 83, no. 2, p. 023110, Feb. 2012, doi: 10.1063/1.3687430.

[366] A. M. Fosnight, B. L. Moran, and I. R. Medvedev, "Chemical analysis of exhaled human breath using a terahertz spectroscopic approach," *Appl. Phys. Lett.*, vol. 103, no. 13, p. 133703, Sep. 2013, doi: 10.1063/1.4823544.

[367] J. Pereira *et al.*, "Breath Analysis as a Potential and Non-Invasive Frontier in Disease Diagnosis: An Overview," *Metabolites*, vol. 5, no. 1, Art. no. 1, Mar. 2015, doi: 10.3390/metabo5010003.

[368] O. Lawal, W. M. Ahmed, T. M. E. Nijsen, R. Goodacre, and S. J. Fowler, "Exhaled breath analysis: a review of 'breath-taking' methods for off-line analysis," *Metabolomics*, vol. 13, no. 10, p. 110, Aug. 2017, doi: 10.1007/s11306-017-1241-8.

[369] K. Schwarz *et al.*, "Breath acetone-aspects of normal physiology related to age and gender as determined in a PTR-MS study," *J. Breath Res.*, vol. 3, no. 2, p. 027003, Jun. 2009, doi: 10.1088/1752-7155/3/2/027003.

[370] C. Wang and P. Sahay, "Breath Analysis Using Laser Spectroscopic Techniques: Breath Biomarkers, Spectral Fingerprints, and Detection Limits," *Sensors*, vol. 9, no. 10, Art. no. 10, Oct. 2009, doi: 10.3390/s91008230.

[371] C. Turner, P. Španěl, and D. Smith, "A longitudinal study of methanol in the exhaled breath of 30 healthy volunteers using selected ion flow tube mass spectrometry, SIFT-MS," *Physiol. Meas.*, vol. 27, no. 7, pp. 637–648, Jul. 2006, doi: 10.1088/0967-3334/27/7/007.

[372] H. Haick, Y. Y. Broza, P. Mochalski, V. Ruzsanyi, and A. Amann, "Assessment, origin, and implementation of breath volatile cancer markers," *Chem. Soc. Rev.*, vol. 43, no. 5, pp. 1423–1449, 2014, doi: 10.1039/C3CS60329F.

[373] V. Vaks, E. Domracheva, E. Sobakinskaya, and M. Chernyaeva, "High-precision terahertz spectroscopy for noninvasive medicine diagnostics," *Photonics & Lasers in Medicine*, vol. 3, no. 4, pp. 373–380, Nov. 2014, doi: 10.1515/plm-2014-0026.

[374] F. C. De Lucia, "The submillimeter: A spectroscopist's view," *Journal of Molecular Spectroscopy*, vol. 261, no. 1, pp. 1–17, May 2010, doi: 10.1016/j.jms.2010.01.002.

[375] L. Chen and S. Oishi, "Terahertz Time-Domain Spectroscopy of Organic Gases," *rle*, vol. 34, no. 3, pp. 251–254, 2006, doi: 10.2184/lsj.34.251.

[376] N. Rothbart, O. Holz, R. Koczulla, K. Schmalz, and H.-W. Hübers, "Analysis of Human Breath by Millimeter-Wave/Terahertz Spectroscopy," *Sensors*, vol. 19, no. 12, Art. no. 12, Jan. 2019, doi: 10.3390/s19122719.

[377] K. Schmalz, N. Rothbart, P. F.-X. Neumaier, J. Borngräber, H.-W. Hübers, and D. Kissinger, "Gas Spectroscopy System for Breath Analysis at mm-wave/THz Using SiGe BiCMOS Circuits," *IEEE Transactions on Microwave Theory and Techniques*, vol. 65, no. 5, pp. 1807–1818, May 2017, doi: 10.1109/TMTT.2017.2650915.

[378] L. N. Ge, H. L. Zhan, W. X. Leng, K. Zhao, and L. Z. Xiao, "Optical Characterization of the Principal Hydrocarbon Components in Natural Gas Using Terahertz Spectroscopy," *Energy Fuels*, vol. 29, no. 3, pp. 1622–1627, Mar. 2015, doi: 10.1021/ef5028235.

[379] W. Leng *et al.*, "Rapidly determinating the principal components of natural gas distilled from shale with terahertz spectroscopy," *Fuel*, vol. 159, pp. 84–88, Nov. 2015, doi: 10.1016/j.fuel.2015.06.072.

[380] S. Fan, K. Jeong, V. P. Wallace, and Z. Aman, "Use of Terahertz Waves To Monitor Moisture Content in High-Pressure Natural Gas Pipelines," *Energy Fuels*, vol. 33, no. 9, pp. 8026–8031, Sep. 2019, doi: 10.1021/acs.energyfuels.9b01112.

[381] G. Ren, Z. Zhu, J. Zhang, H. Zhao, Y. Li, and J. Han, "Broadband terahertz spectroscopy of paper and banknotes," *Optics Communications*, vol. 475, p. 126267, Nov. 2020, doi: 10.1016/j.optcom.2020.126267.

[382] S. Brinkmann, N. Vieweg, G. Gärtner, P. Plew, and A. Deninger, "Towards Quality Control in Pharmaceutical Packaging: Screening Folded Boxes for Package Inserts," *J Infrared Milli Terahz Waves*, vol. 38, no. 3, pp. 339–346, Mar. 2017, doi: 10.1007/s10762-016-0345-y.

[383] D. Banerjee, W. von Spiegel, M. D. Thomson, S. Schabel, and H. G. Roskos, "Diagnosing water content in paper by terahertz radiation," *Opt. Express, OE*, vol. 16, no. 12, pp. 9060–9066, Jun. 2008, doi: 10.1364/OE.16.009060.

[384] P. Mousavi, F. Haran, D. Jez, F. Santosa, and J. S. Dodge, "Simultaneous composition and thickness measurement of paper using terahertz time-domain spectroscopy," *Appl. Opt., AO*, vol. 48, no. 33, pp. 6541–6546, Nov. 2009, doi: 10.1364/AO.48.006541.

[385] J. L. M. van Mechelen, A. B. Kuzmenko, and H. Merbold, "Stratified dispersive model for material characterization using terahertz time-domain spectroscopy," *Opt. Lett., OL*, vol. 39, no. 13, pp. 3853–3856, Jul. 2014, doi: 10.1364/OL.39.003853.

[386] M. Fan, B. Cao, and G. Tian, "Enhanced Measurement of Paper Basis Weight Using Phase Shift in Terahertz Time-Domain Spectroscopy," *Journal of Sensors*, vol. 2017, p. e3520967, May 2017, doi: 10.1155/2017/3520967.

[387] G. Yan, A. Markov, Y. Chinifooroshan, S. M. Tripathi, W. J. Bock, and M. Skorobogatiy, "Resonant THz sensor for paper quality monitoring using THz fiber Bragg gratings," *Opt. Lett., OL*, vol. 38, no. 13, pp. 2200–2202, Jul. 2013, doi: 10.1364/OL.38.002200.

[388] P. Huber, P. Martinez, C. Guers, F. Garet, and P. Borel, "Dielectric Losses of Paper in the THz Domain: Literature Review, Needs for Future Research, and Prospective Solutions," *physica status solidi (a)*, vol. 214, no. 12, p. 1700356, 2017, doi: 10.1002/pssa.201700356.

[389] V. Vassilev, B. Stoew, J. Blomgren, and G. Andersson, "A mm-Wave Sensor for Remote Measurement of Moisture in Thin Paper Layers," *IEEE Transactions on Terahertz Science and Technology*, vol. 5, no. 5, pp. 770–778, Sep. 2015, doi: 10.1109/TTHZ.2015.2462716.

[390] L. Wang, C. Tang, S. Zhu, and S. Zhou, "Terahertz Time Domain Spectroscopy of Transformer Insulation Paper after Thermal Aging Intervals," *Materials*, vol. 11, no. 11, Art. no. 11, Nov. 2018, doi: 10.3390/ma11112124.

[391] M. Peccianti *et al.*, "Terahertz Absorption by Cellulose: Application to Ancient Paper Artifacts," *Phys. Rev. Applied*, vol. 7, no. 6, p. 064019, Jun. 2017, doi: 10.1103/PhysRevApplied.7.064019.

[392] E. Abraham, A. Younus, A. El Fatimy, J. C. Delagnes, E. Nguéma, and P. Mounaix, "Broadband terahertz imaging of documents written with lead pencils," *Optics Communications*, vol. 282, no. 15, pp. 3104–3107, Aug. 2009, doi: 10.1016/j.optcom.2009.04.039.

[393] Y. Ma *et al.*, "Banknotes anti-counterfeiting system based on THz-TDS confocal imaging," in *AOPC 2021: Infrared Device and Infrared Technology*, SPIE, Nov. 2021, pp. 335–343. doi: 10.1117/12.2606730.

[394] Y. Cui, W. Fu, X. Guan, M. Hu, Y. Yan, and S. Liu, "Experiment Studies on Two-Dimension Terahertz Raster Scan Imaging," *J Infrared Milli Terahz Waves*, vol. 33, no. 5, pp. 513–521, May 2012, doi: 10.1007/s10762-012-9885-y.

[395] Z. Y. Tan, T. Zhou, J. C. Cao, and H. C. Liu, "Terahertz Imaging With Quantum-Cascade Laser and Quantum-Well Photodetector," *IEEE Photonics Technology Letters*, vol. 25, no. 14, pp. 1344–1346, Jul. 2013, doi: 10.1109/LPT.2013.2265303.

[396] T. Inagaki, B. Ahmed, I. D. Hartley, S. Tsuchikawa, and M. Reid, "Simultaneous prediction of density and moisture content of wood by terahertz time domain spectroscopy," *J Infrared Milli Terahz Waves*, vol. 35, no. 11, pp. 949–961, Nov. 2014, doi: 10.1007/s10762-014-0095-7.

[397] T. Inagaki, I. D. Hartley, S. Tsuchikawa, and M. Reid, "Prediction of oven-dry density of wood by time-domain terahertz spectroscopy," *Holzforschung*, vol. 68, no. 1, pp. 61–68, Jan. 2014, doi: 10.1515/hf-2013-0013.

[398] J. B. Jackson *et al.*, "Terahertz pulse imaging for tree-ring analysis: a preliminary study for dendrochronology applications," *Meas. Sci. Technol.*, vol. 20, no. 7, p. 075502, Jun. 2009, doi: 10.1088/0957-0233/20/7/075502.

[399] K. Krügener, S. Sommer, E. Stübling, R. Jachim, M. Koch, and W. Viöl, "THz Properties of Typical Woods Important for European Forestry," *J Infrared Milli Terahz Waves*, vol. 40, no. 7, pp. 770–774, Jul. 2019, doi: 10.1007/s10762-019-00601-4.

[400] K. Krügener, E.-M. Stübling, R. Jachim, B. Kietz, M. Koch, and W. Viöl, "THz tomography for detecting damages on wood caused by insects," *Appl. Opt.*, vol. 58, no. 22, p. 6063, Aug. 2019, doi: 10.1364/AO.58.006063.

[401] C. Daher, C. Paris, A.-S. Le Hô, L. Bellot-Gurlet, and J.-P. Échard, "A joint use of Raman and infrared spectroscopies for the identification of natural organic media used in ancient varnishes," *J. Raman Spectrosc.*, vol. 41, no. 11, pp. 1494–1499, Nov. 2010, doi: 10.1002/jrs.2693.

[402] B. Borg, M. Dunn, A. Ang, and C. Villis, "The application of state-of-the-art technologies to support artwork conservation: Literature review," *Journal of Cultural Heritage*, vol. 44, pp. 239–259, Jul. 2020, doi: 10.1016/j.culher.2020.02.010.

[403] J.-P. Guillet *et al.*, "Art Painting Diagnostic Before Restoration with Terahertz and Millimeter Waves," *J Infrared Milli Terahz Waves*, vol. 38, no. 4, pp. 369–379, Apr. 2017, doi: 10.1007/s10762-017-0358-1.

[404] K. Fukunaga and M. Picollo, "Terahertz spectroscopy applied to the analysis of artists' materials," *Appl. Phys. A*, vol. 100, no. 3, pp. 591–597, Sep. 2010, doi: 10.1007/s00339-010-5643-y.

[405] D. Giovannacci *et al.*, "Time-domain imaging system in the terahertz range for immovable cultural heritage materials," *Strain*, vol. 55, no. 2, p. e12292, 2019, doi: 10.1111/str.12292.

[406] M. Inuzuka, Y. Kouzuma, N. Sugioka, K. Fukunaga, and T. Tateishi, "Investigation of Layer Structure of the Takamatsuzuka Mural Paintings by Terahertz Imaging Technique," *J Infrared Milli Terahz Waves*, vol. 38, no. 4, pp. 380–389, Apr. 2017, doi: 10.1007/s10762-017-0365-2.

[407] R. M. Groves, B. Pradarutti, E. Kouloumpi, W. Osten, and G. Notni, "2D and 3D non-destructive evaluation of a wooden panel painting using shearography and terahertz imaging," *NDT & E International*, vol. 42, no. 6, pp. 543–549, Sep. 2009, doi: 10.1016/j.ndteint.2009.04.002.

[408] M. Picollo, K. Fukunaga, and J. Labaune, "Obtaining noninvasive stratigraphic details of panel paintings using terahertz time domain spectroscopy imaging system," *Journal of Cultural Heritage*, vol. 16, no. 1, pp. 73–80, Jan. 2015, doi: 10.1016/j.culher.2014.01.006.

[409] J. B. Jackson *et al.*, "Terahertz imaging for non-destructive evaluation of mural paintings," *Optics Communications*, vol. 281, no. 4, pp. 527–532, Feb. 2008, doi: 10.1016/j.optcom.2007.10.049.

[410] C. Seco-Martorell, V. López-Domínguez, G. Arauz-Garofalo, A. Redo-Sanchez, J. Palacios, and J. Tejada, "Goya's artwork imaging with Terahertz waves," *Opt. Express, OE*, vol. 21, no. 15, pp. 17800–17805, Jul. 2013, doi: 10.1364/OE.21.017800.

[411] A. M. Gomez-Sepulveda *et al.*, "History of Mexican Easel Paintings from an Altarpiece Revealed by Non-invasive Terahertz Time-Domain Imaging," *J Infrared Milli Terahz Waves*, vol. 38, no. 4, pp. 403–412, Apr. 2017, doi: 10.1007/s10762-016-0346-x.

[412] C. L. Koch-Dandolo, T. Filtenborg, K. Fukunaga, J. Skou-Hansen, and P. U. Jepsen, "Reflection terahertz time-domain imaging for analysis of an 18th century neoclassical easel painting," *Appl. Opt., AO*, vol. 54, no. 16, pp. 5123–5129, Jun. 2015, doi: 10.1364/AO.54.005123.

[413] J. Dong, A. Locquet, M. Melis, and D. S. Citrin, "Global mapping of stratigraphy of an old-master painting using sparsity-based terahertz reflectometry," *Sci Rep*, vol. 7, no. 1, Art. no. 1, Nov. 2017, doi: 10.1038/s41598-017-15069-2.

[414] A. J. L. Adam, P. C. M. Planken, S. Meloni, and J. Dik, "TeraHertz imaging of hidden paint layers on canvas," *Opt. Express, OE*, vol. 17, no. 5, pp. 3407–3416, Mar. 2009, doi: 10.1364/OE.17.003407.

[415] A. Redo-Sanchez *et al.*, "Terahertz time-gated spectral imaging for content extraction through layered structures," *Nat Commun*, vol. 7, no. 1, p. 12665, Nov. 2016, doi: 10.1038/ncomms12665.

[416] A. S. Skryl, J. B. Jackson, M. I. Bakunov, M. Menu, and G. A. Mourou, "Terahertz time-domain imaging of hidden defects in wooden artworks: application to a Russian icon painting," *Appl. Opt., AO*, vol. 53, no. 6, pp. 1033–1038, Feb. 2014, doi: 10.1364/AO.53.001033.

[417] J. Dong, X. Wu, A. Locquet, and D. S. Citrin, "Terahertz Superresolution Stratigraphic Characterization of Multilayered Structures Using Sparse Deconvolution," *IEEE Transactions on Terahertz Science and Technology*, vol. 7, no. 3, pp. 260–267, May 2017, doi: 10.1109/TTHZ.2017.2673542.

[418] M. Yin, S. Tang, and M. Tong, "The application of terahertz spectroscopy to liquid petrochemicals detection: A review," *Applied Spectroscopy Reviews*, vol. 51, no. 5, pp. 379–396, May 2016, doi: 10.1080/05704928.2016.1141291.

[419] H. Zhan, S. Wu, R. Bao, L. Ge, and K. Zhao, "Qualitative identification of crude oils from different oil fields using terahertz time-domain spectroscopy," *Fuel*, vol. 143, pp. 189–193, Mar. 2015, doi: 10.1016/j.fuel.2014.11.047.

[420] H. Zhan, Y. Yang, Y. Zhang, X. Miao, K. Zhao, and W. Yue, "Terahertz for the detection of the oil bearing characteristics of shale," *Energy Reports*, vol. 7, pp. 5162–5167, Nov. 2021, doi: 10.1016/j.egyr.2021.08.109.

[421] X. Miao, M. Chen, Y. Li, H. Zhan, K. Zhao, and W. Yue, "Simultaneous Determination of Organic Distribution and Content in Oil Shale by Terahertz Imaging," *Energy Fuels*, vol. 34, no. 2, pp. 1664–1668, Feb. 2020, doi: 10.1021/acs.energyfuels.9b04038.

[422] M. M. Matoug and R. Gordon, "Crude Oil Asphaltenes Studied by Terahertz Spectroscopy," *ACS Omega*, vol. 3, no. 3, pp. 3406–3412, Mar. 2018, doi: 10.1021/acsomega.8b00017.

[423] C. Jiang, K. Zhao, C. Fu, and L. Xiao, "Characterization of Morphology and Structure of Wax Crystals in Waxy Crude Oils by Terahertz Time-Domain Spectroscopy," *Energy Fuels*, vol. 31, no. 2, pp. 1416–1421, Feb. 2017, doi: 10.1021/acs.energyfuels.6b02900.

[424] R. E. Correa Pabón and C. R. de Souza Filho, "Crude oil spectral signatures and empirical models to derive API gravity," *Fuel*, vol. 237, pp. 1119–1131, Feb. 2019, doi: 10.1016/j.fuel.2018.09.098.

[425] Z. X. Li, J. Zhou, X. S. Guo, B. B. Ji, W. Zhou, and D. H. Li, "Terahertz Spectral Properties of Coal Tar," *J Appl Spectrosc*, vol. 85, no. 5, pp. 840–844, Nov. 2018, doi: 10.1007/s10812-018-0726-1.

[426] W.-J. Jin, K. Zhao, C. Yang, C.-H. Xu, H. Ni, and S.-H. Chen, "Experimental measurements of water content in crude oil emulsions by terahertz time-domain spectroscopy," *Appl. Geophys.*, vol. 10, no. 4, pp. 506–509, Dec. 2013, doi: 10.1007/s11770-013-0404-2.

[427] L. Guan, H. Zhan, X. Miao, J. Zhu, and K. Zhao, "Terahertz-dependent evaluation of water content in high-water-cut crude oil using additive-manufactured samplers," *Sci. China Phys. Mech. Astron.*, vol. 60, no. 4, p. 044211, Feb. 2017, doi: 10.1007/s11433-016-0491-3.

[428] I. M. Saied, M. Meribout, E. Kato, and X. H. Zhao, "Terahertz Spectroscopy for Measuring Multiphase Fractions," *IEEE Transactions on Terahertz Science and Technology*, vol. 7, no. 3, pp. 250–259, May 2017, doi: 10.1109/TTHZ.2017.2679602.

[429] Y. Song *et al.*, "Simultaneous Characterization of Water Content and Distribution in High-Water-Cut Crude Oil," *Energy Fuels*, vol. 30, no. 5, pp. 3929–3933, May 2016, doi: 10.1021/acs.energyfuels.6b00340.

[430] J. P. Laib and D. M. Mittleman, "Temperature-Dependent Terahertz Spectroscopy of Liquid n-alkanes," *J Infrared Milli Terahz Waves*, vol. 31, no. 9, pp. 1015–1021, Sep. 2010, doi: 10.1007/s10762-010-9678-0.

[431] H. Ni and L. Tian, "The vibrational dynamics of n-alkanes in the terahertz region," *Sci. Sin.-Phys. Mech. Astron.*, vol. 45, no. 8, pp. 084205–084205, Jul. 2015, doi: 10.1360/SSPMA2015-00138.

[432] J. P. Laib, D. V. Nickel, and D. M. Mittleman, "Terahertz vibrational modes induced by heterogeneous nucleation in n-alkanes," *Chemical Physics Letters*, vol. 493, no. 4, pp. 279–282, Jun. 2010, doi: 10.1016/j.cplett.2010.05.075.

[433] E. Arik, H. Altan, and O. Esenturk, "Dielectric Properties of Diesel and Gasoline by Terahertz Spectroscopy," *J Infrared Milli Terahz Waves*, vol. 35, no. 9, pp. 759–769, Sep. 2014, doi: 10.1007/s10762-014-0081-0.

[434] J. Li, Z. Tian, Y. Chen, W. Cao, and Z. Zeng, "Distinguishing octane grades in gasoline using terahertz metamaterials," *Appl. Opt., AO*, vol. 51, no. 16, pp. 3258–3262, Jun. 2012, doi: 10.1364/AO.51.003258.

[435] F. M. Al-Douseri, Y. Chen, and X.-C. Zhang, "THz wave sensing for petroleum industrial applications," *Int J Infrared Milli Waves*, vol. 27, no. 4, pp. 481–503, Apr. 2006, doi: 10.1007/s10762-006-9102-y.

[436] H. Zhao *et al.*, "Spectrum features of commercial derv fuel oils in the terahertz region," *Sci. China Phys. Mech. Astron.*, vol. 55, no. 2, pp. 195–198, Feb. 2012, doi: 10.1007/s11433-011-4597-1.

[437] H. Zhao, K. Zhao, and R. Bao, "Fuel Property Determination of Biodiesel-Diesel Blends By Terahertz Spectrum," *J Infrared Milli Terahz Waves*, vol. 33, no. 5, pp. 522–528, May 2012, doi: 10.1007/s10762-012-9886-x.

[438] Y. Li, J. Li, Z. Zeng, J. Li, Z. Tian, and W. Wang, "Terahertz spectroscopy for quantifying refined oil mixtures," *Appl. Opt., AO*,

vol. 51, no. 24, pp. 5885–5889, Aug. 2012, doi: 10.1364/AO.51.005885.

[439] E. Arik, H. Altan, and O. Esenturk, "Dielectric Properties of Ethanol and Gasoline Mixtures by Terahertz Spectroscopy and an Effective Method for Determination of Ethanol Content of Gasoline," *J. Phys. Chem. A*, vol. 118, no. 17, pp. 3081–3089, May 2014, doi: 10.1021/jp500760t.

[440] H. Zhan, K. Zhao, H. Zhao, Q. Li, S. Zhu, and L. Xiao, "The spectral analysis of fuel oils using terahertz radiation and chemometric methods," *J. Phys. D: Appl. Phys.*, vol. 49, no. 39, p. 395101, Oct. 2016, doi: 10.1088/0022-3727/49/39/395101.

[441] F. Qin, Q. Li, H. Zhan, W. Jin, H. Liu, and K. Zhao, "Probing the sulfur content in gasoline quantitatively with terahertz time-domain spectroscopy," *Sci. China Phys. Mech. Astron.*, vol. 57, no. 7, pp. 1404–1406, Jul. 2014, doi: 10.1007/s11433-014-5409-1.

[442] A. M. Adbul-Munaim, M. Reuter, M. Koch, and D. G. Watson, "Distinguishing Gasoline Engine Oils of Different Viscosities Using Terahertz Time-Domain Spectroscopy," *J Infrared Milli Terahz Waves*, vol. 36, no. 7, pp. 687–696, Jul. 2015, doi: 10.1007/s10762-015-0164-6.

[443] L. Tian *et al.*, "Optical property and spectroscopy studies on the selected lubricating oil in the terahertz range," *Sci. China Ser. G-Phys. Mech. Astron.*, vol. 52, no. 12, pp. 1938–1943, Dec. 2009, doi: 10.1007/s11433-009-0310-z.

[444] M. Naftaly, A. P. Foulds, R. E. Miles, and A. G. Davies, "Terahertz Transmission Spectroscopy of Nonpolar Materials and Relationship with Composition and Properties," *Int J Infrared Milli Waves*, vol. 26, no. 1, pp. 55–64, Jan. 2005, doi: 10.1007/s10762-004-2033-6.

[445] S. Zhu *et al.*, "Terahertz spectroscopy properties of the selected engine oils," in *Infrared, Millimeter Wave, and Terahertz Technologies*, SPIE, Nov. 2010, pp. 64–69. doi: 10.1117/12.868883.

[446] A. M. Abdul-Munaim, M. Méndez Aller, S. Preu, and D. G. Watson, "Discriminating gasoline fuel contamination in engine oil by terahertz time-domain spectroscopy," *Tribology International*, vol. 119, pp. 123–130, Mar. 2018, doi: 10.1016/j.triboint.2017.10.026.

[447] S. Gorenflo, U. Tauer, I. Hinkov, A. Lambrecht, R. Buchner, and H. Helm, "Dielectric properties of oil–water complexes using terahertz transmission spectroscopy," *Chemical Physics Letters*, vol. 421, no. 4, pp. 494–498, Apr. 2006, doi: 10.1016/j.cplett.2006.01.108.

[448] A. M. Abdul-Munaim, M. Reuter, O. M. Abdulmunem, J. C. Balzer, M. Koch, and D. G. Watson, "Using terahertz time-domain spectroscopy to discriminate among water contamination levels in diesel engine oil," *Transactions of the ASABE*, vol. 59, no. 3, pp. 795–801, 2016, doi: doi: 10.13031/trans.59.11448.

[449] N. Nishimura, R. Ogura, S. Matsumoto, M. Mizuno, and K. Fukunaga, "Study of molecular behavior in oxidation of insulating oil using terahertz spectroscopy," *Electrical Engineering in Japan*, vol. 183, no. 1, pp. 9–15, 2013, doi: 10.1002/eej.22335.

[450] K. S, Y. M, A. Rawson, and S. C. K, "Recent Advances in Terahertz Time-Domain Spectroscopy and Imaging Techniques for Automation in Agriculture and Food Sector," *Food Anal. Methods*, vol. 15, no. 2, pp. 498–526, Feb. 2022, doi: 10.1007/s12161-021-02132-y.

[451] D. M. Mittleman, R. H. Jacobsen, and M. C. Nuss, "T-ray imaging," *IEEE J. Select. Topics Quantum Electron.*, vol. 2, no. 3, pp. 679–692, Sep. 1996, doi: 10.1109/2944.571768.

[452] B. Li, X. Zhao, Y. Zhang, S. Zhang, and B. Luo, "Prediction and monitoring of leaf water content in soybean plants using terahertz time-domain spectroscopy," *Computers and Electronics in Agriculture*, vol. 170, p. 105239, Mar. 2020, doi: 10.1016/j.compag.2020.105239.

[453] V. Dworak, B. Mahns, J. Selbeck, R. Gebbers, and C. Weltzien, "Terahertz Spectroscopy for Proximal Soil Sensing: An Approach to Particle Size Analysis," *Sensors*, vol. 17, no. 10, Art. no. 10, Oct. 2017, doi: 10.3390/s17102387.

[454] G.-J. Lee, S. Kim, and T.-H. Kwon, "Effect of Moisture Content and Particle Size on Extinction Coefficients of Soils Using Terahertz Time-Domain Spectroscopy," *IEEE Transactions on Terahertz Science and Technology*, vol. 7, no. 5, pp. 529–535, Sep. 2017, doi: 10.1109/TTHZ.2017.2731369.

[455] R. A. Lewis, "Invited Review Terahertz Transmission, Scattering, Reflection, and Absorption—the Interaction of THz Radiation with Soils," *J Infrared Milli Terahz Waves*, vol. 38, no. 7, pp. 799–807, Jul. 2017, doi: 10.1007/s10762-017-0384-z.

[456] V. Dworak, S. Augustin, and R. Gebbers, "Application of Terahertz Radiation to Soil Measurements: Initial Results," *Sensors*, vol. 11, no. 10, Art. no. 10, Oct. 2011, doi: 10.3390/s111009973.

[457] F. Qu *et al.*, "Terahertz Multivariate Spectral Analysis and Molecular Dynamics Simulations of Three Pyrethroid Pesticides," *J Infrared Milli Terahz Waves*, vol. 39, no. 11, pp. 1148–1161, Nov. 2018, doi: 10.1007/s10762-018-0519-x.

[458] F. Qu *et al.*, "Spectral Characterization and Molecular Dynamics Simulation of Pesticides Based on Terahertz Time-Domain Spectra Analyses and Density Functional Theory (DFT) Calculations," *Molecules*, vol. 23, no. 7, Art. no. 7, Jul. 2018, doi: 10.3390/molecules23071607.

[459] B. Qin, Z. Li, Z. Luo, Y. Li, and H. Zhang, "Terahertz time-domain spectroscopy combined with PCA-CFSFDP applied for pesticide detection," *Opt Quant Electron*, vol. 49, no. 7, p. 244, Jun. 2017, doi: 10.1007/s11082-017-1080-x.

[460] H. Ge, Y. Jiang, and Y. Zhang, "THz Spectroscopic Investigation of Wheat-Quality by Using Multi-Source Data Fusion," *Sensors*, vol. 18, no. 11, Art. no. 11, Nov. 2018, doi: 10.3390/s18113945.

[461] L. Hui, W. Jingzhu, L. Cuiling, S. Xiaorong, and Y. le, "Study on Pretreatment Methods of Terahertz Time Domain Spectral Image for Maize Seeds," *IFAC-PapersOnLine*, vol. 51, no. 17, pp. 206–210, Jan. 2018, doi: 10.1016/j.ifacol.2018.08.142.

[462] R. Gente *et al.*, "Quality Control of Sugar Beet Seeds With THz Time-Domain Spectroscopy," *IEEE Transactions on Terahertz Science and Technology*, vol. 6, no. 5, pp. 754–756, Sep. 2016, doi: 10.1109/TTHZ.2016.2593985.

[463] H. Luo, J. Zhu, W. Xu, and M. Cui, "Identification of soybean varieties by terahertz spectroscopy and integrated learning method," *Optik*, vol. 184, pp. 177–184, May 2019, doi: 10.1016/j.ijleo.2019.02.148.

[464] W. Liu *et al.*, "Discrimination of geographical origin of extra virgin olive oils using terahertz spectroscopy combined with chemometrics," *Food Chemistry*, vol. 251, pp. 86–92, Jun. 2018, doi: 10.1016/j.foodchem.2018.01.081.

[465] X. Wei, W. Zheng, S. Zhu, S. Zhou, W. Wu, and Z. Xie, "Application of terahertz spectrum and interval partial least squares method in the identification of genetically modified soybeans," *Spectrochimica Acta Part A: Molecular and Biomolecular Spectroscopy*, vol. 238, p. 118453, Sep. 2020, doi: 10.1016/j.saa.2020.118453.

[466] R. Zhao, B. Zou, G. Zhang, D. Xu, and Y. Yang, "High-sensitivity identification of aflatoxin B1 and B2 using terahertz time-domain spectroscopy and metamaterial-based terahertz biosensor," *J. Phys. D: Appl. Phys.*, vol. 53, no. 19, p. 195401, Mar. 2020, doi: 10.1088/1361-6463/ab6f90.

[467] W. Liu, P. Zhao, C. Wu, C. Liu, J. Yang, and L. Zheng, "Rapid determination of aflatoxin B1 concentration in soybean oil using terahertz spectroscopy with chemometric methods," *Food Chemistry*, vol. 293, pp. 213–219, Sep. 2019, doi: 10.1016/j.foodchem.2019.04.081.

[468] X. Yang, K. Yang, Y. Luo, and W. Fu, "Terahertz spectroscopy for bacterial detection: opportunities and challenges," *Appl Microbiol Biotechnol*, vol. 100, no. 12, pp. 5289–5299, Jun. 2016, doi: 10.1007/s00253-016-7569-6.

[469] X. Yang *et al.*, "Rapid and label-free detection and assessment of bacteria by terahertz time-domain spectroscopy," *Journal of Biophotonics*, vol. 9, no. 10, pp. 1050–1058, 2016, doi: 10.1002/jbio.201500270.

[470] X. Sun *et al.*, "Terahertz Spectroscopy Determination of Benzoic Acid Additive in Wheat Flour by Machine Learning," *J Infrared Milli Terahz Waves*, vol. 40, no. 4, pp. 466–475, Apr. 2019, doi: 10.1007/s10762-019-00579-z.

[471] C. Li, B. Li, and D. Ye, "Analysis and Identification of Rice Adulteration Using Terahertz Spectroscopy and Pattern Recognition Algorithms," *IEEE Access*, vol. 8, pp. 26839–26850, 2020, doi: 10.1109/ACCESS.2020.2970868.

[472] J. Liu and L. Fan, "Qualitative and quantitative determination of potassium aluminum sulfate dodecahydrate in potato starch based on terahertz spectroscopy," *Microwave and Optical Technology Letters*, vol. 62, no. 2, pp. 525–530, 2020, doi: 10.1002/mop.32061.

[473] G. Ok, K. Park, M.-C. Lim, H.-J. Jang, and S.-W. Choi, "140-GHz subwavelength transmission imaging for foreign body inspection in food products," *Journal of Food Engineering*, vol. 221, pp. 124–131, Mar. 2018, doi: 10.1016/j.jfoodeng.2017.10.011.

[474] X. Chen *et al.*, "Terahertz (THz) biophotonics technology: Instrumentation, techniques, and biomedical applications," *Chem. Phys. Rev.*, vol. 3, no. 1, p. 011311, Mar. 2022, doi: 10.1063/5.0068979.

[475] Y. Peng, C. Shi, Y. Zhu, M. Gu, and S. Zhuang, "Terahertz spectroscopy in biomedical field: a review on signal-to-noise ratio improvement," *PhotoniX*, vol. 1, no. 1, p. 12, Apr. 2020, doi: 10.1186/s43074-020-00011-z.

[476] Q. Sun, Y. He, K. Liu, S. Fan, E. P. J. Parrott, and E. Pickwell-MacPherson, "Recent advances in terahertz technology for biomedical applications," *Quant Imaging Med Surg*, vol. 7, no. 3, pp. 345–355, Jun. 2017, doi: 10.21037/qims.2017.06.02.

[477] H. Yada, M. Nagai, and K. Tanaka, "Origin of the fast relaxation component of water and heavy water revealed by terahertz time-domain attenuated total reflection spectroscopy," *Chemical Physics Letters*, vol. 464, no. 4, pp. 166–170, Oct. 2008, doi: 10.1016/j.cplett.2008.09.015.

[478] X. Yang *et al.*, "Biomedical Applications of Terahertz Spectroscopy and Imaging," *Trends in Biotechnology*, vol. 34, no. 10, pp. 810–824, Oct. 2016, doi: 10.1016/j.tibtech.2016.04.008.

[479] A. Gong, Y. Qiu, X. Chen, Z. Zhao, L. Xia, and Y. Shao, "Biomedical applications of terahertz technology," *Applied Spectroscopy Reviews*, vol. 55, no. 5, pp. 418–438, May 2020, doi: 10.1080/05704928.2019.1670202.

[480] B. Fischer, M. Walther, and P. U. Jepsen, "Far-infrared vibrational modes of DNA components studied by terahertz time-domain spectroscopy," *Physics in Medicine & Biology*, vol. 47, no. 21, p. 3807, 2002, doi: 10.1088/0031-9155/47/21/319.

[481] W. Zhang, E. R. Brown, M. Rahman, and M. L. Norton, "Observation of terahertz absorption signatures in microliter DNA solutions," *Appl. Phys. Lett.*, vol. 102, no. 2, p. 023701, Jan. 2013, doi: 10.1063/1.4775696.

[482] A. Wittlin, L. Genzel, F. Kremer, S. Häseler, A. Poglitsch, and A. Rupprecht, "Far-infrared spectroscopy on oriented films of dry and hydrated DNA," *Phys. Rev. A*, vol. 34, no. 1, pp. 493–500, Jul. 1986, doi: 10.1103/PhysRevA.34.493.

[483] M. V. Tsurkan, N. S. Balbekin, E. A. Sobakinskaya, A. N. Panin, and V. L. Vaks, "Terahertz spectroscopy of DNA," *Opt. Spectrosc.*, vol. 114, no. 6, pp. 894–898, Jun. 2013, doi: 10.1134/S0030400X13060222.

[484] M. Tang *et al.*, "Terahertz spectroscopy of oligonucleotides in aqueous solutions," *JBO*, vol. 20, no. 9, p. 095009, Sep. 2015, doi: 10.1117/1.JBO.20.9.095009.

[485] H. Cheon, H. Yang, S.-H. Lee, Y. A. Kim, and J.-H. Son, "Terahertz molecular resonance of cancer DNA," *Sci Rep*, vol. 6, no. 1, Art. no. 1, Nov. 2016, doi: 10.1038/srep37103.

[486] H. Cheon, J. H. Paik, M. Choi, H.-J. Yang, and J.-H. Son, "Detection and manipulation of methylation in blood cancer DNA using terahertz radiation," *Sci Rep*, vol. 9, no. 1, Art. no. 1, Apr. 2019, doi: 10.1038/s41598-019-42855-x.

[487] Y. Miura, A. Kamataki, M. Uzuki, T. Sasaki, J.-I. Nishizawa, and T. Sawai, "Terahertz-Wave Spectroscopy for Precise Histopathological Imaging of Tumor and Non-tumor Lesions in Paraffin Sections," *Tohoku J. Exp. Med.*, vol. 223, no. 4, pp. 291–296, 2011, doi: 10.1620/tjem.223.291.

[488] Y. C. Sim, J. Y. Park, K.-M. Ahn, C. Park, and J.-H. Son, "Terahertz imaging of excised oral cancer at frozen temperature," *Biomed. Opt. Express, BOE*, vol. 4, no. 8, pp. 1413–1421, Aug. 2013, doi: 10.1364/BOE.4.001413.

[489] A. Rahman, A. K. Rahman, and B. Rao, "Early detection of skin cancer via terahertz spectral profiling and 3D imaging," *Biosensors and Bioelectronics*, vol. 82, pp. 64–70, Aug. 2016, doi: 10.1016/j.bios.2016.03.051.

[490] T. Bowman, Y. Wu, J. Gauch, L. K. Campbell, and M. El-Shenawee, "Terahertz Imaging of Three-Dimensional Dehydrated Breast Cancer Tumors," *J Infrared Milli Terahz Waves*, vol. 38, no. 6, pp. 766–786, Jun. 2017, doi: 10.1007/s10762-017-0377-y.

[491] P. C. Ashworth *et al.*, "Terahertz pulsed spectroscopy of freshly excised human breast cancer," *Opt. Express, OE*, vol. 17, no. 15, pp. 12444–12454, Jul. 2009, doi: 10.1364/OE.17.012444.

[492] W. Liu *et al.*, "Automatic recognition of breast invasive ductal carcinoma based on terahertz spectroscopy with wavelet packet transform and machine learning," *Biomed. Opt. Express, BOE*, vol. 11, no. 2, pp. 971–981, Feb. 2020, doi: 10.1364/BOE.381623.

[493] O. B. Osman *et al.*, "Differentiation of burn wounds in an in vivo porcine model using terahertz spectroscopy," *Biomed. Opt. Express, BOE*, vol. 11, no. 11, pp. 6528–6535, Nov. 2020, doi: 10.1364/BOE.397792.

[494] W. E. Baughman, H. Yokus, S. Balci, D. S. Wilbert, P. Kung, and S. M. Kim, "Observation of Hydrofluoric Acid Burns on Osseous Tissues by Means of Terahertz Spectroscopic Imaging," *IEEE Transactions on Terahertz Science and Technology*, vol. 3, no. 4, pp. 387–394, Jul. 2013, doi: 10.1109/TTHZ.2013.2267416.

[495] D. R. Churchley, R. J. M. Lynch, F. Lippert, J. S. O. Eder, J. Alton, and C. Gonzalez-Cabezas, "Terahertz pulsed imaging study to assess remineralization of artificial caries lesions," *JBO*, vol. 16, no. 2, p. 026001, Feb. 2011, doi: 10.1117/1.3540277.

[496] K. Lee *et al.*, "Measuring water contents in animal organ tissues using terahertz spectroscopic imaging," *Biomed. Opt. Express, BOE*, vol. 9, no. 4, pp. 1582–1589, Apr. 2018, doi: 10.1364/BOE.9.001582.

[497] X. Yang *et al.*, "Label-free bacterial colony detection and viability assessment by continuous-wave terahertz transmission imaging," *Journal of Biophotonics*, vol. 11, no. 8, p. e201700386, 2018, doi: 10.1002/jbio.201700386.

[498] A. A. Lykina *et al.*, "Terahertz high-resolution spectroscopy of thermal decomposition gas products of diabetic and non-diabetic blood plasma and kidney tissue pellets," *JBO*, vol. 26, no. 4, p. 043008, Mar. 2021, doi: 10.1117/1.JBO.26.4.043008.

[499] A. A. Lykina *et al.*, "Terahertz spectroscopy of diabetic and non-diabetic human blood plasma pellets," *JBO*, vol. 26, no. 4, p. 043006, Feb. 2021, doi: 10.1117/1.JBO.26.4.043006.

[500] K. I. Zaytsev *et al.*, "The progress and perspectives of terahertz technology for diagnosis of neoplasms: a review," *J. Opt.*, vol. 22, no. 1, p. 013001, Dec. 2019, doi: 10.1088/2040-8986/ab4dc3.

[501] Y. Peng, C. Shi, X. Wu, Y. Zhu, and S. Zhuang, "Terahertz Imaging and Spectroscopy in Cancer Diagnostics: A Technical Review," *BME Frontiers*, vol. 2020, Sep. 2020, doi: 10.34133/2020/2547609.

[502] A. I. Nikitkina *et al.*, "Terahertz radiation and the skin: a review," *JBO*, vol. 26, no. 4, p. 043005, Feb. 2021, doi: 10.1117/1.JBO.26.4.043005.

[503] J. Dong, P. You, A. Tomasino, A. Yurtsever, and R. Morandotti, "Single-shot ultrafast terahertz photography," *Nat Commun*, vol. 14, no. 1, Art. no. 1, Mar. 2023, doi: 10.1038/s41467-023-37285-3.

[504] L. Gao, J. Liang, C. Li, and L. V. Wang, "Single-shot compressed ultrafast photography at one hundred billion frames per second," *Nature*, vol. 516, no. 7529, Art. no. 7529, Dec. 2014, doi: 10.1038/nature14005.

[505] Z. Li, R. Zgadzaj, X. Wang, Y.-Y. Chang, and M. C. Downer, "Single-shot tomographic movies of evolving light-velocity objects," *Nat Commun*, vol. 5, no. 1, Art. no. 1, Jan. 2014, doi: 10.1038/ncomms4085.

[506] W. Zhang *et al.*, "Recent Developments in Spectroscopic Techniques for the Detection of Explosives," *Materials*, vol. 11, no. 8, Art. no. 8, Aug. 2018, doi: 10.3390/ma11081364.

[507] O. Zandieh and S. Kim, "Sensitive and selective detection of adsorbed explosive molecules using opto-calorimetric infrared spectroscopy and micro-differential thermal analysis," *Sensors and Actuators B: Chemical*, vol. 231, pp. 393–398, Aug. 2016, doi: 10.1016/j.snb.2016.03.046.

[508] W. Lu *et al.*, "Colorimetric sensor arrays based on pattern recognition for the detection of nitroaromatic molecules," *Journal of Hazardous Materials*, vol. 326, pp. 130–137, Mar. 2017, doi: 10.1016/j.jhazmat.2016.12.024.

[509] J. B. Sleiman, B. Bousquet, N. Palka, and P. Mounaix, "Quantitative Analysis of Hexahydro-1,3,5-trinitro-1,3,5, Triazine/Pentaerythritol Tetranitrate (RDX–PETN) Mixtures by Terahertz Time Domain Spectroscopy," *Appl Spectrosc*, vol. 69, no. 12, pp. 1464–1471, Dec. 2015, doi: 10.1366/15-07937.

[510] A. Rahman, "Dendrimer based terahertz time-domain spectroscopy and applications in molecular characterization," *Journal of Molecular Structure*, vol. 1006, no. 1, pp. 59–65, Dec. 2011, doi: 10.1016/j.molstruc.2011.07.004.

[511] N. Palka, "THz reflection spectroscopy of explosives measured by time domain spectroscopy," *Acta Physica Polonica A*, vol. 120, no. 4, pp. 713–715, 2011.

[512] K. Choi *et al.*, "Reflection terahertz time-domain spectroscopy of RDX and HMX explosives," *Journal of Applied Physics*, vol. 115, no. 2, p. 023105, Jan. 2014, doi: 10.1063/1.4861616.

[513] J. Choi, S. Y. Ryu, W. S. Kwon, K. S. Kim, and S. Kim, "Compound Explosives Detection and Component Analysis via Terahertz Time-Domain Spectroscopy," *Journal of the Optical Society of Korea*, vol. 17, no. 5, pp. 454–460, Oct. 2013, doi: 10.3807/JOSK.2013.17.5.454.

[514] U. Puc, A. Abina, M. Rutar, A. Zidanšek, A. Jeglič, and G. Valušis, "Terahertz spectroscopic identification of explosive and drug simulants concealed by various hiding techniques," *Appl. Opt.*, vol. 54, no. 14, p. 4495, May 2015, doi: 10.1364/AO.54.004495.

[515] J. Chen, Y. Chen, H. Zhao, G. J. Bastiaans, and X.-C. Zhang, "Absorption coefficients of selected explosives and related compounds in the range of 0.1–2.8 THz," *Opt. Express, OE*, vol. 15, no. 19, pp. 12060–12067, Sep. 2007, doi: 10.1364/OE.15.012060.

[516] Y. Chen, Y. Ma, Z. Lu, L. Qiu, and J. He, "Terahertz spectroscopic uncertainty analysis for explosive mixture components determination using multi-objective micro-genetic algorithm," *Advances in Engineering Software*, vol. 42, no. 9, pp. 649–659, Sep. 2011, doi: 10.1016/j.advengsoft.2011.04.011.

[517] V. A. Trofimov and S. A. Varentsova, "Efficiency of using the spectral dynamics analysis for pulsed THz spectroscopy of both explosive and other materials," presented at the SPIE Defense + Security, S. S. Bishop and J. C. Isaacs, Eds., Baltimore, Maryland, United States, May 2015, p. 945409. doi: 10.1117/12.2178001.

[518] V. A. Trofimov and S. A. Varentsova, "A Possible Way for the Detection and Identification of Dangerous Substances in Ternary Mixtures Using THz Pulsed Spectroscopy," *Sensors*, vol. 19, no. 10, Art. no. 10, Jan. 2019, doi: 10.3390/s19102365.

[519] A. D. Burnett *et al.*, "Broadband terahertz time-domain spectroscopy of drugs-of-abuse and the use of principal component analysis," *Analyst*, vol. 134, no. 8, p. 1658, 2009, doi: 10.1039/b817839a.

[520] J. F. Federici *et al.*, "THz imaging and sensing for security applications-explosives, weapons and drugs," *Semicond. Sci. Technol.*, vol. 20, no. 7, pp. S266–S280, Jul. 2005, doi: 10.1088/0268-1242/20/7/018.

[521] N. E. Alexander *et al.*, "TeraSCREEN: multi-frequency multi-mode Terahertz screening for border checks," presented at the SPIE Defense + Security, D. A. Wikner and A. R. Luukanen, Eds., Baltimore, Maryland, USA, Jun. 2014, p. 907802. doi: 10.1117/12.2049926.

[522] G. Tzydynzhapov, P. Gusikhin, V. Muravev, A. Dremin, Y. Nefyodov, and I. Kukushkin, "New Real-Time Sub-Terahertz Security Body Scanner," *J Infrared Milli Terahz Waves*, vol. 41, no. 6, pp. 632–641, Jun. 2020, doi: 10.1007/s10762-020-00683-5.

[523] I. E. Carranza, J. Grant, J. Gough, and D. R. S. Cumming, "Metamaterial-Based Terahertz Imaging," *IEEE Transactions on Terahertz Science and Technology*, vol. 5, no. 6, pp. 892–901, Nov. 2015, doi: 10.1109/TTHZ.2015.2463673.

[524] T. Chen, S. Li, and H. Sun, "Metamaterials Application in Sensing," *Sensors*, vol. 12, no. 3, pp. 2742–2765, Feb. 2012, doi: 10.3390/s120302742.

[525] H. Tao *et al.*, "Metamaterials on Paper as a Sensing Platform," *Advanced Materials*, vol. 23, no. 28, pp. 3197–3201, 2011, doi: 10.1002/adma.201100163.

[526] J. H. Woo *et al.*, "Anisotropic change in THz resonance of planar metamaterials by liquid crystal and carbon nanotube," *Opt. Express, OE*, vol. 20, no. 14, pp. 15440–15451, Jul. 2012, doi: 10.1364/OE.20.015440.

[527] L. Deng *et al.*, "Direct Optical Tuning of the Terahertz Plasmonic Response of InSb Subwavelength Gratings," *Advanced Optical Materials*, vol. 1, no. 2, pp. 128–132, Feb. 2013, doi: 10.1002/adom.201200032.

[528] X. He *et al.*, "Carbon Nanotube Terahertz Detector," *Nano Lett.*, vol. 14, no. 7, pp. 3953–3958, Jul. 2014, doi: 10.1021/nl5012678.

[529] K. Serita, H. Murakami, I. Kawayama, and M. Tonouchi, "A Terahertz-Microfluidic Chip with a Few Arrays of Asymmetric Meta-Atoms for the Ultra-Trace Sensing of Solutions," *Photonics*, vol. 6, no. 1, Art. no. 1, Mar. 2019, doi: 10.3390/photonics6010012.

[530] X. Chen, W. Fan, and C. Song, "Multiple plasmonic resonance excitations on graphene metamaterials for ultrasensitive terahertz sensing," *Carbon*, vol. 133, pp. 416–422, Jul. 2018, doi: 10.1016/j.carbon.2018.03.051.

[531] Z. Geng, X. Zhang, Z. Fan, X. Lv, and H. Chen, "A Route to Terahertz Metamaterial Biosensor Integrated with Microfluidics for Liver Cancer Biomarker Testing in Early Stage," *Sci Rep*, vol. 7, no. 1, p. 16378, Dec. 2017, doi: 10.1038/s41598-017-16762-y.

[532] Z. Liu and K. Aydin, "Localized Surface Plasmons in Nanostructured Monolayer Black Phosphorus," *Nano Lett.*, vol. 16, no. 6, pp. 3457–3462, Jun. 2016, doi: 10.1021/acs.nanolett.5b05166.

[533] W. Tang, L. Wang, X. Chen, C. Liu, A. Yu, and W. Lu, "Dynamic metamaterial based on the graphene split ring high-Q Fano-resonnator for sensing applications," *Nanoscale*, vol. 8, no. 33, pp. 15196–15204, Aug. 2016, doi: 10.1039/C6NR02321E.

[534] S. Zeng *et al.*, "Graphene–Gold Metasurface Architectures for Ultrasensitive Plasmonic Biosensing," *Advanced Materials*, vol. 27, no. 40, pp. 6163–6169, 2015, doi: 10.1002/adma.201501754.

[535] R. Zhou *et al.*, "Label-free terahertz microfluidic biosensor for sensitive DNA detection using graphene-metasurface hybrid structures," *Biosensors and Bioelectronics*, vol. 188, p. 113336, Sep. 2021, doi: 10.1016/j.bios.2021.113336.

[536] Y. Hu, M. Tong, S. Hu, W. He, X. Cheng, and T. Jiang, "Multidimensional engineered metasurface for ultrafast terahertz switching at frequency-agile channels," *Nanophotonics*, vol. 11, no. 7, pp. 1367–1378, Mar. 2022, doi: 10.1515/nanoph-2021-0774.

[537] Y. Hu *et al.*, "Bi2Se3-Functionalized Metasurfaces for Ultrafast All-Optical Switching and Efficient Modulation of Terahertz Waves," *ACS Photonics*, vol. 8, no. 3, pp. 771–780, Mar. 2021, doi: 10.1021/acsphotonics.0c01194.

[538] Y. Yang, D. Xu, and W. Zhang, "High-sensitivity and label-free identification of a transgenic genome using a terahertz meta-biosensor," *Opt. Express*, vol. 26, no. 24, p. 31589, Nov. 2018, doi: 10.1364/OE.26.031589.

[539] S. J. Park, S. H. Cha, G. A. Shin, and Y. H. Ahn, "Sensing viruses using terahertz nano-gap metamaterials," *Biomed. Opt. Express, BOE*, vol. 8, no. 8, pp. 3551–3558, Aug. 2017, doi: 10.1364/BOE.8.003551.

[540] H. Hirori, K. Yamashita, M. Nagai, and K. Tanaka, "Attenuated Total Reflection Spectroscopy in Time Domain Using Terahertz Coherent Pulses," *Jpn. J. Appl. Phys.*, vol. 43, no. No. 10A, pp. L1287–L1289, Sep. 2004, doi: 10.1143/JJAP.43.L1287.

[541] S. Ramani, M. T. Reiten, P. L. Colestock, A. J. Taylor, A. K. Azad, and J. F. O'Hara, "Electromagnetic Response of Finite Terahertz Metafilm Arrays Excited on Total Internal Reflection Boundaries," *IEEE Trans. THz Sci. Technol.*, vol. 3, no. 6, pp. 709–720, Nov. 2013, doi: 10.1109/TTHZ.2013.2284858.

[542] M. Nagai, H. Yada, T. Arikawa, and K. Tanaka, "Terahertz time-domain attenuated total reflection spectroscopy in water and biological solution," *Int J Infrared Milli Waves*, vol. 27, no. 4, pp. 505–515, Apr. 2006, doi: 10.1007/s10762-006-9098-3.

[543] M. Tang *et al.*, "Detection of gene mutation responsible for Huntington's disease by terahertz attenuated total reflection microfluidic spectroscopy," *Journal of Biophotonics*, vol. 14, no. 1, p. e202000315, Jan. 2021, doi: 10.1002/jbio.202000315.

[544] K. Hashimoto, P. B. Ishai, E. Bründermann, and S. R. Tripathi, "Dielectric property measurement of human sweat using attenuated total reflection terahertz time domain spectroscopy," *Biomed. Opt. Express, BOE*, vol. 13, no. 9, pp. 4572–4582, Sep. 2022, doi: 10.1364/BOE.467450.

[545] L. Wu *et al.*, "Horizontal-scanning attenuated total reflection terahertz imaging for biological tissues," *NPh*, vol. 7, no. 2, p. 025005, Jun. 2020, doi: 10.1117/1.NPh.7.2.025005.

[546] M. Tang *et al.*, "Detection of single-base mutation of DNA oligonucleotides with different lengths by terahertz attenuated total reflection microfluidic cell," *Biomed. Opt. Express, BOE*, vol. 11, no. 9, pp. 5362–5372, Sep. 2020, doi: 10.1364/BOE.400487.

[547] S. Wang *et al.*, "Terahertz biosensing based on a polarization-insensitive metamaterial," *IEEE Photon. Technol. Lett.*, pp. 1–1, 2016, doi: 10.1109/LPT.2016.2522473.

[548] M. Tang *et al.*, "Detection of DNA oligonucleotides with base mutations by terahertz spectroscopy and microstructures," *PLoS ONE*, vol. 13, no. 1, p. e0191515, Jan. 2018, doi: 10.1371/journal.pone.0191515.

[549] S. Karmakar, D. Kumar, R. K. Varshney, and D. R. Chowdhury, "Strong terahertz matter interaction induced ultrasensitive sensing in Fano cavity based stacked metamaterials," *J. Phys. D: Appl. Phys.*, vol. 53, no. 41, p. 415101, Oct. 2020, doi: 10.1088/1361-6463/ab94e3.

[550] A. Ahmadivand, B. Gerislioglu, Z. Ramezani, A. Kaushik, P. Manickam, and S. A. Ghoreishi, "Functionalized terahertz plasmonic metasensors: Femtomolar-level detection of SARS-CoV-2 spike proteins," *Biosensors and Bioelectronics*, vol. 177, p. 112971, Apr. 2021, doi: 10.1016/j.bios.2021.112971.

[551] N. Cui *et al.*, "High Electric Field-Enhanced Terahertz Metamaterials with Bowtie Triangle Rings: Modeling, Mechanism, and Carbohydrate Antigen 125 Detection," *J. Phys. Chem. C*, vol. 125, no. 35, pp. 19374–19381, Sep. 2021, doi: 10.1021/acs.jpcc.1c05483.

[552] H. Yoshida *et al.*, "Terahertz sensing method for protein detection using a thin metallic mesh," *Appl. Phys. Lett.*, vol. 91, no. 25, p. 253901, Dec. 2007, doi: 10.1063/1.2825411.

[553] T. S. Bui *et al.*, "Metamaterial-enhanced vibrational absorption spectroscopy for the detection of protein molecules," *Sci Rep*, vol. 6, no. 1, Art. no. 1, Aug. 2016, doi: 10.1038/srep32123.

[554] S. J. Park, B. H. Son, S. J. Choi, H. S. Kim, and Y. H. Ahn, "Sensitive detection of yeast using terahertz slot antennas," *Opt. Express, OE*, vol. 22, no. 25, pp. 30467–30472, Dec. 2014, doi: 10.1364/OE.22.030467.

[555] S. J. Park, S. W. Jun, A. R. Kim, and Y. H. Ahn, "Terahertz metamaterial sensing on polystyrene microbeads: shape dependence," *Opt. Mater. Express, OME*, vol. 5, no. 10, pp. 2150–2155, Oct. 2015, doi: 10.1364/OME.5.002150.

[556] C. Zhang *et al.*, "Label-free measurements on cell apoptosis using a terahertz metamaterial-based biosensor," *Appl. Phys. Lett.*, vol. 108, no. 24, p. 241105, Jun. 2016, doi: 10.1063/1.4954015.

[557] T. Hasebe, Y. Yamada, and H. Tabata, "Label-free THz sensing of living body-related molecular binding using a metallic mesh," *Biochemical and Biophysical Research Communications*, vol. 414, no. 1, pp. 192–198, Oct. 2011, doi: 10.1016/j.bbrc.2011.09.055.

[558] T. Hasebe, S. Kawabe, H. Matsui, and H. Tabata, "Metallic mesh-based terahertz biosensing of single- and double-stranded DNA," *Journal of Applied Physics*, vol. 112, no. 9, p. 094702, Nov. 2012, doi: 10.1063/1.4761966.

[559] X. Wu *et al.*, "Sensing self-assembled alkanethiols by differential transmission interrogation with terahertz metamaterials," *Appl. Opt., AO*, vol. 52, no. 20, pp. 4877–4883, Jul. 2013, doi: 10.1364/AO.52.004877.

[560] X. Wu *et al.*, "Alkanethiol-functionalized terahertz metamaterial as label-free, highly-sensitive and specificbiosensor," *Biosensors and Bioelectronics*, vol. 42, pp. 626–631, Apr. 2013, doi: 10.1016/j.bios.2012.10.095.

[561] S. P. Mickan *et al.*, "Label-free bioaffinity detection using terahertz technology," *Phys. Med. Biol.*, vol. 47, no. 21, pp. 3789–3795, Nov. 2002, doi: 10.1088/0031-9155/47/21/317.

[562] B. M. Fischer *et al.*, "Terahertz time-domain spectroscopy and imaging of artificial RNA," *Opt. Express, OE*, vol. 13, no. 14, pp. 5205–5215, Jul. 2005, doi: 10.1364/OPEX.13.005205.

[563] B. Qin *et al.*, "Highly Sensitive Detection of Carbendazim by Using Terahertz Time-Domain Spectroscopy Combined With Metamaterial," *IEEE Transactions on Terahertz Science and Technology*, vol. 8, no. 2, pp. 149–154, Mar. 2018, doi: 10.1109/TTHZ.2017.2787458.

[564] J. Qin, L. Xie, and Y. Ying, "A high-sensitivity terahertz spectroscopy technology for tetracycline hydrochloride detection using metamaterials," *Food Chemistry*, vol. 211, pp. 300–305, Nov. 2016, doi: 10.1016/j.foodchem.2016.05.059.

[565] W. Xu *et al.*, "Terahertz sensing of chlorpyrifos-methyl using metamaterials," *Food Chemistry*, vol. 218, pp. 330–334, Mar. 2017, doi: 10.1016/j.foodchem.2016.09.032.

[566] P. Nie, D. Zhu, Z. Cui, F. Qu, L. Lin, and Y. Wang, "Sensitive detection of chlorpyrifos pesticide using an all-dielectric broadband terahertz metamaterial absorber," *Sensors and Actuators B: Chemical*, vol. 307, p. 127642, Mar. 2020, doi: 10.1016/j.snb.2019.127642.

[567] L. Xie, W. Gao, J. Shu, Y. Ying, and J. Kono, "Extraordinary sensitivity enhancement by metasurfaces in terahertz detection of antibiotics," *Sci Rep*, vol. 5, no. 1, Art. no. 1, Mar. 2015, doi: 10.1038/srep08671.

[568] J. Liu *et al.*, "Split ring resonators: using the redshift of terahertz responses peak to identify transgenic products with similar spectral characteristics," *Opt Quant Electron*, vol. 47, no. 7, pp. 1819–1828, Jul. 2015, doi: 10.1007/s11082-014-0040-y.

[569] C. R. Williams, S. R. Andrews, S. A. Maier, A. I. Fernández-Domínguez, L. Martín-Moreno, and F. J. García-Vidal, "Highly confined guiding of terahertz surface plasmon polaritons on structured metal surfaces," *Nature Photon*, vol. 2, no. 3, Art. no. 3, Mar. 2008, doi: 10.1038/nphoton.2007.301.

[570] B. Ng *et al.*, "Broadband Terahertz Sensing on Spoof Plasmon Surfaces," *ACS Photonics*, vol. 1, no. 10, pp. 1059–1067, Oct. 2014, doi: 10.1021/ph500272n.

[571] B. You, J.-Y. Lu, T.-A. Liu, and J.-L. Peng, "Hybrid terahertz plasmonic waveguide for sensing applications," *Opt. Express, OE*, vol. 21, no. 18, pp. 21087–21096, Sep. 2013, doi: 10.1364/OE.21.021087.

[572] J. Liu, "High-sensitivity detection method for organochlorine pesticide residues based on loop-shaped absorber," *Materials Chemistry and Physics*, vol. 242, p. 122542, Feb. 2020, doi: 10.1016/j.matchemphys.2019.122542.

[573] B. Li, J. Bai, and S. Zhang, "Low concentration noroxin detection using terahertz spectroscopy combined with metamaterial," *Spectrochimica Acta Part A: Molecular and Biomolecular Spectroscopy*, vol. 247, p. 119101, Feb. 2021, doi: 10.1016/j.saa.2020.119101.

[574] J. F. O'Hara, W. Withayachumnankul, and I. Al-Naib, "A Review on Thin-film Sensing with Terahertz Waves," *J Infrared Milli Terahz Waves*, vol. 33, no. 3, pp. 245–291, Mar. 2012, doi: 10.1007/s10762-012-9878-x.

[575] M. Labidi, J. B. Tahar, and F. Choubani, "Meta-materials applications in thin- film sensing and sensing liquids properties," *Opt. Express, OE*, vol. 19, no. 104, pp. A733–A739, Jul. 2011, doi: 10.1364/OE.19.00A733.

[576] A. G. Markelz, "Terahertz Dielectric Sensitivity to Biomolecular Structure and Function," *IEEE Journal of Selected Topics in Quantum Electronics*, vol. 14, no. 1, pp. 180–190, Jan. 2008, doi: 10.1109/JSTQE.2007.913424.

[577] J. Y. Ou, E. Plum, L. Jiang, and N. I. Zheludev, "Reconfigurable Photonic Metamaterials," *Nano Lett.*, vol. 11, no. 5, pp. 2142–2144, May 2011, doi: 10.1021/nl200791r.

[578] Y. Zhao, K. Vora, X. Liu, G. vom Bögel, K. Seidl, and J. C. Balzer, "Photonic Crystal Resonator in the Millimeter/Terahertz Range as a Thin Film Sensor for Future Biosensor Applications," *J Infrared Milli Terahz Waves*, vol. 43, no. 5, pp. 426–444, Jun. 2022, doi: 10.1007/s10762-022-00859-1.

[579] J. Zhang and D. Grischkowsky, "Waveguide terahertz time-domain spectroscopy of nanometer water layers," *Opt. Lett., OL*, vol. 29, no. 14, pp. 1617–1619, Jul. 2004, doi: 10.1364/OL.29.001617.

[580] J. F. O'Hara *et al.*, "Thin-film sensing with planar terahertz metamaterials: sensitivity and limitations," *Opt. Express, OE*, vol. 16, no. 3, pp. 1786–1795, Feb. 2008, doi: 10.1364/OE.16.001786.

[581] C. Debus and P. H. Bolivar, "Frequency selective surfaces for high sensitivity terahertz sensing," *Appl. Phys. Lett.*, vol. 91, no. 18, p. 184102, Oct. 2007, doi: 10.1063/1.2805016.

[582] F. Miyamaru, Y. Sasagawa, and M. W. Takeda, "Effect of dielectric thin films on reflection properties of metal hole arrays," *Appl. Phys. Lett.*, vol. 96, no. 2, p. 021106, Jan. 2010, doi: 10.1063/1.3292024.

[583] M. Tanaka, F. Miyamaru, M. Hangyo, T. Tanaka, M. Akazawa, and E. Sano, "Effect of a thin dielectric layer on terahertz transmission characteristics for metal hole arrays," *Opt. Lett., OL*, vol. 30, no. 10, pp. 1210–1212, May 2005, doi: 10.1364/OL.30.001210.

[584] S. Yoshida, E. Kato, K. Suizu, Y. Nakagomi, Y. Ogawa, and K. Kawase, "Terahertz Sensing of Thin Poly(ethylene Terephthalate) Film Thickness Using a Metallic Mesh," *Appl. Phys. Express*, vol. 2, no. 1, p. 012301, Jan. 2009, doi: 10.1143/APEX.2.012301.

[585] T. Suzuki, T. Kondo, Y. Ogawa, S. Kamba, and N. Kondo, "Detection of $\rm SiO_2$ Thin Layer by Using a Metallic Mesh Sensor," *IEEE Sensors Journal*, vol. 13, no. 12, pp. 4972–4976, Dec. 2013, doi: 10.1109/JSEN.2013.2278760.

[586] B. Reinhard, K. M. Schmitt, V. Wollrab, J. Neu, R. Beigang, and M. Rahm, "Metamaterial near-field sensor for deep-subwavelength thickness measurements and sensitive refractometry in the terahertz frequency range," *Appl. Phys. Lett.*, vol. 100, no. 22, p. 221101, May 2012, doi: 10.1063/1.4722801.

[587] W. Withayachumnankul *et al.*, "Sub-diffraction thin-film sensing with planar terahertz metamaterials," *Opt. Express, OE*, vol. 20, no. 3, pp. 3345–3352, Jan. 2012, doi: 10.1364/OE.20.003345.

[588] H.-R. Park, X. Chen, N.-C. Nguyen, J. Peraire, and S.-H. Oh, "Nanogap-Enhanced Terahertz Sensing of 1 nm Thick (λ/106) Dielectric Films," *ACS Photonics*, vol. 2, no. 3, pp. 417–424, Mar. 2015, doi: 10.1021/ph500464j.

[589] B. You *et al.*, "Terahertz plasmonic waveguide based on metal rod arrays for nanofilm sensing," *Opt. Express, OE*, vol. 22, no. 9, pp. 11340–11350, May 2014, doi: 10.1364/OE.22.011340.

[590] T. L. Cocker, V. Jelic, R. Hillenbrand, and F. A. Hegmann, "Nanoscale terahertz scanning probe microscopy," *Nat. Photon.*, vol. 15, no. 8, Art. no. 8, Aug. 2021, doi: 10.1038/s41566-021-00835-6.

[591] E. M. Hassan *et al.*, "High-sensitivity detection of metastatic breast cancer cells via terahertz chemical microscopy using aptamers," *Sensors and Actuators B: Chemical*, vol. 287, pp. 595–601, May 2019, doi: 10.1016/j.snb.2019.02.019.

[592] A. Toma *et al.*, "Squeezing Terahertz Light into Nanovolumes: Nanoantenna Enhanced Terahertz Spectroscopy (NETS) of Semiconductor Quantum Dots," *Nano Lett.*, vol. 15, no. 1, pp. 386–391, Jan. 2015, doi: 10.1021/nl503705w.

[593] G. Ji *et al.*, "Terahertz virus-sized gold nanogap sensor," *Nanophotonics*, vol. 12, no. 1, pp. 147–154, Jan. 2023, doi: 10.1515/nanoph-2022-0706.

[594] H.-R. Park, S. Namgung, X. Chen, and S.-H. Oh, "High-density metallic nanogap arrays for the sensitive detection of single-walled carbon nanotube thin films," *Faraday Discuss.*, vol. 178, no. 0, pp. 195–201, May 2015, doi: 10.1039/C4FD00233D.

[595] F. Hu, L. Zhang, X. Xu, Y. Wang, T. Zou, and W. Zhang, "Study on split-ring-resonator based terahertz sensor and its application to the identification of product oil," *Opt Quant Electron*, vol. 47, no. 8, pp. 2867–2879, Aug. 2015, doi: 10.1007/s11082-015-0175-5.

[596] Z. Jakšic, O. Jakšic, and J. Matovic, "Performance limits to the operation of nanoplasmonic chemical sensors: noise-equivalent refractive index and detectivity," *JNP*, vol. 3, no. 1, p. 031770, Apr. 2009, doi: 10.1117/1.3124792.

[597] Z. Djurić, O. Jakšić, and D. Randjelović, "Adsorption–desorption noise in micromechanical resonant structures," *Sensors and Actuators A: Physical*, vol. 96, no. 2, pp. 244–251, Feb. 2002, doi: 10.1016/S0924-4247(01)00834-2.

[598] Z. Jakšić, O. Jakšić, Z. Djurić, and C. Kment, "A consideration of the use of metamaterials for sensing applications: field fluctuations and ultimate performance," *J. Opt. A: Pure Appl. Opt.*, vol. 9, no. 9, p. S377, Aug. 2007, doi: 10.1088/1464-4258/9/9/S16.

[599] L. Peng, L. Ran, H. Chen, H. Zhang, J. A. Kong, and T. M. Grzegorczyk, "Experimental Observation of Left-Handed Behavior in an Array of Standard Dielectric Resonators," *Phys. Rev. Lett.*, vol. 98, no. 15, p. 157403, Apr. 2007, doi: 10.1103/PhysRevLett.98.157403.

[600] S. Walia *et al.*, "Flexible metasurfaces and metamaterials: A review of materials and fabrication processes at micro- and nano-scales," *Applied Physics Reviews*, vol. 2, no. 1, p. 011303, Mar. 2015, doi: 10.1063/1.4913751.

[601] H. o. Moser and C. Rockstuhl, "3D THz metamaterials from micro/nanomanufacturing," *Laser & Photonics Reviews*, vol. 6, no. 2, pp. 219–244, 2012, doi: 10.1002/lpor.201000019.

[602] N. Krumbholz *et al.*, "Monitoring polymeric compounding processes inline with THz time-domain spectroscopy," *Polymer Testing*, vol. 28, no. 1, pp. 30–35, Feb. 2009, doi: 10.1016/j.polymertesting.2008.09.009.

[603] M. Tang *et al.*, "Rapid and label-free metamaterial-based biosensor for fatty acid detection with terahertz time-domain spectroscopy," *Spectrochimica Acta Part A: Molecular and Biomolecular Spectroscopy*, vol. 228, p. 117736, Mar. 2020, doi: 10.1016/j.saa.2019.117736.

[604] P. Martín-Mateos *et al.*, "Hyperspectral terahertz imaging with electro-optic dual combs and a FET-based detector," *Sci Rep*, vol. 10, no. 1, Art. no. 1, Sep. 2020, doi: 10.1038/s41598-020-71258-6.

[605] Y. Li, P. Ferreyra, A. K. Swan, and R. Paiella, "Current-Driven Terahertz Light Emission from Graphene Plasmonic Oscillations," *ACS Photonics*, vol. 6, no. 10, pp. 2562–2569, Oct. 2019, doi: 10.1021/acsphotonics.9b01037.

[606] C. Lan *et al.*, "Highly Efficient Active All-Dielectric Metasurfaces Based on Hybrid Structures Integrated with Phase-Change Materials: From Terahertz to Optical Ranges," *ACS Appl. Mater. Interfaces*, vol. 11, no. 15, pp. 14229–14238, Apr. 2019, doi: 10.1021/acsami.8b22466.

[607] D. A. Bandurin *et al.*, "Resonant terahertz detection using graphene plasmons," *Nat Commun*, vol. 9, no. 1, Art. no. 1, Dec. 2018, doi: 10.1038/s41467-018-07848-w.

[608] Y. Li, K. Tantiwanichapan, A. K. Swan, and R. Paiella, "Graphene plasmonic devices for terahertz optoelectronics," *Nanophotonics*, vol. 9, no. 7, pp. 1901–1920, Jul. 2020, doi: 10.1515/nanoph-2020-0211.

[609] X. Liu, T. Ytterdal, and M. Shur, "Plasmonic FET Terahertz Spectrometer," *IEEE Access*, vol. 8, pp. 56039–56044, 2020, doi: 10.1109/ACCESS.2020.2982275.

[610] M. E. Khani *et al.*, "Supervised machine learning for automatic classification of in vivo scald and contact burn injuries using the terahertz Portable Handheld Spectral Reflection (PHASR) Scanner," *Sci Rep*, vol. 12, no. 1, Art. no. 1, Mar. 2022, doi: 10.1038/s41598-022-08940-4.

[611] A. W. M. Lee, Q. Qin, S. Kumar, B. S. Williams, Q. Hu, and J. L. Reno, "Real-time terahertz imaging over a standoff distance (>25meters)," *Applied Physics Letters*, vol. 89, no. 14, p. 141125, Oct. 2006, doi: 10.1063/1.2360210.

[612] D. Liang, J. Pan, Y. Yu, and H. Zhou, "Concealed object segmentation in terahertz imaging via adversarial learning," *Optik*, vol. 185, pp. 1104–1114, May 2019, doi: 10.1016/j.ijleo.2019.04.034.

[613] X. Shi and J. Chen, "Development of a standoff terahertz imaging system for concealed weapon detection," *Microw Opt Technol Lett*, vol. 61, no. 4, pp. 1116–1120, Apr. 2019, doi: 10.1002/mop.31688.

[614] V. A. Trofimov and S. A. Varentsova, "An Effective Method for Substance Detection Using the Broad Spectrum THz Signal: A 'Terahertz Nose,'" *Sensors*, vol. 15, no. 6, Art. no. 6, Jun. 2015, doi: 10.3390/s150612103.

[615] I. N. Dolganova, K. I. Zaytsev, A. A. Metelkina, and S. O. Yurchenko, "The active-passive continuous-wave terahertz imaging system," *J. Phys.: Conf. Ser.*, vol. 735, no. 1, p. 012075, Aug. 2016, doi: 10.1088/1742-6596/735/1/012075.

[616] A. V. Shchepetilnikov *et al.*, "New Ultra-Fast Sub-Terahertz Linear Scanner for Postal Security Screening," *J Infrared Milli Terahz Waves*, vol. 41, no. 6, pp. 655–664, Jun. 2020, doi: 10.1007/s10762-020-00692-4.

[617] M. Kato, S. R. Tripathi, K. Murate, K. Imayama, and K. Kawase, "Non-destructive drug inspection in covering materials using a terahertz spectral imaging system with injection-seeded terahertz parametric generation and detection," *Opt. Express, OE*, vol. 24, no. 6, pp. 6425–6432, Mar. 2016, doi: 10.1364/OE.24.006425.

[618] R. Jintamethasawat *et al.*, "Non-uniformity Correction Algorithm for THz Array Detectors in High-Resolution Imaging Applications," *J Infrared Milli Terahz Waves*, vol. 41, no. 8, pp. 940–956, Aug. 2020, doi: 10.1007/s10762-020-00698-y.

[619] A. Azan *et al.*, "Monitoring the molecular composition of live cells exposed to electric pulses via label-free optical methods," *Sci Rep*, vol. 10, no. 1, Art. no. 1, Jun. 2020, doi: 10.1038/s41598-020-67402-x.

[620] L. Wei, L. Yu, H. Jiaoqi, H. Guorong, Z. Yang, and F. Weiling, "Application of terahertz spectroscopy in biomolecule detection," *Frontiers in Laboratory Medicine*, vol. 2, no. 4, pp. 127–133, Dec. 2018, doi: 10.1016/j.flm.2019.05.001.

[621] Q. Wang, L. Xie, and Y. Ying, "Overview of imaging methods based on terahertz time-domain spectroscopy," *Applied Spectroscopy Reviews*, vol. 57, no. 3, pp. 249–264, Mar. 2022, doi: 10.1080/05704928.2021.1875480.

[622] N. Karpowicz, H. Zhong, J. Xu, K.-I. Lin, J.-S. Hwang, and X.-C. Zhang, "Comparison between pulsed terahertz time-domain imaging and continuous wave terahertz imaging," *Semicond. Sci. Technol.*, vol. 20, no. 7, pp. S293–S299, Jun. 2005, doi: 10.1088/0268-1242/20/7/021.

[623] T. Hochrein, R. Wilk, M. Mei, R. Holzwarth, N. Krumbholz, and M. Koch, "Optical sampling by laser cavity tuning," *Opt. Express, OE*, vol. 18, no. 2, pp. 1613–1617, Jan. 2010, doi: 10.1364/OE.18.001613.

[624] A. Bartels *et al.*, "Ultrafast time-domain spectroscopy based on high-speed asynchronous optical sampling," *Review of Scientific Instruments*, vol. 78, no. 3, p. 035107, Mar. 2007, doi: 10.1063/1.2714048.

[625] M. Beck *et al.*, "High-speed THz spectroscopic imaging at ten kilohertz pixel rate with amplitude and phase contrast," *Opt. Express, OE*, vol. 27, no. 8, pp. 10866–10872, Apr. 2019, doi: 10.1364/OE.27.010866.

[626] R. Wilk, T. Hochrein, M. Koch, M. Mei, and R. Holzwarth, "Terahertz spectrometer operation by laser repetition frequency tuning," *J. Opt. Soc. Am. B, JOSAB*, vol. 28, no. 4, pp. 592–595, Apr. 2011, doi: 10.1364/JOSAB.28.000592.

[627] A. Bassli *et al.*, "Three-Dimensional Imaging of Materials at 0.1 THz for Inner-Defect Detection Using a Frequency-Modulated Continuous-Wave Radar," *IEEE Transactions on Instrumentation and Measurement*, vol. 69, no. 8, pp. 5843–5852, Aug. 2020, doi: 10.1109/TIM.2020.2966312.

[628] M. C. Giordano, L. Viti, O. Mitrofanov, and M. S. Vitiello, "Phase-sensitive terahertz imaging using room-temperature near-field nanodetectors," *Optica, OPTICA*, vol. 5, no. 5, pp. 651–657, May 2018, doi: 10.1364/OPTICA.5.000651.

[629] J. B. Perraud *et al.*, "Terahertz imaging and tomography as efficient instruments for testing polymer additive manufacturing objects," *Appl. Opt.*, vol. 55, no. 13, p. 3462, May 2016, doi: 10.1364/AO.55.003462.

[630] R. Safian, G. Ghazi, and N. Mohammadian, "Review of photomixing continuous-wave terahertz systems and current application trends in terahertz domain," *OE*, vol. 58, no. 11, p. 110901, Nov. 2019, doi: 10.1117/1.OE.58.11.110901.

[631] J. Suszek *et al.*, "3-D-Printed Flat Optics for THz Linear Scanners," *IEEE Transactions on Terahertz Science and Technology*, vol. 5, no. 2, pp. 314–316, Mar. 2015, doi: 10.1109/TTHZ.2015.2398313.

[632] Y. Amarasinghe, D. M. Mittleman, and R. Mendis, "A Luneburg Lens for the Terahertz Region," *J Infrared Milli Terahz Waves*, vol. 40, no. 11, pp. 1129–1136, Dec. 2019, doi: 10.1007/s10762-019-00635-8.

[633] E. Castro-Camus, M. Koch, and A. I. Hernandez-Serrano, "Additive manufacture of photonic components for the terahertz band," *Journal of Applied Physics*, vol. 127, no. 21, p. 210901, Jun. 2020, doi: 10.1063/1.5140270.

[634] Z. Zhang, H. Zhang, and K. Wang, "Diffraction-Free THz Sheet and Its Application on THz Imaging System," *IEEE Transactions on Terahertz Science and Technology*, vol. 9, no. 5, pp. 471–475, Sep. 2019, doi: 10.1109/TTHZ.2019.2926630.

[635] D. Headland, W. Withayachumnankul, M. Webb, H. Ebendorff-Heidepriem, A. Luiten, and D. Abbott, "Analysis of 3D-printed metal for rapid-prototyped reflective terahertz optics," *Opt. Express, OE*, vol. 24, no. 15, pp. 17384–17396, Jul. 2016, doi: 10.1364/OE.24.017384.

[636] S. A. Mikhailov, "Graphene-based voltage-tunable coherent terahertz emitter," *Phys. Rev. B*, vol. 87, no. 11, p. 115405, Mar. 2013, doi: 10.1103/PhysRevB.87.115405.

[637] S.-W. Huang *et al.*, "Globally Stable Microresonator Turing Pattern Formation for Coherent High-Power THz Radiation On-Chip," *Phys. Rev. X*, vol. 7, no. 4, p. 041002, Oct. 2017, doi: 10.1103/PhysRevX.7.041002.

[638] N. A. Aghamiri, F. Huth, A. J. Huber, A. Fali, R. Hillenbrand, and Y. Abate, "Hyperspectral time-domain terahertz nano-imaging," *Opt. Express, OE*, vol. 27, no. 17, pp. 24231–24242, Aug. 2019, doi: 10.1364/OE.27.024231.

[639] C. Maissen, S. Chen, E. Nikulina, A. Govyadinov, and R. Hillenbrand, "Probes for Ultrasensitive THz Nanoscopy," *ACS Photonics*, vol. 6, no. 5, pp. 1279–1288, May 2019, doi: 10.1021/acsphotonics.9b00324.

[640] H. Guerboukha, Y. Cao, K. Nallappan, and M. Skorobogatiy, "Super-Resolution Orthogonal Deterministic Imaging Technique for Terahertz Subwavelength Microscopy," *ACS Photonics*, vol. 7, no. 7, pp. 1866–1875, Jul. 2020, doi: 10.1021/acsphotonics.0c00711.

[641] A. Pizzuto, D. M. Mittleman, and P. Klarskov, "Laser THz emission nanoscopy and THz nanoscopy," *Opt. Express, OE*, vol. 28, no. 13, pp. 18778–18789, Jun. 2020, doi: 10.1364/OE.382130.

[642] X. Chen *et al.*, "THz Near-Field Imaging of Extreme Subwavelength Metal Structures," *ACS Photonics*, vol. 7, no. 3, pp. 687–694, Mar. 2020, doi: 10.1021/acsphotonics.9b01534.

[643] J. Wang, S. Yan, Z. Li, Z. Zang, X. Lu, and H.-L. Cui, "Single-cell terahertz spectral characteristics in simulated scattering near-field imaging mode," *OSA Continuum, OSAC*, vol. 3, no. 8, pp. 2096–2105, Aug. 2020, doi: 10.1364/OSAC.400827.

[644] C. L. K. Dandolo *et al.*, "Toward a multimodal fusion of layered cultural object images: complementarity of optical coherence tomography and terahertz time-domain imaging in the heritage field," *Appl. Opt., AO*, vol. 58, no. 5, pp. 1281–1290, Feb. 2019, doi: 10.1364/AO.58.001281.

[645] J. Hu, Y. Liu, Y. He, X. Sun, and B. Li, "Optimization of quantitative detection model for benzoic acid in wheat flour based on CARS variable selection and THz spectroscopy," *Food Measure*, vol. 14, no. 5, pp. 2549–2558, Oct. 2020, doi: 10.1007/s11694-020-00501-5.

[646] F. Alves, L. Pimental, D. Grbovic, and G. Karunasiri, "MEMS terahertz-to-infrared band converter using frequency selective planar metamaterial," *Sci Rep*, vol. 8, no. 1, Art. no. 1, Aug. 2018, doi: 10.1038/s41598-018-30858-z.

[647] A. Calabrese *et al.*, "Coulomb forces in THz electromechanical meta-atoms," *Nanophotonics*, vol. 8, no. 12, pp. 2269–2277, Dec. 2019, doi: 10.1515/nanoph-2019-0314.

[648] C. G. Wade, N. Šibalić, N. R. de Melo, J. M. Kondo, C. S. Adams, and K. J. Weatherill, "Real-time near-field terahertz imaging with atomic optical fluorescence," *Nature Photon*, vol. 11, no. 1, Art. no. 1, Jan. 2017, doi: 10.1038/nphoton.2016.214.

[649] Y. Wen *et al.*, "Photomechanical meta-molecule array for real-time terahertz imaging," *Microsyst Nanoeng*, vol. 3, no. 1, Art. no. 1, Dec. 2017, doi: 10.1038/micronano.2017.71.

[650] N. B. Lawler, D. Ho, C. W. Evans, V. P. Wallace, and K. S. Iyer, "Convergence of terahertz radiation and nanotechnology," *J. Mater. Chem. C*, vol. 8, no. 32, pp. 10942–10955, 2020, doi: 10.1039/D0TC01716G.

Walter Nsengiyumva is an experienced engineer and researcher with proficient technical skills and strong educational background in the field of electrical, mechanical, and mechatronic engineering. Dr. Nsengiyumva graduated with his first Bachelor of Engineering in Electrotechnology and Industrial Informatics from Institut des Sciences et des Technologies Industrielles de Brazzaville (Brazzaville, Congo), and his second Bachelor of Technology in Electrical Engineering from Durban University of Technology (Durban, South Africa) in 2008 and 2014, respectively. Dr. Nsengiyumva graduated with his Master's in Mechanical Engineering from Fujian Agriculture and Forestry University (Fuzhou, China) and Ph.D. in Mechatronic Engineering from Fuzhou University (Fuzhou, China) in 2018 and 2022, respectively. With a career spanning over 10 years within academic and industrial sectors, Dr. Nsengiyumva has expertise in research and development, mechanical engineering, electrical engineering, control systems, automation, higher education, project management, intelligent sensing, systems diagnosis, and consulting. Dr. Nsengiyumva is currently an Associate Professor of Mechatronic Engineering in the School of Mechanical Engineering and Automation at Fuzhou University and a member of the Fujian Key Laboratory of Terahertz Functional Devices and Intelligent Sensing. His research interests include intelligent sensing and diagnosis, nondestructive testing and evaluation, structural health monitoring, optics, terahertz spectroscopy and imaging, mechanics of composite materials and structures, signal/image processing and pattern recognition for diagnosis and prognosis of materials and structural systems, renewable energy, and energy management systems. As part of his scientific activities, Dr. Nsengiyumva has published more than 30 research papers in peer-reviewed international journals and 1 book, given several presentations at both national and international conferences, and is constantly a referee of several international journals on the topics of nondestructive testing, composite materials, structural mechanics, optics, terahertz spectroscopy and imaging, and structural health monitoring.

Shuncong Zhong received his Ph.D. degree from the University of Manchester, U.K., in 2007. He has had a many-year industrial and academic career at Imperial College London, University of Liverpool, University of Strathclyde, Shanghai Jiao Tong University, and Mindray Company, Ltd., China. He is currently a Chair Professor at Fuzhou University, China. He has already published more than 200 papers and authorized more than 34 Chinese, US, and UK patents and 13 software

copyrights. He has also published 3 books/chapters, and 5 ISO and Chinese standards. His research interests include intelligent sensing and diagnosis, optics and terahertz systems, structural health monitoring, nondestructive testing and evaluation, signal and image processing, and pattern recognition for diagnosis and prognostics. Prof. Zhong is currently the vice-chairman of the Fujian Society of Mechanical Engineering, the vice-chairman of the Fujian Society of Mechanics, chairman of the Nondestructive Testing Branch of the Fujian Mechanical Engineering Society, executive member of the Fault Diagnosis Committee of the Chinese Society of Vibration Engineering, and executive member of the Equipment Intelligent Operation and Maintenance Branch of the Chinese Society of Mechanical Engineering. He is also an associate editor, guest editor, and editorial board member of 8 international journals. He got 2 Fujian Provincial Science and Technology Progress Awards (1st Prize, ranking first) and 1 Fujian Provincial Higher Education Teaching Achievement Award (Top Prize, ranking first). He was elected as a Fellow of the Society of Engineering and Technology (IET Fellow), a Fellow of the International Institute of Acoustics and Vibration (IIAV Fellow), and a Fellow of the International Society for Condition Monitoring (ISCM Fellow).

Longhui Zheng received his Ph.D. degree in Material Science at Soochow University, Suzhou, China. He is currently an Associate Professor at the Fujian Institute of Research on the Structure of Matter, Chinese Academy of Sciences. His research interests focus on the development of functional nano and micro-materials, dielectric materials, and high-performance composites.

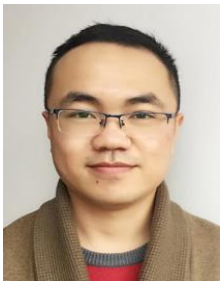

Wei Liang was born in Fujian, China, in 1987. He received his B.S. and Ph.D. degrees from the School of Mechanical Engineering and Automation, Fuzhou University, Fuzhou, China, in 2009 and 2019, respectively. Dr. Liang is currently an Assistant Professor at Fuzhou University, Fuzhou, China. He has authored/co-authored 21 papers and holds 18 patents. His current research interests include force and mass measurement using optical methods and mechanics.

Bing Wang is a Professor of Mechanical Engineering at Fuzhou University, Fuzhou, China. He received his Ph.D. at the University of Hull (UoH) in Jan 2017 and then became a Research Fellow. He moved to the University of Cambridge as a Research Associate in bistable composite technologies from July 2017 to April 2020. His research interests include smart materials, composite structures, mechanics, nondestructive testing & evaluation, multiscale analysis, Elasticity & Viscoelasticity.

Yi Huang is an Associate Professor at Fuzhou University, Fuzhou, China. He received his Ph.D. degree from Fuzhou University in 2021, Fuzhou, China. Up till now, he has published 20 SCI papers. He was awarded the First Prize in the Science and Technology Progress of Fujian Province in 2022. His research interests include terahertz metasurfaces, plasmonic sensors, and terahertz spectroscopy analysis and imaging.

Xuefeng Chen (Senior Member, IEEE) received his Ph.D. degree from Xi'an Jiaotong University, Xi'an, China, in 2004. He is currently a Full Professor and the Dean of the School of Mechanical Engineering, at Xi'an Jiaotong University. He has authored over 100 SCI publications in areas of composite structure, aeroengine, wind power equipment, and so on. Dr. Chen won the National Excellent Doctoral Thesis Award in 2007, the First Technological Invention Award of the Ministry of Education in 2008, the Second National Technological Invention Award in 2009, the First Provincial Teaching Achievement Award in 2013, and the First Technological Invention Award of the Ministry of Education in 2015. He was awarded the Science & Technology Award for Chinese Youth in 2013. He is also the Executive Director of the Fault Diagnosis Branch in the China Mechanical Engineering Society.

Yaochun Shen is a Professor at the University of Liverpool, United Kingdom. He received his Ph.D. degree from Nanjing University in 1992. After that, he held various positions at Southeast University, Heriot-Watt University, Heidelberg University, and Cambridge University. He joined the University of Liverpool as a Senior Lecturer in 2007 and became a full Professor in 2016. He has been working on terahertz-related technology for many years, first as a Research Associate (2001-2004) at the Cavendish Laboratory, University of Cambridge, and then as a Senior Scientist (2004-2007) at TeraView Limited, Cambridge. The influence of his work can also be seen in his excellent publication metrics: h-index 41 and over 5560 citations (Google Scholar), 5 book chapters, 7 patents, over 200 conference & journal publications, and many invited talks.